Aston University

Some pages of this thesis may have been removed for copyright restrictions.

If you have discovered material in AURA which is unlawful e.g. breaches copyright, (either yours or that of a third party) or any other law, including but not limited to those relating to patent, trademark, confidentiality, data protection, obscenity, defamation, libel, then please read our Takedown Policy and contact the service immediately

VIBRATION IN ELECTROMAGNETICALLY HEATED STEEL

Richard Timothy Baker

Doctor of Philosophy

The University of Aston in Birmingham

October 1995

This copy of the thesis has been supplied on condition that anyone who consults it is understood to recognise that its copyright rests with its author and that no quotation from the thesis and no information derived from it may be published without proper acknowledgement.

The University of Aston in Birmingham

Vibration in Electromagnetically Heated Steel

Richard Timothy Baker

Doctor of Philosophy

October 1995

Thesis Summary

When a ferromagnetic steel billet was heated by induction a large increase in the amplitude of longitudinal vibration frequently occurred as a result of resonance. This happened when a natural frequency of the bar coincided with twice the heating frequency or multiples thereof.

The temperature at which resonance occurred depended on a number of factors including billet length and heating power. Resonance was most often observed when the surface temperature of the billet reached the Curie point. It is well established that magnetostrictive vibrations occur in a ferromagnetic material subjected to an alternating electromagnetic field, but existing data suggests that linear magnetostriction decreases towards the Curie point. Linear magnetostriction was measured in a sample of mild steel up to 800°C using a high temperature strain gauge.

The magnetostriction constant λ_{100} was calculated assuming an average grain orientation in mild steel. The data was found to be comparable to that published for single crystals of iron.

It was discovered that linear magnetostriction was responsible for resonance below 600°C but not for temperatures near the Curie point.

Other possible causes of resonance such as forces produced by the interaction between eddy currents and the alternating electromagnetic field, the alpha to gamma phase transformation and the existence of a thin ferromagnetic layer were investigated. None were found to account for resonance in bars of mild steel heated by induction.

Experimental work relating to the induction heating of steel is compared to previous work on the subject of electromagnetic generation of ultrasound where a similar increase of the amplitude of longitudinal waves in steel is reported at the Curie point. It is concluded that the two phenomena are related as they show strong similarities.

Keywords:

Induction Heating, Steel, Curie Point, Resonance, Magnetostriction.

To my girlfriend Anne and my parents.

ACKNOWLEDGEMENTS

I am grateful to my supervisors, Dr Trevor Oliver and Professor Toby Norris for their continuous advice with this work.

Much of the project consisted of practical work and the assistance from Mr Joe Thomas was gratefully received. I am especially thankful to Joe for all the help in constructing the different sets of apparatus required for the tests.

Thanks also go to Mr Brian Harrison and Mr Les Radford for their contributions to my practical work.

I am appreciative for the advice from Dr. Seamus Garvey concerning vibration measurements and theory.

I would like to thank my industrial supervisor, Dr Malcolm Booth, and Midlands Electricity plc for both financial support and for the use of facilities at the Energy Technology Centre.

I am very grateful to David Stickland of Crossley Electronic Sales Ltd for the supply of a 60kW, 3.2 kHz Crossley induction heater at a considerably reduced price.

Many thanks to Mr Jack Sugden from Berkeley Technology Centre, Nuclear Electric plc for the kind loan of an Ometron Laser Vibrometer.

I am thankful to Professor Moses from the University of Wales, College of Cardiff for his advice on measuring magnetostriction.

Finally, I am grateful to The Engineering and Physical Sciences Research Council (EPSRC) for their continuous financial support and to the Royal Academy of Engineering for their financial support regarding the presentation of a paper at EPM '94 in Nagoya, Japan.

CONTENTS

LIST OF FIGURES

LIST OF TABLES

NOMENCLATURE

a	Radius of coil (m)
b	Distortion (%)
c	Specific heat (J $kg^{-1}K^{-1}$)
c	Actual damping coefficient (N s m^{-1})
c_c	Critical damping coefficient (N s m^{-1})
d	Diameter (m)
d	Distance between striations (cm)
d	Heated thickness of the bar (m)
e_{xx}	Strain tensor component
e_{yy}	Strain tensor component
e_{zz}	Strain tensor component
f	Frequency (Hz)
f_L	Force due to interaction of eddy currents with magnetic field (N)
f_n	n^{th} natural frequency (Hz)
f_{ref}	Reference frequency (Hz)
g	Acceleration due to gravity (m s^{-2})
g	Exchange term
h	Height (m)
j	Eddy current density (A m^{-1})
k	Thermal conductivity (W $m^{-1}K^{-1}$)
l	Length (m)
l	Coefficient of dipole-dipole interaction
l_0	Original length (m)
n	Integer ($n \geq 0$)
p	A function of flux distribution in a cylinder
p	Radius to point P (m)
q	Coefficient of quadrupole interaction
q	Charge (C)
r	Mode of vibration
r	Atomic distance (m)
t	Time (s)
u	Displacement (m)
v	Velocity (m s^{-1})
v	Volume (m^3)
v	RMS voltage (V)
w	Pair energy
x	Distance along bar (m)

x	Displacement (m)
$\ddot{x}$	Acceleration (m s^{-2})
y	Distance (m)
z	Distance from centre line (m)
A_1	Transition temperature of steel (723°C)
A_{c1}	Transition temperature of steel (760°C)
A	Cross section area (m^2)
B	Magnetic flux density (T)
B_p	Radial component of flux density (T)
B_z	Axial component of flux density (T)
C	Capacitance (F)
D	Wavelength of striations (cm)
E	Young's modulus (N m^{-2})
E	Electric field strength (V m^{-1})
E	Complete elliptic integral of the second kind of parameter m
F	Force (N)
H	Magnetic field strength (A m^{-1})
H_0	Static magnetic field (A m^{-1})
H_p	Radial component of magnetic field (A m^{-1})
H_z	Axial component of magnetic field (A m^{-1})
I	Current (A)
I_{coil}	Current in heating coil (A)
I_{ref}	Reference current (A)
J	Eddy current density (A m^{-1})
K	Gauge factor
K	Complete elliptic integral of the first kind of parameter m
L_1	Lower critical temperature of steel (°C)
L	Length (m)
L	Noise level (dBA)
M_s	Saturation magnetisation (T)
M	Magnetisation (T)
N	Number of turns
N	Number of active arms
P	Stress (Pa)
P_{in}	Power input (W m^{-2})
P_0	Power density at surface (W m^{-2})
P_R	Heat loss due to radiation (W m^{-2})
P_{con}	Heat loss due to convection (W m^{-2})
Q	Quality factor

R	Radius of bar (m)
R	Resistance (Ω)
R	Response
R_v	Response factor (velocity)
R_d	Response factor (amplitude)
R_a	Response factor (acceleration)
T	Temperature (K)
T	Time period (s)
T_c	Curie temperature (K)
U_1	Upper critical temperature of steel (°C)
U_2	Upper critical temperature of steel with C > 0.8% (°C)
$U_n(x)$	Eigenvalues
V_{dc}	dc voltage (V)
V_{in}	Bridge volts (V)
V_{out}	Output voltage (V)
V_p	Peak sinusoidal voltage (V)
V_{ref}	Reference voltage (V)
V_{steel}	Velocity of sound in hot steel (cm s^{-1})
α	Coefficient of expansion (°C^{-1})
α	Alpha phase of steel
$\alpha_1, \alpha_2, \alpha_3$	Direction cosines
$\alpha_{x,h}$	Receptance between sections x and h
γ	Density (kg m^{-3})
γ	Gamma phase of steel
δ	Skin depth (m)
$\Delta\theta$	Temperature rise above ambient (K)
$\Delta l / l_f$	Strain due to form effect
ΔT	Magnetocaloric temperature rise (K)
$\Delta\omega$	Frequency increment (Hz)
ε	Emissivity
ε	Strain
θ_s	Surface temperature (K)
θ_c	Centre temperature (K)
θ	Angle between magnetisation vector and field (rads)
θ_a	Absolute temperature of surroundings (K)
θ_m	Mean absolute temperature (K)
λ	Magnetostriction
λ_t	Transverse magnetostriction
λ_{sat}	Saturation magnetostriction

λ_{100}	Saturation magnetostriction in the [100] direction
λ_{111}	Saturation magnetostriction in the [111] direction
λ_p	Saturation magnetostriction of a polycrystal
μ	Permeability (Hm^{-1})
μ_r	Relative permeability
μ_0	Permeability of free space (Hm^{-1})
ν	Poisson's ratio
ξ	Fraction of critical damping
π	Constant (= 3.142)
ρ	Resistivity (Ωm)
$d\rho / dT$	Coefficient of resistance ($\Omega\ ^\circ C^{-1}$)
σ	Stress ($N\ m^{-2}$)
τ	Normalised time
ϕ	Flux (Wb)
ϕ	Angle between magnetic moment and dipole pair (rads)
ω	Angular frequency ($rads\ s^{-1}$)
ω_n	Undamped natural angular frequency ($rads\ s^{-1}$)
ω_v	Volume magnetostriction

CHAPTER ONE

INTRODUCTION

1.1 Introduction

Induction heating is used extensively throughout the metals processing industry for applications such as melting, surface hardening, through heating and welding. It is a well established technique with uses ranging from the preparation of pure silicon wafers for the IC industry to the melting of 25 tonnes of metal for casting purposes.

The basis of this type of heating was discovered in 1831 by Michael Faraday (1832). Electromagnetic induction occurs when a voltage is induced in a secondary circuit as a result of varying a current in a primary circuit. The important factor is the change in flux linkage with the secondary circuit. Lenz (1834) showed that the induced current opposes the inducing flux and varies directly with frequency. The principle of induction is used in motors, generators and transformers where any heating effect is undesirable. This heating can be minimised by laminating the magnetic cores, thus reducing the eddy currents, figure 1.1. Large eddy currents, due to the low resistance of the core, arise from the induced e.m.f. in the magnetic circuit. However, with the laminated circuit, the e.m.f.s induced across the five insulated sheets are one fifth of that generated in a solid core. Also, the cross sectional area is reduced to about a fifth, giving a resistance of five times that of a solid core. The overall effect is an eddy current value about 1/25 of that of a solid core.

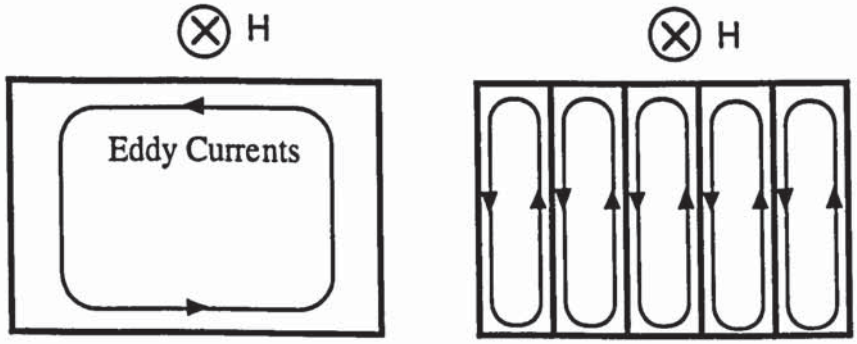

Figure 1.1 Eddy Currents in a Solid and Laminated Core of a Magnetic Circuit

The eddy current effect can be put to good use and is very efficient for heating purposes. Induction heating requires no external heat sources resulting in low heat losses and clean operation. There is no direct contact between the workpiece and the coil and

very high power densities are available, leading to short heating times. These factors combine to produce a method of heating that can be readily used in an automated process.

The induced voltages in an induction heated billet give rise to circulating currents, the magnitude of which decay with depth into the billet. The skin depth, δ is defined as the depth at which the current density has fallen to e^{-1} of its surface value and depends on the material properties and frequency.

Induction heating engineers may be aware of a change in pitch of the noise produced when heating a steel billet as it reaches the magnetic transformation or Curie point. This encouraged an undergraduate student, Dibben (1991), to investigate the source of the sound using a simple microphone attached to the cold end of a mild steel billet and discovered that the bar itself showed a significant increase in extensional vibration when its surface temperature reached the Curie point. Due to the alternating magnetic field, small vibrations (magnetostriction) will occur in ferromagnetic steels when heated by induction, caused by the constant change in magnetisation, although it is generally assumed that magnetostriction is very small at the magnetic transformation point. Magnetostrictive vibrations are most commonly found in transformers. The alternating magnetic field through the laminated steel core produces vibrations at twice the field frequency which can be heard as a distinct hum. To the author's knowledge very little work has been published describing increases in vibration that occur during induction heating. However, much literature on the subject of ultrasonic vibrations generated in steel reveals that an increase in the amplitude of ultrasound increases around the magnetic transformation point, section 2.9.

This research was carried out in collaboration with Midlands Electricity to study the vibrations in steel when heated electromagnetically and to attempt to discover the cause of any increase in vibration amplitude that may occur. Midlands Electricity were also interested in a possible use of the phenomenon. Any increase that occurred near the magnetic phase transformation point was of most interest because of the potential for using the phenomenon in an industrial application.

Induction heaters cover a large range of frequencies depending upon their application, using a number of different supply systems. Low or medium frequency systems (50 Hz to 10 kHz) are used where relatively long heating times are necessary such as through heating and annealing. High frequencies (up to 10 MHz) are used for surface heating such as hardening, welding and crystal growing.

Mains frequency systems require no frequency conversion and use only transformers and associated switchgear. These produce current depths from 10 to 100 millimetres and power levels can be as high as several hundred megawatts.

With the advance of electronics, solid state inverters are available to supply frequencies between 500 Hz and 250 kHz. Power ratings can be as high as two megawatts using thyristors to switch the current. These systems are also capable of varying the frequency over a heating cycle to ensure the changing impedance is matched for maximum power input.

Radio frequency systems supply frequencies from 50 kHz to 10 MHz and produce very small current depths, leading to localised heating at fast rates. The power levels attainable are about one megawatt and are used mainly for high speed tube welding.

There are a number of advantages of using induction heating as opposed to fossil fuelled furnace heating. The induction method of electrically heating is clean and requires no extraction of combustion products. This also lowers the risk of injury to the workforce through explosion or fumes. The process produces far less scaling of material because no combustion takes place and very little decarburization occurs. The power densities available for heating are large which means short heating times, ideal for use in a production line. The heater has a rapid starting time allowing energy to be saved when the equipment is switched off for breaks and hold ups, whereas a conventional furnace takes hours to reach operating temperature and cannot be turned on and off during short breaks. Induction heating installations are normally small compared to furnaces leading to saving in floor space. Finally, the process is highly controllable.

1.2 Types of Heater

The type of heating arrangement will depend upon the nature of the process. For example, some through heating applications use a continuous tunnel heater. Billets are loaded into a magazine that uses a ram to push the billets along the tunnel. At the end of the tunnel will be the heating coil before the billets are discharged ready for processing. Figure 1.2 shows a typical industrial tunnel heater.

Other applications include bar end heating prior to forging. The coil or coils are arranged as a pigeon hole heater. Only one end of the bar is heated before being removed and processed.

For uses such as hardening, the heating arrangement must be customised to the part to be hardened. For example, the teeth of a gear wheel can be induction hardened using a single turn coil surrounding the gear. Figure 1.3 shows gear hardening in 25 seconds using a 100 kHz, 50 kW generator.

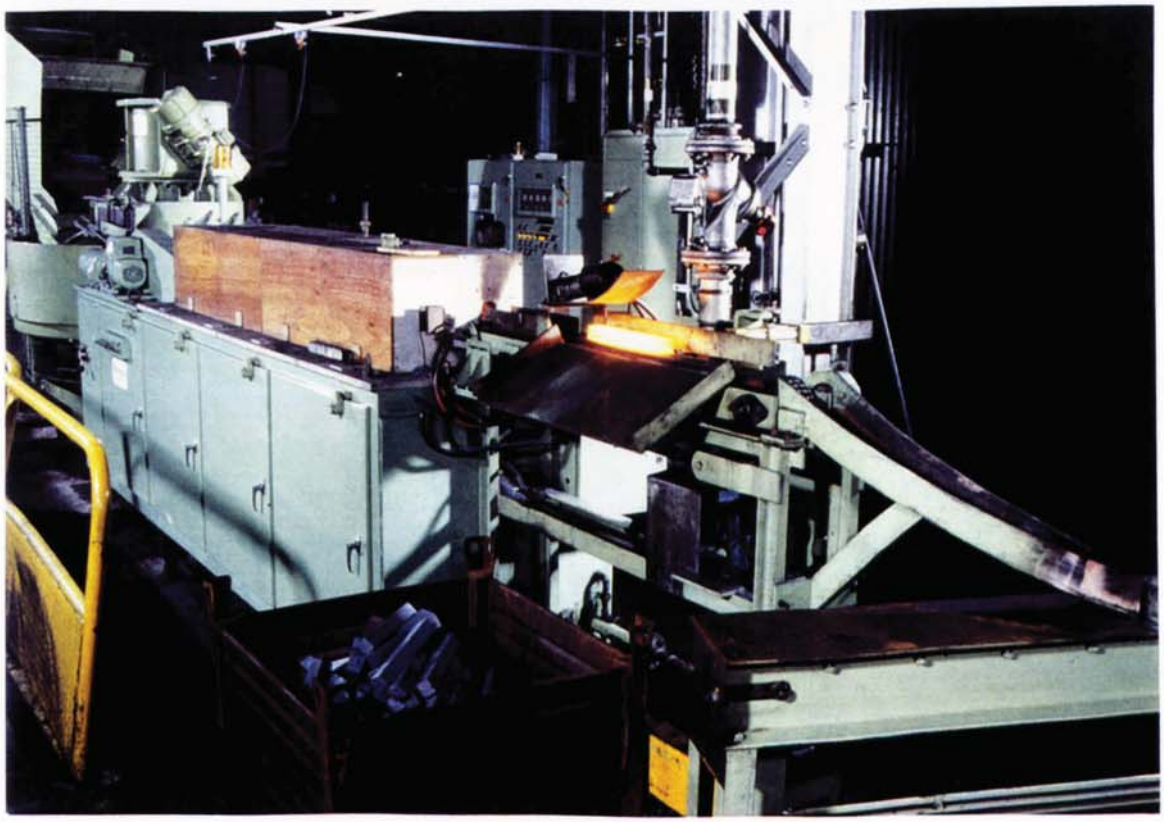

Figure 1.2 An Industrial Induction Tunnel Heater

Figure 1.3 Induction Hardening of Gear Wheel Teeth

Induction heating is also used for melting. Figure 1.4 shows an example of a coreless furnace. The power supply and control panel can be seen to the right of the figure.

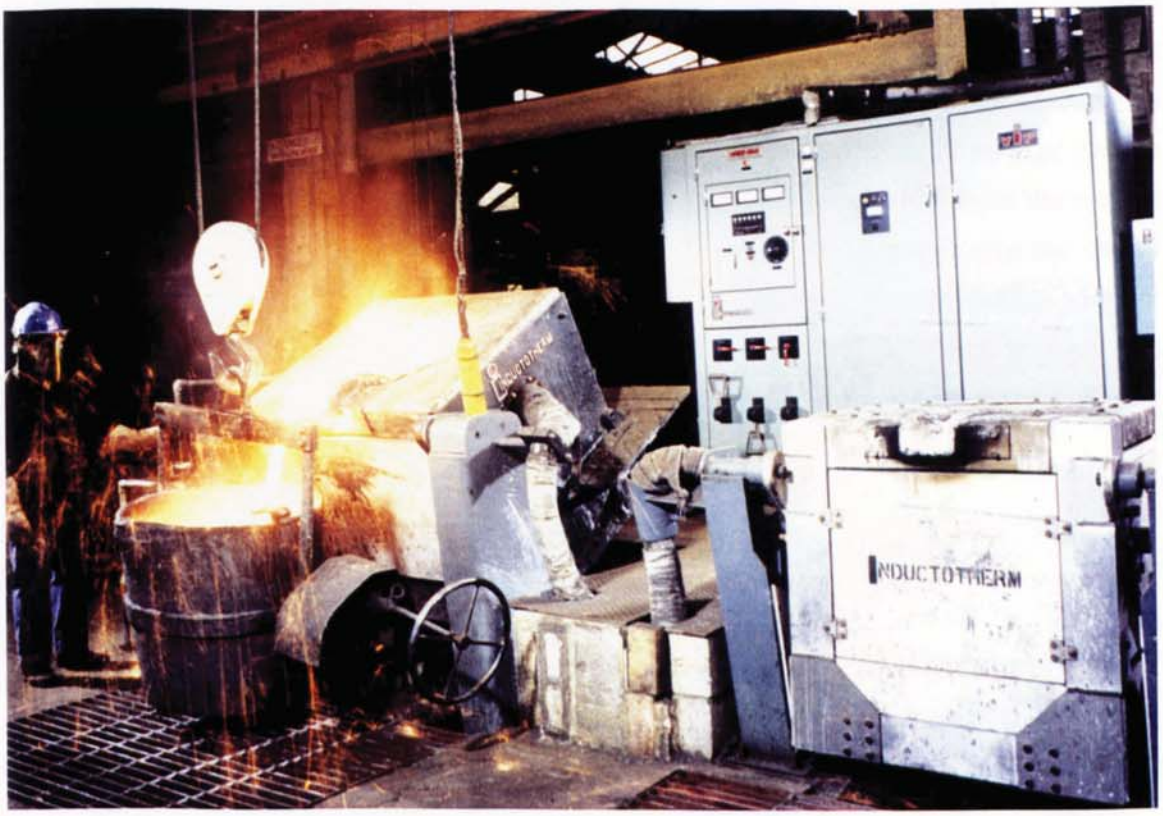

Figure 1.4 Induction Melting Furnace

There is little restriction to coil size and shape. For this reason induction heating can be adapted to a wide range of processes.

The heater used in this research was a 60 kW, 3.2 kHz Crossley machine. It was supplied by Crossley Electronics Ltd, Birmingham, together with a coil designed to allow easy access to bars during heating for instrumentation purposes. The specification for the induction heater can be found in Appendix A.1.1.

1.3 Inverter Operation

The Crossley parallel circuit inverter uses solid state electronics to change the three phase input at 50 Hz to a single phase 3.2 kHz output. Figure 1.5 shows a simplified diagram of the main components in the inverter circuit.

The three phase mains input is converted to DC by a three phase bridge arrangement of thyristors. It is therefore a fully controllable rectifier in which the firing angle of the thyristors is varied to give voltage control. These run at mains frequency with a diode to allow the DC current to circulate freely. The DC output is smoothed using

a large inductor which then provides the inverter circuit with a constant current source. The capacitor also isolates the MF (medium frequency) supply from the mains supply. The inverter is a single phase bridge arrangement consisting of eight thyristors which are fired in alternate double pairs so that the constant DC current is switched in alternate directions with the load circuit. The method used for switching the thyristors off makes use of the alternating voltage which is generated across the load resonant circuit. By firing the alternate thyristors at an appropriate point in advance of each voltage zero, a reverse voltage is created across the devices which are conducting, and forces the current to zero. Since this reverse voltage must be maintained for a period not less than the device turn off time, it follows that the current waveform will lead the sinusoidal voltage waveform by a given period known as the extinction time. For this particular inverter it is 25 μs at 3 kHz and corresponds to a phase angle of 10°. The inverter cannot then operate at a power factor better than 0.92 leading.

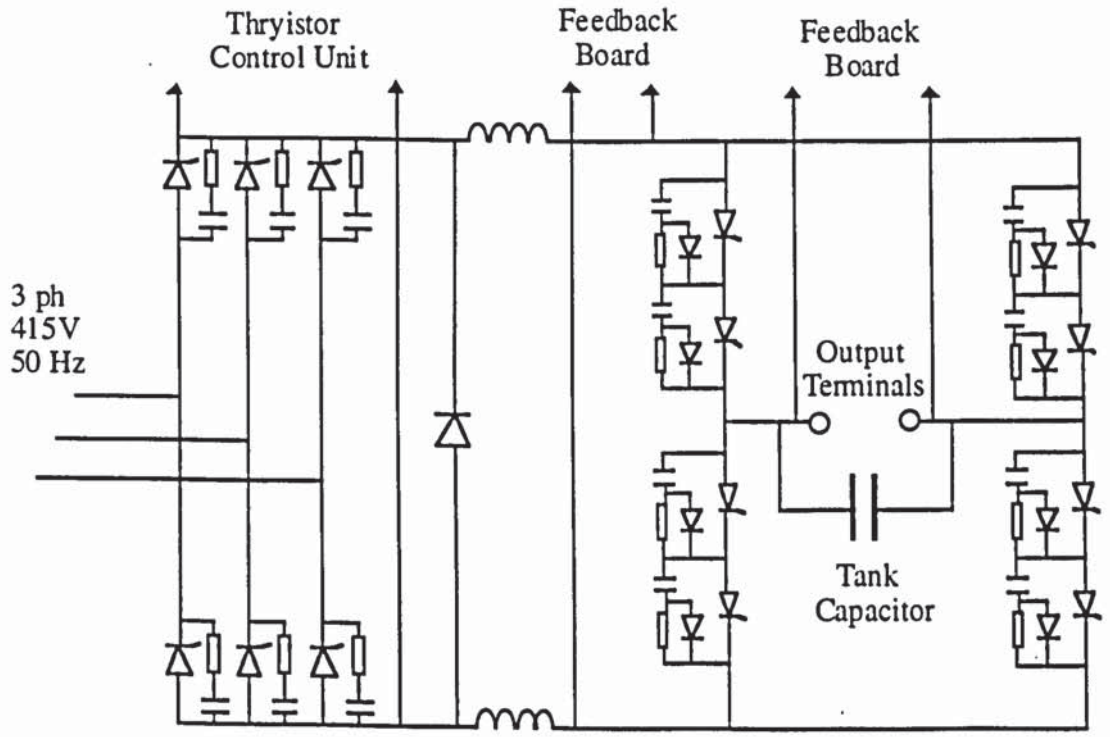

Figure 1.5 Circuit Diagram of the Crossley 60kW Inverter

The inverter circuit operating frequency is determined solely by the load circuit characteristics and should the load resonant frequency change, the operating frequency will shift automatically. Power control is obtained by varying the output voltage of the controlled rectifier, by altering the firing angle.

The parallel circuit type inverter is not self starting because the control circuit providing the correctly timed firing signals cannot do so until the first tank circuit oscillation has been detected. The backward voltage swing, necessary to turn the thyristors off, needs time to build up across the load circuit. An auxiliary starting circuit

is therefore necessary to kick the inverter into operation. It only functions for the first few cycles of MF power (a few milliseconds).

Another feature of the inverter circuit is that since thyristor turn off is achieved by using the oscillation of the load circuit, the thyristors and associated components are able to operate over a fairly broad frequency range (2.5 kHz to 11 kHz). However, the tank capacitor is more critically rated regarding frequency (2.5 kHz to 3.5 kHz).

1.4 Load Resonant System

The Crossley 60kW medium frequency parallel circuit inverter has many advantages over the other basic inverter circuit, the series type. It is more efficient in terms of losses, especially under reduced load conditions and provides a greater range of power control, independent of load. Figure 1.6 illustrates the method of power control. Note the small decrease in operating frequency as the power is reduced.

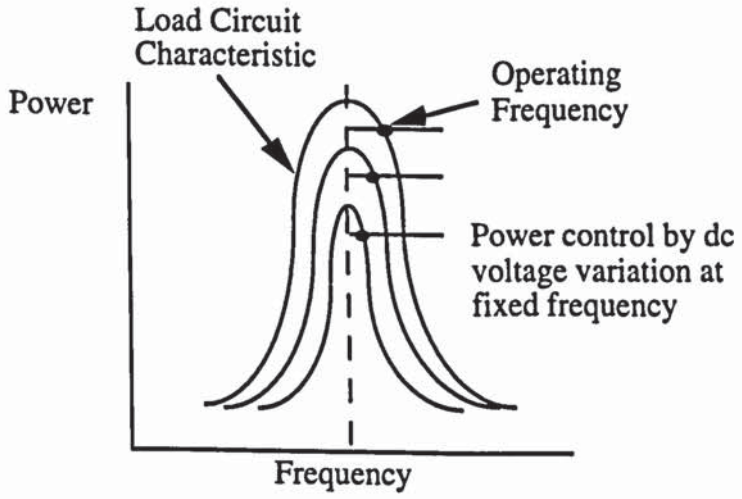

Figure 1.6 Load Resonant Generator Characteristics

This system operates by tapping the output to the load and feeding it back as a commutation circuit, which is used to fire and turn off the thyristors. The difference between the natural load frequency and the inverter frequency is controlled.

1.5 Aims of the Investigation

The main aims of this work at the outset were to:

• Describe and quantify the vibrations that occur near the magnetic transformation point in electromagnetically heated steel and elucidate their causes.

• Seek an industrial application of the phenomenon.

The aims changed as the project progressed and work included the study of magnetostriction in a mild steel as a function of temperature. Little published data exists on this subject, especially with reference to the magnetic transformation point.

The research was not only limited to the magnetic transformation point and covers the vibration in steel at temperatures ranging from -100°C to 1000°C.

Initial objectives of the work included studying non-ferromagnetic materials such as copper, titanium and stainless steel. The influence of bar diameter on the amplitude of longitudinal vibrations, along with different power settings and initial temperatures of the bars were studied.

As the research progressed, the factors affecting the increase in vibration were described in detail and the most likely cause was investigated in depth. The results from this investigation did not reveal the precise mechanism for the increase in vibration near the Curie point and as a result it was difficult to assess whether the phenomenon could be utilised for an industrial application. However, two areas were considered; the control of the heating process and the inspection of hot steel.

1.6 Simulation of an Induction Heater

Before any experimental work was started, simple simulations were carried out using an electromagnetic software package developed by GEC called SLIM (Stafford Laboratory Integrated Modelling). This used finite element analysis to solve magnetic problems and it was envisaged that it could be used to simulate induction heating. Although the package was able to simulate flux density and eddy currents, it was unable to simulate the whole induction heating process. This was due to two reasons; it could not calculate heat flow and did not allow for changes in material property, such as conductivity. The simulation of a simple heater consisting of a steel bar inside a four turn inductor was carried out. The magnetic potential and flux density are shown in figure 1.7 and the eddy current density in the bar is shown in figure 1.8. The frequency was 50 Hz and the current through the coil was 100 Amperes. A thin slice of the upper half of the bar and non-helical coil is shown in the figures. The lower half is not shown because it is symmetric. The potential is shown in red and the flux density shown in green. The high flux density at the corners of the bar gives rise to high eddy currents.

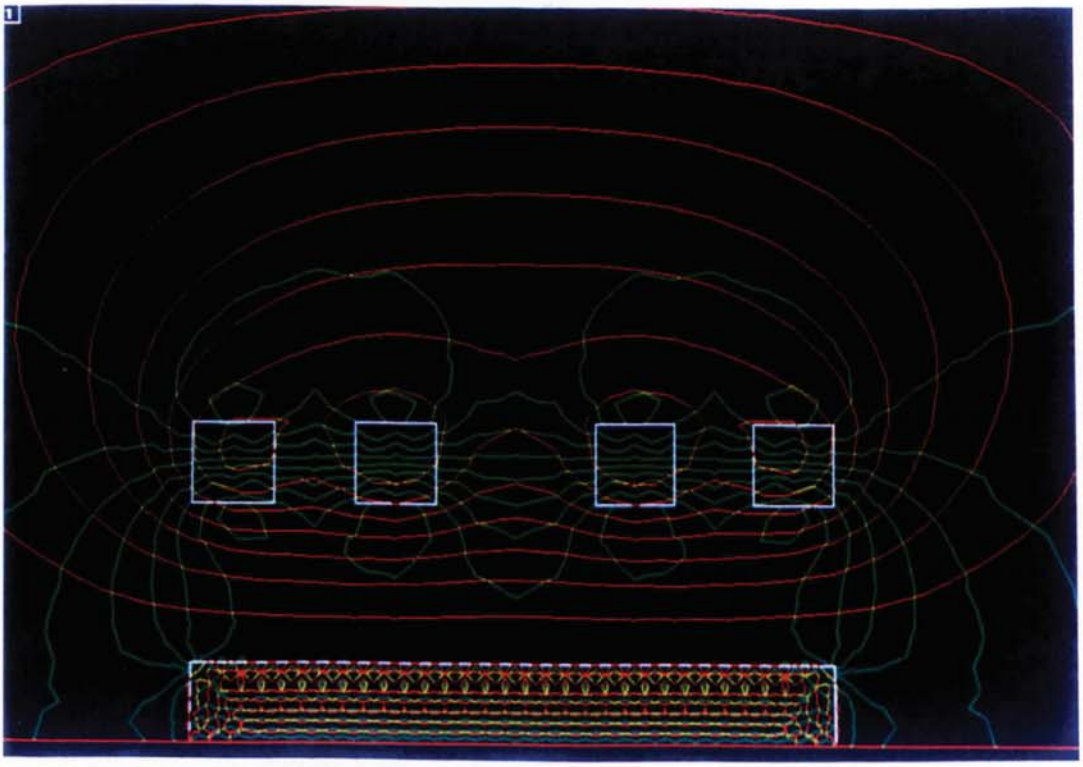

Figure 1.7 Simulated Potential and Flux Density in an Induction Heated Steel Bar

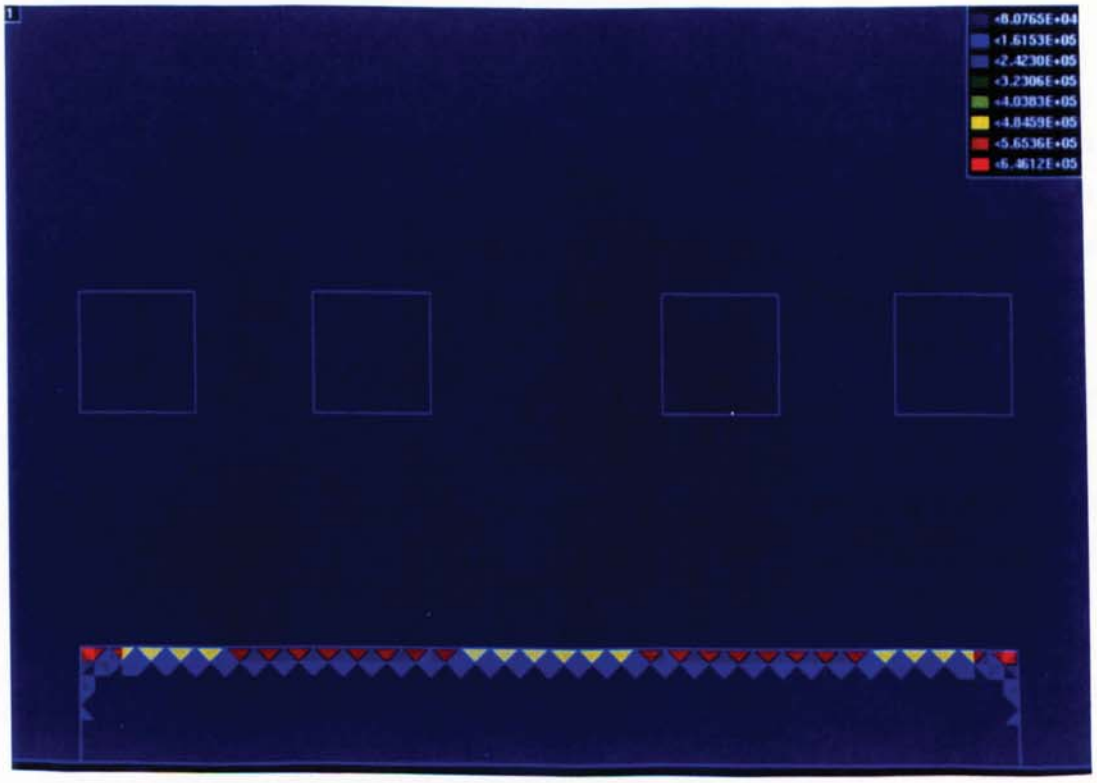

Figure 1.8 Simulated Eddy Current Density in an Induction Heated Steel Bar

Notice how the regions of highest eddy current density are opposite the coils and at the ends of the bar. In reality, the turns of a multi turn coil are equally spaced in order to produce uniform heating. However, for a single turn coil, the eddy current density is greatest opposite the coil. Apart from this simple simulation no further work was carried out using SLIM.

1.7 IHD (Interdisciplinary Higher Degree) Scheme

This research was undertaken as part of the IHD, Total Technology Scheme. It was closely linked with industry, Midlands Electricity in this case, and the coursework was part of a standard MBA course. Four management modules, each consisting of 30 hours of teaching together with tutorials and a form of assessment, were completed. A pass at Masters level was attained in each case. A copy of the Total Technology certificate can be located in Appendix A.4. The four modules studied were:

Management of Innovation
Operations Management
Marketing Management
Financial Accounting and Finance.

1.8 Thesis Outline

Chapter two consists of a detailed literature review containing both background information to this work together with existing published data on subjects such as magnetostriction and the electromagnetic generation of acoustic waves. No discussion is presented in this chapter regarding other authors' findings as comparisons are made in the more appropriate subsequent chapters.

Experimental work on the subject of longitudinal vibration in steel bars during induction heating can be found in chapter three. The apparatus used is discussed and the method of testing explained. Other materials such as stainless steel, copper and titanium are also investigated. The metallurgical structures of a sample of heated and unheated mild steel are shown. Tests carried out on specimens of 0.4% carbon steel to establish whether there was a relationship between resonance and the alpha to gamma phase transformation is covered.

Results obtained in chapter three suggested that a possible cause of resonance was magnetostriction. Since published data on magnetostriction in mild steels as a function of temperature was rare, it was decided to measure magnetostriction in the laboratory. Two sets of apparatus were constructed; the first using displacement transducers and the

second using a high temperature strain gauge. Data is presented for linear magnetostriction as a function of temperature up to 800°C.

Other possible causes of resonance are investigated in chapter five along with discussion of results from this research with reference to existing work. In particular attention is drawn to the similarities between the resonance in steel billets heated by induction and the generation of ultrasound using electromagnetic acoustic transducers (EMATs). Industrial applications using this resonance phenomenon are briefly mentioned.

Chapter six lists the conclusions arising from this research followed in chapter seven by proposals for further work. Suggestions are made requiring further experimental work to pinpoint the exact cause of resonance. The most important being the measurement of magnetostriction in mild steel in high alternating magnetic fields (50 - 100 kAm^{-1}).

The remainder of this thesis consists of references and appendices. The appendices contain specifications of the equipment used and calculations used in determining the forces produced by the interaction between the eddy currents and magnetic field.

Finally, three published papers are added relating to the conferences attended.

1.9 Conclusions

An introduction to induction heating has been given. Types of heater have been discussed and a description of the operation of a load resonant inverter outlined. Simulations have shown how the eddy current and flux densities vary in a bar when placed in an electromagnetic field. Published work on the subject of vibration in steel heated by induction was found to be limited, although work by Dibben (1991) has shown that an increase in longitudinal vibration occurred as the surface temperature of a bar of mild steel reached the Curie point when heated by induction. A summary of the coursework undertaken as part of the IHD Scheme is listed.

CHAPTER TWO

BACKGROUND

2.1 Introduction

Before detailed investigation is carried out into the vibration of steel when heated by electromagnetic induction, it is necessary to familiarise oneself with all the different subjects concerning this work. Both well established theory and modern ideas are covered in this chapter. The wide range of literature discussed includes basic induction heating principles, the metallurgy of steels, vibration theory, magnetic properties of steels (especially magnetostrictive) and electromagnetic acoustic transducers (EMATs).

2.2 Induction Heating

Eddy currents, the basis of induction heating, were initially studied by engineers so that unwanted heating effects could be eliminated from transformers, motors and generators. Induction heating theory is in practice almost identical to transformer theory. Many texts describe the principles of induction heating such as Davies and Simpson (1979). The coil acts as a primary winding coupled to a metallic billet which acts as the secondary. The primary is normally many turns but can be a single turn depending upon the application. The secondary is considered to be a single short circuited turn. The current flowing in the secondary will therefore be high and the heating losses associated with it will vary as the square of this induced current. The eddy currents within a billet will be distributed according to the skin depth, δ, figure 2.1.

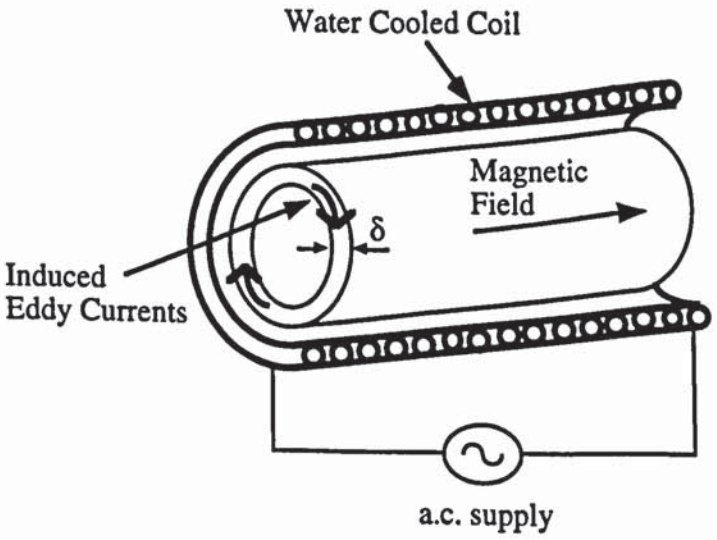

Figure 2.1 Typical Induction Heating Arrangement

The skin depth is approximately the depth at which the current density has fallen to one third of the surface value and is given by:

$$\delta = \sqrt{\frac{\rho}{\mu f \pi}} \qquad (2.1)$$

where δ is the skin depth (m)
ρ is the resistivity of the material (Ωm)
μ is the permeability (Hm^{-1})
f is the frequency (Hz)

The skin depth is usually very small in comparison to the size of the billet or workpiece being heated and conduction is the method of heat transfer from the surface to the inner regions. Large temperature differentials, producing time constants, may arise with induction heating which may be advantageous depending on the application. For example, through heating of a large billet will need to soak prior to forging to allow heat generated in the skin to conduct to the centre of the billet. On the other hand if surface hardening is required, then it is possible to rapidly heat the surface to the required temperature, followed by immediate quenching, thereby limiting heat transfer to the remainder of the material.

Much work concerning eddy current loss in plates, rods and conductors has been undertaken. Gillott and Calvert (1965) solve the eddy current loss problem when the magnetisation process extends into the non-linear region of the magnetisation curve. The calculations are solved by numerical methods which require a computer. Unfortunately, work involving the heat transfer calculations, especially with induction heating, is sparse because of the difficulty of modelling changes in parameters such as conductivity and permeability.

One of the main problems associated with induction heating is the difficulty in directly measuring temperature and power input to a billet. However, it is possible to calculate these values approximately, as shown by Horoszko (1985). Both longitudinal and transverse magnetic flux heating is studied and equations given for calculating the heating power.

2.2.1 Skin Depth

As the temperature of a billet increases other parameters such as resistivity, specific heat and conductivity change. Appendix A.1.2 shows a table of these as a function of temperature for a 0.23% carbon steel. For mild steel the resistivity increases approximately six times between ambient temperature and the Curie point (760°C), at

which the relative permeability falls to unity. These changes are gradual and produce a continuously increasing skin depth with temperature. A billet being heated rapidly by induction can be thought of as being made up of many thin cylinders all tightly inside one another. Each of these in turn will reach the Curie point during the heating process, which itself can be imagined to consist of an electromagnetic wave steadily moving from the surface of the billet towards the centre.

Induction heating creates very complicated temperature profiles across a billet which can only be modelled accurately using a computer. A good example of this type of work is shown by Dibben (1991) in which a computer program was written to predict the temperature rise in an induction heated cylinder.

2.2.2 Heat Transfer and Temperature Distribution In A Cylinder

The reason why induction heating is so rapid and efficient, is that the heat is generated directly in the workpiece and does not rely totally on convection and conduction to heat the material, as with conventional methods. Eddy currents in a depth equivalent to two skin depths create 98% of the heat. The power densities can be enormous leading to a rapid response ideal for surface heating applications where the power density can be as high as 50 MWm^{-2}. A typical temperature profile through an induction heated steel billet is shown in figure 2.2, from Davies and Simpson (1979).

Aston University

Illustration removed for copyright restrictions

Figure 2.2 Temperature Distribution in a Billet (From Davies and Simpson (1979))

The problem of temperature distribution in a cylinder, heated at constant power has been solved by Carslaw and Jaeger (1959) and by Baker (1958). They show that after a transient temperature rise, the temperature distribution becomes parabolic and thereafter the temperature profile remains the same, with all parts rising at the same rate. This is very important in the understanding of induction heating and it can be shown that the temperature difference between the surface and centre of a bar is fixed and is given by:

$$(\theta_s - \theta_c) = \frac{P_0 R}{2k} \qquad \text{valid for } \tau \geq 0.25 \qquad (2.2)$$

where θ_s and θ_c are the surface and centre temperatures respectively (K)
P_0 is the power density at the surface (W m^{-2})
R is the radius of the bar (m)
k is the thermal conductivity (W m^{-1} K^{-1})

and τ is the normalised time given by $[kt / \gamma c R^2]$

where t is the time (s)
γ is the density (kg m^{-3})
c is the specific heat (J kg^{-1} K^{-1})

The power input to a bar heated by induction is very difficult to calculate. Davies and Simpson (1979) give an approximate value as:

$$P_{in} = 2 \mu f \pi H^2 (l A) p \quad Wm^{-2} \qquad (2.3)$$

where μ is the permeability (Hm^{-1})
f is the frequency (Hz)
H is the field strength (Am^{-1})
l is the length (m)
A is the cross sectional area (m^2)

and $$p = \frac{2}{1.23 + d/\delta} \qquad \text{when } d/\delta > 8 \qquad (2.4)$$

where p is a function of flux distribution within the cylinder
d is the diameter (m)
δ is the skin depth (m)

2.2.3 Convection and Radiation

Heat will be lost from the surface of an induction heated cylinder by radiation, P_R according to the Stefan-Boltzmann relationship:

$$P_R = 5.67 \times 10^{-8} \varepsilon (\theta_s^4 - \theta_a^4) \quad Wm^{-2} \tag{2.5}$$

where ε is the emissivity of the surface

θ_s is the absolute temperature of the surface of the cylinder (K)

θ_a is the absolute temperature of the surroundings (K)

5.67×10^{-8} is the Stefan-Boltzmann constant ($W\ m^{-2}\ K^4$)

Radiation losses become significant when the temperature of the surface of the bar reaches 800°C.

An approximation of the rate of heat loss by convection, P_{con} is given by Davies and Simpson (1979) for a billet in the open air:

$$P_{con} = 1.54 (\Delta\theta)^{4/3} \quad Wm^{-2} \tag{2.6}$$

where $\Delta\theta$ is the temperature rise above ambient (K)

For through heating convection losses are small compared with the losses due to radiation, and for most purposes may be neglected. The rate of heat loss from the surface during induction heating is normally lower than the power input to the bar. The overall effect can be taken to be a reduction in the power input to the bar as radiation increases.

2.2.4 Striated Heating

Induction heating was studied in great detail by Babat and Lozinskii (1940) using high frequency fields. They noted that the power input to a bar changed during the heating cycle, increasing at the start of heating and falling to a lower value as the steel reached the Curie point.

Babat (1944) and Lozinskii (1969) also describe a phenomenon known as striated heating. When heating steel at high frequency (242 kHz - 477 kHz) bright and dull bands form on the surface of the steel at regular intervals. This interval depends on the frequency used. The bands move apart as heating continues until the whole surface reaches 900°C when they disappear. This phenomenon is thought to be produced as a result of the interaction of standing waves and magnetostrictive vibrations in the surface of the steel, resulting in spontaneous changes in length between vibration nodes. The properties of the steel at the nodes become different to that of the intermediate zones

during heating. Under the action of magnetostriction the intermediate zones are elastically deformed and therefore possess a higher resistance than the steel at the vibration nodes. Hence, more intense heating takes place at the vibration nodes, leading to striations. Simple relationships of the distance between striations are given.

$$\text{Babat:} \qquad d = 2000 / \sqrt{f} \tag{2.7}$$

$$\text{Lozinskii:} \qquad D = V_{steel} / f \tag{2.8}$$

where V_{steel} is the acoustic velocity in steel (cm s^{-1})
f is the frequency (Hz)
D/2 is the distance between nodes (cm)

For a frequency of 3.2 kHz the values are d = 35 cm and D/2 = 78 cm. No striated heating occurred when heating 600 mm mild steel bars at 3.2 kHz.

2.3 The Metallurgy of Plain Carbon Steels

During the induction heating of steel phase changes occur when its temperature is increased. A brief summary follows describing the types of transformation involved for plain carbon steels of varying carbon content. The iron carbon thermal equilibrium diagram can be found in most good metallurgy texts such as Higgins (1983).

The iron carbon diagram is of the type where two substances are completely soluble in each other in the liquid state but only partially soluble in the solid state. The main phases to consider are:

i) austenite (γ), the solid solution formed when carbon dissolves in face centred cubic iron in amounts up to 2.0%.

ii) ferrite (α), a very dilute solid solution of carbon in body centred cubic iron containing at the most only 0.02% carbon. For most purposes this can be regarded as pure iron.

iii) cementite, or iron carbide, Fe_3C, an interstitial compound of iron and carbon containing 6.69% carbon.

Plain carbon steels are generally defined as being those alloys of iron and carbon that contain up to 2.0% carbon. In practice most ordinary steels contain small amounts of manganese from the casting process. This will be ignored and steels will be regarded as being simple iron-carbon alloys.

The pure metal iron has a body centred cubic structure below 910°C and will change to a face centred structure if heated above this temperature. This phase change is reversible on cooling. The importance of this reversible transformation is that up to 2.0% carbon can dissolve in the f.c.c. iron, whilst in b.c.c. iron no more than 0.02% carbon can dissolve. A steel in its f.c.c. form cooling slowly will change to its b.c.c. form and any carbon in excess of 0.02% will be precipitated out unless the steel is quickly quenched to prevent this. When carbon is precipitated from austenite it is not in the form of graphite but as the compound cementite. This substance is very hard and the greater the proportion of carbon, and hence cementite, the harder the slowly cooled steel.

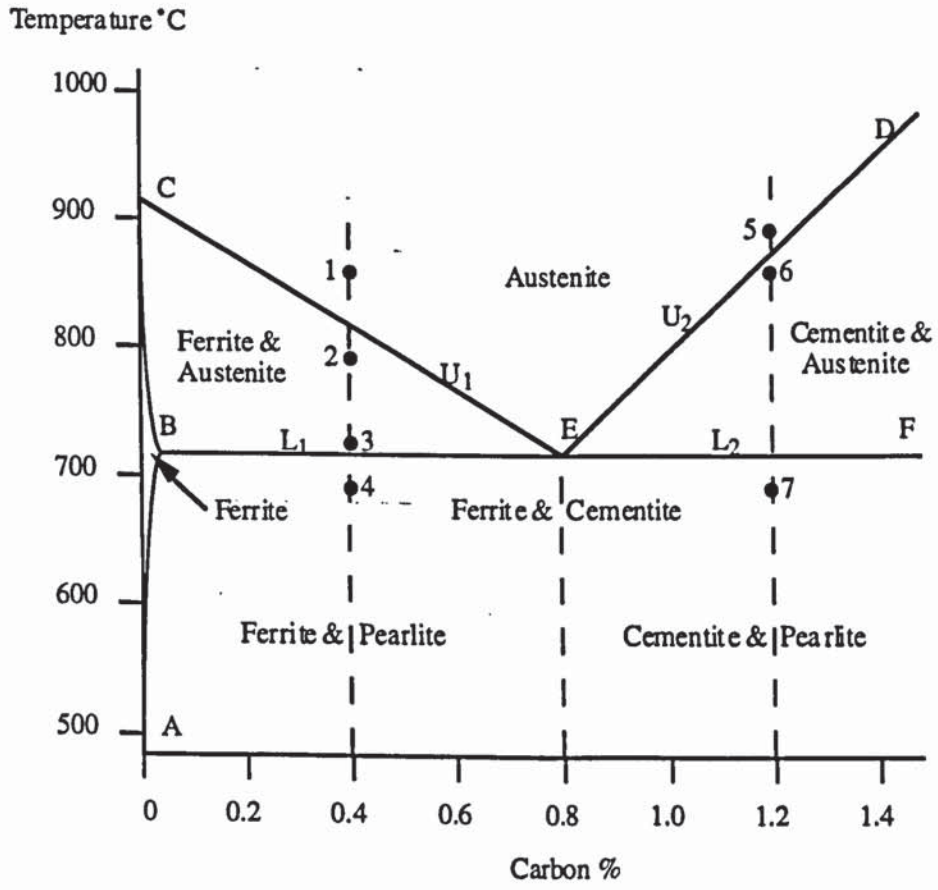

Figure 2.3 Part of the Iron Carbon Equilibrium Diagram

The diagram in figure 2.3 taken from Higgins (1983) shows the temperatures at which transformation begins and ends for any solid (austenite) solution of carbon and f.c.c. iron. The temperature is lowered by adding carbon. This is the line CE.

On the left of the diagram is the line AB. To the left of this line all carbon present is dissolved in b.c.c. iron, forming the solid solution ferrite, whilst any point on the right indicates that the solid solution is saturated, so that some of the carbon contained in the steel will be present as cementite. The line AB indicates that the solubility of carbon in b.c.c. iron increases from 0.006% at room temperature to 0.02% at 723°C.

If three different carbon steels are heated so that they become austenitic they will undergo certain transformations as they cool. If a 0.4% carbon steel is heated above its U_1 temperature (the upper critical temperature) it will become completely austenitic (point 1). On cooling just below U_1 (point 2) the structure changes from face centred cubic to body centred cubic. As a result small crystals of body centred cubic iron begin to separate out from the austenite. These crystals retain a small amount of carbon (less than 0.02%) and can be referred to as ferrite. As the temperature falls further (point 3) the crystals of ferrite grow in size at the expense of the austenite, and because ferrite is almost pure iron the carbon must accumulate in the shrinking austenite crystals. By the time the steel has reached a temperature L_1 (the lower critical temperature) it is composed of half ferrite (containing 0.02% carbon) and half austenite (containing 0.8% carbon). The composition is now represented by point E on the diagram. Austenite can hold no more than 0.8% carbon in solid solution at this temperature of 723°C, and as the temperature falls further, carbon begins to precipitate as cementite. At the same time ferrite is still separating out and the two substances, ferrite and cementite form as alternate layers until all the austenite is used up (point 4). This laminated structure of ferrite and cementite will then contain exactly 0.8% carbon and will account for half the volume of the 0.4% carbon steel. This is an example of a eutectoid and this particular one is known as pearlite.

Any steel containing less than 0.8% carbon will transform from austenite to a mixture of ferrite and pearlite in a similar way when cooled from its austenitic temperature. Transformation will begin at the appropriate upper critical temperature (given by a point on CE which corresponds to the composition of the steel) and end at the lower critical temperature of 723°C. The relative amounts of ferrite and pearlite will depend upon the carbon content of the steel, but the ferrite will be almost pure iron and the pearlite will contain 0.8% carbon exactly.

A steel containing 0.8% carbon will not begin to transform from austenite until the point E has been reached. Transformation will begin and end at this temperature of 723°C. Since the steel contained 0.8% carbon, the final structure will be entirely pearlite.

A steel containing more than 0.8% carbon, for example 1.2%, will begin to transform from austenite (point 5) when the temperature falls to its upper critical at U_2. Since the carbon is in excess of the eutectoid composition, it will first begin to precipitate; not as pure carbon but as needle shaped crystals of cementite round the austenite grain boundaries (point 6). This causes the austenite to become less rich in carbon and by the time it reaches 723°C the remaining austenite will contain 0.8% carbon. This remaining austenite will transform to pearlite (point 7).

Any steel containing more than 0.8% carbon will have a structure of cementite and pearlite if allowed to cool slowly from its austenitic state. Since pearlite always contains 0.8% carbon overall in the form of alternate layers of ferrite and cementite, it follows that any variation in the total carbon content above 0.8% will cause a corresponding variation in the amount of primary cementite present. (Primary simply refers to the first formation before any residual transformation occurs).

2.4 Properties of Iron and Steel With Temperature

Some important properties of iron and steel in the region of the Curie point are outlined in this section. Where data could not be found for steel, data for iron is quoted.

2.4.1 Thermal Expansion

Figure 2.4 from Bozorth (1951) shows the linear expansion of iron against temperature. Mild steel will behave in a similar manner except for its transformation temperature. Density is shown on the right hand scale. The earlier data was obtained by Schmidt (1933) and derived from X-ray data and later by Esser and Eusterbrock (1941). Notice how there is a large change in thermal expansion when the structure changes from body centred cubic to face centred cubic during its α to γ phase transformation.

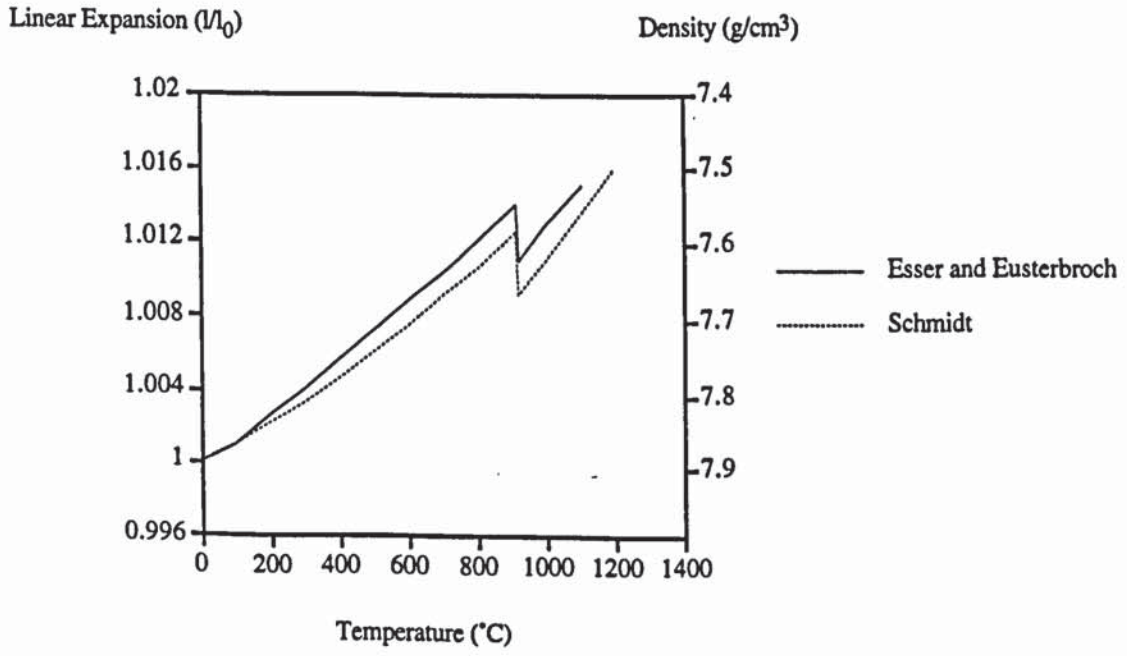

Figure 2.4 Thermal Expansion Data for Iron

2.4.2 The Curie Point and Permeability

The magnetic transformation point or Curie point is the temperature at which the permeability drops to unity. Lozinskii (1969) states that the Curie point of pure iron is 768°C whilst 0.83% carbon steel has a lower Curie point at 721°C. Figure 2.5 shows a diagram of the permeability of both these metals against temperature. Cementite (Fe_3C) losses its magnetic properties at 256°C. The Curie point of a 0.15% carbon mild steel is approximately 760°C.

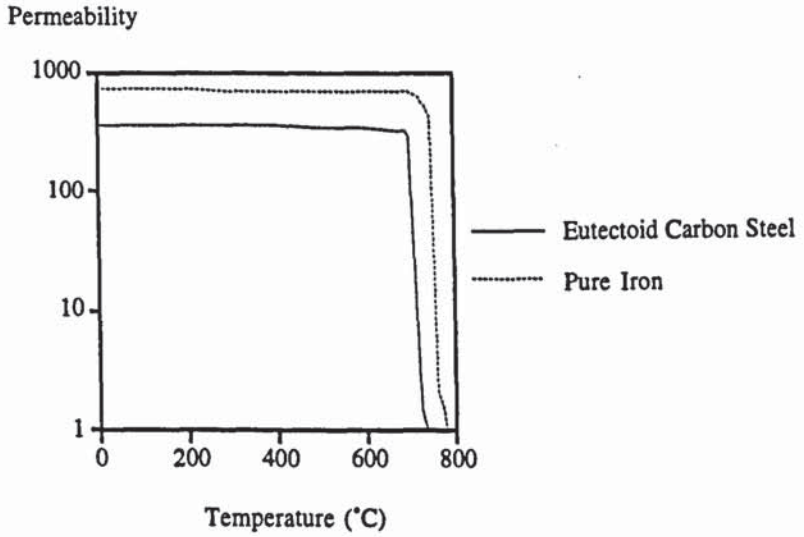

Figure 2.5 Permeability of Iron and Eutectoid Steel with Temperature

Babat (1944) reported that permeability depends widely upon the magnetic field strength. In fields of medium strength the relative permeability of low carbon steels ranged from 100 to 10 000. In high carbon steels the permeability depended largely upon the thermal treatment. The permeability of cementite is considerably less than that of ferrite, therefore the permeability will have different values depending upon the percentage of carbides and residual austenite. Permeability is also reported to vary very little with frequency up to 10 MHz.

The permeability of a vacuum is given by μ_0. Air is assumed to have the same value. The permeability, μ of a material is the product of relative permeability, μ_r and the permeability of a vacuum μ_0:

$$\mu = \mu_r \mu_0 \tag{2.9}$$

For paramagnetic materials and ferromagnetic materials above the Curie point, the value of μ_r is usually between 1.000 and 1.001. For diamagnetic substances, the magnetisation is directed opposite to the field and have permeabilities less than unity.

2.4.3 Young's Modulus, E

The effect of temperature on E is shown in figure 2.6 for iron, from Bozorth (1951). The diagram also shows the Young's Modulus for magnetised iron. There is a significant reduction in E with temperature increase. Plain carbon steels are assumed to show a similar decrease, although the actual values of E may be different.

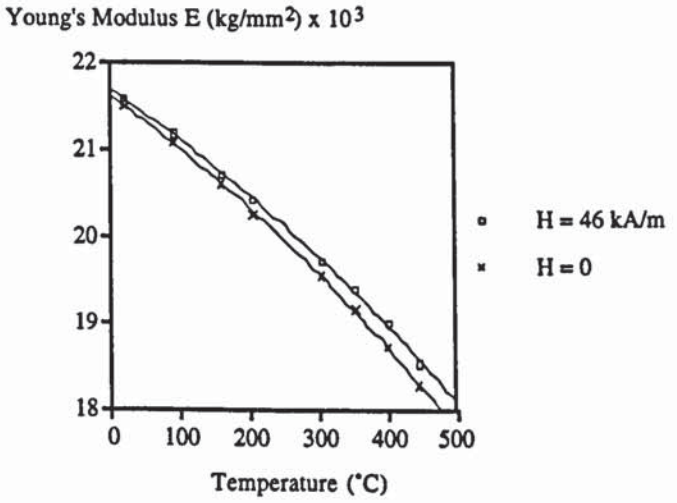

Figure 2.6 Young's Modulus for Magnetised and Unmagnetised Iron at Various Temperatures.

2.4.4 Magnetisation Curves

Together with magnetic field and stress, temperature is one of the important factors in causing change in magnetisation. The greatest influence is just below the Curie point or phase transformation point. The way in which temperature affects the magnetisation curves is shown in figure 2.7, taken from Bozorth (1951), for iron which had been annealed at 800°C.

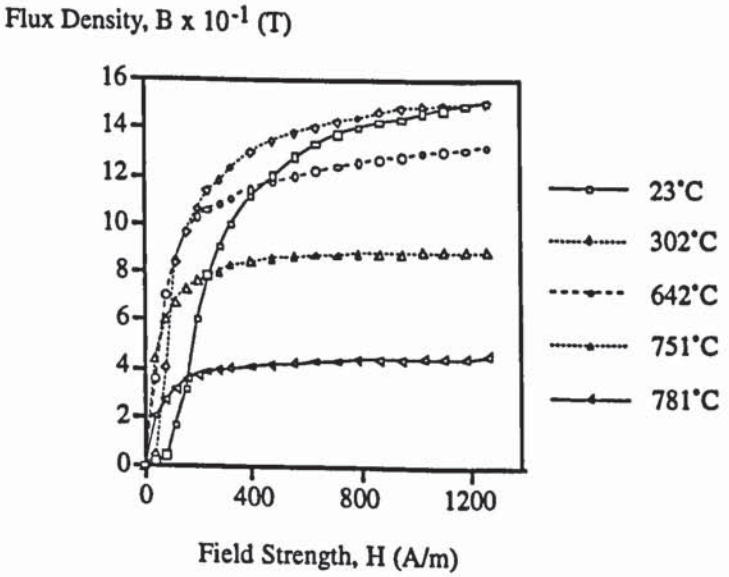

Figure 2.7 Magnetisation Curves of Iron at Different Temperatures.

At high temperatures the curves rise quickly, at lower values of H, and then level out and finally saturate at lower flux densities. The saturation continues to decrease and approaches zero at the Curie point. When a magnetic material is subjected to a high constant field, an increase in temperature usually brings about a continuously accelerating decrease in flux density, reducing almost to zero at the Curie point.

2.4.5 Hysteresis

The way in which the size and shape of the hysteresis loop changes in iron with increase in temperature near the Curie point is indicated by Bozorth (1951) in figure 2.8. The size decreases considerably at the Curie magnetic transformation point.

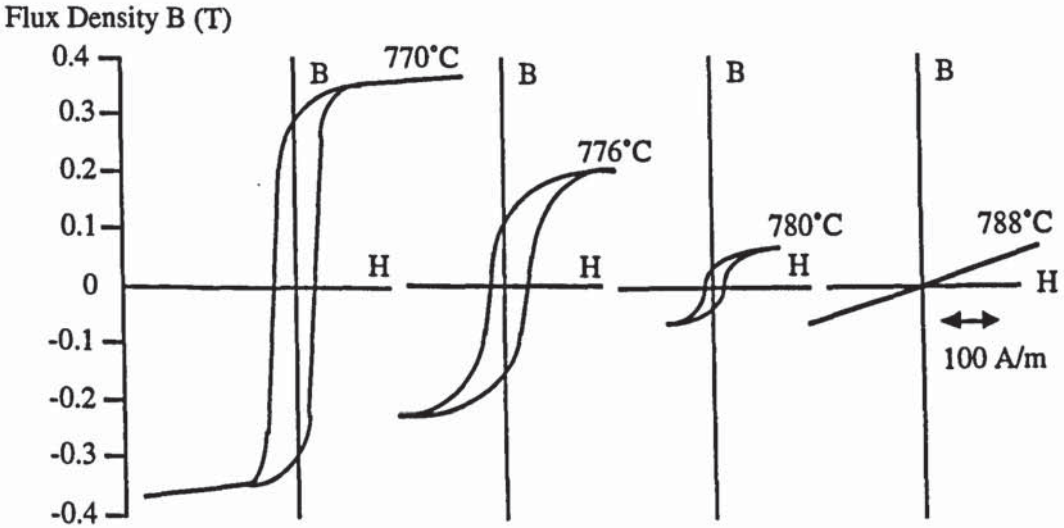

Figure 2.8 Hysteresis Loops of Iron Near the Curie Point.

2.4.6 Magnetocaloric Effect

Weiss and Picard (1918) showed that a sudden application of a high field will increase the temperature of a ferromagnetic material, and the increase is a measure of the molecular field. This is a maximum at the Curie point and is quoted for a field strength of 600 kAm^{-1} producing a temperature change of 2°C.

2.4.7 Summary

Changes in other physical properties become evident as the saturation magnetisation decreases and finally disappears at the Curie point, T_c. These properties are shown in figure 2.9 as schematic curves which summarise the changes, from Bozorth (1951).

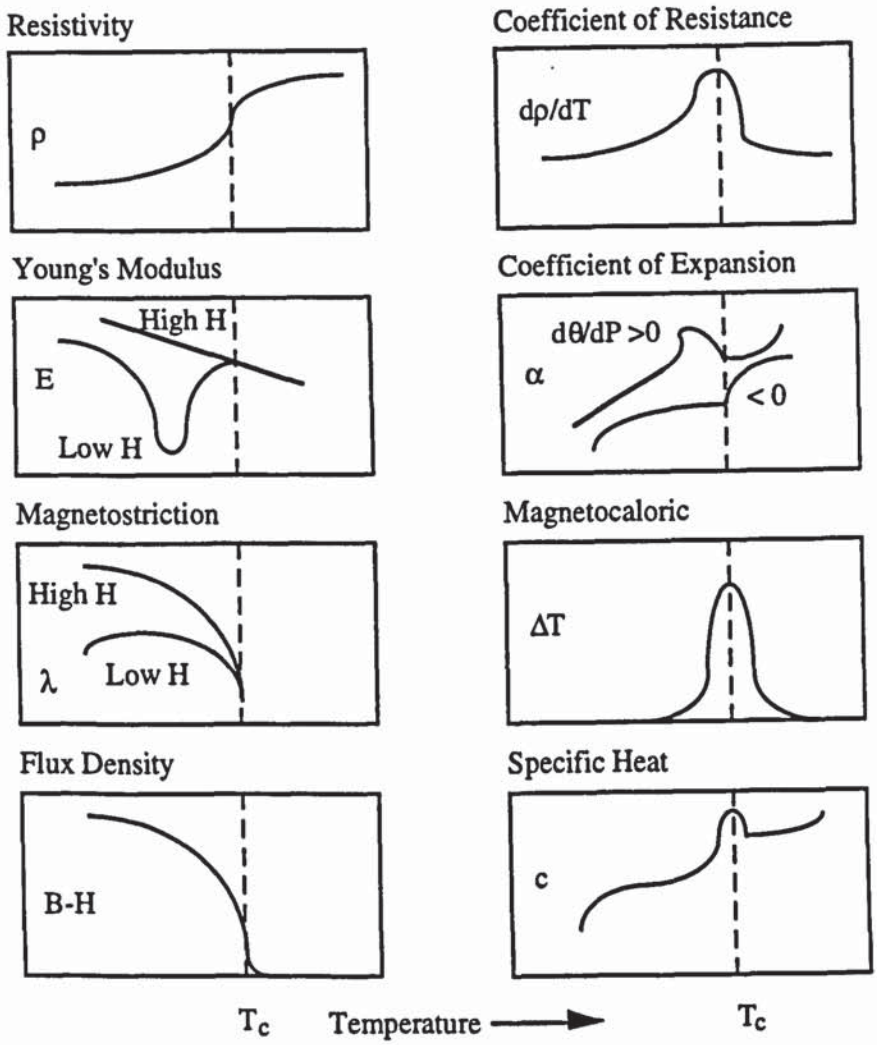

Figure 2.9 Schematic Representation of the Change of Various Properties With Temperature Near the Curie Point.

2.5 Longitudinal Vibration in Mild Steel Rods

The field produced by the induction heating coil is such as to induce extensional or longitudinal vibration in steel bars.

2.5.1 Natural Frequency

Many texts have methods of calculating natural vibration modes of a rod such as Bishop and Johnson (1960). The frequency of natural longitudinal vibration is given by:

$$f_n = \frac{n}{2l}\sqrt{\frac{E}{\gamma}} \qquad (2.10)$$

where f_n is the nth natural frequency (Hz)

n is an integer ≥ 0

l is the length of the bar (m)

E is Young's Modulus (N/m^2)

γ is the density (kg/m^3)

Figure 2.10 shows the longitudinal modes which arise from a free-free bar, taken from Meirovitch (1967);

where l is the length of the bar (m)

x is the displacement (m)

r is the mode

$U_n(x)$ are the eigenvalues, n is an integer ≥ 0

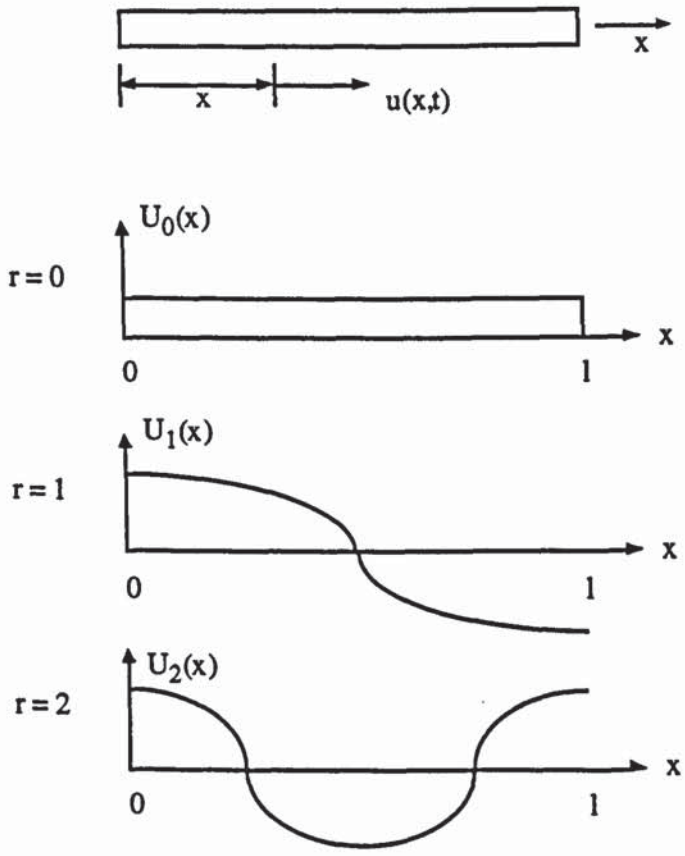

Figure 2.10 Modes of Longitudinal Vibration of a Rod

The mode r = 0 is interpreted as the displacement of the rod as a whole, known as a rigid body mode and is typical of unrestrained systems for which there are no forces or moment exerted by the supports.

2.5.2 Damping

Damping in a system can be determined by noting the maximum response i.e. the response at the resonant frequency. This is defined as the factor Q by Harris and Crede (1976) with respect to mechanical vibration as:

$$Q = (R_v)_{max} = 1 / 2\xi \tag{2.11}$$

where R_v is the velocity response of the system and ξ is the fraction of critical damping.

The maximum acceleration and displacement responses are slightly larger:

$$(R_d)_{max} = (R_a)_{max} = (R_v)_{max} / (1 - \xi^2)^{1/2} \tag{2.12}$$

The damping in a system is also indicated by the sharpness or width of the response curve in the vicinity of a resonant frequency ω_n, figure 2.11. Designating the width as a frequency increment $\Delta\omega$ measured at the half power point, (i.e. at a value of R equal to $R_{max}/\sqrt{2}$), the damping of the system is defined as:

$$\frac{\Delta\omega}{\omega_n} = \frac{1}{Q} = 2\xi \qquad \text{for } \xi < 0.1 \tag{2.13}$$

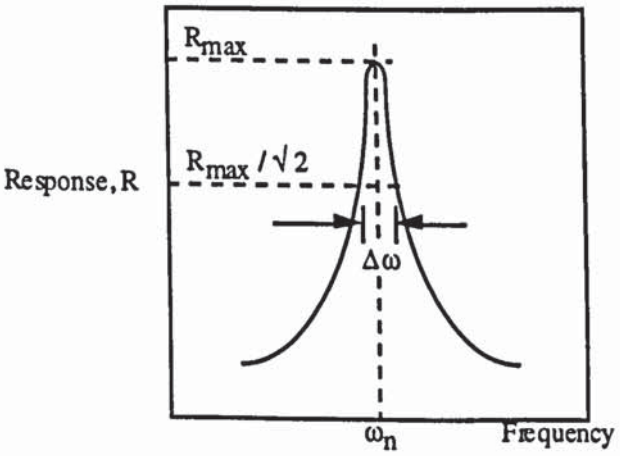

Figure 2.11 Response Curve Showing Bandwidth at Half Power Point

Information regarding damping in ferromagnetic alloys by Cochardt (1953) describes how the magnetomechanical effect contributes significantly to the large damping capacity in high strength ferromagnetic alloys. Tests carried out in strong magnetic fields showed that steel had practically no damping other than that exhibited by the eddy currents set up. Cullity (1972) found that when a specimen was magnetised to saturation, the domain walls were removed and the damping was reduced significantly.

2.6 Ferromagnetism and The Domain Theory

No explanation of ferromagnetism was made until Weiss (1907) put forward his hypothesis of the molecular field. He assumed that a molecular field acted in a ferromagnetic substance below its Curie temperature as well as above it, and that this field was so strong that it could magnetise the substance to saturation even in the absence of an applied field. The substance is then self saturating or spontaneously magnetised. The theory that a ferromagnetic material is composed of many regions or domains, each magnetised to saturation in some direction was proposed. Each domain is spontaneously magnetised to the saturation value M_S, but the directions of magnetisation of the various domains are such that the substance has no net magnetisation. The process of magnetisation is then one of converting it from a multi domain state to that of a single domain magnetised in the same direction as the applied field. Figure 2.12 shows the illustrated process.

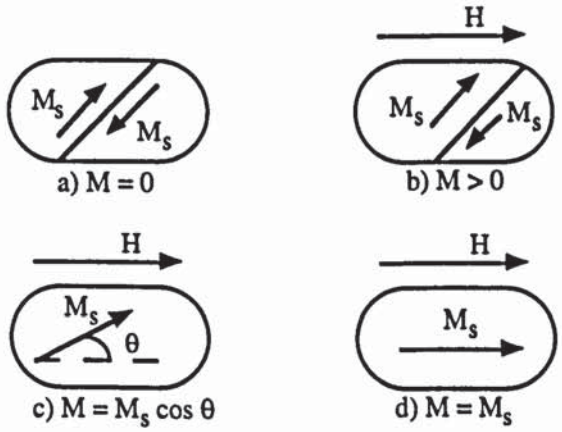

Figure 2.12 The Magnetisation Process

The line in (a) shows a portion of a crystal in which there are parts of two domains; the boundary separating them is called a domain wall. The two domains are spontaneously magnetised in opposite directions so that the magnetisation of this part of the crystal is zero. In (b) a field H has been applied causing the upper domain to grow in expense of the lower domain by downward motion of the domain wall. In (c) the wall has moved outside the region. At higher fields the magnetisation rotates parallel to the applied field and the material is saturated in (d). It should be noted that during this process there has been no change in the magnitude of the magnetisation of any region.

In the unmagnetised state the directions in which the domains are saturated are either distributed at random or in some way such that the resultant magnetisation of the specimen as a whole is zero. Application of a field only changes the direction of magnetisation and not the magnitude.

Two important problems in ferromagnetism are to explain; one, the manner in which magnetisation is changed by the presence of an applied field and two, the anisotropic character of the magnetic crystal which determines the direction in which the domain is spontaneously saturated.

In the absence of an external field the direction of magnetisation in a single domain is affected by the crystal structure or by strain. In iron the magnetisation proceeds most readily in a direction parallel to a cubic axis. It is concluded that in a domain in a crystal of iron not subjected to strain or external magnetic field the magnetisation is always parallel to one of the crystal axes [100]. Since there are six such directions that are equivalent, a demagnetised crystal of iron will normally have one sixth of its domains oriented in each of these directions of easy magnetisation.

Ordinarily at constant temperature the moment of a domain, and therefore the magnetisation of the ferromagnetic body of which it is a part, is changed by:

i) A change in the direction of magnetisation of the domain - "rotational"; or
ii) A change in the volume of the domain - "moving boundary".

Processes may be classified as irreversible or reversible according to whether the energy dissipated as heat is a relatively large or small fraction of the potential energy. Considering these classifications the three main parts of the magnetisation curve may be identified with the following processes:

i) Reversible boundary displacement.
ii) Irreversible boundary displacement.
iii) Reversible rotation.

A fourth process, irreversible rotation may occur in a rotating field.

As previously mentioned the direction of magnetisation in a domain is determined by the crystal structure, provided strain and magnetic field are absent, but when the latter are present either of them may be controlling.

2.7 Phase Transformations in Magnetic Field

The first transformations discovered, involving magnetic fields, were that of hardness. Herbert (1929), claimed that a slowly rotating field could increase the hardness of certain metals. He proposed a hypothesis of lattice resonance. He believed that at certain temperatures the lattice resonated as its natural frequency coinciding with that of the heat vibration.

Measurements by Chaloupecky (1980) of the α to γ phase transformation using a dilatometer were carried out to determine the transformation time in eutectoid steel heated at different rates by induction. He found that the time of the α to γ transformation differed greatly, not only with different heating conditions, but also with different positions in the induction heater coil in relation to the rate at which energy was supplied to the sample.

Verhoeven, Downing and Gibson (1986) studied the ferromagnetic to paramagnetic transition in steel heated by induction. They concluded that there were two cases for the steel undergoing this transition. The first was the normal magnetic Curie transition and the second was the α - γ phase transformation which produces paramagnetic austenite. It was claimed that with large heating rates it is possible for the A_1 transition temperature to change. Normally this is 723°C but could be as high as 770°C. They describe how metallographic data provided clear evidence that the magnetic transformation was due wholly, or in part, to the α - γ transformation. Even in fields of 3 x 10^4 A/m the A_{c1} temperature was lower than 770°C. They conclude that it is very difficult to separate the first and second order transformations which occur near the Curie point.

Thermomagnetic treatment was studied by Ghosh and Roy (1987) for constructional and tool steels. They state that the diffusion of interstitial carbon is expected to be different when in a magnetic field and is due to the distortion of void spaces. In high alloy steels the austenite can be made to transform quickly to produce a more uniform, completely transformed structure with low hardness in a considerably reduced isothermal treatment time.

2.8 Magnetostriction

2.8.1 Definition

When a body is magnetised its dimensions change slightly by not more than a few parts per million. This effect is referred to as magnetostriction. The change in length in the direction parallel to the magnetisation is that most often measured and this change is the Joule magnetostriction. The symbol λ is usually used for $\Delta l/l$. Changes in length can be both positive and negative and are usually dependent on field strength. Volume magnetostriction is that phenomenon in which the volume of a specimen is changed by magnetisation. Changes of volume are measurable, but the relative change in volume $\Delta v/v$, is much smaller than the relative change in length, λ.

The value of λ measured at magnetic saturation is called the saturation magnetostriction λ_{sat} and when magnetostriction is used without qualification, it is λ_{sat} that is usually meant. Figure 2.13 below shows how λ typically varies with field H, for a substance with positive magnetostriction (from Cullity (1972)).

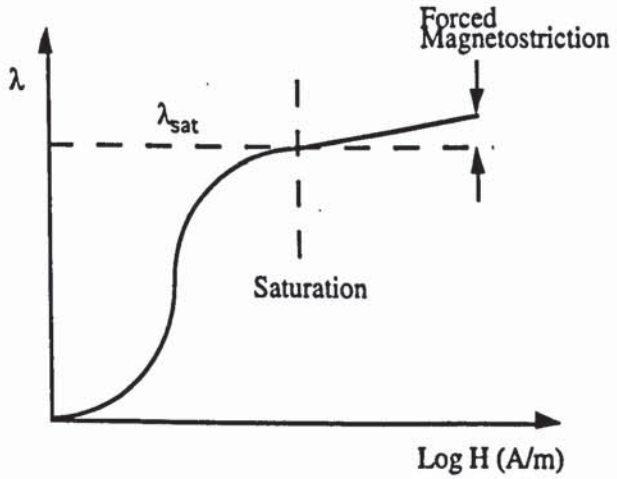

Figure 2.13 Variation of λ with Field H for a Material with Positive Magnetostriction

Between the demagnetised state and saturation, the volume of a specimen remains almost constant. This means that there is a transverse magnetostriction λ_t which is one-half the longitudinal magnetostriction and negative in sign.

$$\lambda_t = -\lambda / 2 \qquad (2.14)$$

When saturation is reached at any given temperature, in other words the specimen has become a single domain magnetised in the direction of the field, further increase in field causes forced magnetisation. This represents an increase in the magnetisation of the domain itself by way of an increase in the degree of spin order which can be produced by very high fields. This causes a small change in λ with H called forced magnetostriction,

and as is apparent from figure 2.13, a large field is required for this effect to become appreciable. The longitudinal, forced magnetostriction λ shown in the figure is a consequence of a small volume change occurring beyond saturation and called volume magnetostriction. It causes an equal expansion or contraction in all directions. Forced magnetostriction is a very small effect and has no bearing on the behaviour of practical magnetic materials in ordinary fields.

In an alternating magnetic field, the change in length will be continuously changing and as a result magnetostrictive vibrations are induced. The frequency of the vibrations produced by magnetostriction are twice the field frequency.

2.8.2 Physical Origin of Magnetostriction

According to Cullity (1972), magnetostriction is mainly due to spin-orbit coupling. This is fairly weak because a field of a few hundred amperes per meter can rotate the spins away from the easy directions. When a field tries to reorbit the spin of a particular electron, the orbit of that electron also tends to be reorientated. The orbit is very strongly coupled to the lattice and resists the attempt to rotate the spin axis. Figure 2.14 shows the relation between magnetostriction and spin-orbit coupling. The black dots are the atoms' nuclei, the arrows show the net magnetic moment and the ovals contain the electrons belonging to each atom.

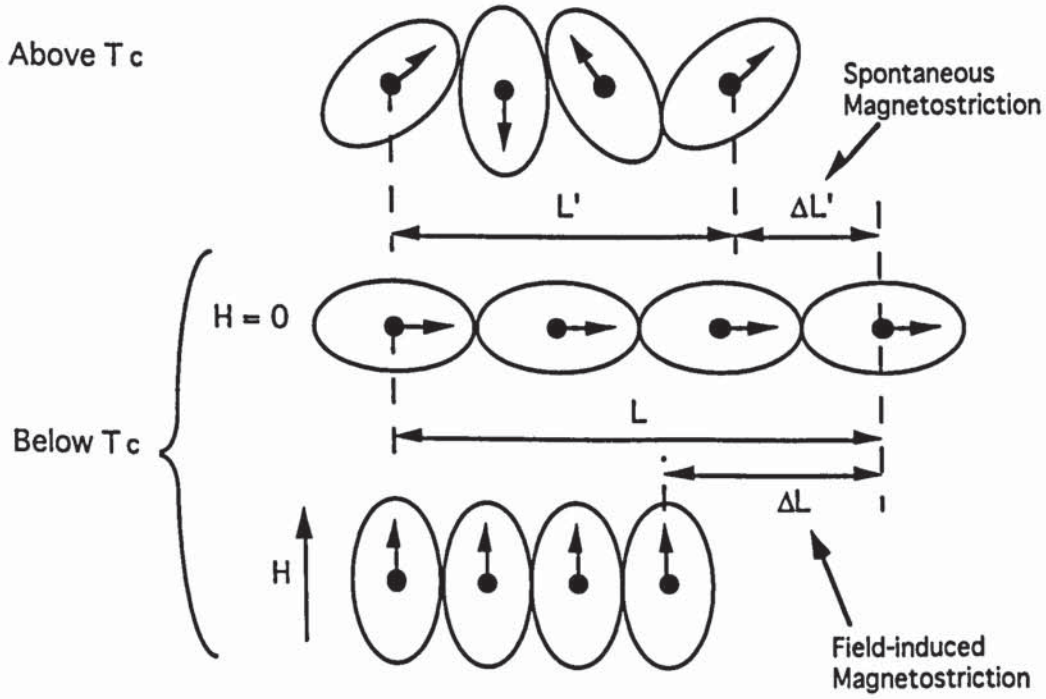

Figure 2.14 Physical Origin of Magnetostriction

The top row of atoms are in their paramagnetic state above the Curie temperature. Below the Curie temperature the effect of spontaneous magnetisation would be to rotate the spins and the electron clouds into a certain orientation determined by the crystal anisotropy. (We must assume that the spin-orbit coupling is very strong. This is not so for iron since it has been shown by X-ray techniques that the orbit is not significantly reorientated).

2.8.3 Review of Magnetostriction

The measurements of Joule (1842) and Joule (1847) established the fact that iron, when magnetised, increased its length in the direction of magnetisation and contracted at right angles thereto. As closely as he could determine its volume did not change.

Barrett (1882) observed for the first time a change in volume. It was reported by Bidwell (1886) that iron contracts in high fields and ultimately becomes shorter than the unmagnetised specimen. Bidwell (1890) showed that tension decreases the expansion of iron and that a sufficient force will prevent any expansion at all and will increase the contraction.

At the turn of the century Nagaoka and Honda (1902) investigated the magnetostriction of iron, cobalt and nickel at high and low temperatures. Webster (1925) reported the first systematic study of the magnetostriction of single crystals.

The effect of temperature was investigated when Honda and Shimizu (1903) collected data for iron, figure 2.15. The mechanical arrangement used claimed to have a resolution of 5×10^{-8} for a change in length of the specimen. This is one of the earliest papers describing magnetostriction at high temperature (800°C). The results for soft iron show that in weak fields the specimen increased in length whereas in high fields the specimen decreased in length. The general trend with temperature was that the contraction in high fields disappeared, followed by an elongation. With further increase in temperature (above 500°C) and after reaching a maximum, the elongation decreased until it ceased at 970°C.

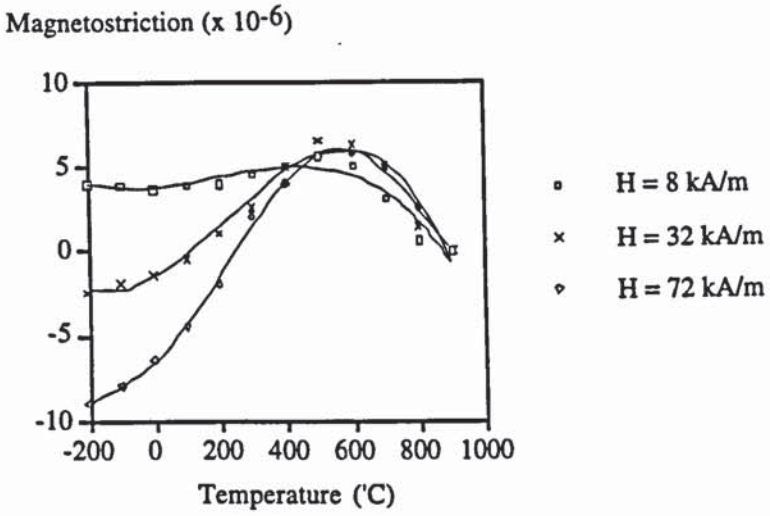

Figure 2.15 Magnetostriction of Iron at Various Temperatures.

Vibration in steel in a magnetic field was observed by Pierce (1929). He used magnetostriction to produce and control electrical and mechanical resonance from 300 Hz to 300 kHz. The procedure was relatively simple; a rod was placed inside two coils and a current was passed through one of the coils so that mechanical vibrations were induced in the rod. These reacted with the second coil to maintain a constant frequency in the electrical circuit. It was necessary to alter the length of rod if a change in frequency was desired. The rods were magnetised so that the alternating field did not change the sign of magnetisation, only its magnitude. This gave rise to vibrations at the same frequency of the field. If the rods were not magnetised, the vibration would be at twice the frequency of the field, which was undesirable for the reaction on the second part of the electrical circuit. Although Pierce did not study the influence of temperature on the magnetostrictive vibrations, he had shown how a mechanical and electrical set-up lead to very precise oscillators.

Rankin (1932) investigated magnetostriction using 0.13% carbon steel rods, 1/4" to 1/16" diameter, and discovered that magnetostriction decreased with a decrease in diameter. The rods had all been cold drawn from an initial diameter to give smaller specimens. Rankin is not sure whether the results are due to changes in internal stress of the rods or not.

Williams (1933) studied the measurement of hardness using magnetostrictive effects. The change in length of a material was found to be a measure of its hardness. Tests were performed on steels with carbon contents ranging from 0.1% to 1.1% with the higher carbon steels being the harder. Using flux densities up to 1 Tesla Williams found that magnetostriction increased with decrease in carbon content and concluded that grain size had effected magnetostriction.

A review of magnetostriction and some magnetomechanical effects has been published by Lee (1955). A ferromagnetic substance comprises of three types of energy; the exchange, anisotropy and magnetostatic (demagnetising) energies. These vary with the state of the strain of the substance and will deform spontaneously if the total energy becomes a minimum. The three energies give rise to volume magnetostriction, linear magnetostriction and the form effect.

Magnetostriction constants λ_{100} and λ_{111} are characteristics of a material and are changed only if the interactions responsible for magnetostriction are altered. For example, measurements have been made by Takaki (1937) of the values of the constants with increase in temperature for iron. The variation is complicated and points towards a spin-orbit interaction. Results are expected to be similar for a low carbon steel since the carbon acts as a diluent. The graph in figure 2.16 shows that λ_{111} is -20×10^{-6} at 20°C and decreases with increase in temperature to zero at 700°C. λ_{100} on the other hand starts at 20×10^{-6} and falls only to 10×10^{-6} at 750°C. No reference is made to the field strength.

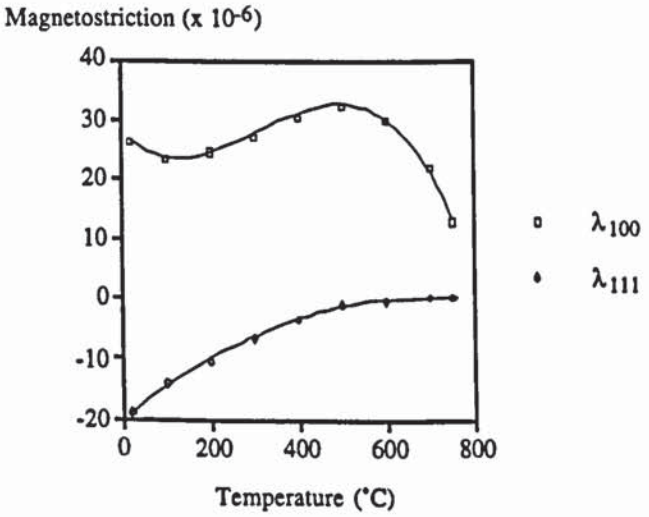

Figure 2.16 The Temperature Dependence of the Magnetostriction Constants in Iron.

A review of the volume magnetostriction by Lee (1955) leads to a thermal expansion anomaly. As temperature is increased towards the Curie point there is a volume change caused by the destruction of the spontaneous magnetisation. This has been investigated in nickel. The peak of thermal expansion plotted against temperature shows in figure 2.17 that the area between the full and broken curves is equal to the total volume change associated with spontaneous magnetisation. However, it cannot be assumed that magnetostriction in iron is isotropic and theories which describe the behaviour of nickel, including the thermal expansion anomaly, are not appropriate.

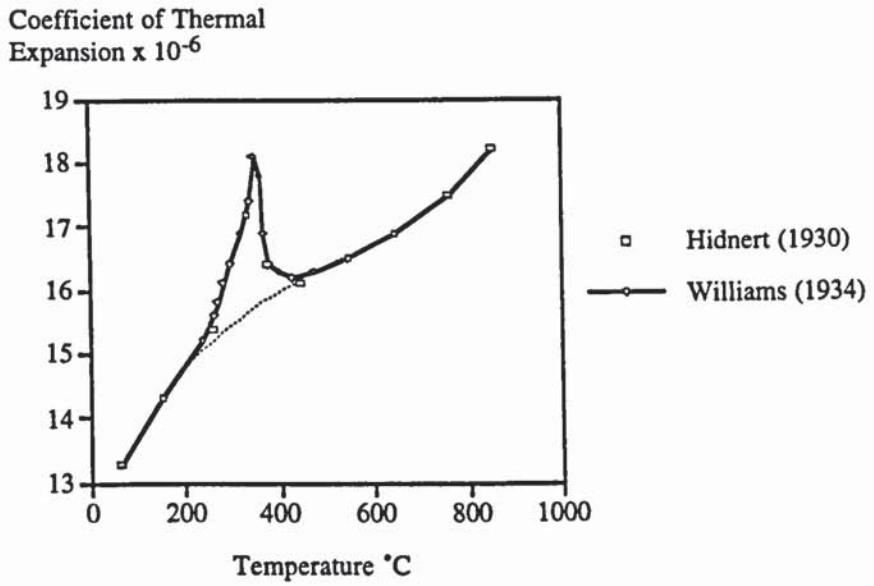

Figure 2.17 Thermal Expansion Anomaly in Nickel

Only recently, have the effects of alternating magnetic fields been investigated. Chow and Nembach (1976) reported that when an axial a.c. field is applied to a cylindrical ferromagnet, magnetostriction causes the specimen to vary longitudinally in length, periodically with time. The a.c. field adds a strain to the specimen. In their tests a specimen was deformed at a constant resolved strain rate. The total strain rate changes its sign four times in a cycle.

Work studying the effects of temperature on magnetostriction by Hoekstra, Gyorgy, Zydzik and Flanders (1977) describe a rotating magnetostrictometer, which automatically recorded magnetostriction as a function of temperature. A strain gauge was used together with a lock in amplifier to only record the signal which was at twice the frequency of the rotating specimen. The magnetostriction constants were recorded in a fixed field as a function of temperature between -196°C and 250°C with a sensitivity of 3×10^{-8}.

The a.c. magnetostriction of grain-oriented 3.25% silicon iron was measured by Pike and Moses (1977), from room temperature to the Curie point using high temperature strain gauges. Heating was carried out in a resistively heated tube furnace (wound non-inductively) in an atmosphere of argon with a separate magnetising coil added to provide the field. A small high temperature strain gauge was attached to each specimen to measure magnetostriction along its length, perpendicular to the rolling direction. The specimen was magnetised at 50 Hz with the output from the strain gauge measured using a carrier frequency bridge and the demodulated output signal analysed on an f.f.t. analyser to obtain the 100 Hz component. The dB/dt waveform was also recorded at the same time. The magnetising coil was capable of producing a maximum flux density of 1.1 T. The

results are presented in figure 2.18. Two types of grain-oriented silicon iron were used. Type A had the conventional degree of orientation and type B was very highly oriented.

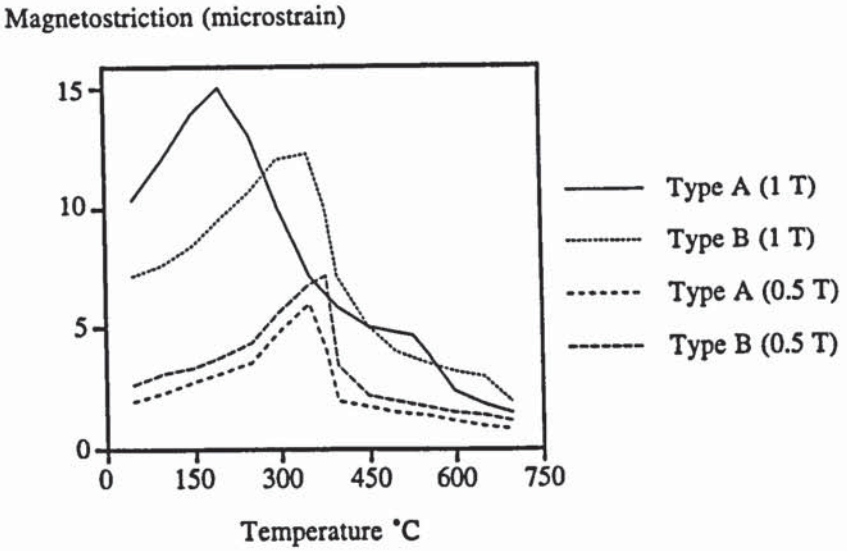

Figure 2.18 Fundamental Magnetostriction In Grain Oriented Silicon Iron

The graph shows that there was a distinct increase in magnetostriction in the material between 300°C and 400°C and was explained by the fact that magnetic annealing took place and the presence of the phosphate coating created stresses. Magnetostriction in this electrical steel generally decreased with increase in temperature.

In order to compare the experimental results to theory, Pike and Moses used an approximate equation for the a.c. magnetostriction of a single grain:

$$\lambda = (3 / \sqrt{2})\, \lambda_{100}\, (B / M_s) \sin\theta\, (\sin^2(\theta/2) - \cos^2\theta) \qquad (2.15)$$

where θ represents the misorientation in the plane of the sheet with reference to the perfect [110] [001] structure and λ_{100} is the magnetostriction in the [100] direction. M_S is the saturation magnetisation and B is the flux density. The equation is valid for flux densities up to 1.1 T. For perfectly oriented grains in the [011] direction, $\theta = 90°$. Substituting in the above equation gives:

$$\lambda = (3 / 2\sqrt{2})\, \lambda_{100}\, (B / M_s) \qquad (2.16)$$

In this range, magnetostriction is proportional to flux density and λ_{100} can be calculated for different temperatures. Experimental and theoretical results were found to agree, apart from in the temperature range 300°C to 400°C.

Forced volume magnetostriction, $\partial\omega_v/\partial H$ of the f.c.c. Fe-Ni Invar alloys was measured from 77 to 900 K (-196°C to 627°C) by Ishio and Takahashi (1985). They found that large increases in $\partial\omega_v/\partial H$ occurred at the Curie points of the alloys

investigated where ω_v is the volume expansion. The volume expansion was assumed to be a function of both the amplitude of the local magnetic moment and the spin-spin correlation between local magnetic moments. Forced volume magnetostriction was measured using a three terminal capacitance technique in fields up to 1600 kAm^{-1}.

The volume expansion ω_v is defined as:

$$\omega_v = (\Delta l / l)_{parallel} + 2(\Delta l / l)_{perpendicular} \qquad (2.17)$$

the directions being with reference to the applied magnetic field.

For Ni-Fe the volume expansion increases linearly with increasing H at lower temperatures. However, just below the Curie point the value of $\partial\omega_v/\partial H$ is dependent upon H. Therefore it is not adequate to discuss the magnetovolume effect in terms of $\partial\omega_v/\partial H$. Above T_c the volume expansion becomes quadratic against H. Values of $\partial\omega_v/\partial H$ increase gradually with increase in temperature until a sharp maximum occurs at about $T = 0.9T_c$.

With the use of ever increasing transformer size, the effects of magnetostriction in electrical steel have been studied. Eingorn (1989) investigated the magnetostriction of electrical steel by measuring transformer noise and discovered that over a temperature range of 20-100°C magnetostriction increased by 45%. This was measured at a flux density of 1.7 T and 50 Hz. The graph, figure 2.19, shows the plot of both noise level of the transformer and magnetostriction against temperature. No information is given on the vibrational characteristics of the transformers.

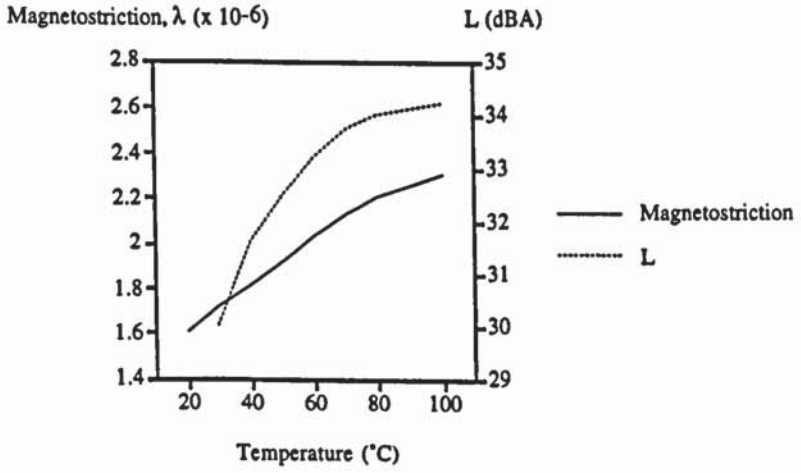

Figure 2.19 Noise Level (L) of the Magnetic Circuit and Magnetostriction (λ) Against Temperature.

Recently, direct measurements of magnetostriction with change in temperature have been measured. Yamano, Nakagiri, Shinke and Maeda (1990) studied the effects of temperature on magnetostriction in a medium carbon steel due to an alternating field. The authors used magnetostriction for stress relieving at low temperatures and showed that a 10% relief of surface residual stress was possible. Magnetostrictive vibrations were induced in rods of the ferromagnetic material which produced resonance. A low intensity variable frequency (50 Hz - 20 kHz) magnetic field was tuned to produce the resonance in the rods. Both ends of the specimen were free and the vibration displacement was detected using non-contact eddy current probes with a measuring accuracy of 1 μm. Tests were carried out at a constant flux density of 40 mT. The relationship between the vibration amplitude due to magnetostriction and testing temperature is shown in figure 2.20. The solid and dotted lines represent the measurements taken in liquid and air respectively. The distortion, b when initial tensile loading had been carried out is shown.

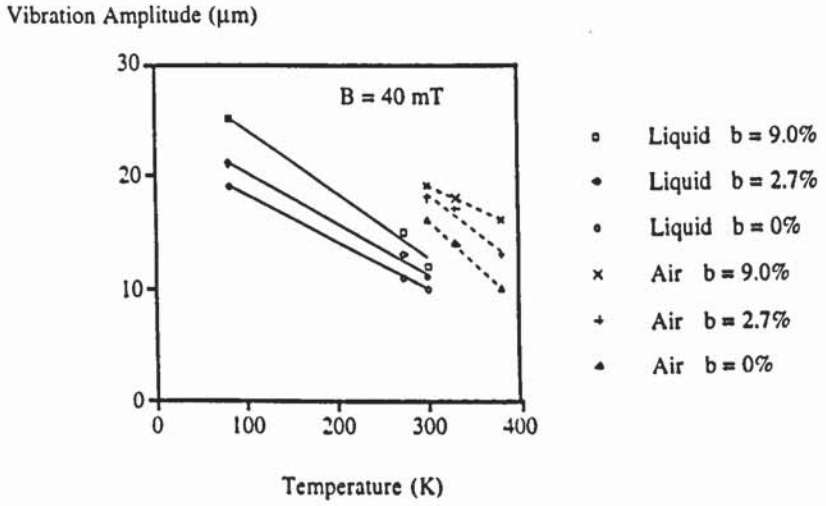

Figure 2.20 Relationship Between Testing Temperature and Vibration Amplitude.

Results suggest that magnetostriction decreases with increase in temperature over the range 77-373K. The authors believe that this is due to the fact that spontaneous magnetisation decreases when the surface temperatures of the specimens rise as high as the testing temperature. The reason for the difference between readings in air and liquid was thought to be due to the type of bath used.

Tests involving low carbon steel have been performed by Pravdin and Burtseva (1992). Differential magnetoelastic and magnetostriction constants of sensitivity were measured as a function of small increases of elastic stress - for the case of the variation of the initial magnetic state of a specimen of plain carbon steel along its limiting hysteresis loop. Resultant, irreversible and reversible components of the constants were obtained in relation to the internal field. The data was necessary to understand the process of magnetic rearrangement of 90° domains, evaluation of internal stresses and for

developing the acoustic method. The constants were calculated as the field was reduced by a small amount and as a cyclic load was applied to the specimen. No change in temperature was mentioned. The fields employed were many times smaller than those used in induction heating.

2.8.4 Magnetostriction of Single Crystals

Most information on magnetostriction of materials is given in terms of single crystals. This is because the saturation magnetostriction depends on crystal direction and an empirical theory for cubic crystals, based on constants was developed by Akulov (1930).

A summary of work carried out on this subject is given by Cullity (1972). A single crystal of iron is found to increase in length in the [100] direction when magnetised to saturation in the same direction, figure 2.21. The shape of the cell cannot therefore be cubic and must be tetragonal. If a [010] domain is replaced by a [100] domain by the mechanism of wall motion then the region will expand in the [100] direction and contract at right angles to it. The magnetostrictive effect of the motion of the two kinds of walls is quite different. Spontaneous strain is independent of the sense of the magnetisation and the dimensions of a domain do not change when the direction of spontaneous magnetisation is reversed. Since passage of a 180° wall through a region reverses the magnetisation of that region, 180° wall motion does not produce any magnetostrictive change in dimensions.

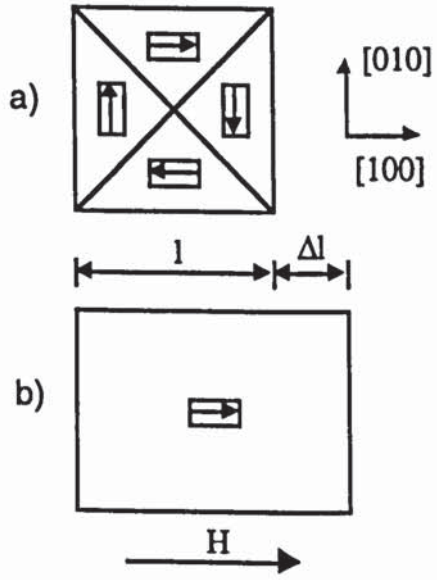

Figure 2.21 Magnetostriction of an Iron Crystal in the [100] Direction.

Rotation of the M_s vector always produces a dimensional change because the spontaneous magnetostriction depends on the direction of the vector relative to the crystal axes. In general a crystal magnetised in a non easy direction will involve 180° and 90° wall motion and domain rotation. The last two of these processes will be accompanied by magnetostriction.

The saturation magnetostriction of a cubic crystal, λ_{sat} in the same direction as the magnetisation defined by the cosines α_1, α_2, α_3 is given by :

$$\lambda_{sat} = 3/2\,\lambda_{100}\,(\alpha_1^4 + \alpha_2^4 + \alpha_3^4 - 1/3) + 3\,\lambda_{111}\,(\alpha_1^2\alpha_2^2 + \alpha_2^2\alpha_3^2 + \alpha_3^2\alpha_1^2) \qquad (2.18)$$

This is known as the two constant equation for magnetostriction. The next approximation in the series involves five constants but is rarely required.

Using the relation:

$$(\alpha_1^2 + \alpha_2^2 + \alpha_3^2)^2 = (\alpha_1^4 + \alpha_2^4 + \alpha_3^4) + 2(\alpha_1^2\alpha_2^2 + \alpha_2^2\alpha_3^2 + \alpha_3^2\alpha_1^2) = 1 \qquad (2.19)$$

$$\lambda_{sat} = \lambda_{100} + 3\,(\lambda_{111} - \lambda_{100})(\alpha_1^2\alpha_2^2 + \alpha_2^2\alpha_3^2 + \alpha_3^2\alpha_1^2) \qquad (2.20)$$

where λ_{100} and λ_{111} are the saturation magnetostrictions when the crystal is magnetised in the [100] and [111] directions respectively. This equation is valid for both crystals with easy directions [100] or [111].

Equation 2.18 gives the field-induced strain when a crystal is saturated from a demagnetised state. The saturated state being when the specimen is a single domain with M_s parallel to the applied field. In the demagnetised state however, the domain magnetisations when weighted by volume add up to zero. This means that there are infinite ways in which the domain arrangements and volumes can result in zero net magnetisation. The equation assumes that in the demagnetised state, all types of domain have equal volume. For iron the total volume of the crystal will be equally divided by the domains; [100], [$\underline{1}$00], [010], [0$\underline{1}$0], [001], [00$\underline{1}$]. If this is not achieved then the equations are not valid.

Differences in the magnetostriction values observed by different investigators for the same metal are usually due to differences in the demagnetised state. Typical values of the constants for iron are $\lambda_{100} = 21$, $\lambda_{111} = -21$ and $\lambda_p = -7$. The final value being an experimental value for a polycrystalline structure.

Magnetostriction constants are said to usually decrease in absolute magnitude with temperature increase and approach zero at the Curie point. This has been found by Tatsumoto and Okamoto (1959) and is shown in figure 2.22 for iron.

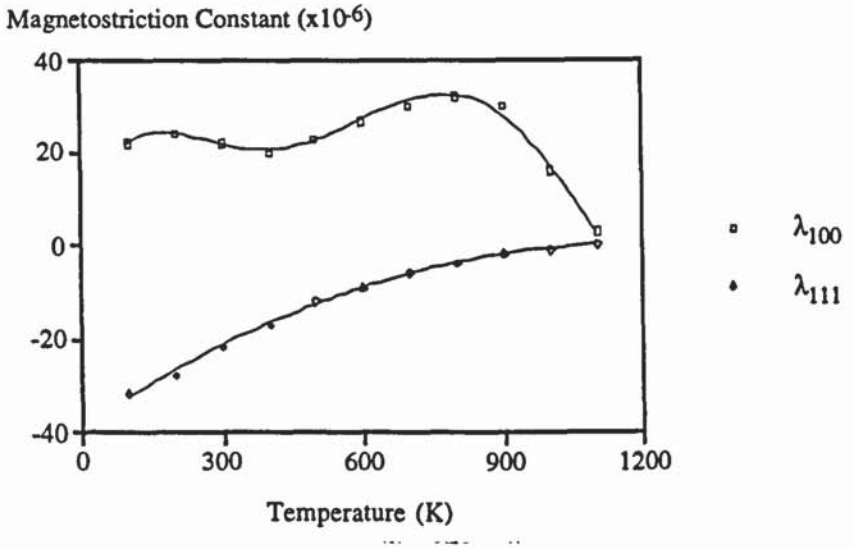

Figure 2.22 Magnetostriction Constants of Single Crystals of Iron As a Function of Temperature

2.8.5 Magnetostriction of Polycrystals

The saturation magnetostriction of a polycrystal, parallel to the magnetisation is represented by λ_p. Its value is dependent on the magnetostrictive properties of the individual crystals and the way in which they are arranged; the presence or absence of preferred domain or grain orientation. Some sort of averaging is necessary to describe the effects so we may assume that either the stress of the specimen is uniform and strain varies from grain to grain or strain is uniform and the stress varies.

Cullity (1972) uses the latter of these statements. The magnetostriction in the field direction is averaged over all the crystal orientations or averaging the above equation over all orientations of the M_s vector with respect to a set of crystal axes. The magnetostriction of a polycrystal is given by:

$$\lambda_{sat}\,(av) = \frac{(2\lambda_{100} + 3\lambda_{111})}{5} \qquad (2.21)$$

2.8.6 Volume Magnetostriction

According to Chikazumi (1978), magnetostriction originates from the interaction between atomic magnetic moments, as in magnetic anisotropy. We can discuss the origin with reference to Neel's theory. When the distance between the atomic magnetic moments is variable, the interaction energy is:

$$w(r, \cos\phi) = g(r) + l(r)(\cos^2\phi - 1/3) + q(r)(\cos^4\phi - 6/7\cos^2\phi + 3/35) + .., \qquad (2.22)$$

where r is the atomic distance

w is the pair energy

ϕ is the angle between the direction of the dipole and its pair

l is the coefficient of dipole-dipole interaction

q is the coefficient of quadrupole interaction

The first term g(r) is independent of the direction of magnetisation and is the exchange interaction. This does not contribute to the usual magnetostriction, but to volume magnetostriction. The second term is the dipole-dipole interaction which does depend upon the direction of magnetisation and can be the main origin. The remainder of the terms also contribute but are usually small compared to the second. The fractional change in volume is given by the strain tensor components as:

$$\delta v / v = e_{xx} + e_{yy} + e_{zz} \qquad (2.23)$$

If spontaneous strain is put into this formula the result is zero. This is because a rotation of magnetisation does not give rise to any volume change. It is necessary to lower the specimen to below the Curie temperature to observe the volume change. Previously, parallelism was assumed for spin pairs but this is no longer the case because the g term does not include the direction cosines of magnetisation. It is assumed that g represents the average exchange energy for thermally agitated spin pairs.

This phenomenon is referred to as forced magnetostriction. Both this and the anomalous thermal expansion are isotropic for cubic crystals as they originate in the exchange interaction.

The change in volume, ω_v caused by the application of a magnetic field is usually much smaller than the change in length. The graph of ω_v verses H for iron is shown in figure 2.23 in relation to the length magnetostriction from Bozorth (1951). Here $\omega_v/3$ is plotted to bring out the fact that the change in length measured in high fields (above 320 kA/m) is mainly due to a volume change.

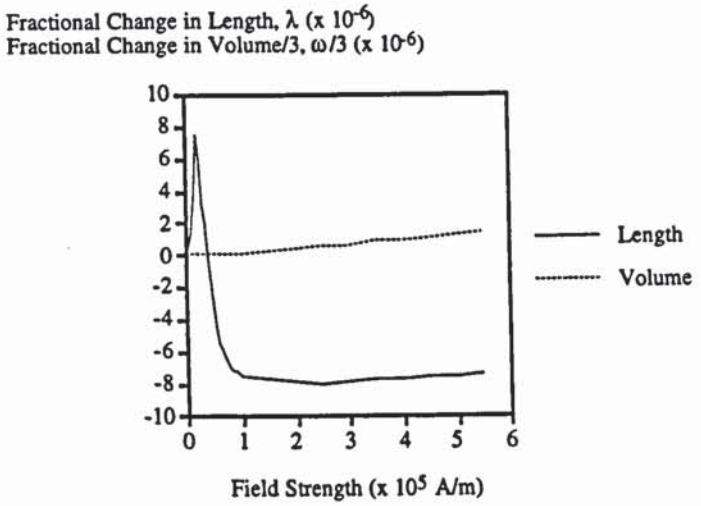

Figure 2.23 Length and Volume Magnetostriction of Iron.

The magnetic or quasi magnetic forces between atoms give rise to an expansion (or contraction) of the lattice by opposing the purely elastic forces between atoms. The equilibrium distortion or magnetostriction occurs when the sum of the two corresponding energies is a minimum. If the linear magnetostriction is calculated using magnetic dipole moments alone, the calculated value is too small by an order of magnitude. This is because the spin-orbit coupling must be taken into account.

2.8.7 Form Effect

When a specimen is magnetised a strain ($\Delta l / l_f$) occurs which has a physical origin entirely different from that of magnetostriction but which can be erroneously ascribed to magnetostriction if not aware of it. The strain depends on the shape of the specimen and is due to the form effect.

This effect occurs because of the tendency of a magnetised body to minimise its magnetostatic energy. Superimposed on the form effect strain is the strain due to magnetostriction and the two make up the observed strain. Cullity (1972) reports that for an iron sphere the strain due to the form effect is 4×10^{-6} so it is not negligible for short specimens. If the length to diameter ratio of a rod specimen is greater than 5, then the magnetostatic energy will then be so small that $\Delta l / l_f$ may be ignored, compared to that from magnetostriction.

Chikazumi (1978) gives a more mathematical approach to the form effect. Volume magnetostriction of a specimen is described as follows. First the volume will increase in proportion to H^2 as a result of the form effect, then as the rotation of magnetisation starts the volume begins to decrease because of the crystal effect. This is negative for iron. After saturation has been reached, the volume increases once again due to forced

magnetostriction. Volume magnetostriction as a whole is a small effect but in a very strong field can give rise to a large deformation since forced magnetostriction is proportional to H. It must be noted that the form effect gives rise to Joule magnetostriction as well as volume magnetostriction.

2.9 Electromagnetic Generation of Ultrasonic Waves in Metals

2.9.1 Lorentz Force

It was shown back in 1820 by Ampere that parallel currents in adjacent wires attract one another and in antiparallel wires repel. The wires are electrically neutral so the force is not electrostatic or Coulomb. Further experiments have shown that there is no force between a stationary charge and a current, but charges moving parallel to a current are attracted, while charges circulating round in a plane normal to the current produce no effects. This can be found in many textbooks such as Dobbs (1984).

A similar effect is found when a current is placed between the poles of a magnet. The force depends upon the direction of the current. Today we attribute a magnetic field, B to both the current in the wire and atomic currents in the magnet. Experiments on charges, q moving at a velocity, v in a uniform field, B of a magnet then show that the forces, F can be explained in terms of a new force acting on a moving charge in a magnetic field called the Lorentz Force.

$$F = qv \times B \tag{2.24}$$

This topic is investigated in detail here because it is postulated that this phenomenon and the vibration in steel heated by induction show distinct similarities.

2.9.2 Electromagnetic Generation of Acoustic Waves

The Lorentz force effect has been used for creating ultrasound in metal. The mechanism for this is best explained by considering a conductor which is near an alternating current carrying conductor. Eddy currents are induced in the first conductor. If a static magnetic field is superimposed an additional force, f_L acts on the electrons given by:

$$f_L = \mu_0 J \times H_0 \tag{2.25}$$

where μ_0 is the permeability of free space (Hm^{-1})
J is the current density (Am^{-2})
H_0 is the static magnetic field (Am^{-1})

For the case when the static field is perpendicular to the eddy currents, the Lorentz force on the electrons is longitudinal resulting in a variation in the electron charge density. In the absence of a compensating variation of positive charge, an internal electric field, E also along the same axis as the eddy currents, is set up that forces the lattice of ions into motion. This is commonly known as the EMA (electromagnetic acoustic) method of creating ultrasound.

In a review by Budenkov and Gurevich (1982), the EMA method was first used by Otroumov and Polotovskii (1933) to excite free elastic vibrations in metal rods, and by Randell, Zener and Rose (1939) to inspect grain size and later by Merkulov (1965) for the purpose of directed ultrasonic wave radiation on account of a specimen's geometry.

Kaule (1964) carried out a simple test to discover whether the waves produced by the EMA method were limited to the surface of a metal. He discovered that an ultrasonic pulse was propagated through the material in much the same manner as a plane wave, covering the full cross section. Results taken with increase in temperature of the specimen show that the effect of linear magnetostriction is to increase the amplitude of the ultrasound to a maximum at around 600°C before falling to zero at the Curie point. Figure 2.24 shows Kaule's results.

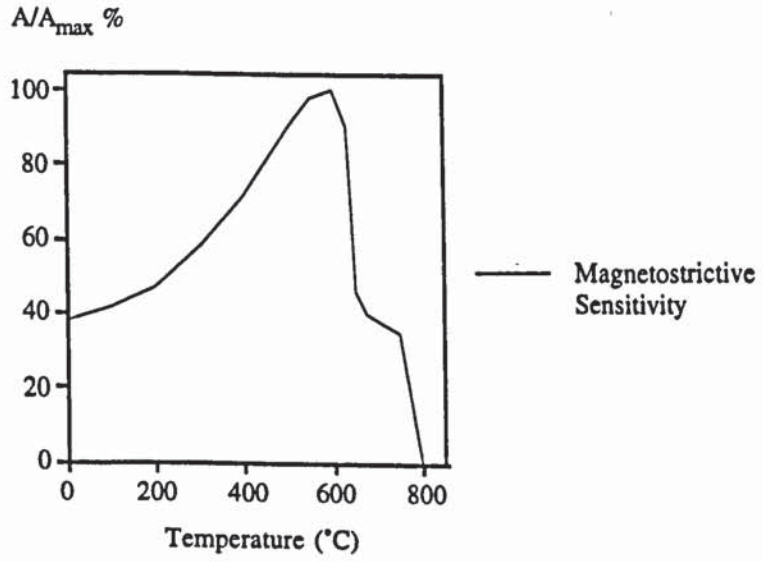

Figure 2.24 Amplitude of Ultrasound As a Function of Temperature

Papadakis, Lynnworth, Fowler and Carnevale (1972) describe how an increase in the longitudinal ultrasonic amplitude in steel is obtained, near the Curie point, when no magnetic field is present, either steady or alternating. The ultrasonic signal was produced by a piezoelectric ceramic transducer and directed into the specimen using a stainless steel buffer rod. Results were very similar to those obtained using an EMAT (Electromagnetic Acoustic Transducer) which creates ultrasound in steel by the interaction of an alternating

current with a steady magnetic field. The velocity of ultrasound using the piezoelectric transducer was found to decrease with temperature rise. A number of hypotheses are presented for the peak in amplitude near the Curie point. These are:

1) An interaction between the motion of the wave and the magnetic properties of the steel, since the overlap integrals of the electron wave functions depend on the interatomic spacing which change in a longitudinal wave.

2) An interaction between the longitudinal wave and the transformation from b.c.c. to f.c.c. where there is a dimension change in steel at this point.

3) An interaction between the longitudinal wave and solubility of the carbides at 723°C, as there is a dilation associated with the introduction of a carbon atom interstitially into the iron lattice.

Substantial work by Budenkov and Maskaev (1973) has shown that, in iron and two different steels, it was possible to use the EMA method to stimulate longitudinal ultrasonic waves at a temperature near the Curie point. The authors assumed that the mechanism of stimulating ultrasound was the same for ferromagnetic and non-ferromagnetic materials and was as a result of Lorentz forces. A round, flat spiral sensor was used as a source and receiver of vibrations mounted on the specimen which was situated between two electromagnetic poles. The cause of the longitudinal ultrasonic wave was due to the reverse magnetoelastic effect from the EMA sensor. An elastic wave was created and spread to the inside of the specimen resulting in a change in the magnetisation characteristics of the material. Changing this in the presence of a magnetic field lead to an electromagnetic wave of identical frequency to the elastic wave. This was quickly damped in the bulk of the material but appeared in the skin layer. Results showed that as the specimen of iron approached the Curie point, the longitudinal ultrasonic impulse increased to a maximum before falling to zero after the Curie point, figure 2.25. With an increase in the magnetic field, the temperature at which the peak occurred fell and the width of the peak widened. Results obtained during heating and cooling of the specimen show distinct differences and was believed to be related to structural changes in the iron.

The hypothesis presented relates to the magnetostrictive properties and the magnetoelastic effect of material in the region of the Curie point. However, little is known about these effects which take place by means of a paraprocess or coupling process. It is known that there is a significant volumetric effect around the Curie point for ferromagnetics (probably on account of their spontaneous magnetisation) which may influence the amplitude of the ultrasonic pulses. Budenkov and Maskaev suggest this explanation for their results. For the specimen placed in a permanent magnetic field near

the Curie temperature, it experiences deformations in all directions due to volume magnetostriction, or the form effect in low fields, and by the coupling process in higher fields. The high frequency of the magnetic field created by the EMA sensor caused elastic collisions in the surface layer of the deformed specimen. The appearance of a longitudinal wave was as a result of an isotropic deformation of the specimen.

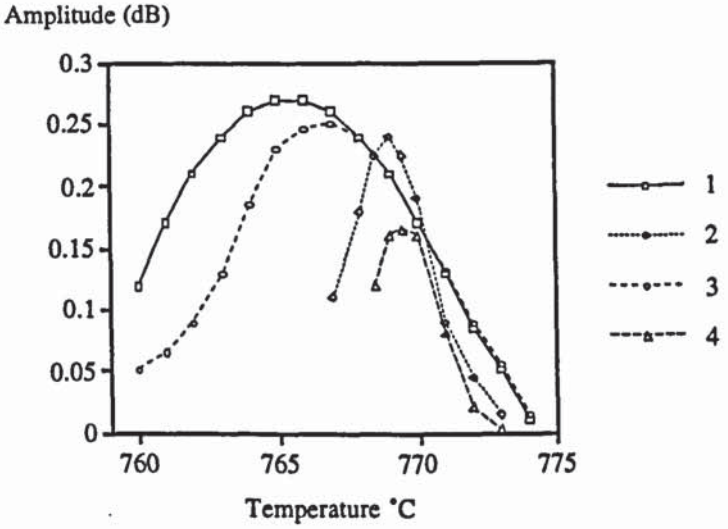

Figure 2.25 Amplitude of Ultrasound in Iron As a Function of Temperature When Heating (1 and 2) and Cooling (3 and 4).
Magnetising Current was 200 A (1 and 3) and 50 A (2 and 4)

The impulse obtained was a result of volume magnetostriction and magnetoelastic effects. It was assumed that the amplitude of the impulse was proportional to the slope of the curve of volume magnetostriction.

The three forms of volume magnetostriction are discussed:

- the form effect by means of rotation (and the paraprocess in larger magnetic fields), especially near the Curie point.

- by means of specimen form in small fields, which increases as the square of the field. In dynamic fields vibrations of the skin layer are linear functions of field.

- by means of a paraprocess at temperatures lower than the Curie point which are linear functions of the field.

At low temperature there is no saturation in the amplitude of vibration with increase in field. This is explained by the fact that the volume magnetostriction arises due to a rotation process. The paraprocess in large fields has been shown to occur at a slightly lower temperature.

Thompson (1978) produced a model to predict the efficiency of ultrasonic waves generated in ferromagnetic materials. Both contributions from Lorentz and magnetostrictive forces are considered. The model was directly compared with experimental results obtained using iron. It was claimed that an increase in resistivity caused an increase in efficiency, as did a decrease in permeability.

Whittington (1978) used the EMA method of creating ultrasound in hot steel and showed that an increase in the amplitude of longitudinal waves occurred in the region 750-800°C. This was referred to as the enhancement region and was thought to occur when the surface of the steel had cooled just below its Curie point while the interior was still hot, so that the steady or d.c. flux was concentrated in the ferromagnetic surface layer. The results of signal amplitude versus temperature for a longitudinal wave are shown in figure 2.26. The frequency of the ultrasound was 2 MHz. Whittington also mentions that it is difficult to generate longitudinal ultrasonic signals in hot steel below 600°C.

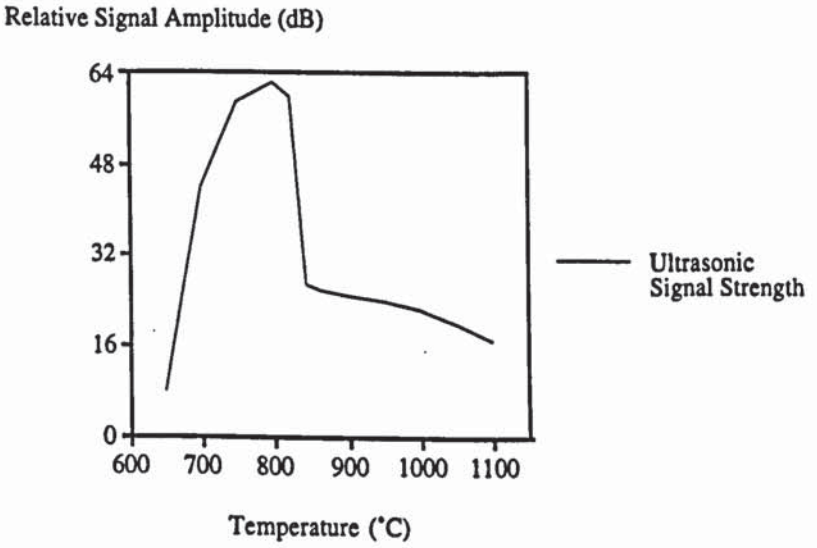

Figure 2.26 Ultrasonic Signal Strength in Mild Steel as a Function of Temperature.

Cole (1978) was another to carry out tests using the EMA method on mild steel up to 1200°C. A zig-zag grid of wires carrying a radio frequency current generated the surface waves. Current to the grid was 600 A at 250 kHz. Results showed a significant increase in signal amplitude near the Curie point. The increase in signal amplitude was seen during both heating and cooling of the mild steel sample as shown in figure 2.27. The hypothesis given is that the surface of the steel cooled below the Curie point and concentrated the steady field in this layer.

ASTON UNIVERSITY
LIBRARY AND
INFORMATION SERVICES

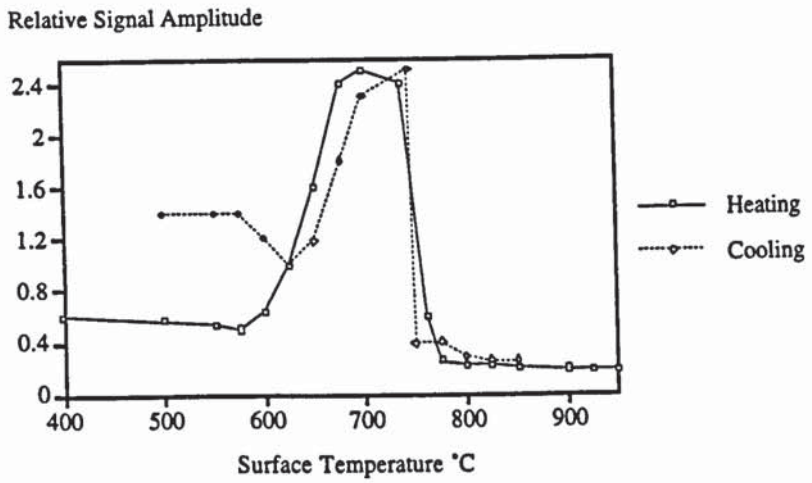

Figure 2.27 Amplitude of Ultrasound in Mild Steel Near the Curie Point.

More results showing an increase in the amplitude of ultrasonic pulses near the Curie temperature were reported by Budenkov and Maskaev (1979). Two increases in amplitude were noted at around 200°C and 768°C and explained as follows. For the lower temperature the ferromagnetic cementite changed into its non-ferromagnetic phase and the volume magnetostriction of cementite was responsible for enhancing the ultrasonic pulse amplitude. The second increase was attributed to an increase in volume magnetostriction in the vicinity of the α to γ phase transformation and not to the second order magnetic phase transformation. The results are compared to those obtained using a piezoelectric transducer which did not show any increases in the amplitude of ultrasound in hot steel. However, this does not agree with the work of Papadakis, Lynnworth, Fowler and Carnevale (1972).

It is possible to create ultrasonic waves without using a steady magnetic field as explained by Kawashima, Murota, Nakamori, Soga and Suzuki (1979). A mild steel and a stainless steel were tested. The amplitude of the ultrasound in the mild steel was found to increase sharply at about 800°C. The frequency of the signal was twice that of the current in the excitation coil, indicating that the waves originated from magnetostriction in the steel. Also reported is the fact that the increase in amplitude near the Curie point only happened with longitudinal waves and not shear waves. The results obtained agree with those from Papadakis, Lynnworth, Fowler and Carnevale (1972) who used the momentary coupling technique of conventional ultrasonic transducers. It was unknown whether the abrupt increase in ultrasound amplitude near the Curie point was due to the temperature dependence of electromagnetic generation and detection or temperature dependence of scattering and absorption mechanisms of ultrasound in steel or a combination of the two.

A review, carried out by Budenkov and Gurevich (1982), describes scientific publications concerning contactless methods of ultrasonic non-destructive inspection. Included is a detailed survey of EMAT devices. The review outlines the three main ways of exciting elastic waves;

1) on the surface of the object being inspected (either by contact, immersion or the EMA method for materials with good conductivity)

2) in some surface volume (due to magnetostrictive forces in the vicinity of the Curie point or by the EMA method at high frequency)

3) within the object being inspected far from the surface (the acoustic emission method)

Work by Budenkov and Gurevich using lasers to produce ultrasound pulses in iron showed that an increase in the amplitude occurred at the Curie point. This method of generation did not use an electromagnetic technique. The increase in amplitude was apparently due to the thermostriction effect. As the temperature approached the Curie point, a change in the temperature of the surface layer, caused by the pulse of laser light, was sufficient to convert the ferromagnetic material to paramagnetic. This was accompanied by a volume change so that the thermostriction effect was added to the usual thermoelastic effect.

Detailed work was undertaken by Trigubovich and Domorod (1984) to produce a mathematical model for the relationship between ultrasound, created by an electromagnetic method, and temperature. Using the Weiss-Heisenberg theory and Landau's theory, expressions were derived for the temperature dependence of the Lorentzian and magnetostriction components of the ultrasonic amplitude. This function was determined by the magnetic induction in the case of the Lorentzian component and by the product of the differential susceptibility of the magnetisation in the case of the magnetostriction component. An abrupt increase in the magnetic susceptibility near the Curie point was said to enhance the magnetostriction mechanism for creating ultrasound.

Trigubovich and Domorod suggested that Landau's theory could explain the increase in amplitude at higher temperatures and was due to a change in the magnetostriction forces. Figure 2.28 shows comparisons between experimental values of the amplitude of ultrasonic vibrations with the mathematical model. The magnetostriction component agreed well with experiment and the Lorentzian component, in contrast to the experimental function, reduced as temperature increased.

The factors influencing the ultrasonic amplitude with temperature increase are magnetisation and magnetic susceptibility; conductivity having no effect. The sharp increase in susceptibility near the Curie point is attributed to an enhancement of the magnetostriction mechanism. The Lorentzian component of the amplitude diminishes together with magnetisation as temperature increases.

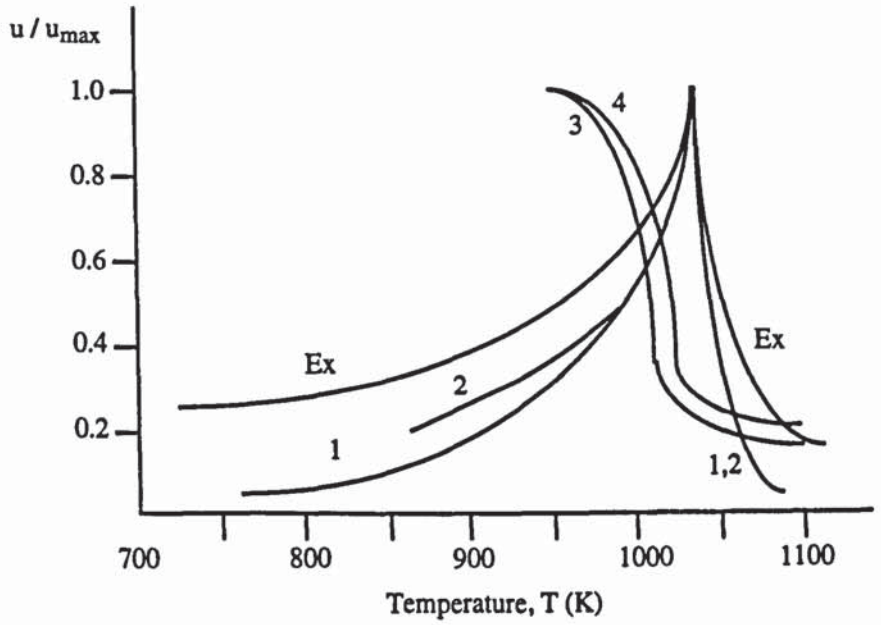

Figure 2.28 Theoretical and Experimental Amplitude of Ultrasonic Vibrations as a Function of Temperature

Curve	Function
Ex	Experimental function
1	Magnetostriction component according to the Weiss-Heisenberg theory
3	Lorentzian component according to the Weiss-Heisenberg theory
2	Magnetostriction component according to Landau's theory
4	Lorentzian component according to Landau's theory

Table 2.1 Key to Figure 2.28

All the typical applications of an EMAT together with some basic principles are listed by Alers and Burns (1987). Included are portable EMATs for hand inspection, water cooled EMATs for use on material up to a temperature of 1300°C, EMATs for rapid on line inspection, an EMAT designed to inspect rail track and EMATs for bar and tube inspection during fabrication.

Boyd and Sperline (1988) showed that ultrasonic waves could be generated using a pulsed laser and detected using an EMAT. The amplitude of ultrasound in a carbon steel was measured up to 900°C and found to increase just before the Curie point. The mechanism responsible was claimed to be the same as that stated by Kawashima, Murota,

Nakamori, Soga and Suzuki (1979). The ability to detect Barkhausen noise at temperatures below the Curie point using this system was reported. Barkhausen noise was due to the relaxation of the pulsed magnetic field used in the EMAT receiver.

The success of EMATs in field trials has been reported by Cook, Jackson and Droney (1989). An increase in amplitude of the signal near the Curie point in ferromagnetic materials is mentioned, but no explanation for the cause is given.

Detection of flaws on the internal wall of a tube could only previously be carried out by eddy current and flux leakage methods if the wall was thin (< 1 cm). Ultrasonics allows the inside of a thicker tube to be inspected. Alers (1991) describes an EMAT as a method for tube inspection at high speeds and high temperatures.

Lee and Ahn (1992) investigated the application of an EMAT at high temperature up to 800°C on specimens of aluminium, stainless steel and mild steel. The velocities and amplitudes of ultrasonic waves were investigated in each of the materials as a function of temperature. The transducer was driven by a high power pulse and was water cooled so that it remained under 100°C even though it was placed in a furnace with a maximum temperature of 800°C.

The results show that in aluminium and stainless steel the velocity decreased linearly with increase in temperature. This was because the temperature dependence of elastic constants is inversely proportional to the square of temperature. The results of amplitude of the ultrasonic wave against temperature show that for aluminium and stainless steel, the amplitude decreases as a function of temperature due to attenuation within the material. In the case of mild steel, the amplitude increased significantly between 600°C and 800°C for shear waves and between 715°C and 735°C for longitudinal waves, figure 2.29. It is hypothesised that the large increase was due to magnetostriction, which occurred when the surface of the steel cooled, so that the interior was still paramagnetic whilst the surface had become ferromagnetic. A spatial variation in the static magnetic field then occurred at the boundary area between the region under the transducer and the region just near the transducer.

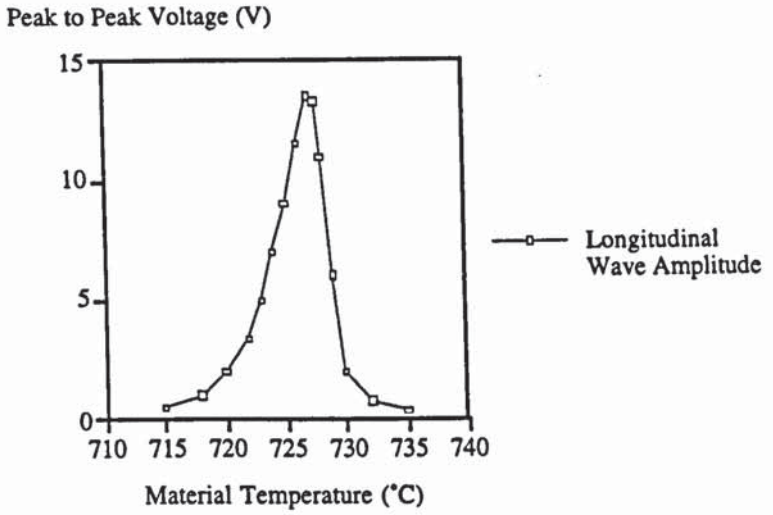

Figure 2.29 Temperature Dependence of Longitudinal Wave Amplitude in Steel.

An investigation into the directional patterns of EMA transducers for high temperature ultrasonic testing was carried out by Gurevich and Gal'tsev (1993). An EMAT was used to create ultrasound in an alloy of invar which had a Curie point of 207°C. The test simulated the properties of ferromagnetic steels in the temperature range 750-800°C. Tests were also carried out in the absence of the steady field indicating that the generation of ultrasound was due to bulk magnetostriction. Near the Curie point an increase in the amplitude of the ultrasound was observed, even without the steady d.c. field. The reason given is that the paraprocess state, described earlier by Budenkov and Maskaev (1973), can be achieved by magnetisation or temperature.

2.10 Conclusions

This chapter has reviewed a wide range of topics directly and indirectly associated with this research. An introduction has been given of the basic theory of induction heating, properties of steels as a function of temperature and longitudinal vibration in bars.

It is shown that there are many changes which take place within iron or steel in the vicinity of the Curie point, which may or may not be linked to the increases in longitudinal vibration when heated by electromagnetic induction.

Work involving the behaviour of iron or steel in magnetic fields has been continuing for almost a century and yet there are aspects which are still not fully understood. Very little data exists for many materials in the area of Joule magnetostriction as a function of temperature and the mechanism responsible for volume magnetostriction has not been established.

Only recently has a phenomenon similar to vibration during induction heating come to light using electromagnetic generation of ultrasound in metals. Many papers have been written postulating that an increase in the amplitude of longitudinal ultrasonic waves in ferromagnetic steel around 720°C is due to the enhancement of magnetostriction. However, ultrasound has also been generated using both lasers and conventional piezoelectric transducers and both report similar increases in attenuation of the ultrasonic waves just before the Curie point. In the latter case there were no magnetic fields involved, suggesting that the enhancement is possibly due to changes in the materials properties near the Curie point rather than external influences.

It is highly likely that there are similarities between the work involving ultrasound and that of induction heating and both are brought together in this chapter for comparison and completeness.

Finally it has been shown that previous published work concerning EMATs is not in agreement when discussing both the results and possible hypotheses.

CHAPTER THREE

MEASUREMENT OF VIBRATION DURING INDUCTION HEATING

3.1 Introduction

The majority of this research involved detailed experimental work in order to collect data concerning vibration in steel when heated by induction. The very nature of induction heating, strong electromagnetic fields and high temperatures, made it difficult to use many types of instrumentation for measuring data. This chapter deals with the measurement of vibration and the study of the microstructure of a mild and medium carbon steel after heating. The measurement of magnetostriction, which was thought to be a possible mechanism for the vibration, is covered in a separate chapter.

Towards the end of the project, a software package called LabView† became available for use with this work. Earlier tests were repeated and the data collected using LabView. Using this package it was possible to obtain data at more frequent time intervals and to save it into data files for later use.

3.2 Apparatus

Most of the equipment used for the practical work in this project was commercially available 'off-the-shelf'. Some equipment however was designed and constructed for specific work where necessary.

3.2.1 Inverters and Coils

The majority of experiments used a commercial 60 kW, 3.2 kHz Crossley induction heater. The results from these tests were compared with results using a 100kW, 2.4 kHz Radyne induction heater. The Radyne heater had a pigeon hole coil arrangement, similar to that used for industrial bar end heating, in which three coils were connected in series. Measurements were made on a bar heated in the central coil with either the bar resting on the refractory or being suspended horizontally just above the refractory using steel cable. The specification for the Radyne induction heater can be found in Appendix A.1.3.

The coil used with the Crossley heater was constructed so that access to the bar was possible during heating. Only half of each turn was embedded in the refractory base

† LabView is a registered trademark of National Instruments Corporation.

with the remaining part of the turn being covered in an insulating resin. The coil consisted of 24 turns and had a gap of approximately 3 mm between each turn. The overall size of the coil and refractory was 350 mm in length by 230 mm wide and 160 mm deep.

The coil could be arranged vertically or horizontally depending on the nature of the test carried out. In the vertical position, bars were hung vertically down through the coil from an overhead support. A sturdy rig was constructed to hold the coil in this position whilst allowing for instrumentation to be attached to the bar, and a supply of cooling water to flow over the lower end. Figure 3.1 shows the arrangement.

For the coil in the horizontal position the bar was supported just above the refractory by cables at either end which were themselves attached to an overhead fixture, figure 3.2. It was also possible to rest a bar directly onto the refractory, as would be the case in industrial heating, but it was decided to separate the bar from the coil to isolate it from external vibrations.

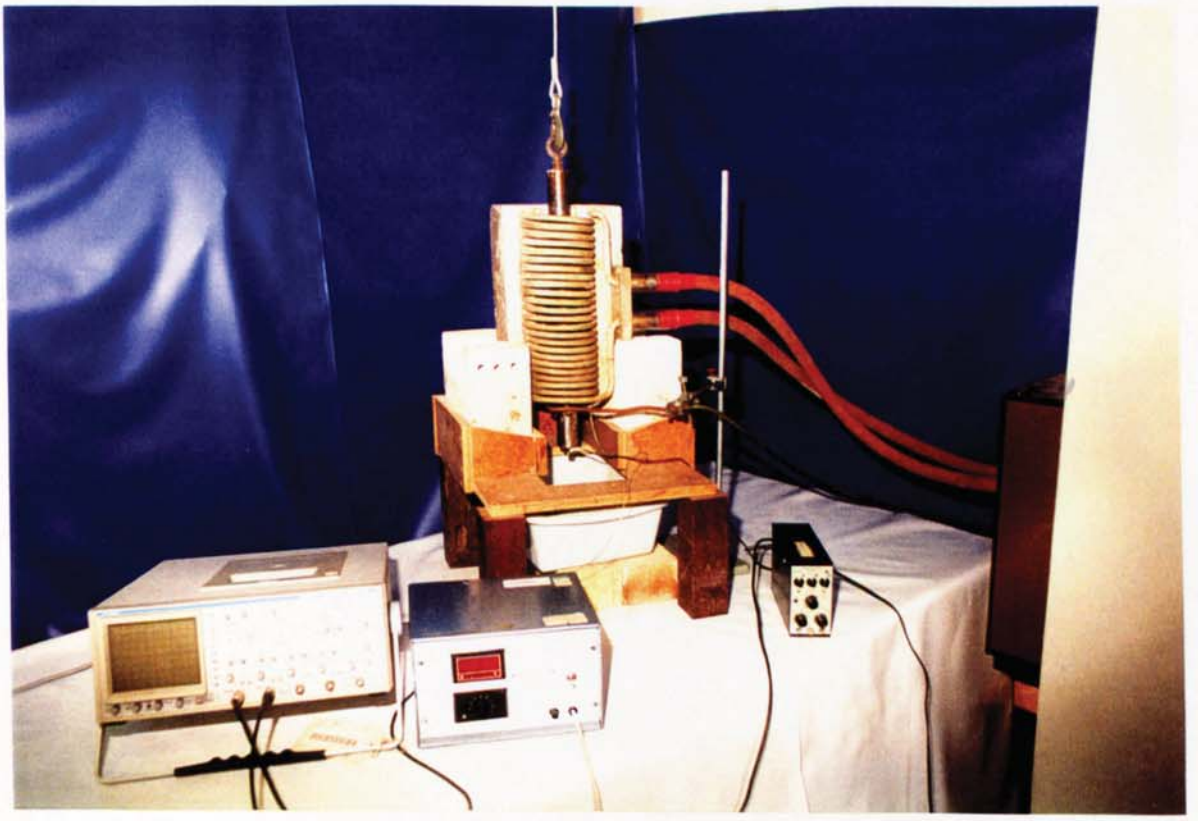

Figure 3.1 Photograph of Vertical Coil Arrangement

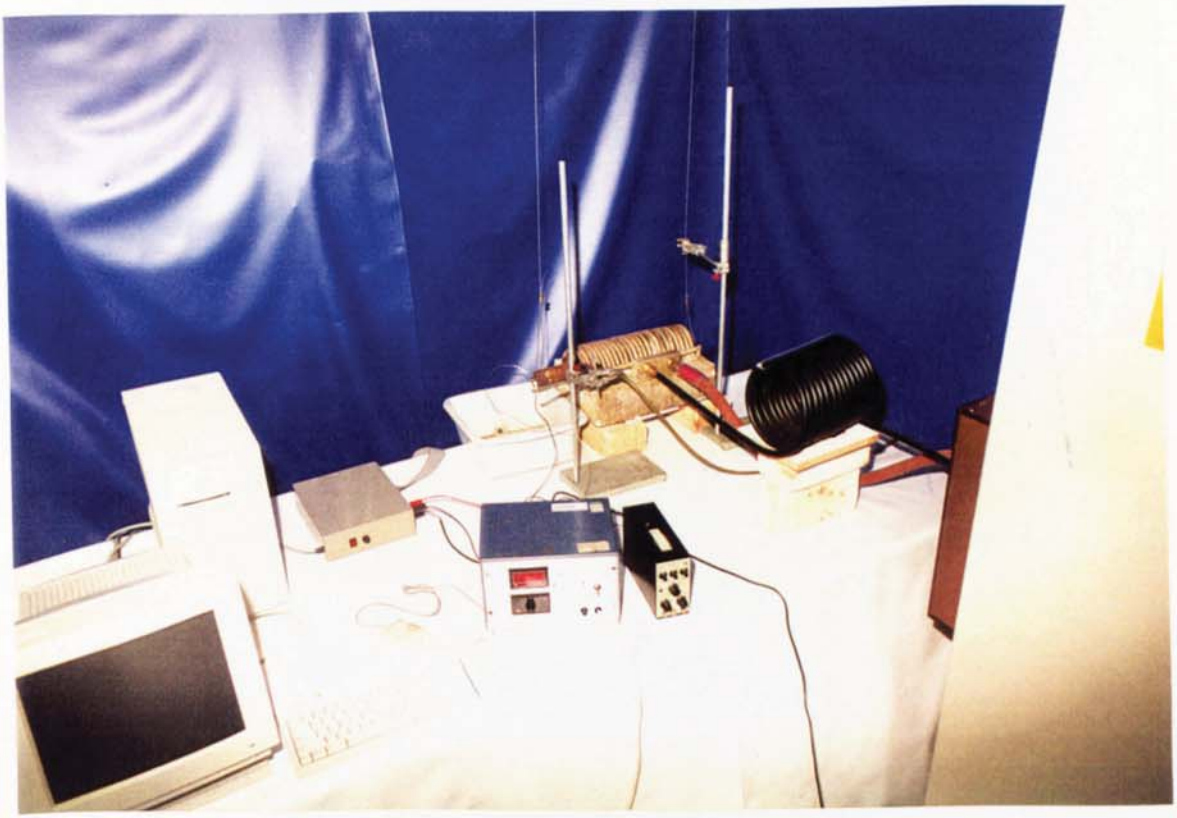

Figure 3.2 Photograph of Horizontal Heating Arrangement

The 24 turn heating coil was not of a high enough inductance for the inverter resonant circuit. To overcome this a matching coil was placed in series with the heating coil. It consisted of 14 turns and was not used for heating. The number of turns on the heating coil could have been increased instead of having a matching coil, but would have increased the length of the coil and made measurements using two accelerometers difficult on 600 mm long bars.

3.2.2 Materials Tested

Bars of different material and of varying dimension were heated in the induction heater. Table 3.1 shows the materials used and their composition.

Material	Dimensions
Copper Bar (C101)	ϕ 38 mm x 500 mm
Austenitic Stainless Steel Bar (304S11)	ϕ 40 mm x 500 mm
Titanium Bar (TI-2) ASTM-B-348 Grade 2	ϕ 40 mm x 500 mm
Monel 400 Bar (70% Ni, 30% Cu)	ϕ 40 mm x 500 mm
Iron Bar (Remko B) (0.025% C)	ϕ 41 mm x 500 mm
0.4% Carbon Steel Bar (BS970-080A42)	ϕ 40 mm x 500 mm
1.5 % Carbon Steel Bar (AISI D2)	ϕ 40 mm x 500 mm
Mild Steel Bar (BS970-En3b) (0.2% C)	6 x ϕ 40 mm x 600 mm
Mild Steel Bar (BS970-En3b) (0.2% C)	2 x ϕ 25 mm x 600 mm
Mild Steel Bar (BS970-En3b) (0.2% C)	2 x ϕ 50 mm x 600 mm
Mild Steel Bar (BS970-En3b) (0.2% C)	2 x 40 mm x 40 mm x 600 mm

Table 3.1 Materials Tested

Phase changes occurred in some of the materials listed above when heated to high temperature. For example, with the low carbon and mild steels, normalising occurred after heating to 1000°C and allowing to cool in air. The medium carbon steel hardened if quenched in water under certain heating conditions. The high carbon steel hardened in air after heating to high temperature, so it was important to correctly carry out the test the first time using this material.

3.2.3 LabView Computer Software

LabView is a powerful virtual instrument (VI) software package. Once raw data has been input to the computer, it can be processed in a variety of ways. For example the software can act as an oscilloscope, a spectrum analyser or a chart recorder. The data can be easily graphed and stored in files.

This package was chosen towards the end of the project because it had the ability to sample and save data quickly, which was important given the short duration (two minutes) of the heating tests. It was possible to record the frequency components of vibration many times during heating to show the changes occurring at different temperatures of the bar. The spectrum analyser VI collected data from an oscilloscope VI, which sampled at 40 kHz, and calculated a power spectrum from it. The maximum frequency that the spectrum analyser VI could depict was 20 kHz. Errors will have arisen

due to the sampling rate of the oscilloscope which was only twice the frequency of the measured signal. The spectrum analyser was tested using a signal generator and coped well up to the maximum of 20 kHz on both square and sinusoidal waveforms.

3.3 Instrumentation

3.3.1 Temperature Measurement

Surface temperature was measured at the mid point of each bar using a K-type thermocouple (NiCr / NiAl). These have a temperature range of -160°C to 1370°C, although their accuracy is only quoted by the manufacturers over the range 0°C to 1100°C as:

$$0°C \text{ to } 400°C = \pm 3°C$$
$$400°C \text{ to } 1100°C = 0.75\%$$

The mid point was chosen because it was the hottest part of the bar during heating. The mineral insulated, inconel sheathed thermocouple was held in place at the surface by filing a groove in the bar, inserting the thermocouple tip and then peening the metal over it to hold it firmly. No adhesive could be used to hold the thermocouple because of the high temperatures involved. The method adopted has some distinct disadvantages. Firstly, the thermocouple does not measure surface temperature but an average temperature over the top two or three millimetres because of its diameter of 2 mm. Secondly, distortion of the eddy currents flowing around the thermocouple fixing will occur and could cause differences in the heat generated in the area of the thermocouple. Other problems arise including a reduction in the temperature of the thermocouple tip due to conduction along the sheath, possible induced voltages in the lead due to high alternating electromagnetic fields in the induction heater, and a small error in the thermocouple and instrumentation itself. The temperature profile through the bar was calculated knowing the surface temperature and power input according to equation 2.2.

Centre temperature was measured on selected bars by drilling a small hole and inserting a K-type thermocouple. It was secured with a high temperature cement. The sheathed thermocouple has its junction at the very tip so it was assumed that the temperature from this arrangement would be a reasonable measure of the temperature at the centre of the bar. Again, errors will occur as outlined above.

Each thermocouple was connected to a meter which gave a visual indication of temperature and a linear output of 1mV/°C to connect to an oscilloscope or LabView.

Surface temperature measurement was also attempted using a pyrometer. This was not adopted as a technique because the emissivity had to be set manually, by estimation. A change of 0.2 in emissivity was found to give a temperature difference of 30°C at 210°C and 61°C at 800°C. That is 1.5°C and 3°C respectively for a change of 0.01 in emissivity. The emissivity also changed from bar to bar and from test to test depending on the amount of scale on the bar and it was decided that the thermocouple would indicate a more accurate value of surface temperature.

3.3.2 Vibration Measurement

For bars of length 400 mm and greater, the longitudinal vibration was measured at one or both faces of the bar using an accelerometer. This was possible because the instrument was not in the region of high field and consequently was not directly heated. However, conduction along the bar would have damaged the accelerometers so it was necessary to cool one or both ends using water. This was delivered from a quench ring which encircled the end of the bar. The specifications of the accelerometers used can be found in Appendix A.1.4. The small, lightweight instrument was attached firmly onto the face of the bar using electrically insulating studs and mica washers. It was necessary to insulate the accelerometer from the bar otherwise earth loops were set up between the instruments, producing often spurious and unreliable results. Silicone rubber was used to cover the connection to the accelerometer to prevent water ingress. Accelerometers were chosen for several reasons; they are very sensitive to the accelerations produced, are relatively compact and lightweight which only affected the measurements to a small degree and when attached to the bar, thermal expansion did not affect the vibration signal.

The accelerometer output was connected to a charge amplifier, with the output sensitivity set to 0.1 V/g, and connected to a spectrum analyser to obtain a set of data with respect to frequency of the vibrations, or via a rectifier to a digital oscilloscope to give the total magnitude of vibration. The latter was often used as it gave a distinct indication of when the amplitude of vibration increased. When connected to LabView, the output sensitivity was set to 0.01 V/g to keep the signal below the 5 volt input level. The full specification can be found in Appendix A.1.5.

The equipment necessary to rectify the a.c. signal consisted of a bridge rectifier with a resistance and capacitance in parallel as shown in figure 3.3. The values of C and R were chosen to give an adequate time constant so that the output waveform had little ripple. When the circuit was switched on, the capacitor charged through the two forward biased diodes to the peak voltage of the unsmoothed rectified waveform. As the sinusoidal voltage feeding the diodes swung below its peak, the diodes became reverse biased. As the other two diodes were still reverse biased, the capacitor discharged

through the resistor with time constant RC for almost half a cycle. When the voltage driving the second pair of diodes exceeded that of the capacitor, they became forward biased and the capacitor recharged to the peak voltage. The discharge, charge cycle repeated with charging alternatively taking place through each diode pair.

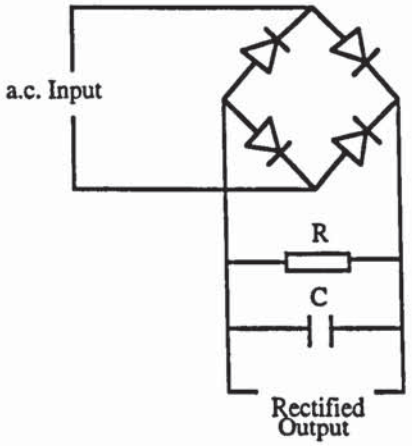

Figure 3.3 Rectifier Used With Vibration Measurements

Using $R = 4200\ \Omega$ and $C = 6.5\ \mu F$

$RC = 27.3$ ms

The lowest frequency to be detected was 3.2 kHz. This became 6.4 kHz after rectification with a time period, T of 0.17 ms. The RC value was much greater than this, leading to a smoothed output with little ripple.

From Hunter (1970) the d.c. voltage, V_{dc} was related to the peak sinusoidal voltage, V_p by:

$$V_{dc} \approx V_p \left[1 - \frac{T}{2RC} \right] \qquad (3.1)$$

Using the above values, $V_{dc} / V_p = 0.997$. Hence, the difference in the voltages was negligible and the output voltage was regarded as being the same magnitude as the input voltage.

For bars shorter than the length of the coil it was impractical to use accelerometers since they would be directly heated and exceed their operating temperature. An Ometron VS100 laser vibrometer was therefore used; its specification can be found in Appendix A.1.6. There was no need to use retro-reflective material or paint on a sample of steel up to 1000°C. The laser was focused by means of a lens until the reflected signal was of maximum intensity, indicated by LED's on the head. An output, taken directly from the head, was connected to a spectrum analyser or through the rectifier to a digital

oscilloscope. This output was directly proportional to the velocity of the surface measured. There was no need to water cool the ends of the bars. This method had the advantage of not having to add weight to the bar being measured. The laser was also used to measure vibration of the coil and transverse vibration of the bar at its mid point, measured through the gaps in the coil. This was not possible with accelerometers.

3.3.3 Noise from Accelerometers

One of the main disadvantages of using accelerometers was the noise produced by the electromagnetic field. This was investigated by placing the accelerometer near to the face of a bar of mild steel when heated at 60kW, figure 3.4. The signal was found to be of low amplitude (100 times lower) when compared to the signal produced when attached to the heated steel bar. The noise at 3.2 kHz was of the greatest magnitude which did not affect the results collected at higher frequencies.

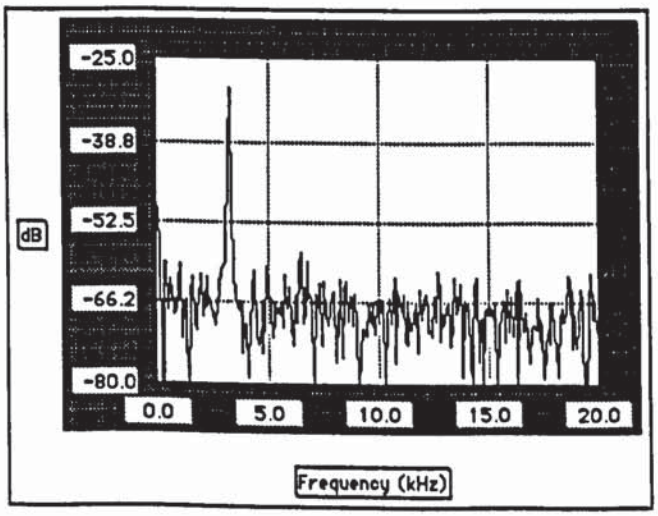

Figure 3.4 Frequency Components of Noise from Accelerometer

Cooling the end of the bar with water produced vibration in the bar and unwanted signals in the accelerometer. However, this signal was at low frequency (< 200 Hz) and was ignored.

When measuring longitudinal vibration at the face of the bar, there was a small amount of pick-up from other vibration modes such as transverse. To overcome this, transverse vibration was measured at the ends of the bar to compare to the longitudinal vibration recorded.

3.3.4 Field Measurement

The magnitude of the magnetic field was measured using a search coil. The values were compared with those calculated for a solenoid. The current flowing in the coil was measured using a Rogowski coil which had an air core, so did not saturate, and was also linear in its measuring range.

The Rogowski coil was calibrated on a known 50 Amp (I_{ref}), 50 Hz (f_{ref}) supply. The voltage output, V_{ref} from the coil was noted. It was then placed around the inverter coil conductor and the voltage output recorded when the inverter was at full power and unloaded. The current flowing through the inverter coil was calculated using:

$$I_{coil} = I_{ref} \frac{V_{out}}{V_{ref}} \frac{f_{ref}}{f} \tag{3.2}$$

giving I_{coil} = 1033 Amps for a frequency, f = 3.2 kHz.

The field strength, H was calculated using Amperes Law:

$$H = \frac{NI_{coil}}{l} \tag{3.3}$$

where H = field strength (Am^{-1})
N = number of turns
I_{coil} = rms coil current (A)
l = length of coil (m)

The Crossley induction heater coil had 24 turns and its overall length was 0.35 m. The field strength, H was calculated to be 70860 A/m (rms).

The measured value of field strength was obtained by using a search coil in the unloaded coil. The field strength was found using:

$$v = -N \frac{d\phi}{dt} \tag{3.4}$$

$$B = \frac{\phi}{A} \tag{3.5}$$

$$H = \frac{B}{\mu_0} \tag{3.6}$$

where N = number of turns on search coil

ϕ = flux (Wb)

A = area of search coil (m^2)

H = field strength (Am^{-1})

B = flux density (T)

μ_0 = permeability of free space (Hm^{-1})

v = rms voltage (V)

t = time (s)

The measured field strength was calculated to be 68580 A/m (rms), equating to a peak flux density of 0.12 T.

The search coil was used to obtain the frequency spectra of the magnetic field. The coil current contained harmonics, produced by the inverter circuit, which led to harmonics in the field. These can be seen in figure 3.5. Peaks were recorded at 3.2 kHz, 9.6 kHz and 16.0 kHz. This was expected since the inverter load current contained both third and fifth harmonics.

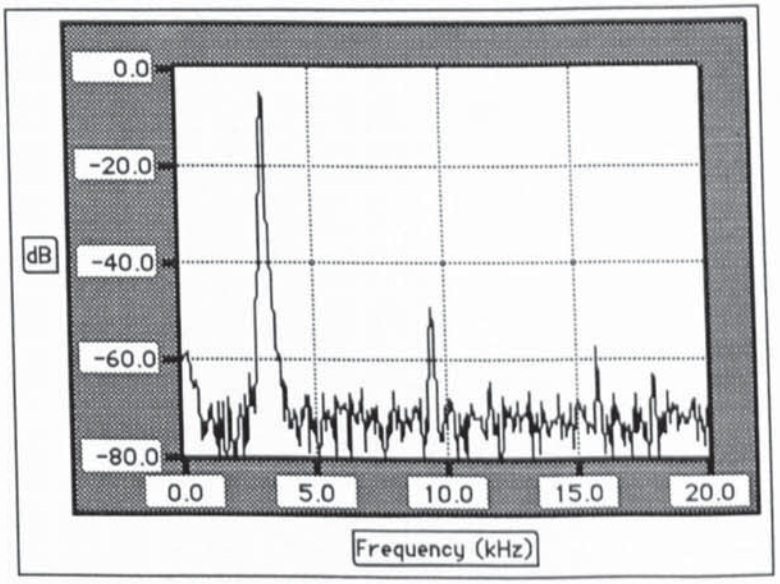

Figure 3.5 Frequency Spectra of Electromagnetic Field

A search coil was also designed to measure the flux density in a mild steel bar when heated at different powers in the induction heater. This was primarily carried out to estimate the saturation magnetisation of a bar of En3b mild steel at different temperatures, to be used in magnetostriction calculations. More detail can be found in chapter 4, together with BH curves for the mild steel.

The field components at 3.2 kHz, 9.6 kHz and 16.0 kHz produced direct magnetostrictive vibrations at twice these frequencies, 6.4 kHz, 19.2 kHz and 32.0 kHz.

3.3.5 Heating Coil Current Measurement

Using the Rogowski coil the current flowing through the heating coil was measured while a 600 mm mild steel bar was heated. The frequency components recorded are shown in table 3.2.

Frequency (kHz)	3.2	9.6	16.0
dBV	8.5	-33.5	-46.3
Voltage (V)	2.66	0.021	0.005
Percentage	99%	0.78%	0.18%

Table 3.2. Frequency Components of the Loaded Coil Current

The proportion of each of the current components in the loaded coil were very similar to the proportion of the measured field components in the unloaded coil.

3.3.6 Power Measurement

The power of the induction heater was monitored by taking a signal from the displayed power output from the inverter and connecting it to the digital oscilloscope or LabView. The power trace could then be compared with the temperature plot. A typical plot is shown in figure 3.6. The power was seen to rise quickly at the start of the heating process. As the temperature of the mild steel bar increased, the power decreased initially. The power reached a maximum when the bar's surface temperature was near the Curie point. The reason for this according to Davies and Simpson (1972) is thought to be due to the changes in skin depth and resistivity of the bar at this point.

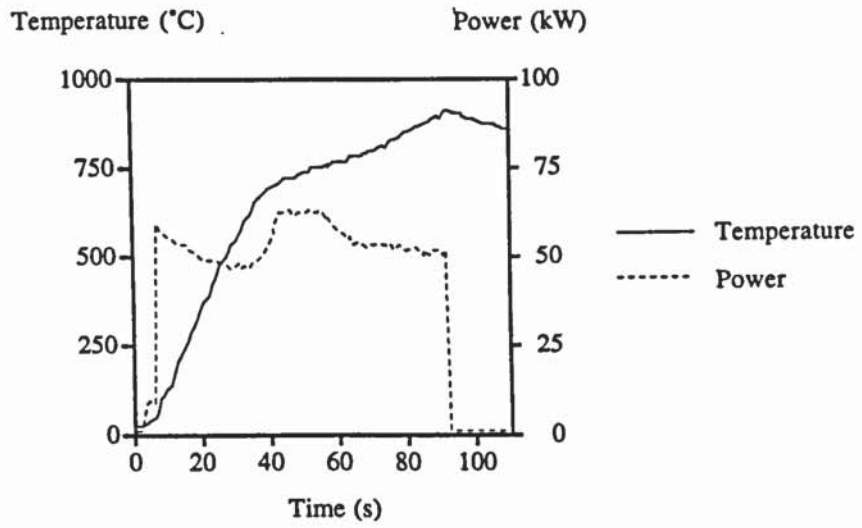

Figure 3.6 Power Input to a Mild Steel Bar During the Heating Process at Full Power

3.4 Temperature Distribution in a Mild Steel Bar

Tests were carried out to measure both the surface temperature and centre temperature of a steel bar, heated at different power levels. Figure 3.7 shows the result of heating a 600 mm long En3b mild steel bar at 60kW and figure 3.8 shows the result of heating the same bar at 30kW.

It can be seen from both graphs that as the surface temperature neared the Curie point, the rate of surface temperature increase fell rapidly. The rate of centre temperature increase of the bar did not fall off at such a rate and the average temperature of the bar continued to increase.

Heating at 30kW showed that the centre temperature actually exceeded the surface temperature after the Curie point had been reached. This was due to the losses at the surface and an increase in the skin depth, leading to lower power densities in the surface layers of the bar.

Davies and Simpson (1972) state that the surface and centre temperature will rise at the same rate after an initial transient. One reason why these results do not agree with this statement is because only part of the length of the bar was heated directly. One end was continuously cooled with a stream of water for instrumentation purposes and the other end cooled in air. This caused heat to flow along the bar as well as towards the centre altering the temperature distribution in the bar.

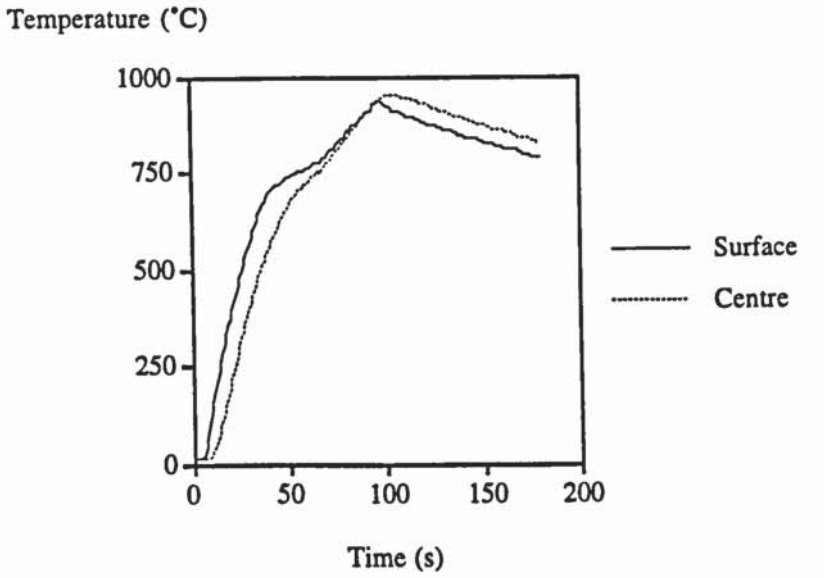

Figure 3.7 Surface and Centre Temperatures of a 600 mm Long Mild Steel Bar Heated at 60kW

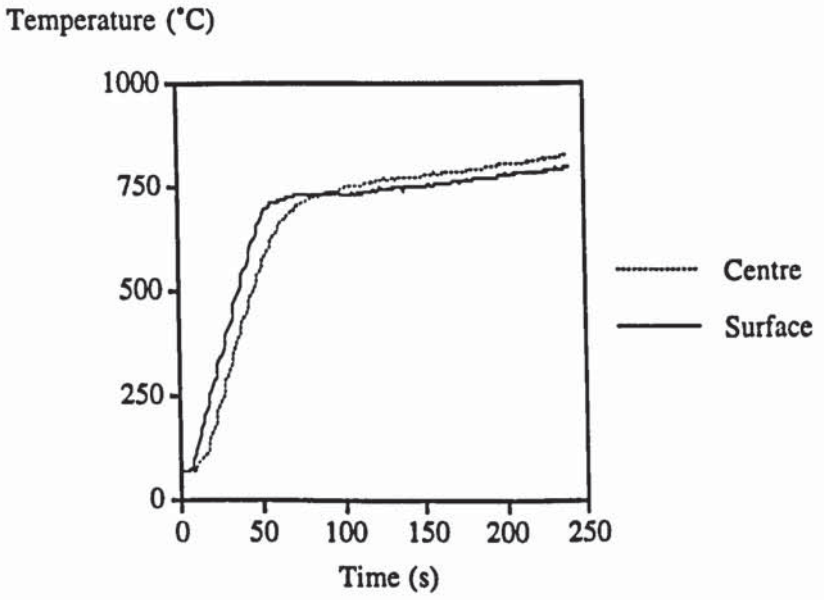

Figure 3.8 Surface and Centre Temperatures of a 600 mm Long Mild Steel Bar Heated at 30kW

3.5 Longitudinal Vibration in Ferromagnetic Steel Bars

When a bar of steel was heated by induction, the surface temperature at the mid point of the bar increased quickly. This was accompanied by vibration of low magnitude at several frequencies, most likely originating from magnetostriction. As the bar increased further in temperature (700°C) the longitudinal vibration often suddenly increased in magnitude for a few seconds before falling to its original lower value.

No striated heating was seen to occur on the bar's surface due to the low frequency used producing nodes at a distance greater than the length of the bar. According to Langman (1987), striated heating is also not observed if:

$$f \geq \frac{10^5}{d^2} \text{ Hz} \tag{3.7}$$

where f is the frequency of the induction heater (Hz)
d is the heated thickness of the bar (mm)

In this case d is equal to the skin depth at the start of heating and for mild steel heated at 3.2 kHz is about 0.16 mm. According to Langman, the frequency must therefore be greater than 3.9 MHz in order to avoid striations. However, the nodal distance between striations for a 600 mm long mild steel bar is calculated to be 78 cm from equation 2.8, which is greater than the length of the bar.

3.5.1 Tests On Steel Bars Resting Horizontally in the Heating Coil

A 600 mm long En3b mild steel bar was placed in the coil, resting on the refractory and heated. An accelerometer was fixed to one face of the bar. The bar was heated from 20°C at 60 kW. Figure 3.9 shows the plot of longitudinal vibration magnitude, power and temperature as a function of time. A significant increase (up to 60g) in acceleration magnitude occurred as the surface temperature of the bar reached the Curie point. Although the power and vibration increases may occur almost simultaneously, this work has suggested that the vibration change is not as a direct result of the power change.

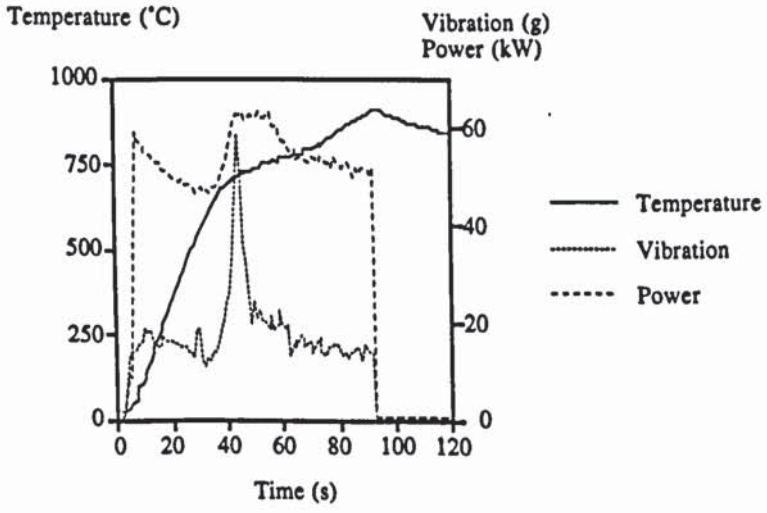

Figure 3.9 Vibration of a 600 mm Long Mild Steel Bar Heated at 60kW

The same bar was allowed to cool and reheated from 20°C at 30kW. Figure 3.10 shows the plot of vibration magnitude for this power. A large peak still occurred (60g) as the surface temperature of the bar reached the Curie point but the power is shown to decrease at this point indicating that there is no direct relation between power and magnitude of vibration. A smaller peak (20g) can be seen at the start of heating at about 200°C.

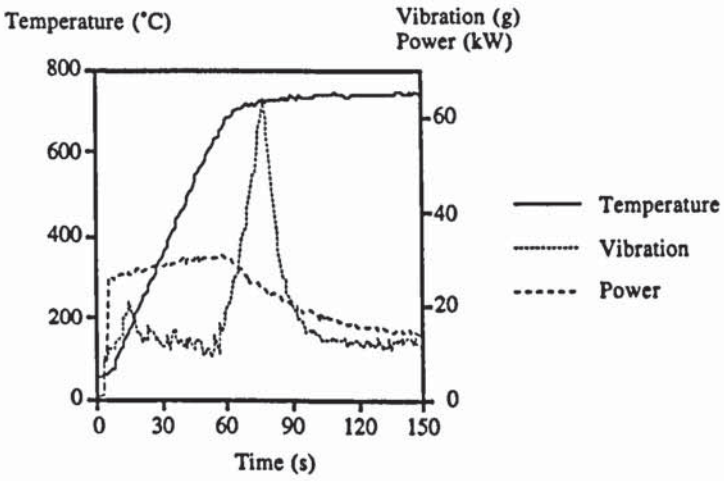

Figure 3.10 Vibration of a 600 mm Long Mild Steel Bar Heated at 30kW

The test at 30kW was repeated with the same mild steel bar, figure 3.11. The increase in vibration as the surface reached the Curie point was seen to be of a greater magnitude (110g) than in the previous similar test. Notice also the smaller peak at about 500°C corresponding to an increase in acceleration of about 40g.

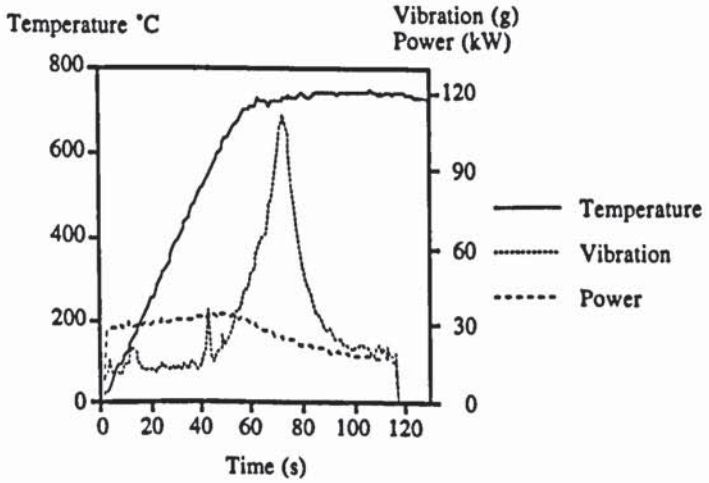

Figure 3.11 Vibration of a 600mm Long Mild Steel Bar Heated at 30kW (Repeat)

The bar was allowed to cool and reheated from 80°C at 20kW. The large increase in acceleration (70g) still occurred as the surface reached the Curie point but a peak (40g) at 500°C was again apparent, figure 3.12.

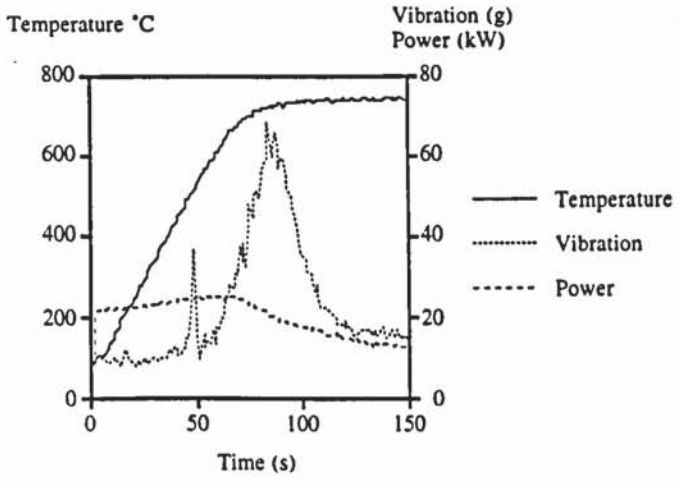

Figure 3.12 Vibration of a 600 mm Long Mild Steel Bar Heated at 20kW

The above figures show the magnitude of vibration over the whole frequency range determined by the conditioning amplifier (30 Hz to 30 kHz). When the frequencies of vibration were analysed at the peaks below the Curie point, figure 3.13 and at the Curie point, figure 3.14 there was a distinct difference.

It was stated in section 2.8.1 that an alternating electromagnetic field produces magnetostrictive vibrations at twice the field frequency and its subsequent harmonics. In this case the fundamental heating frequency was 3.2 kHz and the subsequent harmonic was the third at 9.6 kHz (figure 3.5). Magnetostriction was therefore expected to occur at 6.4 kHz and 19.2 kHz, but the above spectrum shows a considerable amount of vibration at 12.8 kHz. There was no field component at 6.4 kHz which would lead directly to magnetostrictive vibrations at 12.8 kHz. If the signal at 12.8 kHz was due to magnetostriction, then the mechanism for generation of the magnetostrictive vibration must be non-linear in order to produce harmonics.

At or near the Curie point, the main component of the vibration, in terms of acceleration, was at 19.2 kHz. It is already known that magnetostrictive vibration at this frequency is produced from the 9.6 kHz magnetic field component and there were a number of possible reasons as to why there should be an increase in the vibration at this temperature. These included an increase in magnetostriction near the Curie point, an interaction from the phase transformation which occurs near this temperature, or an interaction between the high magnetic field and damping within the material.

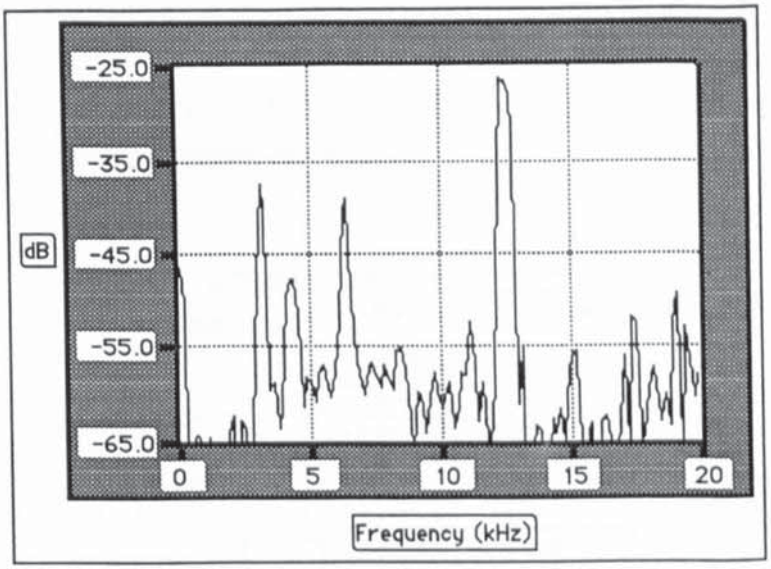

Figure 3.13 Frequency Components of Vibration at 500°C

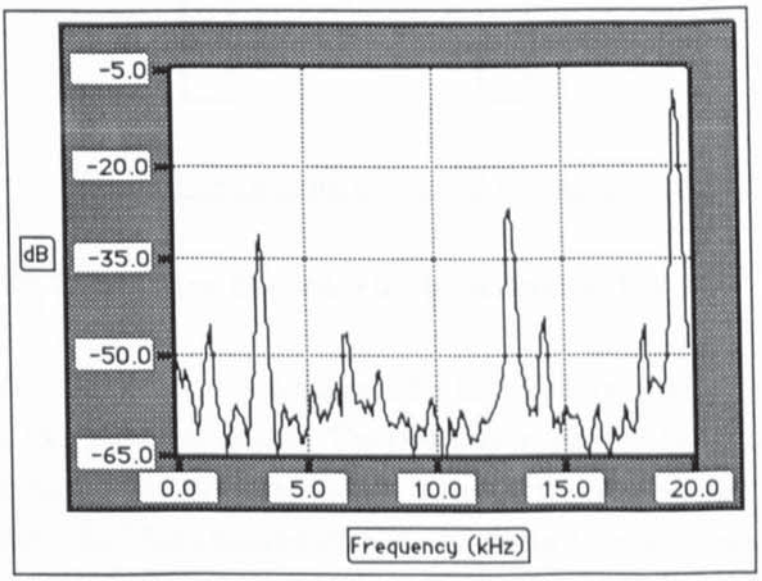

Figure 3.14 Frequency Components of Vibration at the Curie Point.

3.5.2 Tests Using Vertically Suspended Steel Bars

It was known that vibration from the coil was transmitted through the refractory to the bar. To eliminate this vibration from that of the bar, a vertical rig was constructed to hold the coil. The bar was then suspended by a cable from an overhead support. The accelerometer was fixed to the bottom face of the bar, cooled with a flow of water. Figure 3.15 shows the testing arrangement. The results were very similar to those obtained when heating a bar in the horizontal position, resting on the refractory. Further tests using the rig indicated that the position of the bar in the coil altered the results, even when

heated at the same power and from the same initial temperature. The reason for this was thought to be due to uneven lengths protruding from the coil at each end. It was decided not to continue to use this heating arrangement and use a modified horizontal arrangement. Chaloupecky (1980) also reported changes in results when the position of steel inside an induction heater was altered.

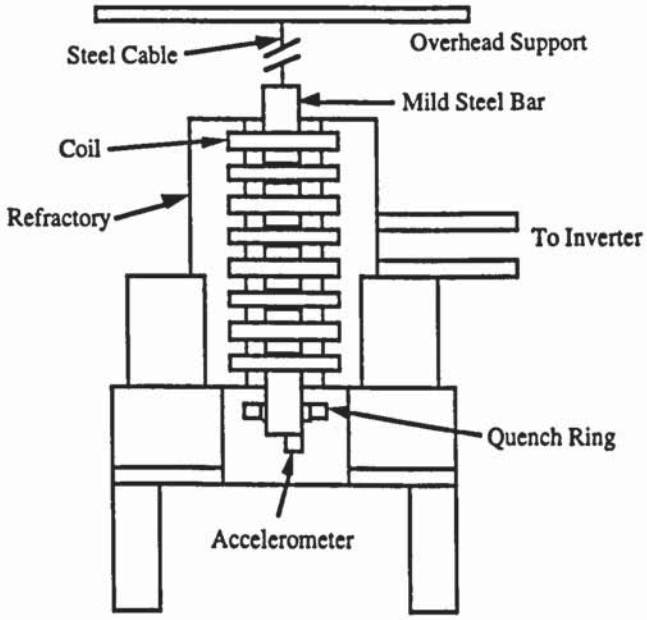

Figure 3.15 Diagram of Vertical Rig Arrangement

3.5.3 Tests on Steel Bars Suspended Horizontally Through Coil

An arrangement which was adopted for the majority of experimental work used ideas from the two previous set-ups. The coil was positioned horizontally and the bar was suspended a couple of millimetres above the refractory using a steel cable at each end of the bar, figure 3.16. This arrangement allowed the bar to be positioned centrally in the coil, with an equal length protruding from each end of the coil. It also allowed the bar to thermally expand in both directions as opposed to only downwards in the vertical arrangement and an accelerometer could be fixed to both faces of a bar during heating. The cables were fixed to a large overhead beam two metres above the coil. Two quench rings were used, one at each end of the bar, to keep the accelerometers cool.

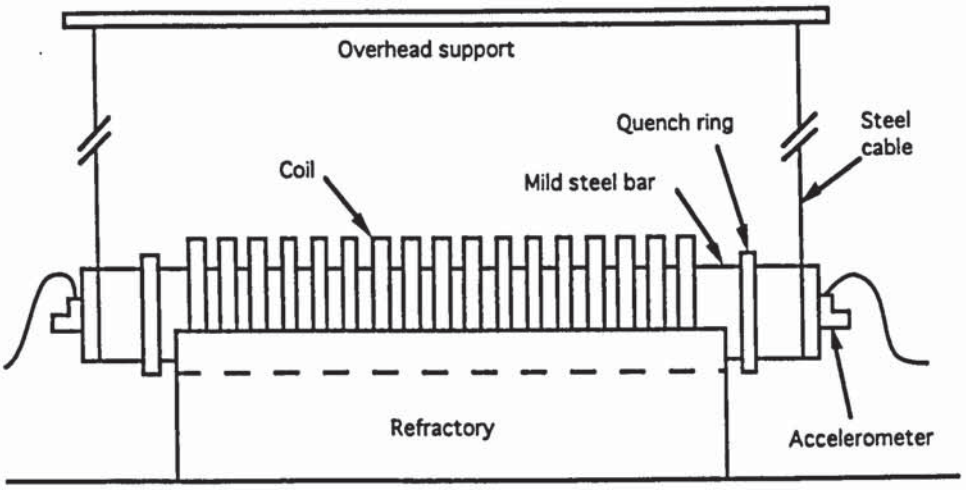

Figure 3.16 Horizontally Suspended Bar Heating Arrangement

Using this arrangement it was possible to allow the bar to swing freely inside the coil, or to hold it in position by lightly clamping the steel cables. Results were collected from a 600 mm En3b mild steel bar when heated from ambient temperature at 60kW, figure 3.17.

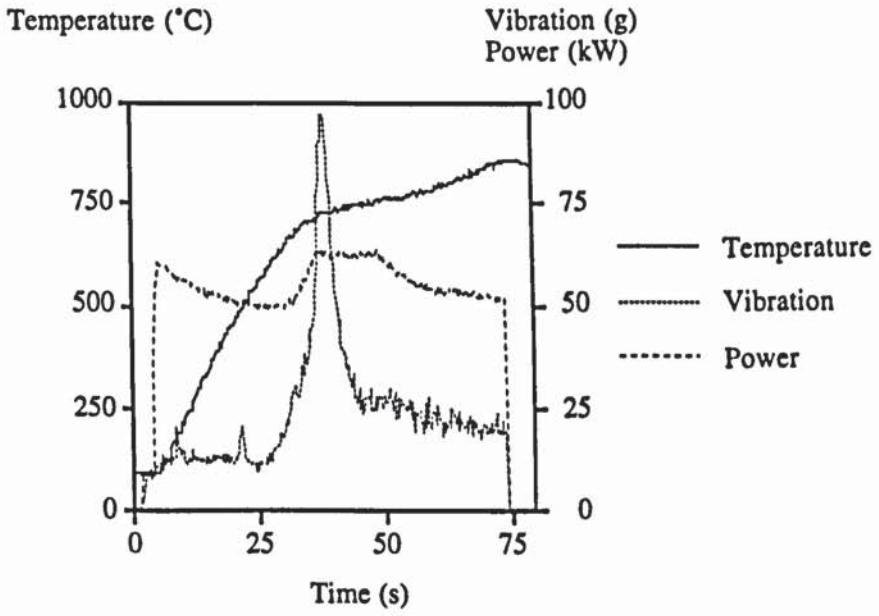

Figure 3.17 Temperature, Vibration and Power of a 600 mm Mild Steel Bar Heated at 60kW

The resulting graph, figure 3.17 is similar to the one obtained when the bar rested on the refractory, figure 3.9. As the surface temperature of the bar approached the Curie point, the magnitude of the longitudinal vibration increased significantly to 98g.

The tests were more or less repeatable with the increase occurring at the same temperature but not always of the same magnitude. Figure 3.18 shows the plots of

power, temperature and vibration when the above bar was heated on a separate occasion with identical conditions. Notice how the magnitude of acceleration only increased to 82g.

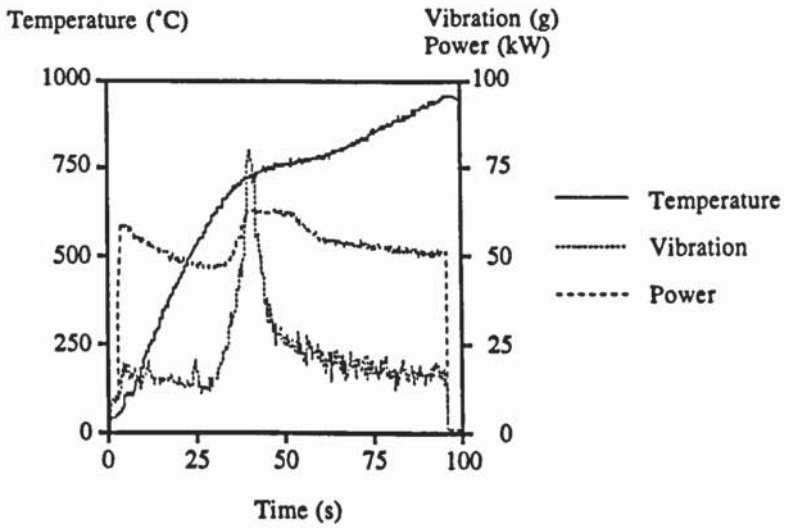

Figure 3.18 Temperature, Vibration and Power of a 600 mm Mild Steel Bar Heated at 60kW (Repeat)

The frequency components of vibration at the peaks near the Curie point were analysed and found to both consist of a large component at 19.2 kHz. Figure 3.19 shows the same bar heated from ambient temperature at 30kW. Again a peak of 70g occurred as the surface of the bar reached the Curie point. The magnitude of the vibration was slightly lower than in the previous figure, but was still due to the component at 19.2 kHz.

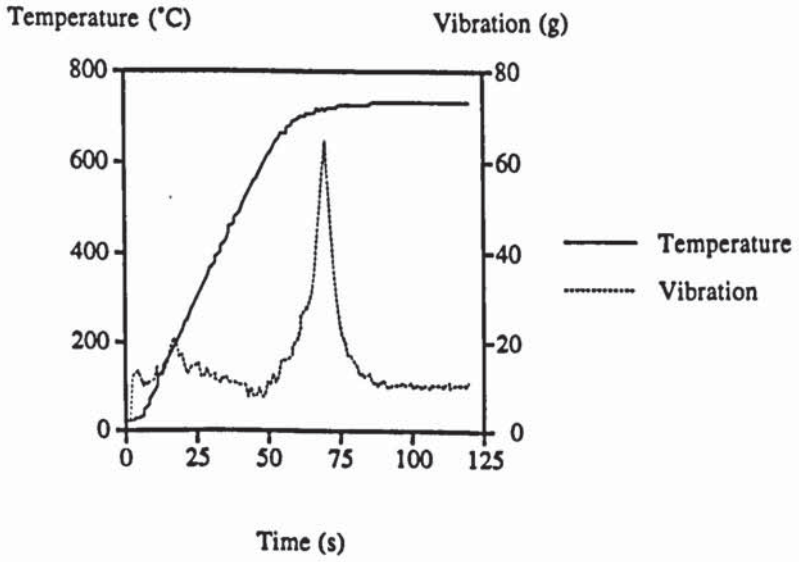

Figure 3.19 Temperature and Vibration of a 600 mm Mild Steel Bar Heated at 30kW.

From the above graphs it is apparent that the results are similar to those obtained when heating a bar when resting directly on the refractory. This indicates that the

vibration from the coil did not greatly affect the results. Even so, it was decided to continue to use the present arrangement.

It was possible, using LabView, to obtain frequency spectra of the vibration acceleration in the bar as heating progressed. Figure 3.20 shows nine such spectra. Each frame was taken 4 seconds apart as the bar was heated at 60kW from 50°C. There is an additional component at 15 kHz which was not apparent when the vibration was analysed using a Hewlett Packard F.F.T. analyser. It must therefore be assumed that the 40 kHz sampling rate of the spectrum analyser in LabView was not fast enough for signals up to 20 kHz and as a result the computation of the power spectrum to obtain the frequency components was not wholly accurate. The frames below should therefore be regarded as schematic indications rather than accurate values. The overall picture shows the component at 19.2 kHz increasing as the surface of the bar approached the Curie point.

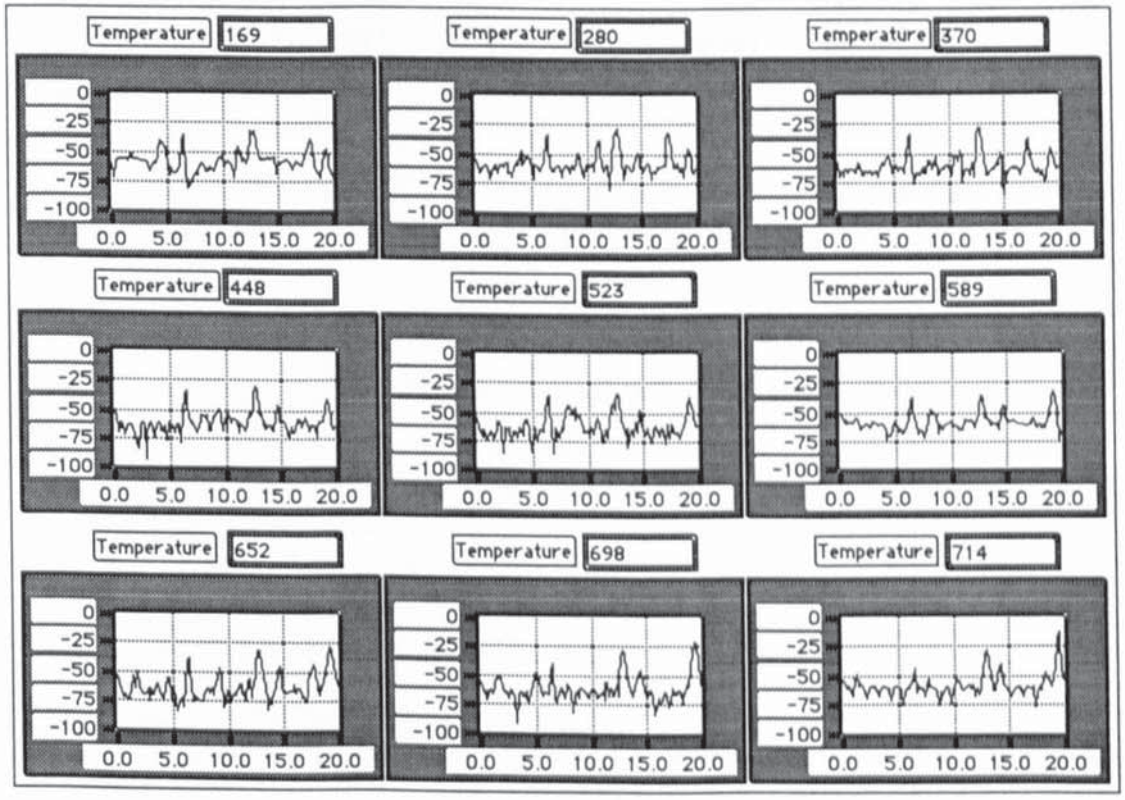

Figure 3.20 Frequency Components of Vibration from Heating a 600 mm Mild Steel Bar at 60kW.

Figure 3.21 shows a similar set of spectra for the same bar heated at 30kW. Each frame was recorded at 15 second intervals because of the increased duration of the test. At the start of heating there was a large component at 12.8 kHz and near the Curie point the 19.2 kHz component increased.

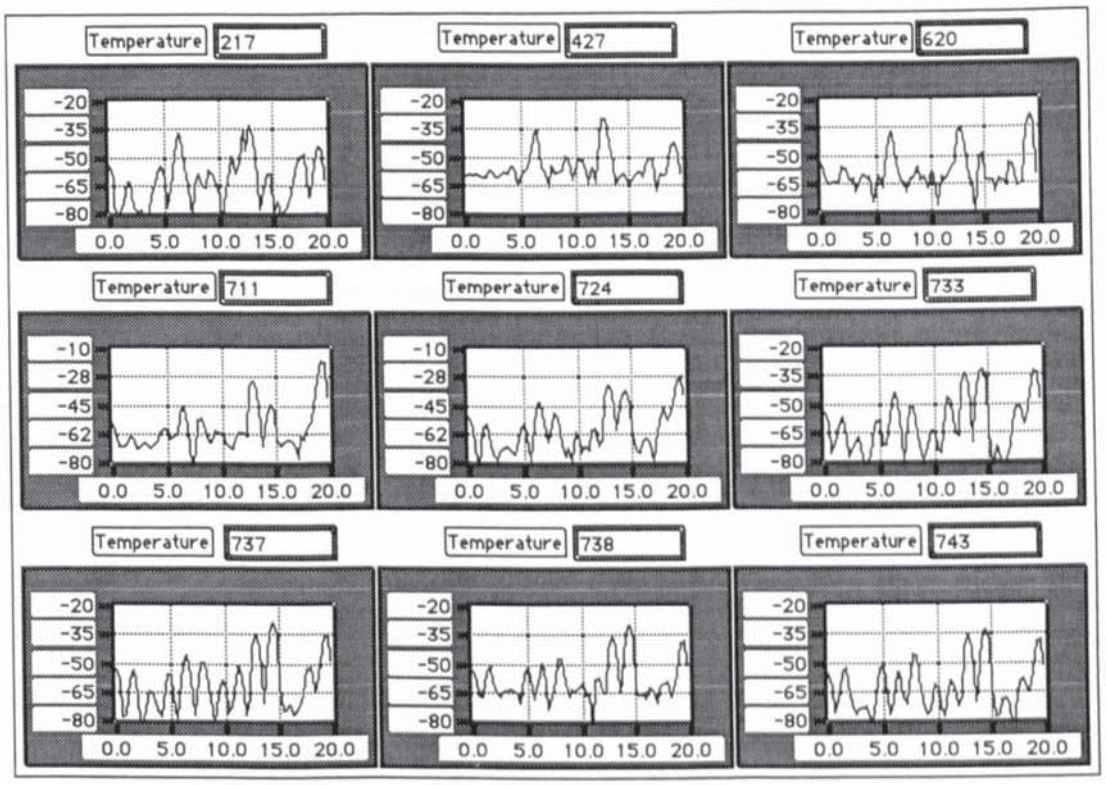

Figure 3.21 Frequency Components of Vibration from Heating a 600 mm Mild Steel Bar at 30kW.

Using the frequency components in figure 3.14 for the increase in acceleration near the Curie point, it was possible to obtain values of the displacement of the face of the bar using:

$$x = - \omega^2 \ddot{x} \tag{3.8}$$

where x is displacement (m)

$\ddot{x}$ is acceleration (ms^{-2})

ω is the angular natural frequency ($rads^{-1}$)

Table 3.3 shows the individual acceleration and calculated displacement components. Assuming that each component is sinusoidal and in phase, the total displacement is the summation of all components.

Frequency (kHz)	dBV	V (volts)	Acceleration (ms^{-2})	Displacement (μm)
19.2	17.4	7.43	728.9	0.050
12.8	5.9	1.98	194.2	0.030
6.4	1.79	1.79	175.6	0.109

Table 3.3 Displacement at Each Frequency Component of Vibration

The total displacement is about 0.2 μm. Considering only one half of the bar (300 mm) since it is assumed that the displacement is symmetrical about the mid-point, the strain is:

$$\frac{\Delta l}{l} = \frac{0.2\ \mu m}{300\ mm} = 0.67 \times 10^{-6} \tag{3.9}$$

The stress can be calculated knowing that:

$$E = \frac{\sigma}{\Delta l / l} \tag{3.10}$$

where Young's Modulus E is approximately 160×10^3 Nmm^{-2} at the Curie point.

$$\sigma = 0.11\ Nmm^{-2} \tag{3.11}$$

Compared to a typical value of 400 Nmm^{-2} for the tensile strength of a mild steel, the stress cause by the vibration is insignificant.

3.6 Natural Frequency Measurements

The natural resonances of a 600 mm mild steel bar were measured from ambient temperature to 850°C. This was carried out by heating the bar in the induction heater to the required temperature, switching the power off to prevent vibration occurring due to the heating process and exciting one face with an impact hammer. An accelerometer was fixed to the other face of the bar. The hammer also had an accelerometer attached to it and the signals from the two accelerometer conditioning amplifiers were connected to a spectrum analyser. The signal from the hammer was then deducted from the signal from the bar to give the spectrum of natural resonances of the bar. The bar was allowed to cool to ambient temperature before heating to the next temperature. The reason for this was to simulate the temperature profile across the bar when vibration occurred during the actual heating process.

Graphs of the natural longitudinal frequencies of the bar were plotted against temperature, figure 3.22.

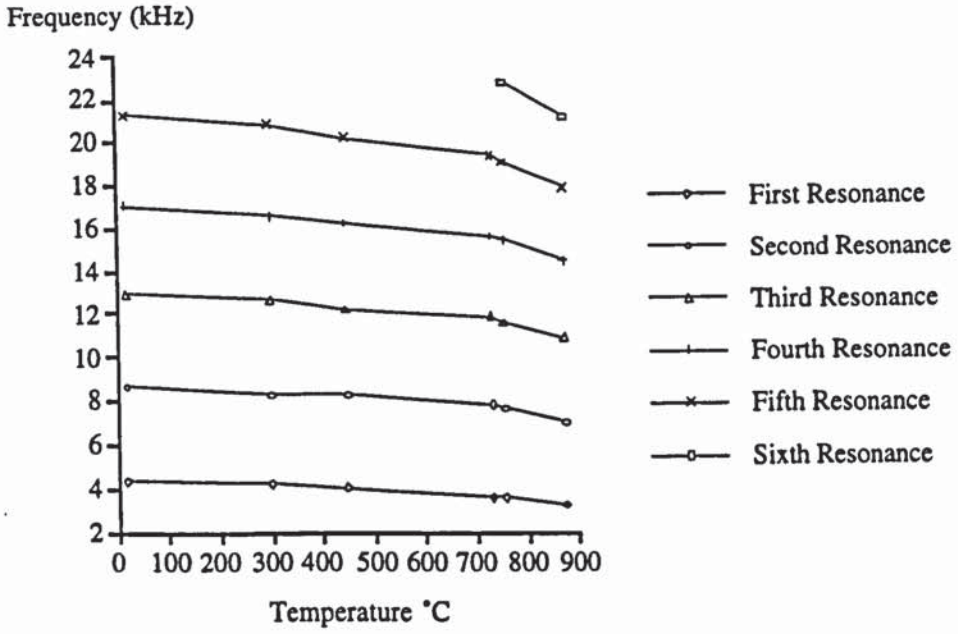

Figure 3.22 Experimental Values of Natural Resonances Against Temperature

The natural modes of a bar were also calculated using equation 2.10.

$$f_n = \frac{n}{2l}\sqrt{\frac{E}{\gamma}} \qquad (3.12)$$

The values for density and Young's modulus with increasing temperature were taken from Metals Handbook (1985). The temperature variation through the bar was simplified using the mean temperature, calculated from Davies and Simpson (1972):

$$\theta_s = \theta_m + \frac{P_0 R}{4k} \qquad (3.13)$$

where θ_s and θ_m are the surface and mean temperatures respectively (°C)
P_0 is the power density at the surface (W m^{-2})
R is the radius of the bar (m)
k is the thermal conductivity (W m^{-1}°C^{-1})

The results however are plotted as a function of surface temperature, figure 3.23, because it was this parameter that was measured in the experiments.

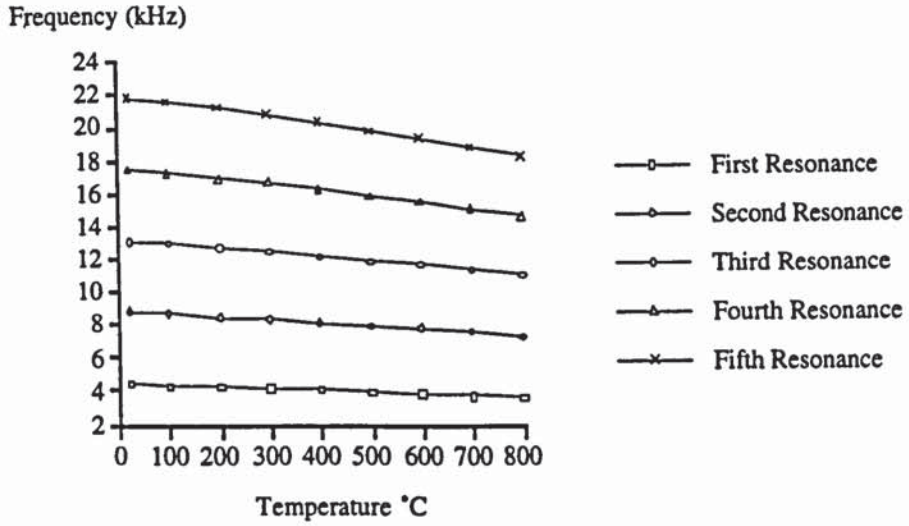

Figure 3.23 Calculated Natural Resonances Against Temperature

The graph showing the measured natural resonances indicates that the natural frequency of the bar decreased sharply in the vicinity of the Curie point. The reason for this is that the frequency was plotted against surface temperature. It was shown in section 3.4 that the surface temperature at the Curie point was almost constant for a short time while the temperature at the centre of the bar continued to increase. This had the effect of reducing the natural frequency of the bar and when plotted against the more constant surface temperature appeared to show a sudden decrease.

For the calculated resonance graph, the curves are much smoother. This is because it was assumed that the surface and centre temperature increased at a constant rate. From both graphs it is apparent that at 500°C the third natural resonance of the bar is about 12.8 kHz and at the Curie point the fifth natural resonance is approximately 19.2 kHz. Both of these coincide with the frequency of vibration observed at these temperatures during induction heating of the steel bar. The increase in longitudinal vibration is therefore as a result of a natural mode being excited leading to resonance. This was checked by heating different lengths of mild steel, which had different longitudinal natural frequencies.

3.7 Length of Bar

The same material, En3b mild steel bar of diameter 40 mm, was cut to various lengths and heated by induction. Bars longer than 600 mm were produced by screwing two lengths of bar together so that their faces were held in very close contact. Longitudinal vibration would still occur in the joined bars and was measured using an accelerometer.

The results below refer to a joined bar of length 1200 mm. Figure 3.24 shows the vibration components from the resonance which occurred near the Curie point during heating at two different power settings and from slightly different initial temperatures. It can be clearly seen that the vibration at resonance occurred at a frequency of 12.8 kHz. Again the magnitudes are shown to change considerably between similar tests.

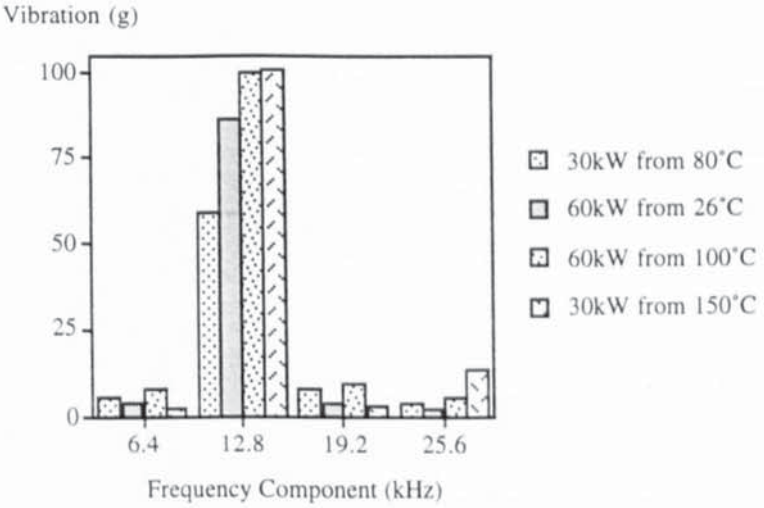

Figure 3.24 Frequency Components of Vibration at the Curie Point of Two Joined 600 mm Mild Steel Bars

A small resonance was also seen to occur at 530°C and the frequency components are depicted in figure 3.25. The vibration appears to be due to a number of components.

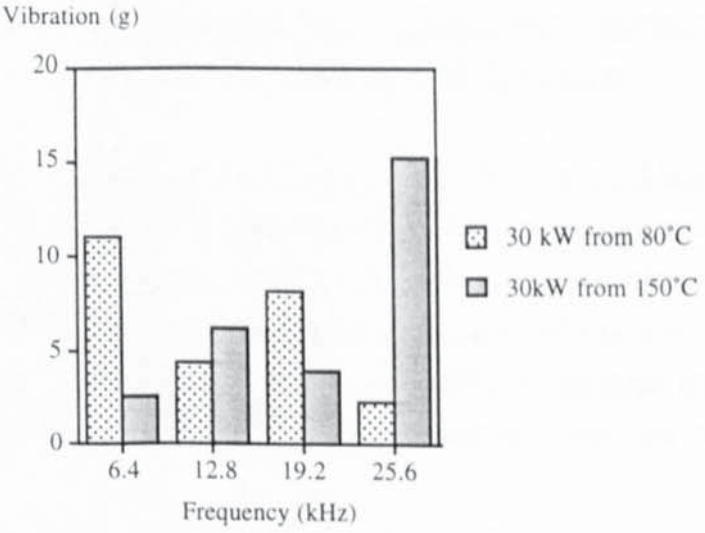

Figure 3.25 Frequency Components of Vibration at 530°C of Two Joined 600 mm Mild Steel Bars

The above results should be compared to results on continuous bars with caution. By joining two 600 mm bars of mild steel together errors will have been produced in the measurements due to the non homogeneous boundary between the two faces of the bars.

The natural longitudinal frequencies of the joined 1200 mm bar were calculated using equation 3.12. The values are plotted in figure 3.26. Near the Curie point, the seventh natural resonance appears to be approximately 12.8 kHz and at 530°C the third natural resonance is about 6.4 kHz.

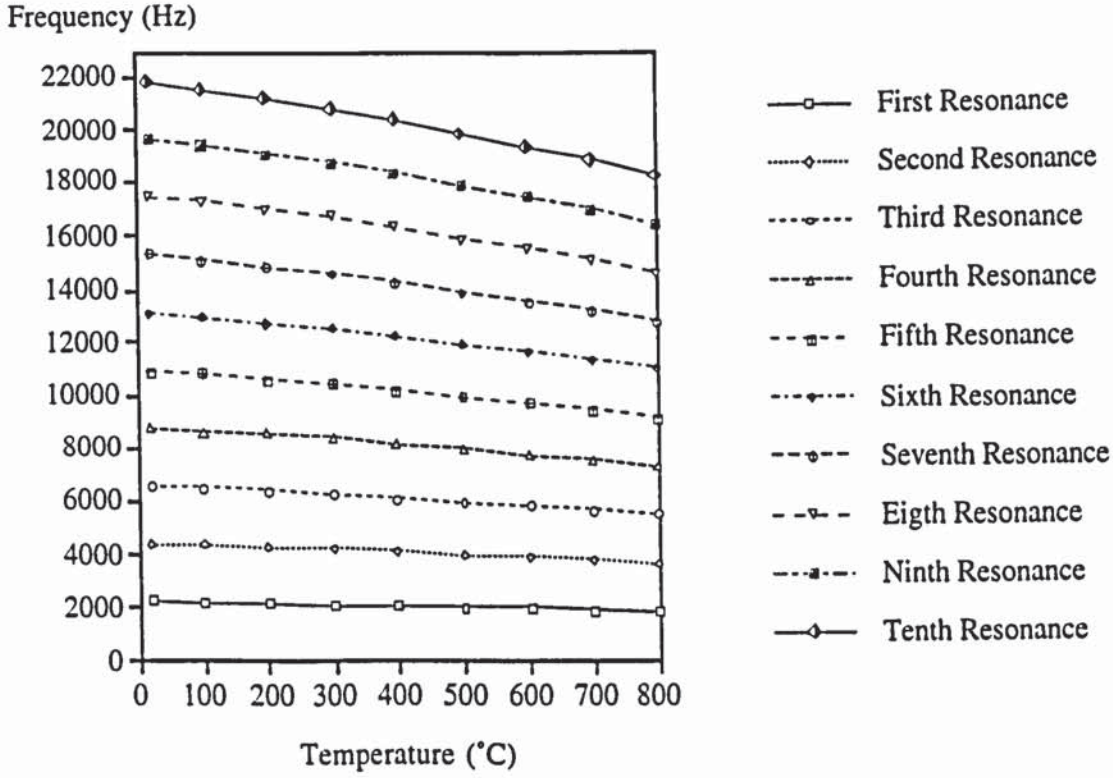

Figure 3.26 Calculated Natural Longitudinal Frequencies of Two Joined 600 mm Mild Steel Bars

The vibration peaks produced in the joined 1200 mm mild steel bar when heated by induction are as a result of a natural resonance of the bar being excited. Although other natural resonances are shown to coincide with twice the heating frequency and subsequent harmonics, these are even resonances and could be a possible reason as to why they are not excited. For example, from figure 3.26 the tenth natural resonance is approximately 19.2 kHz at 650°C but no resonance occurred in the bar at this temperature.

A 500 mm bar was heated and the vibration measured with an accelerometer. A resonance was found to occur at 810°C. Another small resonance occurred at 540°C with the main component being 19.2 kHz corresponding to 13g. When compared to the natural frequencies of the bar, it was discovered that the resonance was in fact an even mode. Figure 3.27 shows the frequency components at 810°C.

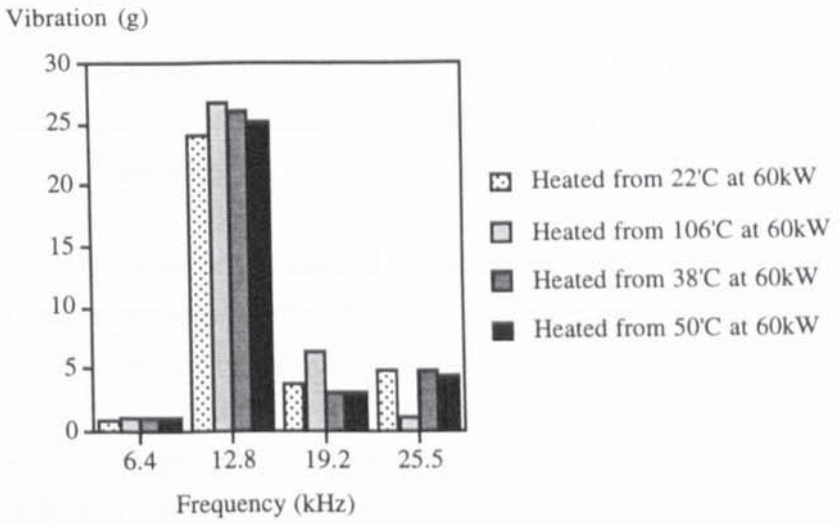

Figure 3.27 Frequency Components of Vibration of a 500 mm Mild Steel Bar at 810°C.

The natural longitudinal frequency was measured as a function of temperature, figure 3.28 and the third natural frequency was found to be approximately 12.8 kHz at 810°C.

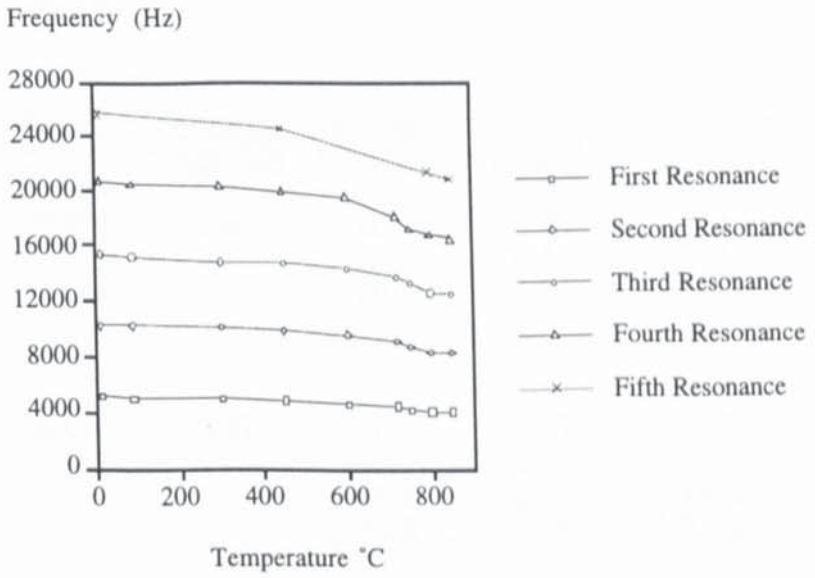

Figure 3.28 Measured Natural Resonances of a 500 mm Bar as a Function of Temperature

In this case the fourth natural resonance may have been excited because the bar was not placed symmetrically in the coil. As a result heating was not concentrated at the mid-point of the bar but at one end.

Resonance was discovered not to always occur near the Curie point and for some lengths of bar resonance did not occur at all during heating to 800°C.

3.8. Ometron Laser Measurements

The Ometron laser vibrometer was used to check both previous results, obtained using accelerometers, and to measure vibration on short lengths of bar. Unfortunately, LabView was not available at the time when the laser was used for this work.

Background noise was measured and found to give an even distribution over the whole of the frequency range studied (0-25 kHz). The velocity signal was measured to be 8 mV (rms), corresponding to a velocity of 0.08 mms^{-1}.

Tests were carried out as before on different lengths of En3b steel bar heated at 20kW to 35kW and any increase in vibration and the corresponding temperature was recorded. The natural resonances of each length of bar were calculated as before. The results were then compared to see whether any of the frequencies coincided. A summary of the results is shown in the table 3.4. The temperature at which a velocity peak occurred is given together with the main frequency components and the velocity magnitude of each component. The last two columns indicate the natural resonances of the bar at room temperature and at the temperature at which the peak occurred. It is shown that the frequency components at the peak coincide with the values of natural resonance at that temperature.

Length	Power	Temp of Peak (°C)	Frequency (kHz)	Velocity (mm/s)	Resonances At 20°C	Resonances at Peak
600 mm	35 kW	710	6.4	0.40	4.2	3.6
			12.8	0.44	8.4	7.8
			19.2	2.09	12.6	11.8
					16.6	15.6
					20.8	19.4
400 mm	35kW	100	6.3	5.42	6.5	6.4
			12.7	5.02	12.9	12.8
			19.1	2.04	19.4	19.2
			25.4	2.8	25.9	25.5
205 mm	20kW	150	12.6	2.0	12.7	12.5
					25.2	24.8
105 mm	30kW	No peaks	None	None	24.8	N/A

Table 3.4 Results Obtained Using the Laser Vibrometer

Harris and Crede (1976) stated that for a force that acts at the centre of a beam the even modes of vibration are not excited. This is because for these modes the centre is a node. It could be a similar case when bars are heated by induction. Most of the time there was an even proportional of bar protruding from the coil at each end. Only the centre of

the bar was directly heated and it is presumed that the vibration was created in the central region. Thus even modes would not be expected. From the results collected it can be seen that the majority of modes excited were odd and would agree with the above explanation.

3.9 Phase of Vibration

By attaching accelerometers to both faces of the bar it was possible to determine the mode of vibration. It was discovered that the two faces resonated 180° out of phase, i.e. both move out or in at the same time. Results were recorded when the vibration was at a resonance peak. It was not discovered where the vibration was induced in the bar, if it was concentrated in the skin layer or evenly across the whole section. The vibration was assumed to be the same at all points on the face of the bar because of the medium frequency used. At much higher frequencies there would there be a difference between vibration at different points on the face if the vibration was in fact created in the skin layer.

3.10 The Effect of Heating Power on the Magnitude of Vibration

Once resonance had been found to occur at certain temperatures during the heating process, a number of tests were undertaken to ascertain what factors affected either the magnitude of vibration or the temperature at which resonance occurred. A 600 mm mild steel bar (En3b) was heated repeatedly from ambient temperature at different power settings. The temperature and vibration during the heating cycle were recorded using LabView and from this data the temperature at which the resonance occurred and its peak magnitude was obtained. These values were then plotted as a function of heating power, figure 3.29.

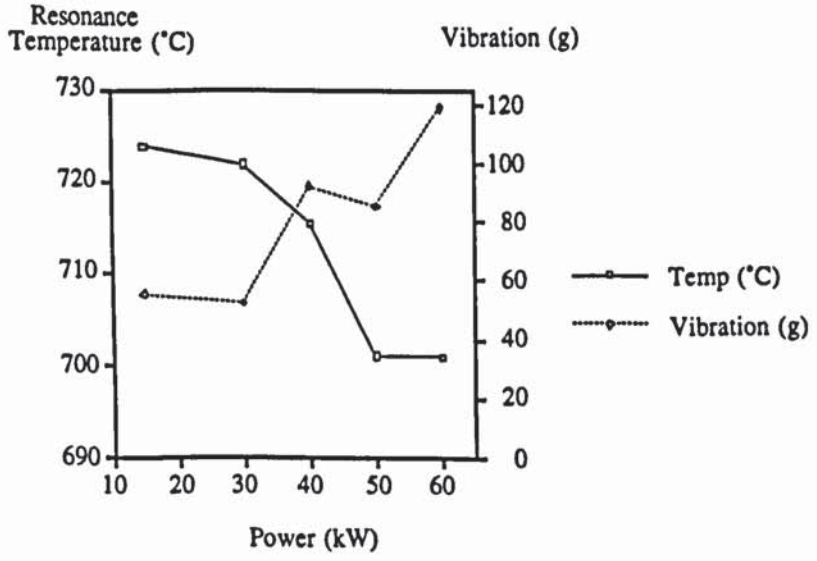

Figure 3.29 Vibration and Resonance Temperature As a Function of Heating Power

The graph shows that the vibration magnitude increased with an increase in heating power. This implies that the mechanism responsible is proportional to the field strength since the field changes directly with power.

With an increase in heating power there appears to be a decrease in the surface temperature at which resonance occurred. The results show resonance to occur very close to the A_1 transition temperature (723°C) and may be connected to the transformation of steel at this point. However, Verhoeven, Downing and Gibson (1986) state that at fast heating rates, such as those produced by induction heating, the A_1 transition temperature may be considerably higher and may in fact be very close to the Curie point. The results here show that the opposite has occurred i.e. the higher the power, and therefore rate of heating, the lower the temperature at which resonance has occurred. It is therefore unlikely that the resonance is caused by the A_1 transition at this temperature.

3.11 The Effect of Initial Temperature of the Bar on the Magnitude of Vibration

It was discovered that a 40 mm diameter bar heated at 60kW from ambient temperature had a large temperature differential across it up to about 800°C and produced an increase in longitudinal vibration when the surface of the bar neared the Curie point. The centre however, was at a temperature of 520°C (measured by experiment and from theory). If the bar was allowed to soak so that the surface and centre were closer in temperature and reheated at the same power, the magnitude of vibration and the temperature at which resonance occurred were both lower. This can be seen from figure 3.30.

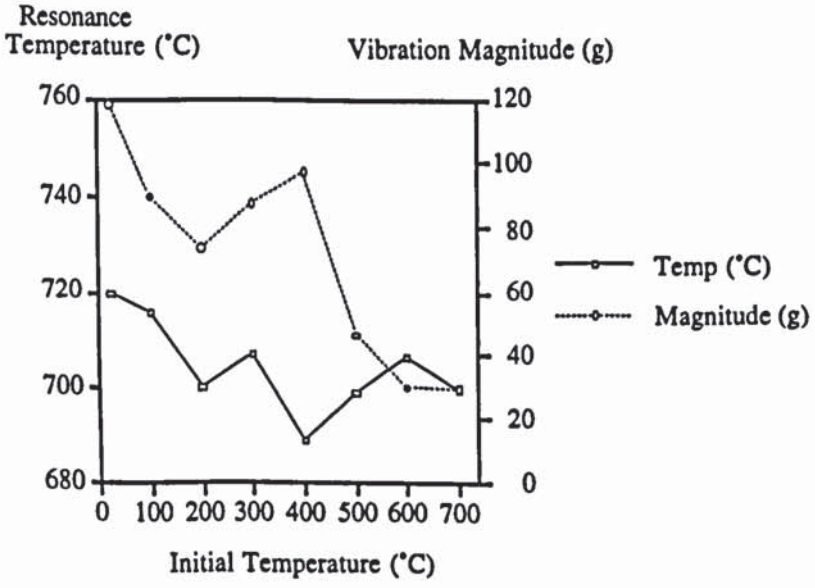

Figure 3.30 The Effect of Different Starting Temperatures on the Magnitude of Vibration at the Curie Point

It was unclear at this stage whether it was the temperature differential across the bar or the surface starting temperature which affected the magnitude of vibration. It was postulated that the average temperature of the bar was the controlling factor since average temperature increases with increase in initial temperature. Natural frequency depends on the average temperature of the bar and for an increase in initial temperature, the surface temperature at resonance (resonance temperature) will decrease. This agrees with the experimental results, figure 3.30 and the magnitude of resonance is therefore likely to be dependent upon the temperature difference across the bar, or average temperature rather than simply the surface temperature of the bar.

3.12 The Effect of Bar Diameter on the Magnitude of Vibration

The effect of heating different diameter mild steel bars was investigated. The bars were all of the same length, 600 mm and were either 25 mm, 40 mm or 50 mm in diameter. They were heated from the same initial temperature at the same inverter power setting for two sets of tests. This was set to 50 kW for the first set of tests and to 30 kW for the second set. Although the power setting on the Crossley inverter indicated the same value for each diameter of bar, it was discovered using calorimetry that the actual power input to the bar changed with diameter. Equations 2.3 and 2.4 were used to calculate the power input to these bars at the above power settings. The power input to a mild steel bar was found to double if the diameter doubled. For the 25 mm diameter bar the power input was lowest and for the 50 mm bar the power input was double this value. This was due to the coupling between the coil and workpiece.

Figure 3.31 shows a graph of the magnitude of vibration recorded at resonance near the Curie point when the different diameter bars were heated at 50kW. The 50 mm diameter bar showed the highest acceleration component at 19.2 kHz and the trend appears to be, the greater the diameter of the bar, the larger the vibration component. Figure 3.32 shows the magnitudes of acceleration of the same bars at each of the frequency components when heated at a power setting of 30kW. This time however the 40 mm bar shows the greatest magnitude at 19.2 kHz.

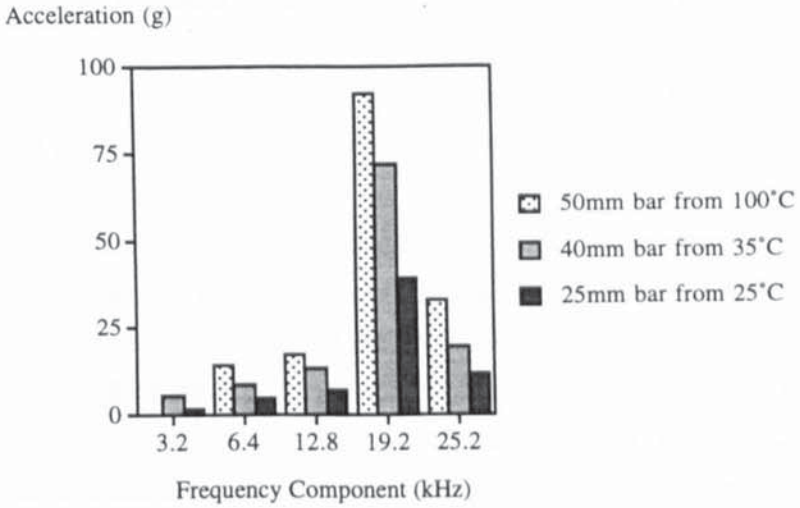

Figure 3.31 Vibration Components for Different Diameter Bar All Heated at 50kW

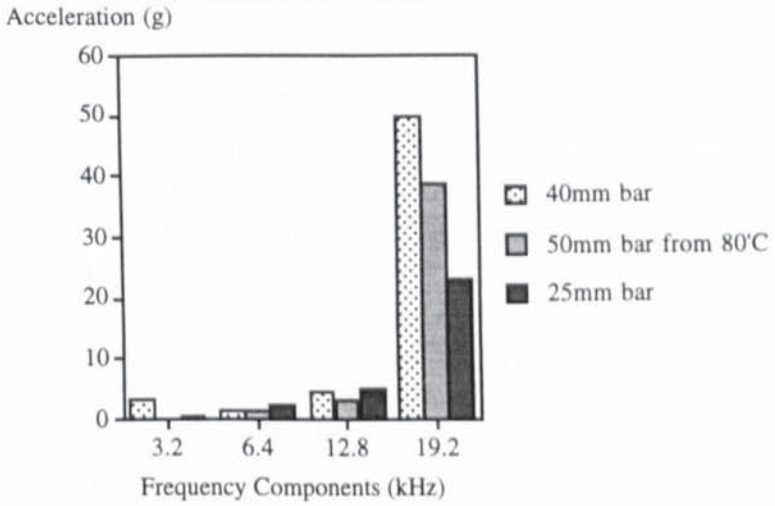

Figure 3.32 Vibration Components for Different Diameter Bar All Heated at 30kW

Davies and Simpson (1979) have calculated coil efficiencies for bar hardening as a function of diameter at a number of frequencies. They show that with an increase in diameter there is an increase in heating efficiency. For example, heating a 25 mm bar at 3 kHz is 60% efficient whereas heating a 50 mm bar is 75% efficient. This value is calculated as the power input to bar / power input to coil. From equation 2.3 the power input to a bar is dependent upon p which is a function of diameter, d. Comparing this with the above results shows that there is a similarity. For instance figure 3.31 shows that the signal at 19.2 kHz for the 50 mm diameter steel bar is about twice that of the 25 mm bar.

The resonance magnitude is therefore a function of bar diameter which itself is a function of power input to the bar.

3.13 The Effect of Carbon Content on the Magnitude of Vibration

Apart from using mild steel as the test material, it was decided to use higher carbon steels and iron. These were all 40 mm diameter bars of length 500 mm.

The 0.4% carbon steel was heated in exactly the same manner as the mild steel bars. Figure 3.33 shows the results from heating the bar at 60kW. There were two major increases in vibration apparent, the first just before the Curie point, 740°C and the second at 810°C. Figure 3.34 shows the frequency components over the heating cycle. Each frame was recorded 4 seconds apart. The peak at the very start of heating was thought to be caused by the sudden increase in power and is not as a result of resonance within the bar.

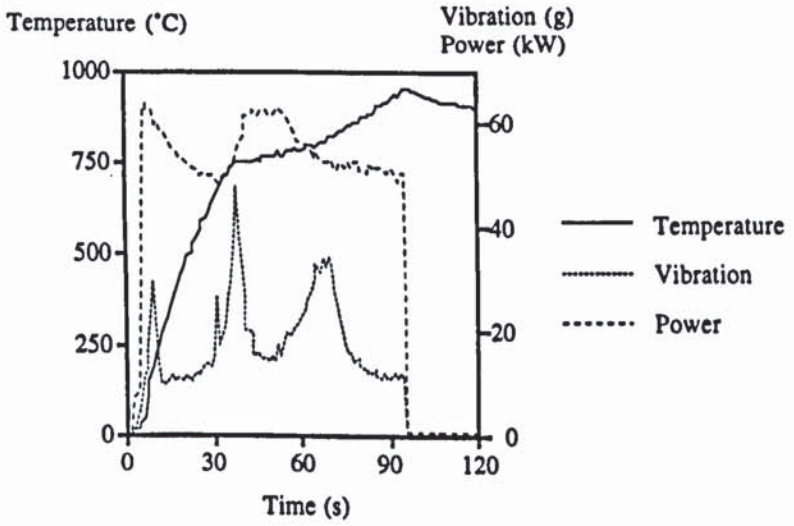

Figure 3.33 Temperature, Vibration and Power for the 0.4% Carbon Steel Heated at Full Power

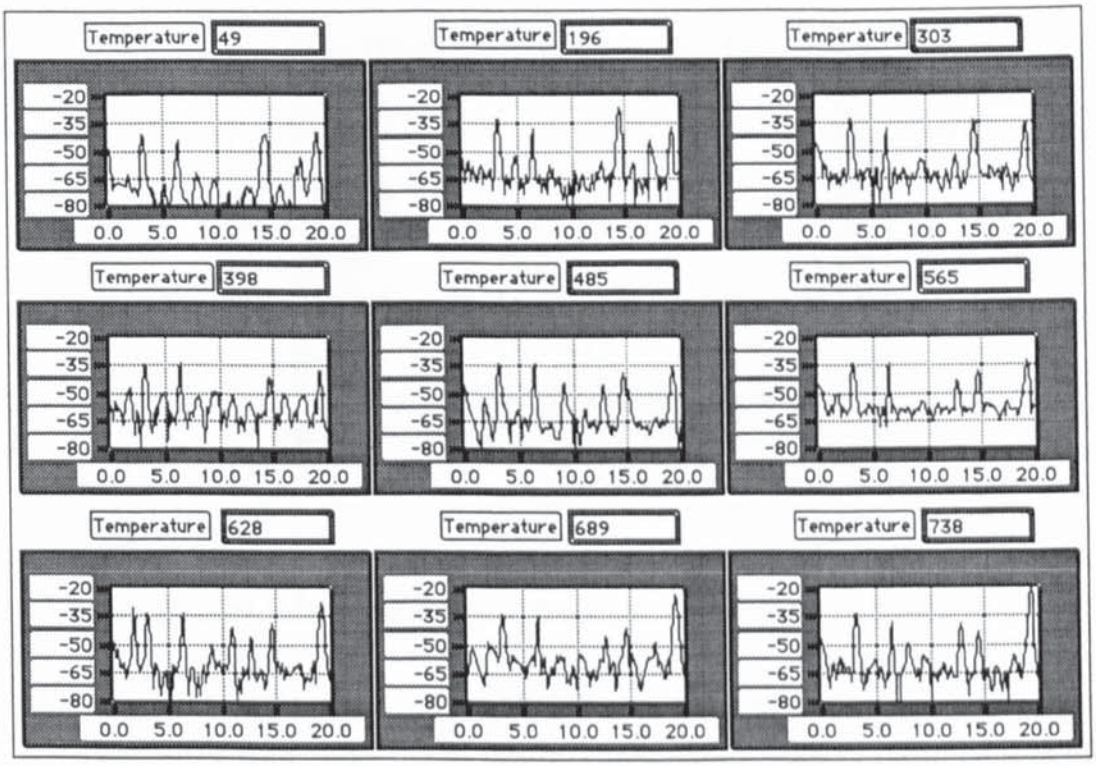

Figure 3.34 Frequency Components of Vibration of a 0.4% Carbon Steel Bar Heated at 60kW

It was discovered that the two peaks were resonances of the bar corresponding to 19.2 kHz and 12.8 kHz at 740°C and 810°C respectively.

The 1.5% carbon bar could only be heated once as there was possibility that it would harden when heated and allowed to cool in air. It was discovered that increases in longitudinal vibration occurred at 540°C and near the Curie point, figure 3.35. The frequency components at 540°C are shown in figure 3.36.

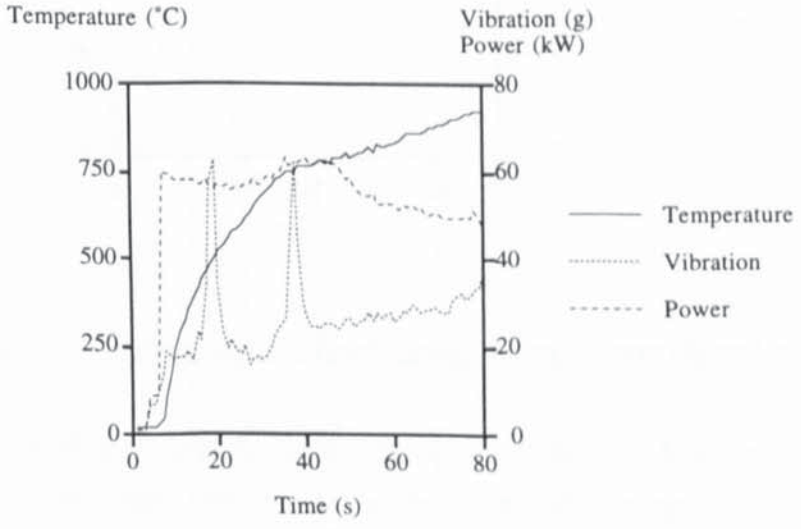

Figure 3.35 Temperature, Vibration and Power for the 1.5% Carbon Steel Heated at 60kW

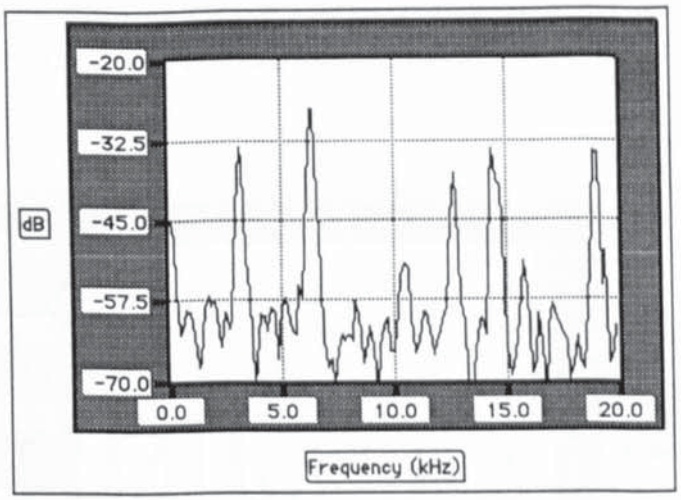

Figure 3.36 Vibration Components of the 1.5% Carbon Steel at 540°C

The two distinct peaks in figure 3.35 correspond to resonances at 6.4 kHz and 19.2 kHz at 540°C and 740°C respectively. Other components are also present but of much lower magnitude, figure 3.36.

Finally, for the iron bar there was very little vibration during heating producing a resonance peak corresponding to about 35g near the Curie point, figure 3.37.

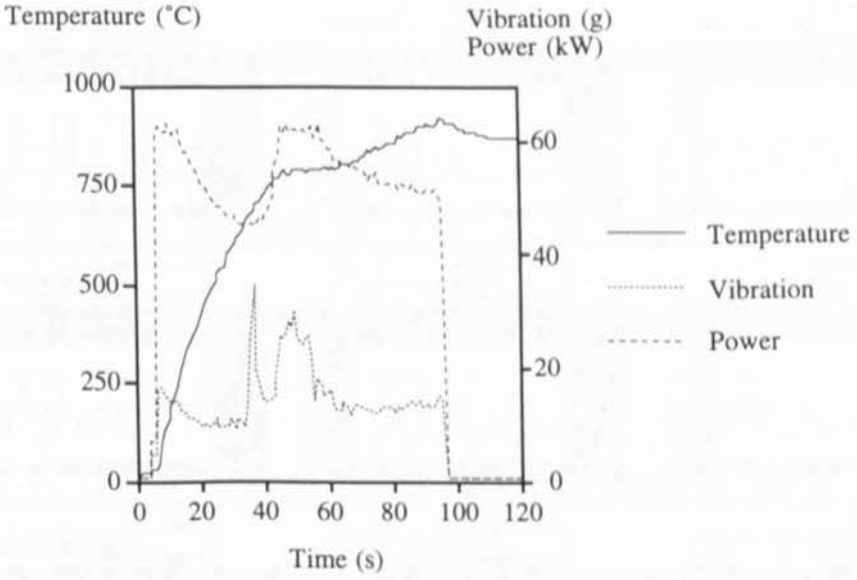

Figure 3.37 Temperature, Vibration and Power of Iron Heated at 60kW

Figure 3.38 shows the frequency components near the Curie point and again the component at 19.2 kHz was found to be of greatest magnitude. The frequency components were recorded at 4 second intervals, figure 3.39. The magnitude of resonance near the Curie point was 5 times lower than that for mild steel. It was discovered that for the iron bar the initial temperature did not seem to have the same effect

on the magnitude of vibration as that for mild steel. This difference may be due to the low carbon content in the iron or to the fact that the transformation temperatures are much higher.

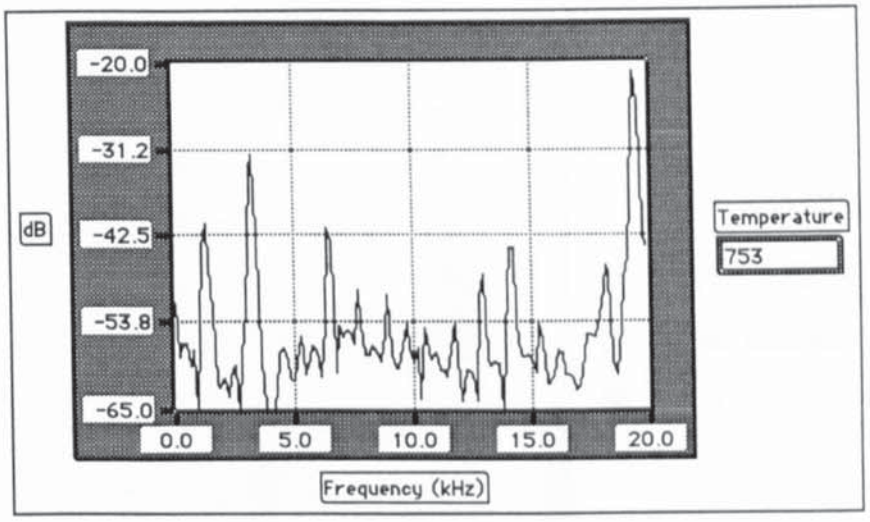

Figure 3.38 Frequency Components of Vibration of the Iron Bar at the Curie Point (Heated at 60kW)

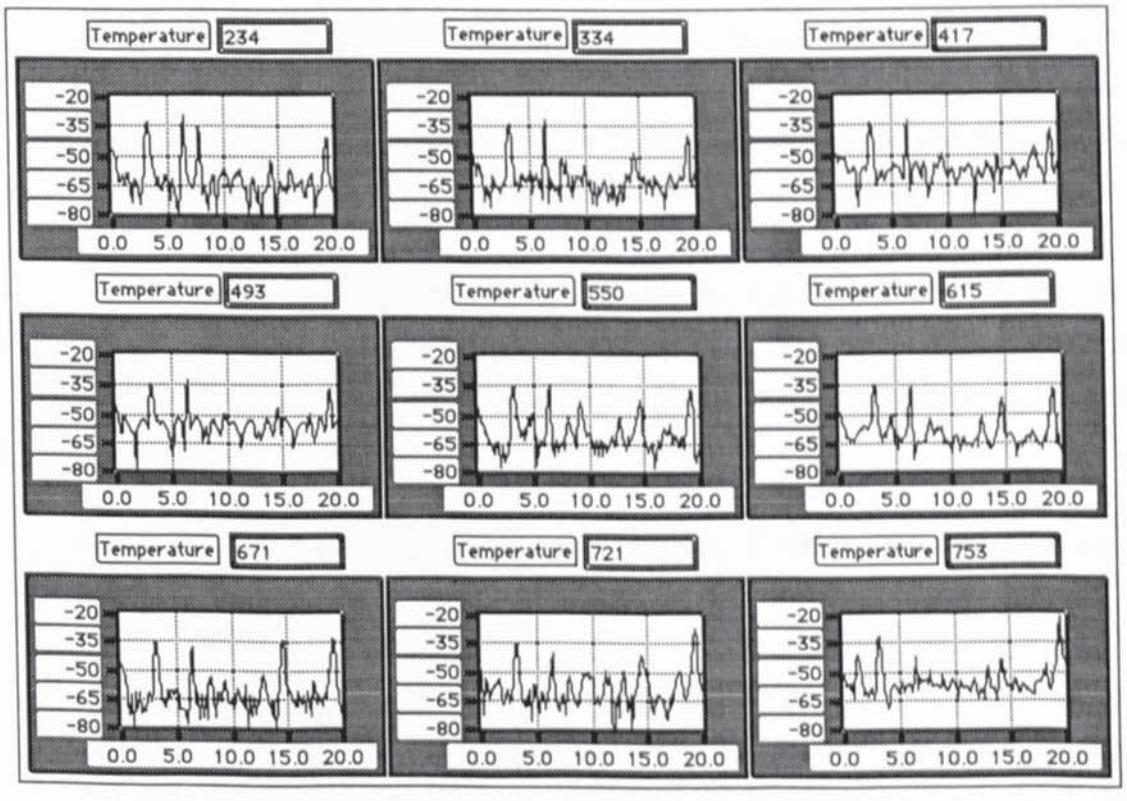

Figure 3.39 Frequency Components of Vibration of the Iron Bar Heated at 60kW

Figure 3.40 shows the comparison between the carbon steels for resonance near the Curie point. It appears that the lower the carbon content of the steel, the greater the magnitude of resonance at the Curie point. However, iron does not agree with this hypothesis.

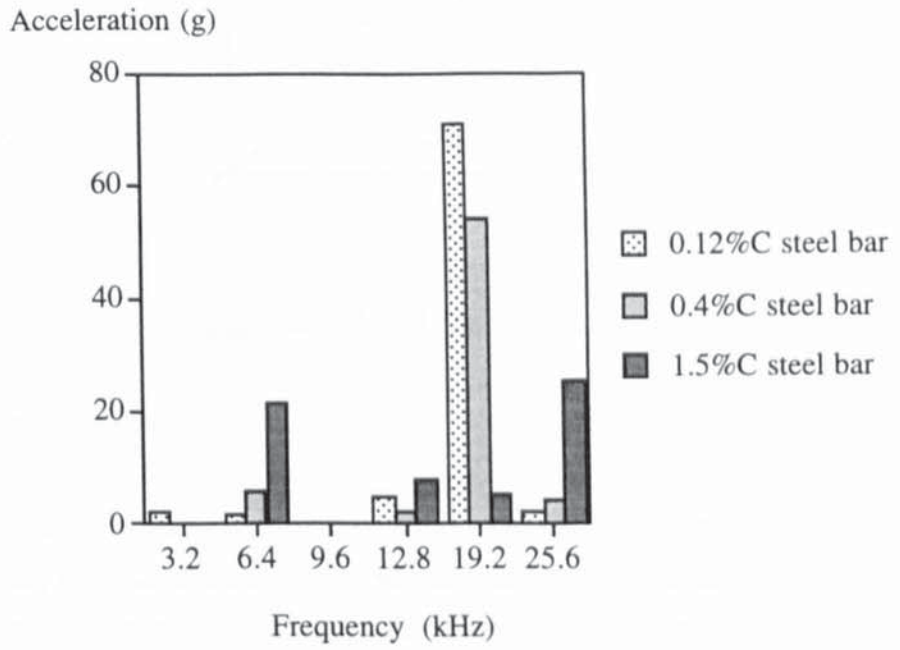

Figure 3.40 Vibration Components of Different Carbon Steels.

Williams (1933) reported that the harder a steel, the smaller the magnetostrictive vibration. Carbon increases the hardness of a steel and if magnetostriction is a cause of vibration, then the vibration should decrease with increase in carbon content for a steel. However iron, which is the softer of the materials showed low magnitudes of resonance.

It is hypothesised that the magnitude of resonance may be linked to the amount of ferrite in the steel. The tests however did not use enough different steels with varying carbon content for a true trend to be observed but shows that resonance is not the same for different steels.

3.14 The Effect of Axial Position in the Heating Coil on the Magnitude of Vibration

A test was undertaken to investigate whether the axial position of a mild steel bar changed the magnitude of resonance at the Curie point. A bar was suspended horizontally through the coil, above the refractory. The height above the refractory was set to 1 cm, 3 cm and the normal central position for the three tests, figure 3.41. The bar was heated from the same initial temperature at the same power. The vibration plots as a function of temperature were all similar, indicating that the vibration was independent of the axial

position of the bar in the coil. Only the longitudinal position affected the vibration during heating.

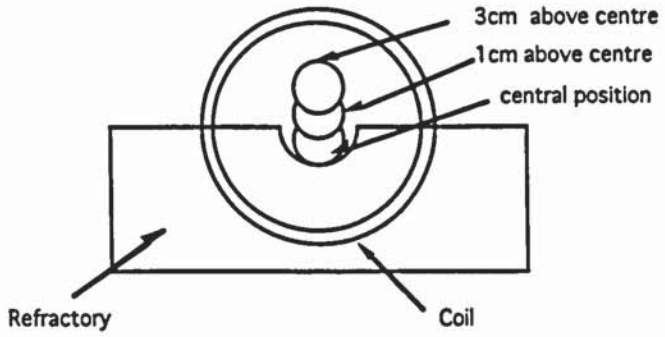

Figure 3.41 Axial Position of Bar in Coil

3.15 Body Forces

It was discovered that when a mild steel bar was suspended horizontally in the coil allowing it to move freely, body forces were present during heating, causing the bar to move axially. Several tests were carried out in which the bar was placed in different positions in the coil so that either one end protruded out of the coil or both ends protruded by the same amount. It was found that if only one end stuck out, the bar was initially pulled into the coil. When the surface of the heated portion reached the Curie temperature the cold end of the bar was quickly pulled into the coil and heated.

With both ends protruding nothing happened until the portion of the bar being heated reached the Curie point. Then the bar moved so that one of the cooler, ferromagnetic ends of the bar was pulled into the coil. This section was heated whilst the previously heated part cooled. The end portion of the bar in the coil then reached the Curie point and the previously heated part of the bar was pulled back into the coil. The bar continued moving in this manner with each end of the bar being alternatively heated and cooled.

The reason for this comes from the fact that a ferromagnetic material will be strongly attracted into a solenoid whereas a paramagnetic material will be weakly attracted. As the heated part of the bar reached the Curie point it became paramagnetic and was forced out of the coil because of the attraction of the ferromagnetic end of the bar into the solenoid.

As the bar moved it was discovered that the longitudinal vibration increased at the same time. It is postulated that the two occurrences are merely coincidental and are only related by the temperature at which they occur.

3.16 Lateral Vibration of Bar

Two accelerometers were fixed opposite each other on the curved surface at one end of a 600 mm long En3b bar. Two were necessary to balance the end of the bar and were continuously quenched by a small water flow. The diagram in figure 3.42 shows the position of the accelerometers. The bar was heated at 40kW and the vibration, temperature and power were recorded as a function of time, figure 3.43. The frequency components were recorded during the heating cycle, figure 3.44, showing the component at 3.2 kHz to be the greatest. This was thought to be due to the pick-up of the accelerometer since the magnitude was 0.03 V and is comparable to the noise level.

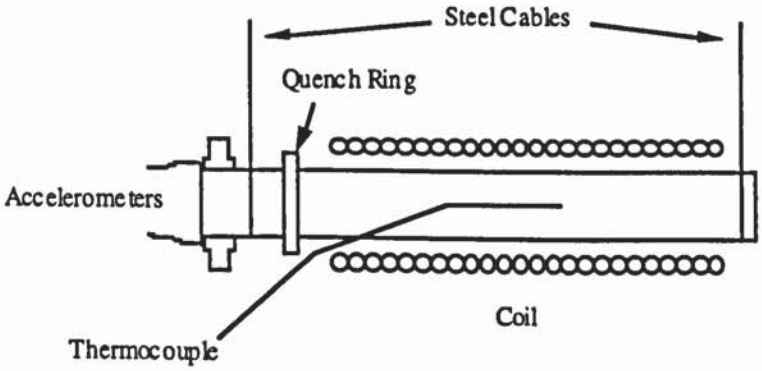

Figure 3.42 Position of Accelerometers for Lateral Vibration Measurement

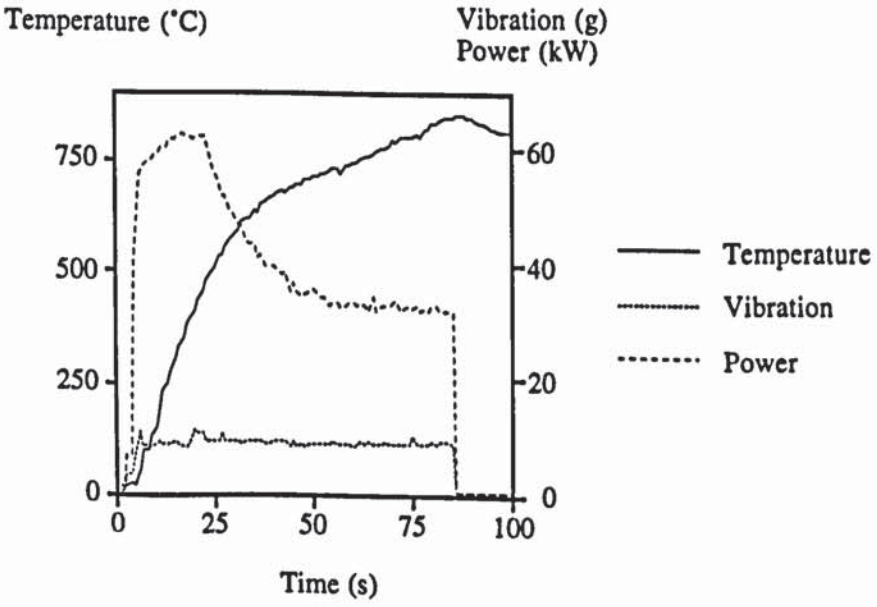

Figure 3.43 Graph of Lateral Vibration, Temperature and Power of a 600 mm Long Mild Steel Bar

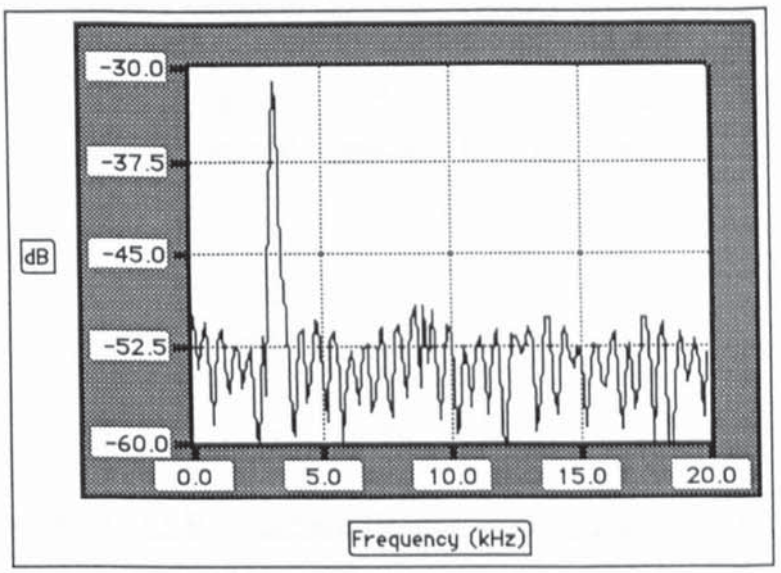

Figure 3.44 Frequency Components of Lateral Vibration

Lateral vibration was also measured on the heated section at the mid-point of a 600 mm long mild steel bar using the laser vibrometer. When the longitudinal vibration increased as the surface temperature approached the Curie point, the transverse vibration was also seen to increase slightly. The frequency responsible was the same as that observed for the longitudinal resonance, 19.2 kHz. The magnitude of the transverse vibration was measured to be 0.04 V with a setting of 0.1 V/mm s^{-1}. Hence, the velocity was 0.4 mm/s. This is equivalent to an acceleration of 5g. Transverse magnetostriction is reported to be half the magnitude of longitudinal magnetostriction, λ up to saturation (equation 2.14). However this is not the case when heating steel bars by induction. An explanation for the difference could be that linear magnetostriction is not responsible for resonance. Perhaps volume magnetostriction is the cause because the volume of the bar appears to increase. There was very little lateral vibration during heating indicating that cross coupling of the longitudinal signal was low.

3.17 Change of Heating Frequency (Measurements by Laser Vibrometer)

Tests were conducted on lengths of En3b mild steel bar using a 100kW, 2.3 kHz Radyne induction heater. The maximum field strength was 100 kAm^{-1}. All measurements were made with the laser vibrometer for convenience. Measurements were recorded as r.m.s. values to reduce noise. The diameters of the bars were 40 mm. The results are presented in table 3.5.

Length (mm)	Power (kW)	Velocity at 2.3 kHz (mm/s)	Velocity at 4.6 kHz (mm/s)	Velocity at 9.2 kHz (mm/s)	Velocity at 13.8 kHz (mm/s)	Velocity at 18.4 kHz (mm/s)	Velocity at 23.0 kHz (mm/s)	Temp at Which Measured (°C)
600	50	0.31	4.58	0.42	0.28	-	-	200
450	30	0.29	7.05	2.29	1.14	0.99	-	720
400	20	0.23	1.66	0.23	0.08	1.51	0.14	400
200	20	0.32	0.58	0.56	0.16	-	1.62	600

Table 3.5 Results from Heating Steel Bars at 2.4 kHz

For the 600 mm long mild steel bar a small increase in vibration was seen to occur at around 200°C. The majority of the vibration occurred at a frequency of 4.6 kHz, twice the exciting frequency of 2.3 kHz which was very close to the first natural resonance of the bar at this temperature. No resonances were excited near the Curie point in the 600 mm bars because no natural resonances coincided with twice the heating frequency or subsequent harmonics. Although the fifth natural resonance fell to around 18.4 kHz at 900°C no increase in vibration occurred. The cause of the vibration was most likely no longer present at 900°C or so low in magnitude that an increase was not detected.

The 450 mm long bar showed resonance at 720°C. The 4.6 kHz natural resonance was excited at this temperature.

The 400 mm long bar gave a resonance peak at a temperature of 400°C. Again the increase in vibration was due to the excitation of natural resonances of the bar at 4.6 kHz and 18.3 kHz.

The 200 mm long bar produced a resonance at 600°C. The frequency components, indicate that a resonance occurred at 22.9 kHz which coincided with the second natural resonance of the bar at this temperature.

Normally only the odd resonances were excited but in this case an even resonance was recorded. This may be due to the fact that the short bar was no longer central in the coil and as a result was subjected to uneven heating, primarily greater heating towards one end.

Longitudinal resonance has been shown to occur in mild steel bars when heated at a different frequency, but the temperatures at which resonance occurred was different from heating at 3.2 kHz.

3.18 Damping in Steel Bars

The fraction of critical damping (damping ratio), ξ for a system with viscous damping is defined as the ratio of actual damping coefficient, c to the critical damping coefficient, c_c. By measuring values from resonance peaks observed on the spectrum analyser it was possible to calculate the fraction of critical damping using equation 2.13.

A set of results was taken from the resonance peaks at the Curie point of a 600 mm bar heated at full power, 60kW. The results show that damping was small, table 3.6. This is to be expected when a resonance occurs. Other authors also report very little damping in steel around the Curie point, e.g. Bozorth (1951).

Resonance Frequency (Hz)	$\Delta\omega$ (Hz)	$\Delta\omega / \omega_n$	$\xi = \Delta\omega / 2\,\omega_n$ for $\xi < 0.1$
19210	2	0.0001	0.00005
19266	2	0.0001	0.00005
19199	1.5	0.00008	0.00004

Table 3.6 Values of Damping Ratio of the Fifth Natural Resonance at the Curie Point for a Mild Steel Bar

The damping ratio of a 600 mm mild steel bar as a function of temperature was also investigated by exciting its natural resonances with an impact hammer, table 3.7. Only the first natural resonance was studied because the strength of the signal of subsequent resonances decreased with temperature and it was not possible to accurately obtain a strong peak on the spectrum analyser.

Temperature °C	Resonance Frequency (kHz)	Damping Ratio ξ
13	4.2	0.0012
18	4.2	0.0010
400	3.9	0.0010
520	3.8	0.0010
560	3.7	0.0008
590	3.7	0.0013
600	3.7	0.0014
700	3.5	0.0073
760	3.4	0.015
800	3.3	0.018

Table 3.7 Damping Ratio for the First Natural Resonance as a Function of Temperature

The results from table 3.7 show that generally the damping ratio has increased with temperature for the first resonance. It must be noted that the results were taken with the induction heater switched off. There was no decrease in damping around the Curie point which may only occur in a magnetic field.

Harris and Crede (1976) state that ferromagnetic materials have significantly greater damping than non-ferromagnetic materials at intermediate stress levels. This is due to the rotation of the magnetic domain vectors produced by an alternating stress field. If the specimen is magnetised to saturation, most of the damping disappears, indicating that it was due to magnetoelastic hysteresis. Magnetoelastic damping is independent of excitation frequency, at least in the range of engineering interest. It decreases only slightly with increase in temperature until the Curie point is reached when it decreases rapidly to zero. A static stress superimposed on an alternating stress will reduce magnetoelastic damping.

Cochardt (1953) reports that alloys with large damping capacities do not exhibit appreciable damping when tested in a strong magnetic field. This is due to the alignment of the domains in the applied field restricting their movement under the influence of an alternating stress. Energy cannot be dissipated and the damping capacity is therefore small. Most of the damping arises from the eddy currents.

3.19 Insulated Tests Using Steel Bars

It was reported by Whittington (1978) and many others, section 2.9 that an increase in the amplitude of ultrasonic vibration near the Curie point of steel was due to the surface of the material cooling below the Curie point and becoming ferromagnetic whilst the inner part of the bar was still paramagnetic. This would increase the steady field in the thin surface layer. To see whether surface cooling affected vibration of a steel bar when heated by induction, an experiment was devised using insulation around the bar. This was carried out with ceramic wool. The steel was heated at 60kW and the vibration recorded. The temperature, measured at the bar's surface was seen to increase throughout the heating period. No difference in vibration was seen, compared to unlagged tests, and since the surface of the bar did not cool below the Curie point during heating, it must be concluded that this is not the cause of the increase in vibration associated with this point. Although Whittington (1978) used a steady (d.c.) field and the occurrence of a thin ferromagnetic layer would have concentrated the field, the tests undertaken using the induction heater used an alternating field which was confined to a very thin skin through most of the heating process. Resonance at the Curie point occurred as the skin depth increased and the flux density became less concentrated. This conflicts with the results published by those such as Whittington (1978) if the mechanisms

responsible for ultrasound enhancement and resonance during induction heating are related.

3.20 Metallography of Heated and Unheated Mild Steel

After one of the En3b mild steel bars had been heated several times and vibration observed, small samples were taken from it. These were cut from the mid-point of the bar and from the end of the bar which had been water cooled. The samples were mounted, etched using a 2% nital solution and studied under a microscope. The microstructures are shown at x500 magnification in figure 3.45. A Vicker's hardness test was carried out and both samples had a value of 272. If the steel had been annealed it would have been expected to have a value around 190. The higher value suggests that some cold working has been introduced into the steel.

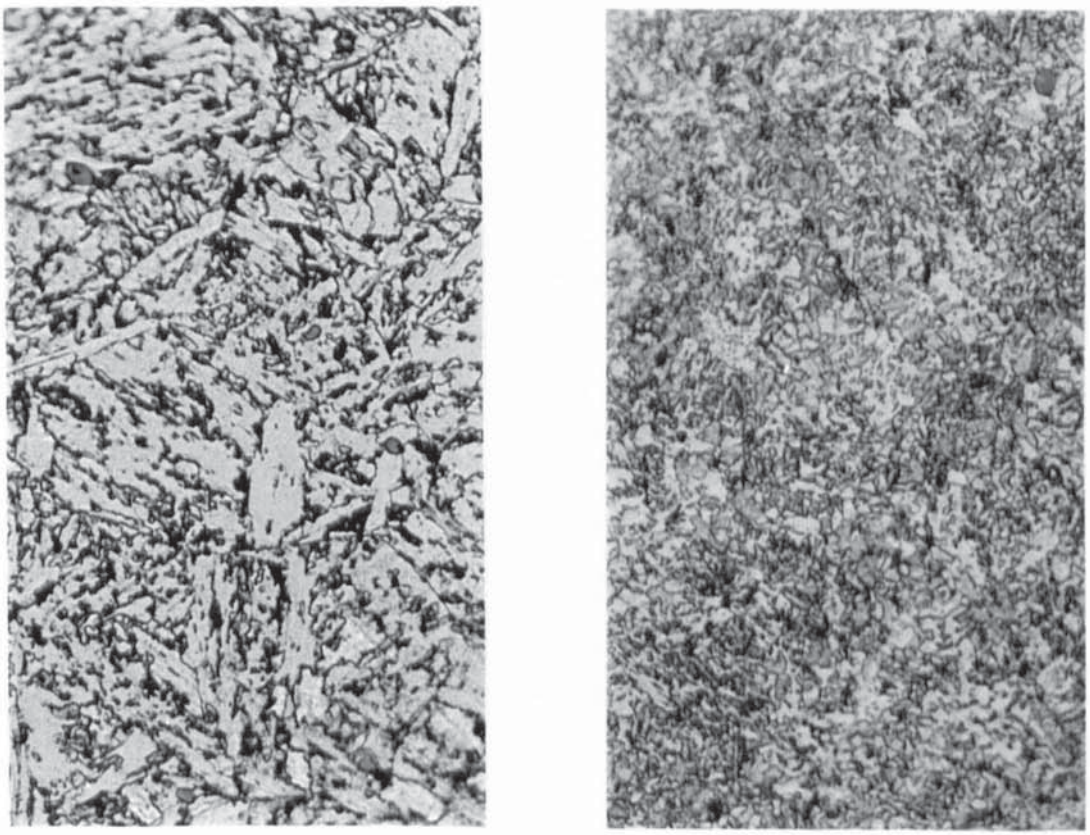

Unheated Heated

Figure 3.45 Microstructures of Induction Heated and Unheated Mild Steel

The unheated specimen shows a fairly course arrangement of the crystals which are sharp or spiky in nature. The heated specimen shows a structure which is much more refined with smaller crystals. Allowing the bar to cool in air or water has probably caused normalising to occur. There seems to be no other immediate change to the material, which would alter its performance after vibration had occurred during induction heating.

3.21 Alpha to Gamma Phase Transformation in a 0.4% Carbon Steel

Plots recorded showing the inverter power may also indicate that phase transformation takes place. The power is closely related to the current in the coil which itself will change with the load. As steel heats up its permeability and resistance change. The largest change in permeability will arise as soon as the α / γ transformation occurs since austenite is paramagnetic. But for a mild steel the Curie point is 760°C and the α / γ transformation has occurred by about 850°C. The magnetic transformation would normally occur before the phase transformation.

Verhoeven, Downing and Gibson (1986) state that the change in current in the coil is a direct result of the α / γ transformation and have results showing structures of samples heated to different temperatures in which the transformation has occurred.

To determine whether this transformation was accompanied by vibration, short rods (300 mm long by 10 mm diameter) of 0.4% carbon steel, BS970-817M40, all cut from one single length, were heated by induction to different temperatures and rapidly quenched in water. The temperature reached by each bar was determined by the amplitude of longitudinal vibration, measured with an accelerometer. Samples from the rods were cut from the centre, mounted, etched in 2% nital solution and examined under a microscope. Comparisons were made to see whether there were any signs of a phase transformation. The rods were heated to the temperatures shown in table 3.8.

Sample Number	Heat Treatment	Temperature Reached
0	Unheated	20°C
1	Heat to start of peak	720°C
2	Heat to vibration peak	740°C
3	Heat just past vibration peak	750°C
4	Heat past vibration peak	850°C

Table 3.8 Samples of 0.4% Carbon Steel Heated to Different Temperatures Before Quenching in Water

The samples were rapidly heated to the temperatures shown above and were not held at these temperatures for any significant amount of time. The structures corresponding to each sample are shown in figure 3.46. All were taken at x200 magnification.

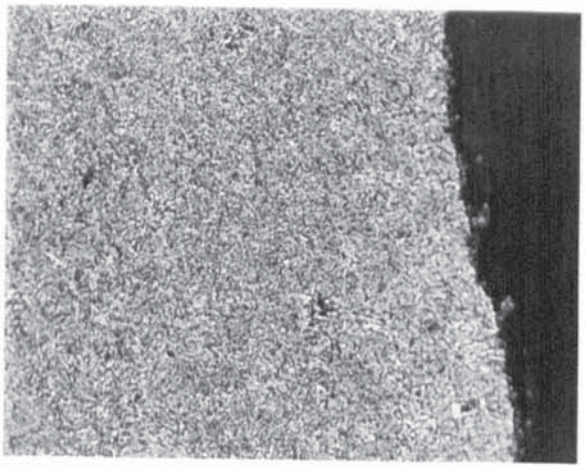

a) Sample 0 (Outer Edge x200)

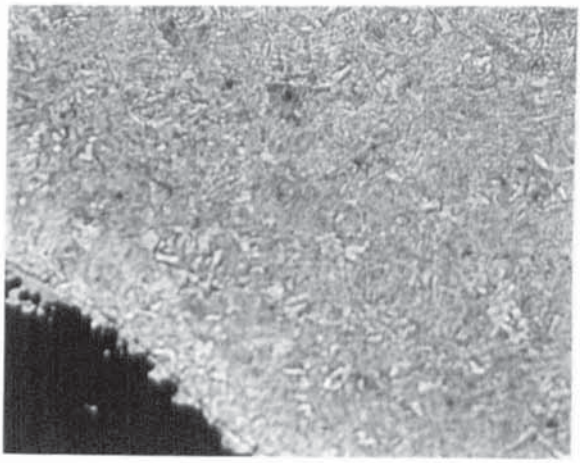

b) Sample 1 (Outer Edge x 200)

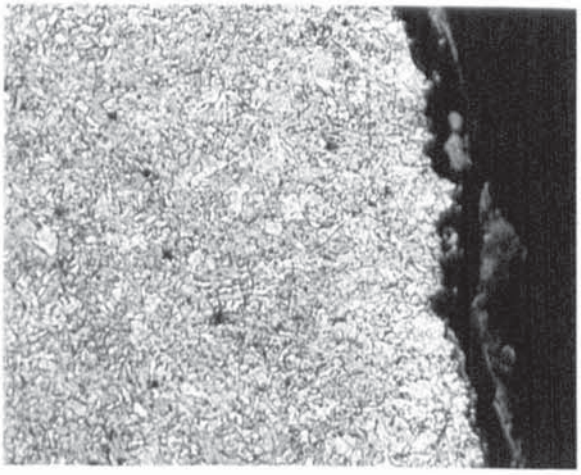

c) Sample 2 (Outer Edge x200)

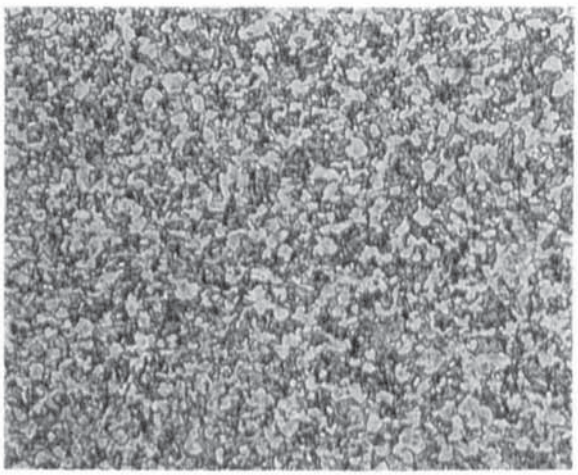

d) Sample 3 (Centre x200)

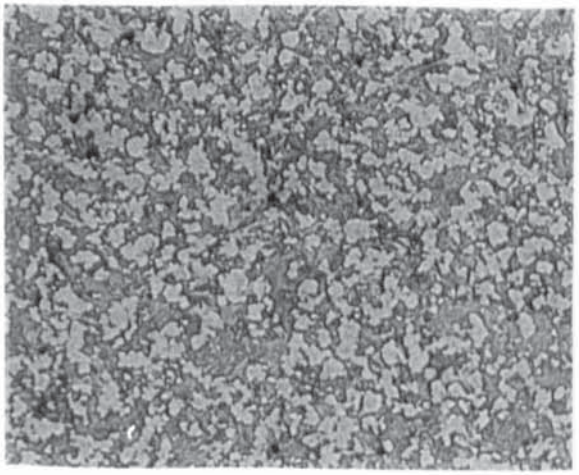

e) Sample 4 (Centre x200)

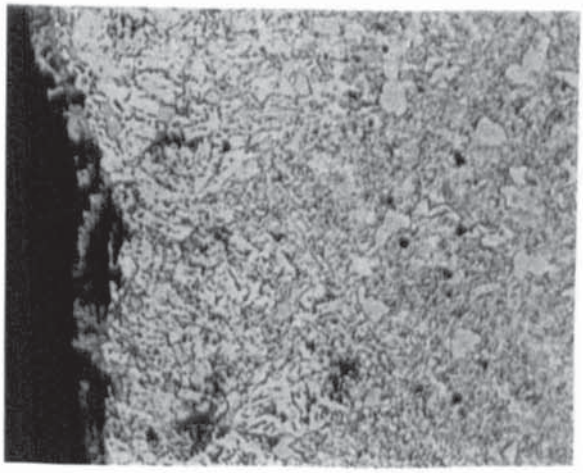

f) Sample 4 (Outer Edge x500)

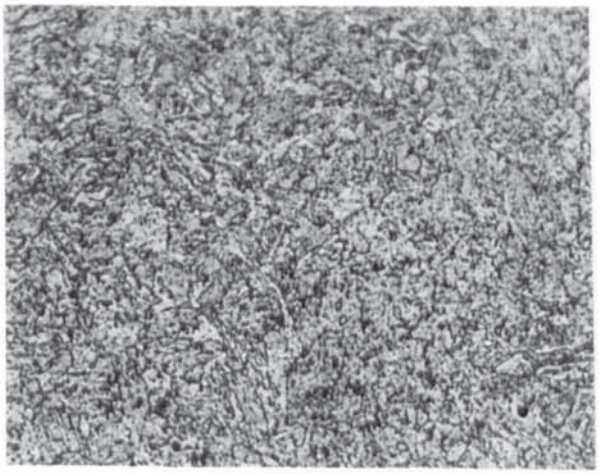

g) Sample 2 (Outer Edge x500)

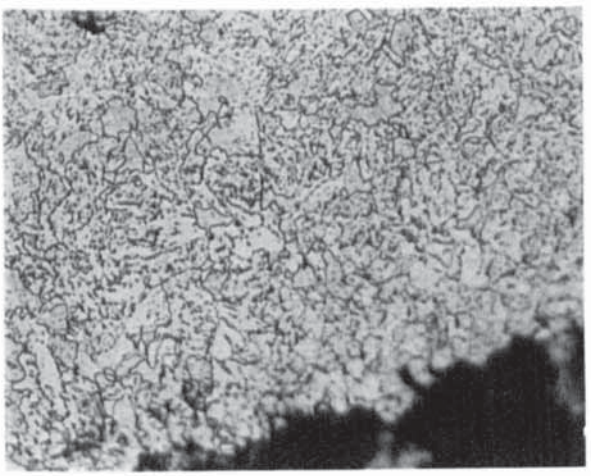

h) Sample 3 (Outer Edge x500)

Figure 3.46 Microstructures of 0.4% Carbon Steel Heated To Different Temperatures By Induction

There is evidence of different size grain structure, but no indication of previous austenite formation. There may be several reasons for this. Firstly the holding time at the various temperatures may be far too short and as a result no transformation occurred. Secondly, the water quench may have been inadequate so the structures were not 'frozen' and did not produce any martensite. However, the final sample was a control because it was heated to 850°C and quenched. If hardening was to take place, then it should be apparent in this sample. It was not and may be as a result of either surface cooling between heating and quenching or due to the absence of time for soaking before quenching. It is difficult to assess whether the test was invalid from the results obtained. There is scope for further work regarding this topic and more tests are required to discover whether resonance near the Curie point is associated with the phase transformation.

It can be seen from the structures in figure 3.46 that the unheated sample in (a) is composed of approximately half ferrite and half pearlite. There is no significant difference between the structure at the centre and edge of the sample.

When heated to the start of resonance, (b) the structure is similar to that of the unheated sample. The sample which was heated to the point at which resonance was a maximum, (c) shows again that there is little difference between this structure and the two previous.

The structure of the sample in (d) is remarkably different from the other structures. The photograph was taken of the centre of the sample. The sample that was heated to 850°C before being quenched (e) shows the structure at the centre of the sample is similar to that of (d). However, the structure at the outer edge of the same sample at x500 magnification (f) is quite different.

Sample 2, heated to the temperature at which vibration was maximum shows the structure at the outer edge, (g). Even at x500 magnification it shows no signs of any transformation.

Finally, the structure of the sample that was heated just past the peak of vibration is shown in (h) taken at x500 magnification. It does not show any indication of a phase transformation having occurred.

3.22 Conventional Heating of Steel Bars

A mild steel bar with accelerometer fixed to one face was heated using an oxy-acetylene torch to discover whether vibration would occur by this method of heating. The bar was placed horizontally on refractory bricks. No vibration was observed. This simple experiment suggested that heat alone was not a mechanism for vibration and the electromagnetic field was the main driving force behind the vibration in steel.

A bar which had a strain gauge welded onto it used for magnetostriction measurements in chapter 4 was heated in a furnace to 800°C with no field. No increase in strain was observed over the temperature range, other than apparent strain due to temperature effects.

3.23 Testing Different Materials

Non-ferromagnetic materials were tested to see whether vibration occurred during heating. Testing of a weakly ferromagnetic alloy, monel is also included in this section. All bars were 40 mm diameter of length 500 mm.

3.23.1 Austenitic Stainless Steel

No increase in vibration occurred during heating from ambient temperature to 900°C, when heated at 15kW, 30kW and 44kW. The results did show that a small amount of vibration was present throughout the heating process at frequencies of 6.4 kHz, 12.8 kHz and 19.2 kHz. The amplitude of vibration at these frequencies increased with increase in power setting. These values are the same magnitude as the noise which

measured a total of 0.06 volts or 6g across the frequency range 0 - 30 kHz. The signal at 6.4 kHz was either produced by the accelerometer itself (noise) or was low magnitude magnetostriction. The former is the most likely. Table 3.9 shows a summary of the results.

Frequency (kHz)	Acceleration at Power = 15kW	Acceleration at Power = 30 kW	Acceleration at Power = 44kW
3.2	0.03 g	0.04 g	0.05 g
6.4	0.11 g	0.62 g	1.10 g
9.6	0.01 g	0.01 g	0.01 g
12.8	0.09 g	0.10 g	0.04 g
16.0	0.01 g	0.01 g	0.01 g
19.2	0.02 g	0.01 g	0.02 g
22.4	0.01 g	0.01 g	0.01 g
25.6	0.01 g	0.01 g	0.02 g

Table 3.9 Vibration of Austenitic Stainless Steel Bar

The stainless steel and mild steel bars had approximately the same natural resonances with increase in temperature. Since resonance did not occur in austenitic steel, it must be assumed that the phenomenon is limited only to the ferromagnetic steels and is possibly associated with the magnetic properties they possess. For example, their high permeabilities and magnetostriction coefficients.

3.23.2 Copper

A bar of copper was heated at a number of power settings. The results were similar to those of the stainless steel and showed no increase in vibration. The vibration detected was due to noise or pick-up and originated from induced signals in the accelerometer. The magnitude of the signal was 0.1 volt with the acceleration component at 6.4 kHz being the greatest. The vibration appeared to be present all the way through the heating process, at low magnitude.

3.23.3 Monel 400

This material is ferromagnetic at room temperature but has a Curie point of about 50°C. It showed no visible increase in the amplitude of vibration when heated to 150°C and this was thought to be due to the fact that the starting temperature was too close to its

Curie temperature. It had been shown, for mild steel, that the closer the initial temperature to the Curie point, the lower the magnitude of resonance, section 3.11.

Further tests involved cooling the monel bar using liquid nitrogen to -120°C before heating but still no resonances were excited. Only noise was measured as shown in table 3.10.

Frequency	dBV	Voltage	Vibration
3.2 kHz	-48.0 dBV	0.004 V	0.04g
6.4 kHz	-20.7 dBV	0.092 V	0.92g
12.8 kHz	-53.1 dBV	0.002 V	0.02g

Table 3.10 Frequency Components of Vibration From Heating Monel 400

3.23.4 Titanium

Titanium is a paramagnetic material which undergoes a phase transformation at 902°C when its structure changes from body centred cubic to face centred cubic. Mild steel also undergoes this transformation at about 850°C. It was decided to use titanium to see whether an increase in longitudinal vibration occurred as it underwent its phase transformation. The titanium bar was heated at various power settings in the induction heater and it was found that no increase in vibration was detected between ambient temperature and 1050°C. It must therefore be concluded that the phase transformation alone does not produce the increase in longitudinal vibration for either titanium or steel.

3.24 Discussion

The results collected in this chapter show a number of significant points. The results agree firstly with those discovered by Dibben (1991) showing that an increase in longitudinal vibration may occur in steel bars during induction heating. This increase, or resonance, arose when a natural frequency of the bar was excited. This appeared to occur most frequently when the surface of the bar was near the Curie temperature but was found to be due to the fact that the surface temperature did not increase greatly at this point while the rest of the bar increased steadily in temperature. The overall temperature distribution was found to be different from that assumed by Davies and Simpson (1972). By changing the length of steel bar, a resonance could be excited at a number of different temperatures ranging from 100°C to 800°C.

The magnitude of vibration at resonance was found to vary with heating power, bar diameter and initial temperature. The first two show that the magnitude is proportional to power input to the bar or field strength. The mechanism responsible for exciting the resonances appeared to be due to a combination of electromagnetic and temperature effects. It was found to only occur in ferromagnetic materials so is possibly connected with the spontaneous magnetisation of the materials or magnetostriction.

Since different results were obtained using different carbon steels the phenomenon could be dependent upon certain phases such as ferrite, cementite, pearlite or martensite. It is known that austenitic materials such as stainless steel do not show resonance when heated by induction.

Hypotheses by other authors as to the mechanism responsible for the increase in ultrasonic wave amplitude near the Curie point have been tested as possible explanations for resonance near the Curie point produced by induction heating. They were found not to be responsible for resonance. These include the alpha to gamma phase transformation and the existence of a thin ferromagnetic surface layer on a steel bar with paramagnetic centre.

Finally, after a mild steel bar had been heated and vibration occurred there was no apparent change to the structure of the material or its hardness. The only change which had occurred was normalising.

3.25 Summary of Results

From these findings, it appears that the most likely cause of resonance near the Curie point is magnetostriction. Magnetostriction was investigated primarily because the longitudinal vibrations in the steel bars were at twice the field frequency and harmonics thereof. Magnetostriction also occurs at twice the field frequency. Resonance was only seen to occur in ferromagnetic steel and magnetostriction is large in these materials.

3.26 Conclusions

It has been shown that longitudinal resonances are excited in ferromagnetic steel bars heated by induction when a natural frequency of the bar coincides with twice the heating frequency or subsequent harmonics. The magnitude of resonance can be a function of many factors such as:

- initial temperature prior to heating - the greater the initial 'soaked' temperature of a bar, the lower the magnitude of resonance.

• inverter power setting - for low powers the magnitude of resonance may be high and at higher powers resonance may not occur because of the rapid rate of heating.

• type of steel - of the different carbon steels tested, the lower carbon steels (with the exception of iron) showed higher magnitudes of resonance.

• diameter of bar - doubling the diameter of steel bar, doubled the power input to the workpiece and the magnitude of resonance.

The phenomenon of resonance only occurs in ferromagnetic steels when heated electromagnetically and is unlikely to be due to the occurrence of the α to γ phase transformation but further tests are required. Also the idea of the surface of a bar cooling below the Curie point, concentrating the field in a skin layer is not responsible for resonance because heating using an alternating field creates a skin throughout the heating process.

Magnetostriction in steel, the mechanism thought to be responsible for resonance is investigated in the next chapter. The main interest in the measurement of this property is around the Curie point. It is possible that there may be two different mechanisms responsible for resonance below and at the Curie point.

CHAPTER FOUR

MAGNETOSTRICTION MEASUREMENTS

4.1 Introduction

As part of this research it was necessary to study the magnetostriction of mild steel as a function of temperature. Published data on this subject is rare, although some data has been published on magnetostriction in electrical materials such as silicon-iron. Existing data for ferromagnetic materials shows that Joule magnetostriction, that is a change in length in the direction parallel to the magnetisation, decreases with temperature until it becomes zero at the Curie point. However, results from the previous chapter suggested that the vibration was most likely caused by magnetostriction. No published data was discovered that showed quantitative measurements of magnetostriction for any steel in the region of the Curie point. Most data was quoted for temperatures up to about 720°C. At high temperatures instrumentation, such as strain gauges, becomes problematic.

The most accurate way to measure such small changes in dimension of a sample of mild steel was to use a strain gauge that was capable of withstanding the high temperatures involved. Initially such a gauge was not readily available and an alternative method of measuring magnetostriction with displacement transducers was used. Magnetostriction was measured up to and including the Curie point where vibration had been seen to increase so frequently when heating steel by induction. A gauge later became commercially available from a manufacturer in Japan which could continuously operate up to 750°C and withstand higher temperatures (800°C) for short periods. This enabled more accurate measurements to be made.

4.2 Displacement Apparatus

The Crossley induction heater was unsuitable for delicate magnetostriction measurements and operated at a fixed medium frequency. An apparatus with a separate heating coil and magnetising coil was designed and constructed. The advantages of using separate coils for heating and producing magnetostriction were that the temperature of the specimen could be controlled more accurately and the magnetising field could be of variable frequency. A sensitive displacement transducer was used to record the magnetostriction in a ring sample of mild steel (BS970-En3b). An alternating field rather than a steady d.c. field was used for several reasons:

a) it was not known whether the a.c.. and d.c. magnetostriction of a specimen were the same for similar field strengths and as resonance of steel heated by induction was thought to be produced by a.c. magnetostriction it was decided to keep the field a.c.

b) it was much easier to measure an alternating signal from the displacement transducer than a d.c. signal because thermal expansion of the mild steel ring did not produce any a.c. component. Even with severe drifting of the signal it was possible to distinguish the smaller alternating signal.

c) a d.c. field would have to be switched on and off in order to see the dimension change due to magnetostriction whereas the a.c. field could be left on.

The equipment designed and constructed incorporated a ring specimen of mild steel as the test piece. Figure 4.1 shows the assembled apparatus which had a diameter of 160 mm and measured 65 mm high. The actual rig can be seen in figure 4.2. The ring dimensions were 88 mm outer diameter, 80 mm inner diameter and height 20 mm. A ring specimen was used because it was easier to thermally insulate, the field created by the toroidal winding would not affect the transducer and a ring shape suffers no end effects. It was undesirable to use accelerometers to measure the ring's acceleration because of the need for cooling parts of the ring and the mass of the accelerometer would affect the measurements. Instead a linear variable differential transformer (LVDT) was used. This was a commercially available model from RDP Electronics; its specification can be found in Appendix A.1.7. The instrument was capable of measuring to high resolution although this depended on the nature of the rest of the equipment regarding noise. Repeatability of the instrument was quoted as being 0.15 μm. Noise from the instrument and associated circuit was found to measure 4 mV peak to peak.

The output from the LVDT was set to give 5 mV/μm. When initially tested, it was found that the signal to noise ratio was almost unity. Signal processing techniques such as averaging or filtering the signal did not give adequate results, so a small lever was constructed and fitted to increase the signal by using mechanical advantage. The mild steel ring was housed inside a concrete jacket which had a small hole in the side for thermocouple access and another for a ceramic probe, which measured 7 mm in diameter and 60 mm long. A glass water jacket was inserted down the centre of the concrete structure. A toroidal coil was wound around the concrete and through the water jacket which kept the winding cool and prevented the insulation from breaking down. Water was also passed through silicon rubber tubing, which was wrapped around the outside of the concrete jacket, to cool the winding. The ceramic probe, in contact with the vertical surface of the ring, pushed against one end of the lever. The other side of the lever pushed against the LVDT. This was spring loaded and kept the probe in constant contact

with the specimen. The ceramic probe was screwed into a length of Nylatron† which is a self-lubricated plastic and fitted into a small housing of the same material (not shown in the diagram). Metal was avoided in the construction because of the close proximity of the heating coil which may have heated the parts causing thermal expansion and hence measuring errors. The lever had a mechanical advantage of 8:1 and a movement of 1 μm produced a movement of 8 μm at the transducer.

† Nylatron is a registered trademark of Polypenco Ltd.

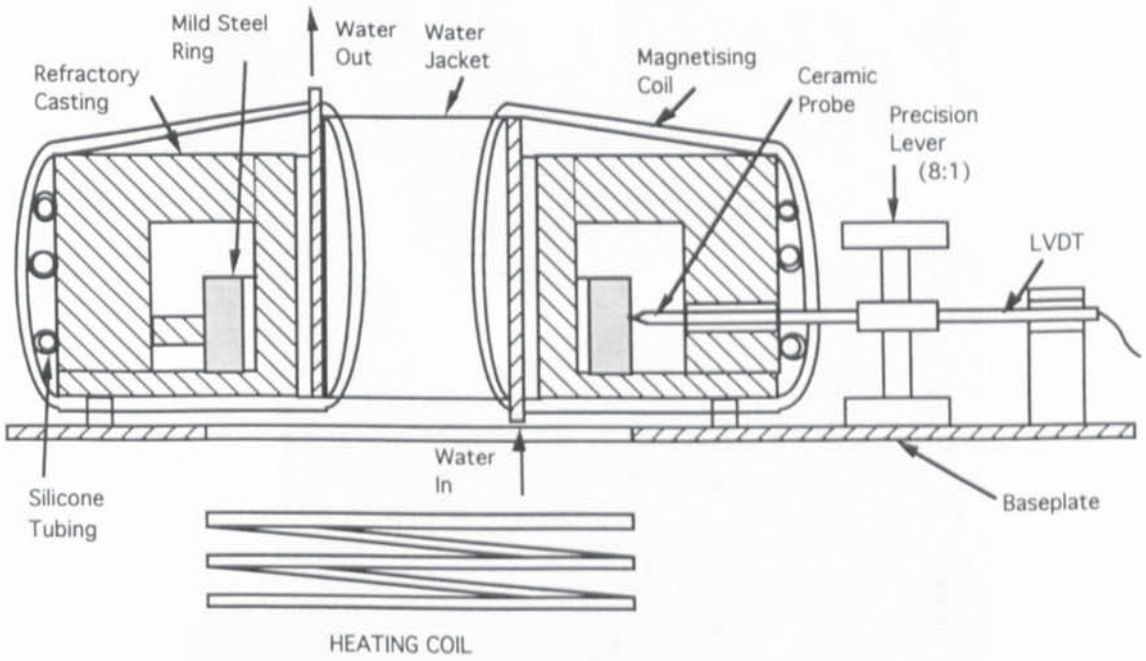

Figure 4.1 Apparatus Used to Measure Magnetostriction

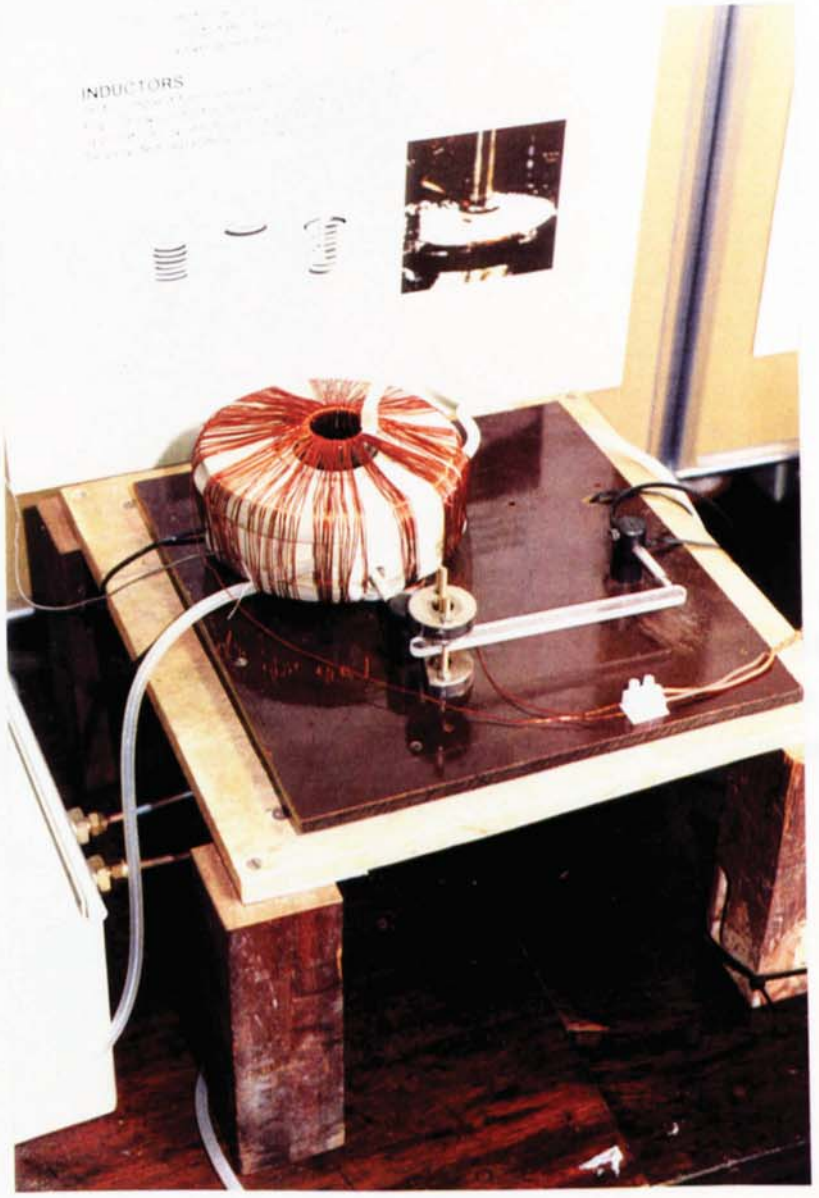

Figure 4.2 Photograph of Apparatus Used to Measure Magnetostriction

The specimen was heated using a 4kW, 150 kHz Cheltenham induction heater. The heating coil was placed underneath the apparatus and was capable of heating the ring to 750°C. The temperature distribution was assumed to be constant across the small section of the ring due to the low heating power used and the long heating duration. The magnetising coil current was obtained from a 3kW amplifier which was fed from a signal generator. Unfortunately, the lowest frequency which could be used without causing distortion was 18 Hz giving a maximum current of 2.5 Amps. This gave a peak field of 2650 Am^{-1} inside the coil. Tests were generally carried out at the lower frequencies to try to avoid exciting any natural modes of the ring. The most likely mode of the rectangular

cross section ring to be excited was believed to be extensional since magnetostriction would cause the ring to increase in diameter and was calculated according to Harris and Crede (1976) using:

$$\omega_n = \sqrt{\frac{E}{\gamma R^2}} \tag{4.1}$$

where E = modulus of elasticity (Nmm^{-2})
γ = density (kgm^{-3})
R = radius of ring (m)

For mild steel $\omega_n = 123148$ rad/s (4.2)

$f_n = 19600$ Hz (4.3)

The output from the LVDT was connected to a spectrum analyser. Measurements of the fundamental, second and third harmonic signals at 36 Hz, 72 Hz and 108 Hz respectively were recorded. These were plotted against temperature, figures 4.3, 4.4 and 4.5.

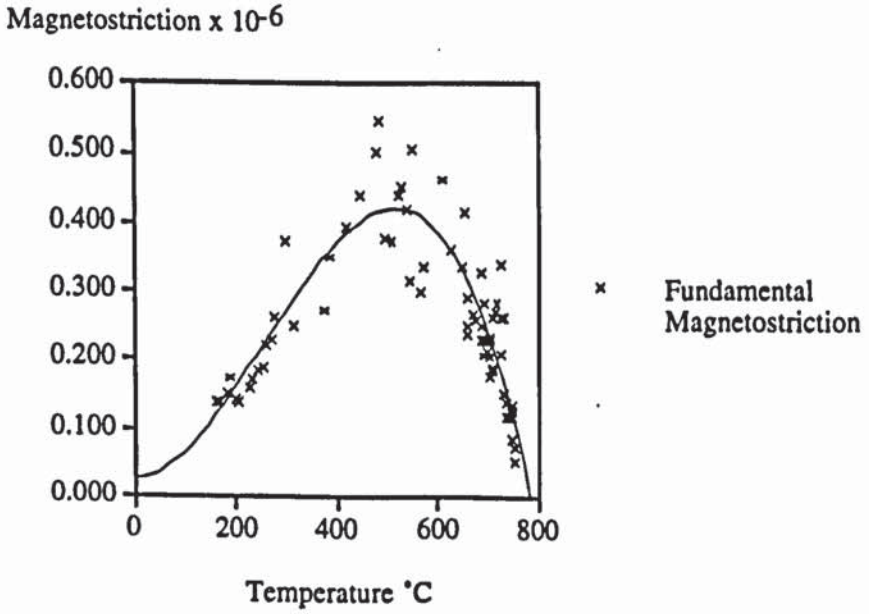

Figure 4.3 Magnetostriction at 36 Hz As a Function of Temperature

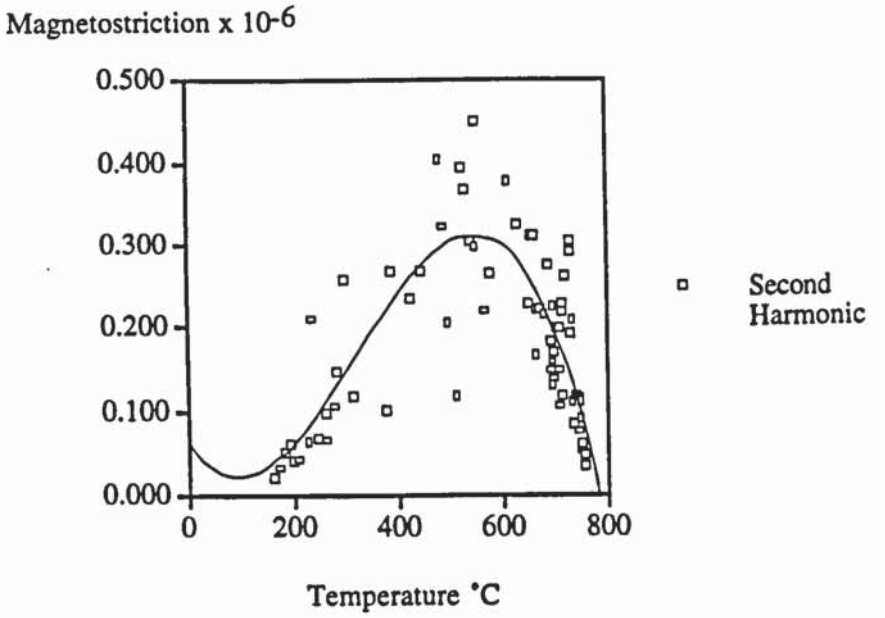

Figure 4.4 Magnetostriction at 72 Hz As a Function of Temperature

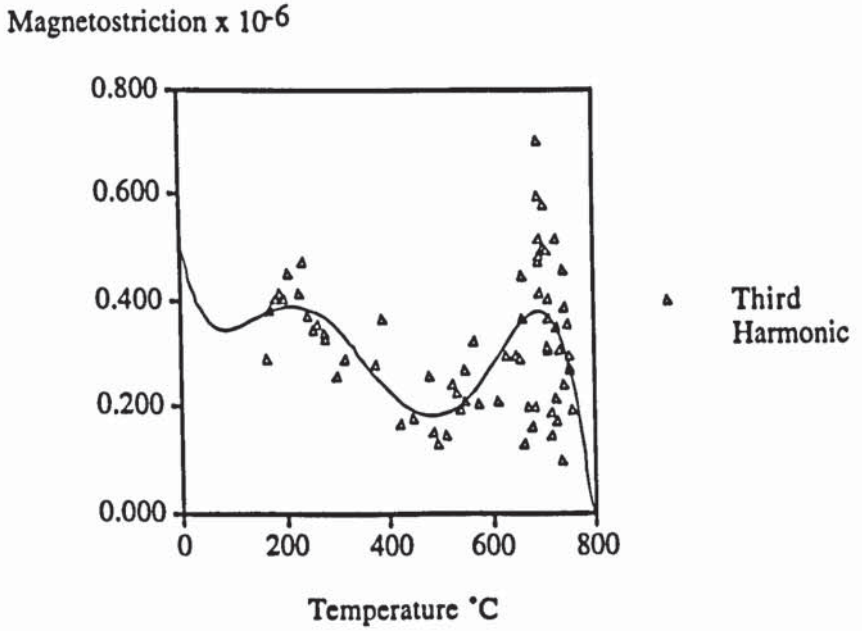

Figure 4.5 Magnetostriction at 108 Hz As a Function of Temperature

The graphs show an increase in signal for the fundamental and second harmonic at about 500°C. It was later found by varying the frequency of the field that the ring had natural resonances at 55 Hz, 110 Hz and 165 Hz at ambient temperature which produced a ten fold increase in the displacement signal when excited by a field at half these

frequencies. The frequency of these resonances were found to decrease with temperature to 36 Hz and 72 Hz at about 500°C which explains the increased signal at this temperature. The third harmonic of magnetostriction at 108 Hz was seen to increase just before the Curie point and was again due to the excitation of a natural resonance of the ring at this temperature. These large increases were not due to an increase in magnetostriction.

The magnitude of magnetostriction and direction of the dimension change both agree with published results for iron. Most texts, such as Bozorth (1951) report positive magnetostriction, or an increase in size in low fields for iron followed by negative, or decrease in size in higher fields (>16 kA/m). All the results collected showed only positive magnetostriction or an increase in the diameter of the ring. This is unlikely to be due to thermal expansion unless the expansion was affected by the magnetic field and produced oscillations as a result. The magnitude of the change in diameter is far less than would be expected from thermal effects in any case. Unfortunately no data could be found of magnetostriction in mild steel as a function of temperature and the results have to be compared to the nearest similar material, iron. Since the field used for the above test was 2650 A/m only positive magnetostriction would be expected, which occurred.

On all three graphs it is evident that magnetostriction at the three measured frequencies decreases rapidly as the Curie point is approached. The maximum ring temperature was 754°C and earlier results showed that the increase in vibration when a bar was heated by induction generally occurred between 710°C and 740°C. However, there are two distinct differences between the results from this test apparatus and the results collected from the vibration of steel bars in the induction heater:

1) the ring had no temperature difference across it due to the duration of heating and low power used.

2) the field strength in the induction heater was 30 times that produced by the magnetostriction measuring apparatus (omitting the field from the heating coil).

The LVDT signal was observed together with a voltage output from the signal generator to observe the minute change in diameter of the ring. The LVDT waveform was found to be at twice the frequency of the signal generator voltage. The LVDT signal was therefore measuring magnetostriction of the ring. The magnetostriction signal was slightly out of phase with the signal generator voltage and was not a sinusoidal waveform due to the high harmonic content.

4.2.1 Magnitude of Magnetostriction

In section 2.8.6 it was reported that for iron, the magnetostriction in a steady field of 2500 A/m was 4.5×10^{-6} from figure 2.23. If this value is assumed to be the same as the total value expected in an a.c. field of the same magnitude then the expected change in diameter of the ring would be:

$$\Delta l / l = 4.5 \times 10^{-6} \tag{4.4}$$

$$\Delta d = 4.5 \times 10^{-6} \times 88 \text{ mm} = 3.96 \times 10^{-4} \text{ mm} \tag{4.5}$$

However, the results at each frequency component gave much smaller changes in diameter and hence lower values of magnetostriction averaging 0.4×10^{-6} for each of the three components measured as a function of temperature. It is anticipated that one of the reasons for the difference is the fact that each frequency component had been measured separately and was an rms value. Also, the magnetostriction measured was the a.c. magnetostriction whereas the quoted figure from section 2.8.6 was for a d.c. field. The two may well have different values. Finally, the material tested was mild steel and is likely to have different magnetostrictive properties from iron.

At room temperature magnetostriction was also measured as a function of field strength. Figure 4.6 shows the results from two sets of data. The signal from the LVDT was measured on a digital meter which gave an rms value of all the harmonics of the a.c. magnetostriction.

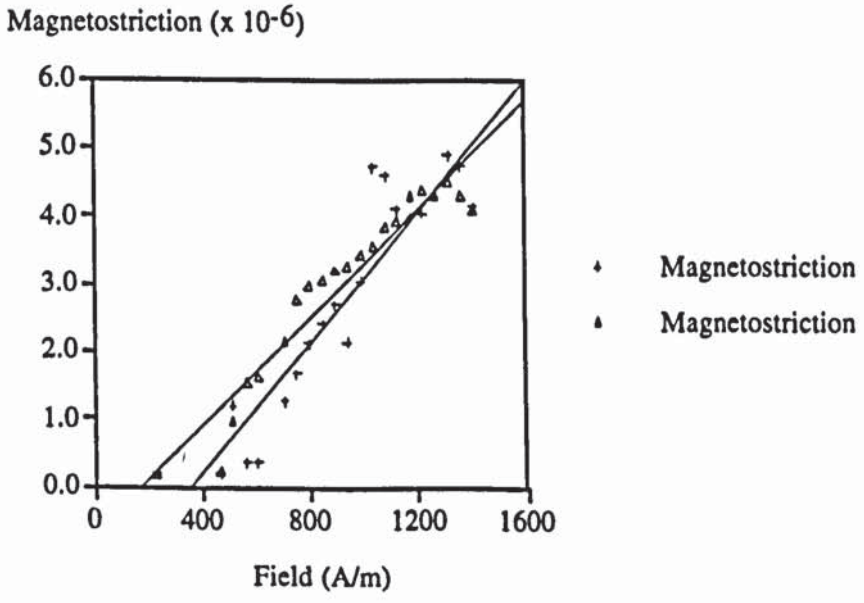

Figure 4.6. A.C. Magnetostriction as a Function of Field Strength

The relationship of magnetostriction as a function of field strength was found to be linear. The values of magnetostriction were much higher than those recorded for the tests involving a temperature rise because the total a.c. magnetostriction was taken into account instead of individual frequency components. The magnitude was in better agreement with published data for iron and the signal was positive over the low range of field strengths used.

4.2.2 Discussion

The constructed apparatus had some problems associated with the accuracy of the recorded measurements. The graphs of magnetostriction in figures 4.3, 4.4 and 4.5 show the general trend as a function of temperature, but as can be seen from the amount of scatter, the measurements vary considerably. Even using the lever arrangement to increase the displacement signal, it was only just greater than the noise level and although an average of the signal was recorded to minimise noise, measurements were poor due to the low signal to noise ratio. The lever, constructed using precision bearings, introduced a small amount of movement into the system, causing some error but it was assumed that any play was taken up by the spring loaded transducer. Finally, the contact between the probe and the mild steel ring was not visible and relied on the spring in the LVDT to keep a good contact. The probe often stuck in its housing and required resetting on the surface of the steel ring introducing errors into the measurements. This could not be avoided because of the tight fit necessary between the parts to prevent errors due to play between the moving pieces. The mild steel ring was heated to 750°C in air and the formation of scale would have certainly affected the results. The magnetostriction measurements taken may have been for the scale rather than the mild steel and could be a valid explanation for the difference in the magnitude when compared to existing data for iron.

Magnetostriction at the three frequencies was recorded simultaneously. If any of the measurements were spurious, for example due to a stuck probe becoming free, then the results collected at all three frequencies would be expected to show similar increases or decreases with temperature. Since this is not the case, the results are considered to be valid, even if not an accurate representation of magnetostriction.

Errors would have been introduced due to the design of the apparatus itself. The transducer arrangement was so sensitive that it could detect traffic noise from the road outside the laboratory. Noise was also produced when cooling water flowed through the silicone rubber tubing. The water flow had to be present in order to prevent the insulation on the winding from breaking down. With the current flowing through the coil, wound directly onto the concrete casing, forces were present between the turns causing vibration and could be heard as a humming noise. It was also possible to feel the movement by

placing a hand on the casing. This vibration would have been transmitted to the mild steel ring, which rested on a ledge inside the casing, or to the baseplate, on which the transducer sat. Ways of eliminating the vibration were looked at but proved too difficult in practice. These included:

a) winding the coil so that it did not contact the concrete casing. This meant that no other components could contact the coil such as the baseplate or fixtures. In practice it would have required the coil to be suspended in mid air.

b) use of a d.c. current in the coil would have only created forces between the turns when switched on or off. This would eliminate vibration in the apparatus but made it extremely difficult to measure magnetostriction as thermal effects would then affect the measurements. With a d.c. field the magnetostriction signal would have to be observed as a d.c. signal. This was undesirable as the transducer was susceptible to drifting. A d.c. field would also magnetise the mild steel ring which would alter its magnetostrictive properties.

By positioning the LVDT on the refractory casing, the vibration signal produced by the winding was found to oscillate around a zero position, whereas the signal from magnetostriction, was found to be always greater than zero. As a result it was possible to distinguish the two signals and when measuring displacement from the ring, the transducer signal was found to consist almost entirely of a signal which was offset from the zero position indicating it to be due to magnetostriction and not vibration from the winding.

4.3 Measurements Using A Strain Gauge

Until recently high temperature strain gauges were very specialised and expensive instruments. They have now become commercially available as a complete package ready to weld onto a specimen to be measured. A Kyowa KHCS-10 gauge was used for these tests. The maximum temperature which it could withstand was quoted as 750°C. However, the manufacturers had performed tests up to 850°C. A specification of the gauge can be found in Appendix A.1.8 along with the data sheet in Appendix A.1.9. The gauge was welded longitudinally, at the mid-point of a 50 mm diameter bar of previously unheated En3b mild steel. The length of this bar was 200 mm. A 50 mm diameter bar was chosen because the strain gauge could only be welded to a bar of minimum radius 20 mm. Surface temperature was recorded using a thermocouple located at the mid-point of the bar. The strain gauge was connected into a bridge amplifier and the output from this to a spectrum analyser. An electrically heated furnace was used to heat the bar during the tests and a magnetising coil was constructed to fit inside the furnace to produce the

alternating magnetic field. The furnace was capable of heating to a temperature of 1000°C and was thyristor controlled. The magnetising coil had three layers, each consisting of 50 turns, wound around a ceramic tube. Each turn and layer was isolated from one other by refractory cement. A maximum current of 9 Amps at 50 Hz could be supplied to the magnetising coil. Argon gas was continuously piped into the furnace during the tests to minimise scale formation on the bar. The apparatus used is shown in figure 4.7.

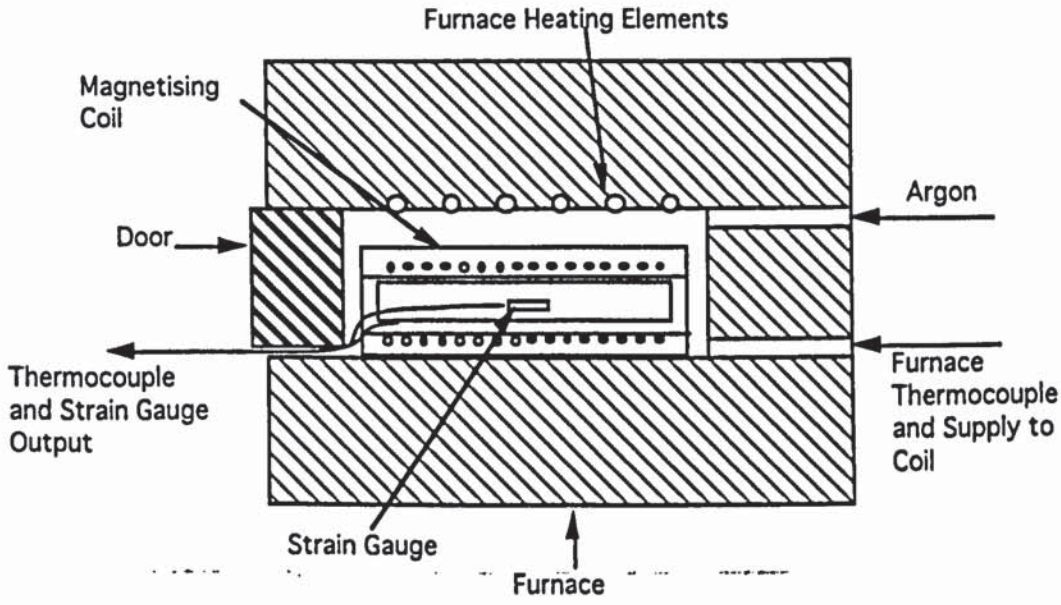

Figure 4.7 Apparatus to Measure Magnetostriction Using A Strain Gauge

The bar was slowly heated in the furnace up to 800°C. At each temperature interval of 10°C the current to the magnetising coil was increased from 0 to 6 Amps in steps of 1 Amp. At each field strength and temperature, the strain at 100 Hz, 200 Hz and 300 Hz was recorded from the spectrum analyser. Thermal expansion and apparent strain from the gauge due to temperature effects could be ignored since they gave d.c. signals and did not alter the a.c. signal when observed on a spectrum analyser. An emf at 50 Hz was induced in the strain gauge when placed in the magnetising coil but did not affect the signals due to magnetostriction at 100 Hz, 200 Hz and 300 Hz. Figure 4.8 shows a photograph of the furnace with the coil and steel bar inside.

Figure 4.8 Photograph of Furnace and Strain Gauge Equipment.

The first longitudinal resonance of the bar was calculated to be approximately 12.9 kHz using equation 2.10, and was not excited using the 50 Hz supply even as the resonance frequency decreased with temperature. Any signal would therefore be a direct measure of a.c. magnetostriction in mild steel.

Although this method of measuring magnetostriction is more accurate than using a displacement transducer there are a number of points to remember when comparing the results with those of vibration in bars heated by induction:

1) the field strength was 25 times lower than that in the induction heater.

2) the mild steel bar had no temperature difference across it since it was heated slowly in a furnace.

3) At high temperature (750°C) the output from the strain gauge showed drifting of the total a.c. signal at ± 10 microstrain / hour. The measurements of magnetostriction

were typically only 2 microstrain at each frequency and taken at about 20 readings per hour. Errors may have been introduced as a result of the drifting.

4) Scale produced on the bar would have directly affected readings from the strain gauge. Results would therefore be expected to vary from test to test as the amount of scale built up.

4.3.1 Field Strength

The field strength was measured using a large search coil and compared to the value calculated using Ampere's Law. The measured field strength was calculated to be 3900 A/m rms using equation (3.4). The calculated field strength was calculated to be 4500 A/m (for a current of 6 Amps) using Ampere's Law, equation (3.3).

4.3.2 Magnetic Properties of BS970-En3b Mild Steel

A similar piece of En3b mild steel bar with a high temperature search coil surrounding it was heated in the furnace to record values of flux density, B together with field strength as a function of temperature. It was assumed that the flux density at each specific temperature and field strength would be the same as for the other mild steel bar with the strain gauge attached to it. It was therefore not necessary to measure the flux density at the same time as measuring magnetostriction. The search coil was constructed from 5 turns of copper wire and insulated from the surface of the bar using ceramic beads threaded onto the wire. At each 20°C temperature step the current in the coil was increased from 0 to 6 Amps and the voltage across the search coil measured. Values of B were calculated at each field strength as a function of temperature. Figure 4.9 shows the graph for a field strength of 3750 A/m.

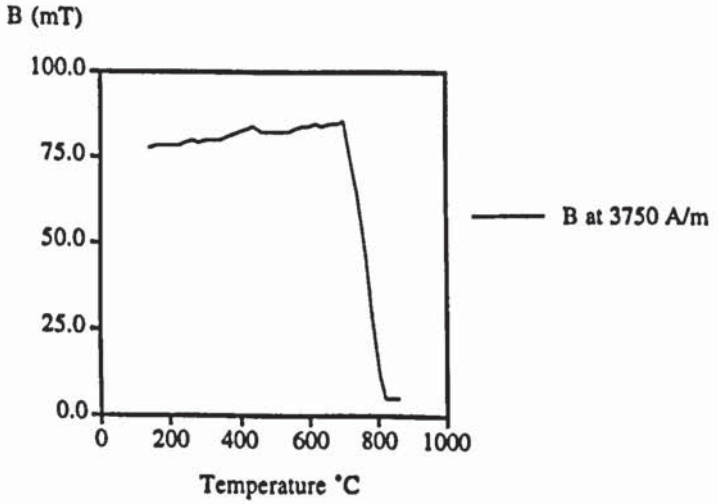

Figure 4.9 Flux Density As a Function of Temperature for a Mild Steel Bar

The flux density was found to increase slowly between 100°C and 700°C before falling rapidly as the Curie point was approached. Similar curves were produced at other field strengths.

4.3.3 Magnetostriction Results

The data collected of magnetostriction at 100 Hz, 200 Hz and 300 Hz was plotted as two types of graph. Strain was calculated using:

$$V_{out} = \frac{K\varepsilon N V_{in}}{4} \tag{4.6}$$

where K is the gauge factor
ε is the strain (microstrain)
N is the number of active arms
V_{in} is the bridge volts (V)
V_{out} is the measured voltage (μV)

The bridge amplifier had the gain set to 2000 so the measured value was actually 2000 times greater than that in equation (4.6).

The first graphs show each frequency component as a function of flux density for a range of temperatures. Figure 4.10 shows the a.c. magnetostriction at 100 Hz plotted against flux density from 95°C to 695°C.

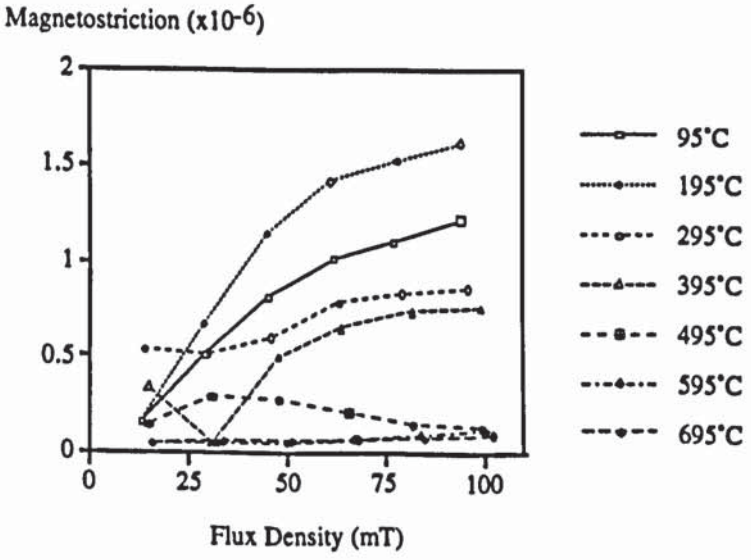

Figure 4.10 Magnetostriction at 100 Hz As a Function of Flux Density

Similar results were obtained when the 200 Hz component was plotted against flux density, figure 4.11.

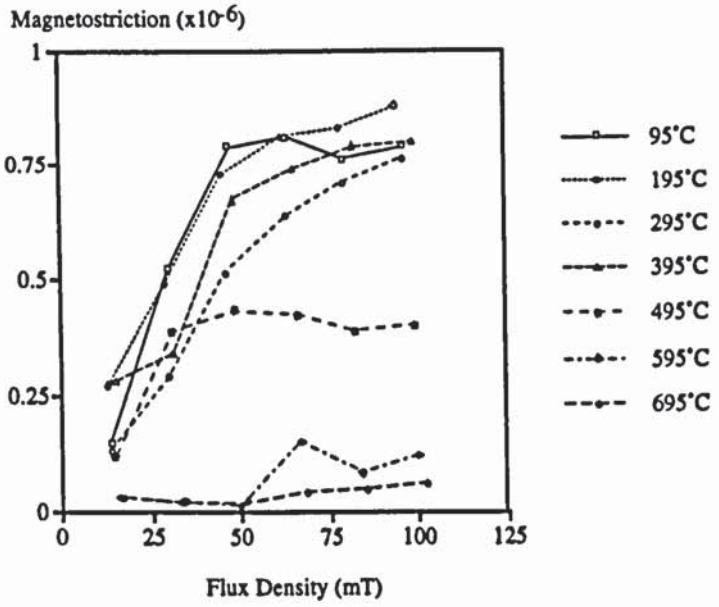

Figure 4.11 Magnetostriction at 200 Hz As a Function of Flux Density

The component at 300 Hz is shown plotted in figure 4.12 as a function of flux density.

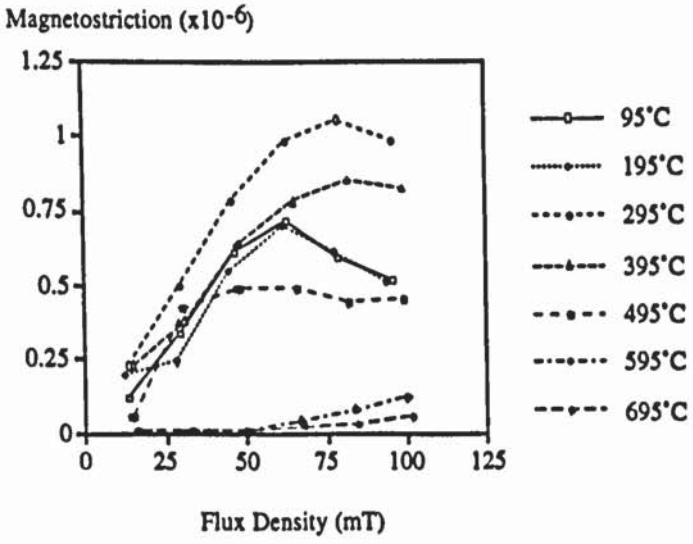

Figure 4.12 Magnetostriction at 300 Hz As a Function of Flux Density

The three graphs indicate that the 100 Hz component is of the greatest magnitude followed by the component at 300 Hz. Magnetostriction increased initially as the temperature increased before falling at higher temperatures. This is similar to the results obtained by Pike and Moses (1977) for silicon-iron.

The trend of magnetostriction as a function of flux density is to increase at low values before reaching a maximum at about 75 mT. The reason why the harmonic at 300 Hz was larger than that at 200 Hz is due to the harmonics in the supply current to the magnetising coil. The 50 Hz supply had harmonics at 150 Hz and 250 Hz and the field also contained similar amounts of these harmonics. The field at 150 Hz produced magnetostriction at twice this frequency or 300 Hz. This added to the 300 Hz magnetostriction signal caused by the 50 Hz signal.

4.3.4 Magnetostriction As a Function of Temperature

Graphs were plotted of magnetostriction at different field strengths as a function of temperature. Figure 4.13 shows the 100 Hz component at three field strengths.

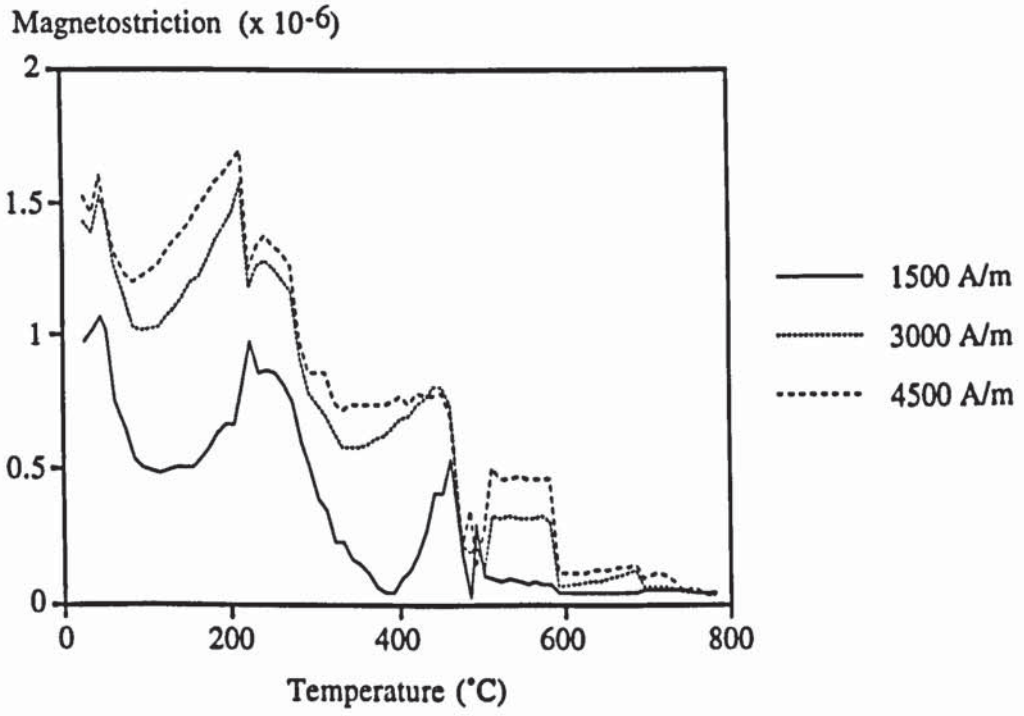

Figure 4.13 Magnetostriction At 100 Hz as a Function of Temperature

Figure 4.14 shows the 200 Hz component of magnetostriction.

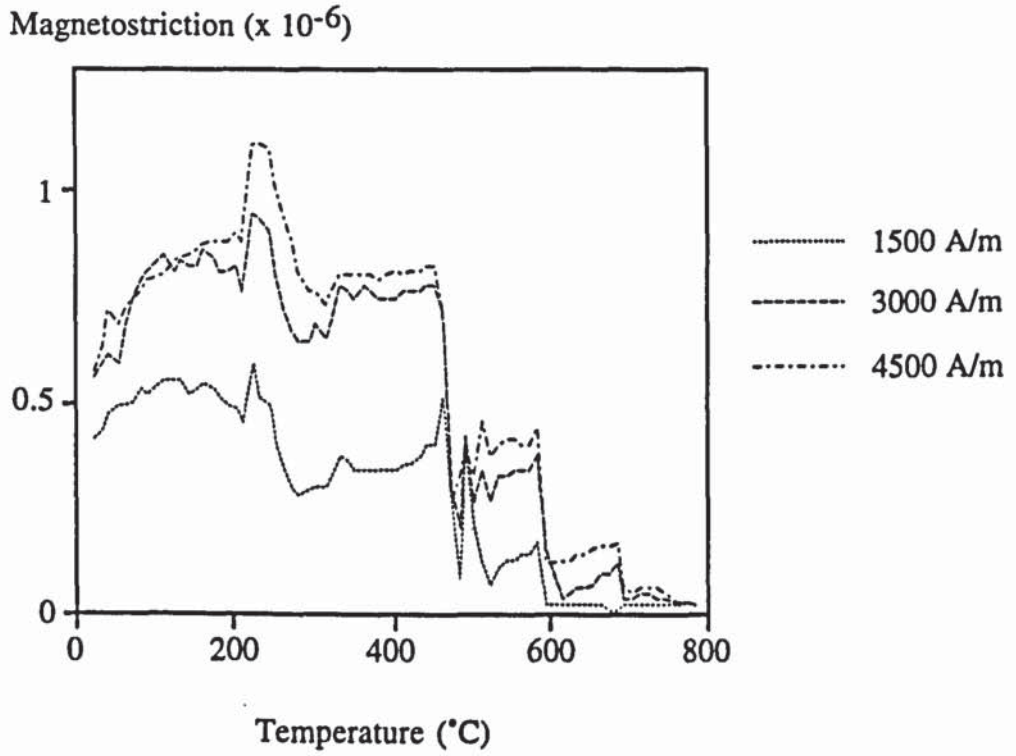

Figure 4.14 Magnetostriction at 200 Hz As a Function of Temperature

Figure 4.15 shows the 300 Hz component of magnetostriction measured as a function of temperature.

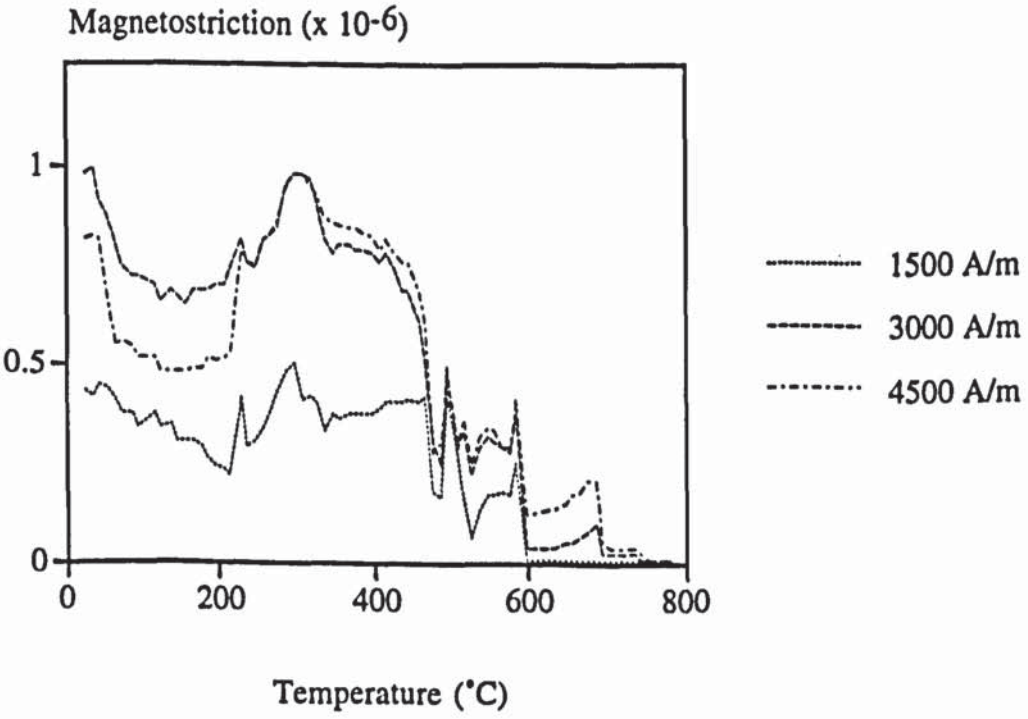

Figure 4.15 Magnetostriction at 300 Hz As a Function of Temperature

All three graphs show distinct increases in magnetostriction between 200°C and 400°C. A possible explanation for this increase is that it is related to the Curie point of cementite. The magnitude of magnetostriction is of the same order of magnitude as those measured using the displacement transducers, but is lower than published literature as each individual frequency component has been measured. The most important observation is that the magnetostriction at all three frequencies measured decreased to its lowest level near and at the Curie point.

The tests above were repeated on another occasion to see whether the results were repeatable. Figure 4.16 shows the comparison at 100 Hz. The magnitude of magnetostriction is different but the trend is similar giving increases at the same temperatures.

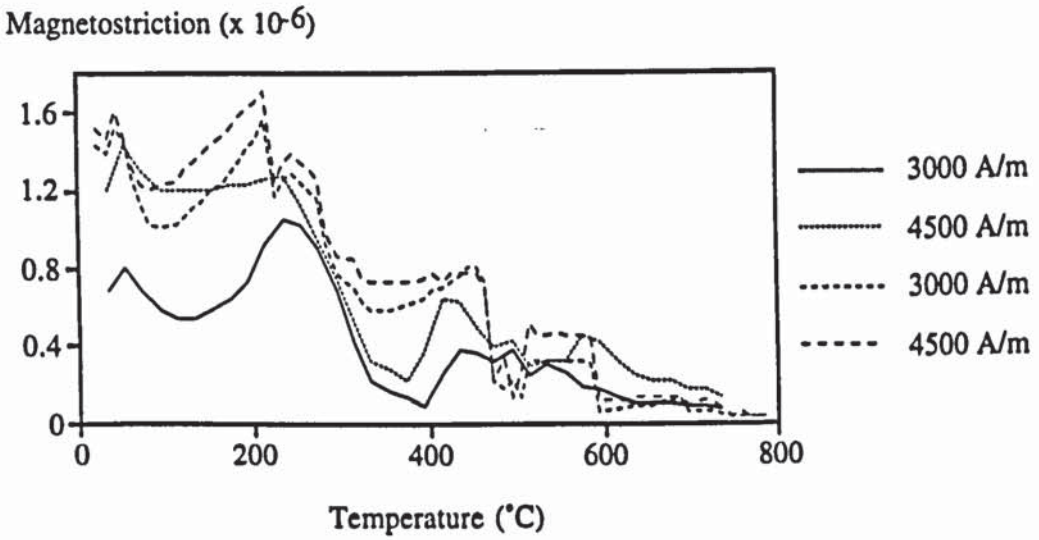

Figure 4.16 Comparison of Similar Tests Carried Out on Different Occasions For 100 Hz Component of Magnetostriction As A Function of Temperature

Figure 4.17 shows the comparison at 200 Hz. It is interesting to observe that the results were quite different at low to medium temperatures. The trend near the Curie point however is similar.

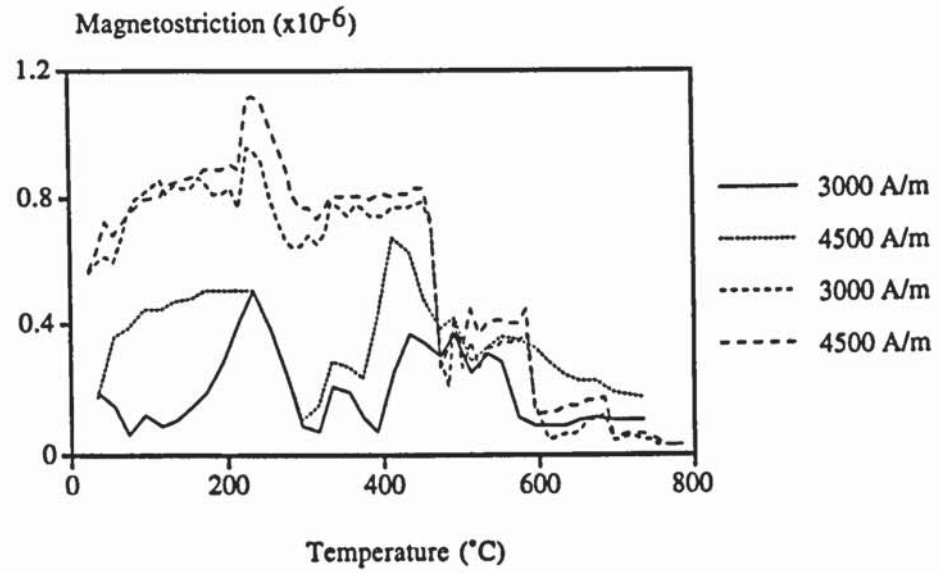

Figure 4.17 Comparison of Similar Tests Carried Out on Different Occasions For 200 Hz Component of Magnetostriction As A Function of Temperature

Figure 4.18 also shows a vast difference in results at 300 Hz between the two tests. The trends are similar but there is a large difference in the magnitudes.

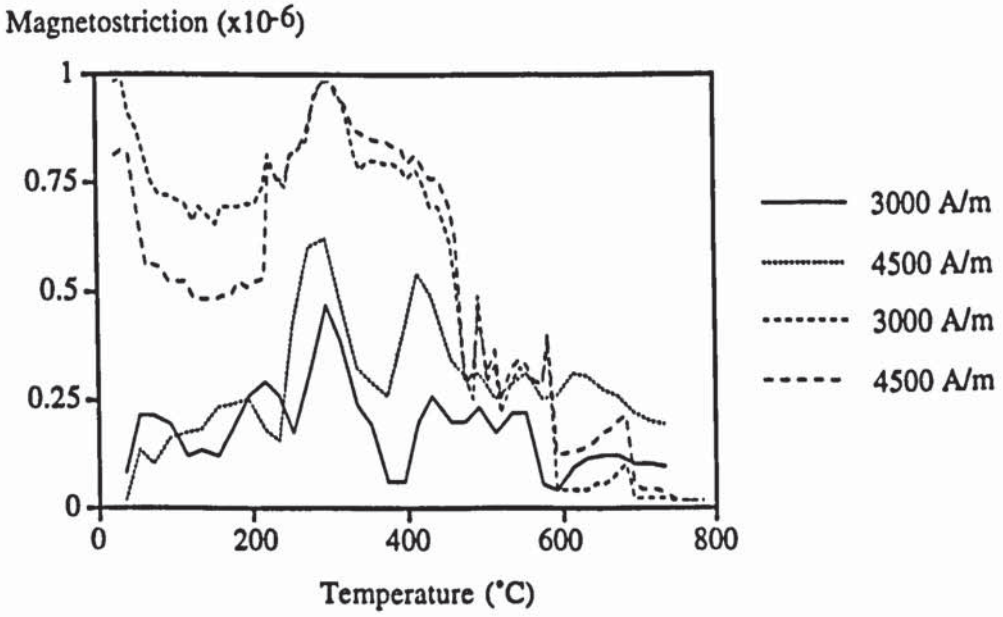

Figure 4.18 Comparison of Similar Tests Carried Out on Different Occasions For 300 Hz Component of Magnetostriction As A Function of Temperature

There are a number of reasons as to why the results differ for the two tests carried out on different occasions:

i) build up of scale around the strain gauge on the bar
ii) errors in the magnitude of coil current used as it was adjusted manually
iii) readings were taken quickly in succession at each field strength and may not have had time to give steady state responses

In order to compare the experimental results with theory the magnetisation process in the mild steel was considered. It was shown by Simmons and Thompson (1971) that for a single grain with a misorientation θ in the plane of the sheet the a.c. magnetostriction λ is approximately given by:

$$\lambda = \frac{3}{\sqrt{2}} \lambda_{100} \frac{B}{M_s} \sin\theta \left(\sin^2\frac{\theta}{2} - \cos^2\theta\right) \tag{4.7}$$

If it is assumed that the grains are perfectly aligned in the [0 1 1] direction giving $\theta = 90^\circ$, the equation becomes:

$$\lambda = \frac{3}{2\sqrt{2}} \lambda_{100} \frac{B}{M_s} \tag{4.8}$$

The grains in mild steel are not perfectly aligned but randomly orientated. An average approximation was calculated in order to compare the results of this work with other authors' work involving magnetostriction constants measured on single grains. Taking the average of equation 4.7 gives:

$$\lambda(av) = \frac{3}{\sqrt{2}} \lambda_{100} \frac{B}{M_s} \frac{1}{\pi} \int_0^{\pi} \sin\theta \left(\sin^2\frac{\theta}{2} - \cos^2\theta\right) \tag{4.9}$$

$$\lambda(av) = \frac{3}{\sqrt{2}} \lambda_{100} \frac{B}{M_s} \frac{1}{\pi} \left(\frac{-6\cos\theta + 3\cos 2\theta + 2\cos 3\theta}{24}\right)_0^{\pi} \tag{4.10}$$

$$\lambda(av) = \frac{3}{\sqrt{2}} \lambda_{100} \frac{B}{M_s} \frac{1}{\pi} \left(\frac{1}{3}\right) \tag{4.11}$$

$$\lambda(av) = \frac{1}{\pi\sqrt{2}} \lambda_{100} \frac{B}{M_s} \tag{4.12}$$

It must be noted that equation 4.12 is an approximate equation assuming that the grains in the mild steel specimen are randomly and equally arranged.

It was necessary to obtain the saturation magnetisation M_s as a function of temperature for the mild steel before calculating the magnetostriction constant from equation 4.12.

4.3.5 Saturation Magnetisation Measurements

The magnetising coil in the furnace did not create a field large enough to saturate the bar of En3b. However, the 60 kW Crossley heater produced a much larger electromagnetic field although at a higher frequency. The higher frequency did not affect the saturation magnetisation values and could therefore be used in calculations at lower frequency fields. A disadvantage of using the induction heater was that rapid heating of the bar occurred. To obtain plots of B and H against temperature all the signals were recorded on a digital oscilloscope. A search coil, consisting of 4 turns of copper wire and insulated using ceramic beads, was wrapped tightly around a 40 mm diameter En3b mild steel bar and the voltage signal rectified to give the magnitude. The field in the heating coil was measured by first of all measuring the current in the coil, using a Rogowski coil. The voltage induced across the Rogowski coil was rectified to give the magnitude and recorded. The current flowing in the heating coil was calculated from the voltage across the Rogowski coil and the field was calculated using Ampere's law. Tests were carried out from ambient temperature at different power settings. The three measured variables were recorded as functions of time. The results obtained were not exact since an integrator was not used with the Rogowski coil.

From plots of the voltages and temperature against time it was possible to extract the values of B and H at similar temperatures and plot B versus H for each temperature. Although these graphs have only eight points it is possible to see saturation beginning to occur. It was then possible to estimate values of saturation magnetisation at each temperature. Figure 4.19 shows the graph of B versus H at 50°C. From this the value of saturation magnetisation was estimated to be 0.57 T. This was repeated using the values of B and H for temperatures up to 750°C.

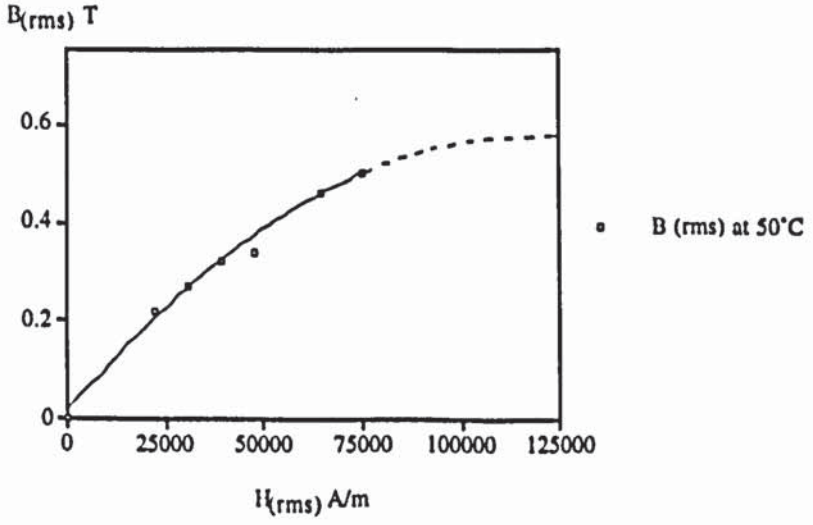

Figure 4.19 A Graph of B as a Function of H at 50°C

Table 4.1 shows the values of saturation magnetisation as a function of temperature.

Temperature °C	50	100	150	200	250
M_S (T)	0.57	0.56	0.61	0.61	0.58
Temperature °C	300	350	400	450	500
M_S (T)	0.57	0.62	0.60	0.59	0.57
Temperature °C	550	600	650	700	750
M_S (T)	0.53	0.53	0.50	0.41	0.27

Table 4.1 Saturation Magnetisation as a Function of Temperature

Figure 4.20 shows a graph of the values in table 4.1. The saturation magnetisation is almost constant up to 500°C before falling rapidly as the Curie point is approached.

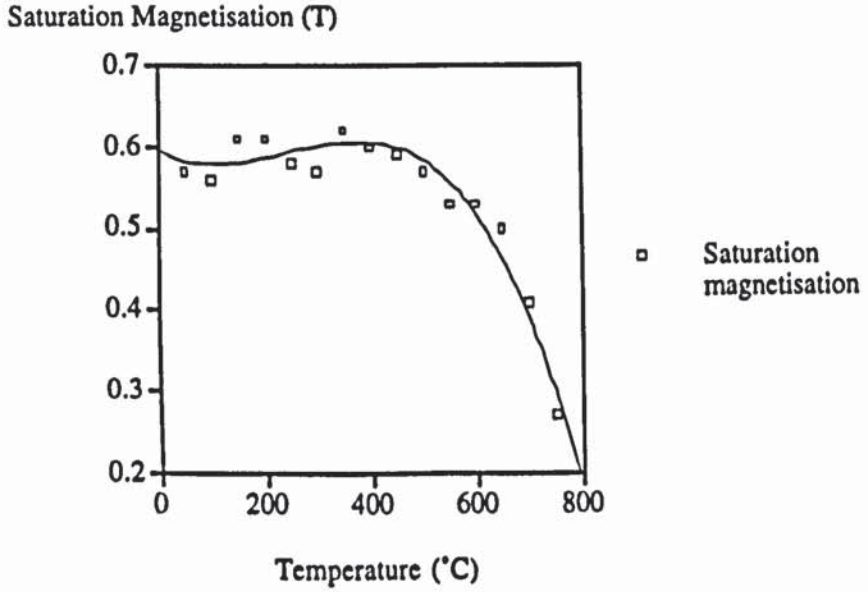

Figure 4.20 Graph of Saturation Magnetisation Against Temperature

4.3.6 Calculations of Magnetostriction Constants

The results of measured magnetostriction were compared with existing data from a single crystal. Using equation 4.12 and values of M_S and λ from the measurements obtained with the strain gauge, values of λ_{100} were calculated. Figure 4.21 shows the magnetostriction constant at 100 Hz as a function of temperature. This was compared to results obtained by Tatsumoto and Okamoto (1959) on tests involving single crystals of iron, figure 2.22. The results obtained using mild steel are of the same order of magnitude as those published for iron. Since the data for mild steel was collected from a polycrystalline specimen there will be errors in the calculations. However, the most

important feature is that the magnetostriction constant λ_{100} for mild steel decreases at the Curie point.

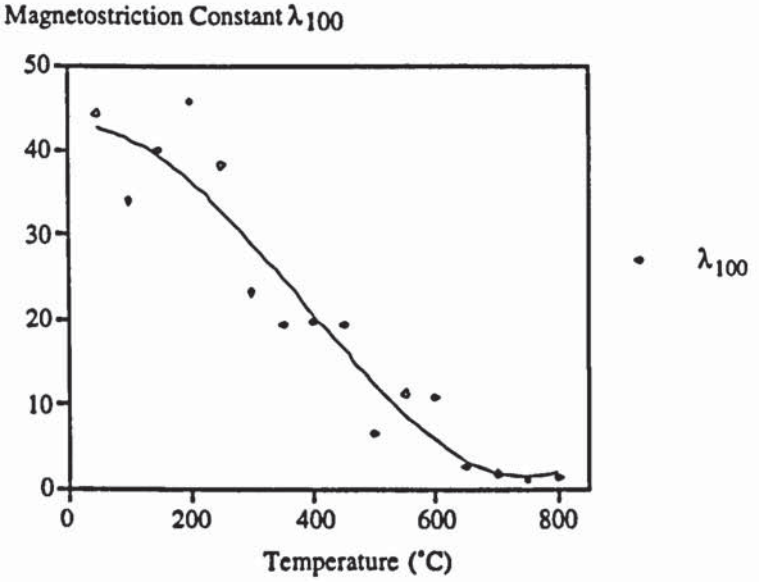

Figure 4.21 Magnetostriction Constant λ_{100} at 100 Hz As a Function of Temperature.

4.3.7 Results Collected Using LabView Software

The above tests were repeated on the mild steel specimen heated in the furnace with the strain gauge voltage recorded and analysed using LabView. The gain on the bridge amplifier was set to 200 for these tests to avoid exceeding the input voltage to the computer. LabView was configured to record the magnitude of the frequency components at 100 Hz, 200 Hz and 300 Hz at regular intervals of 4 seconds. In total 1300 sets of data were collected and figure 4.22 shows magnetostriction as a function of temperature for mild steel in a field of 3000 A/m.

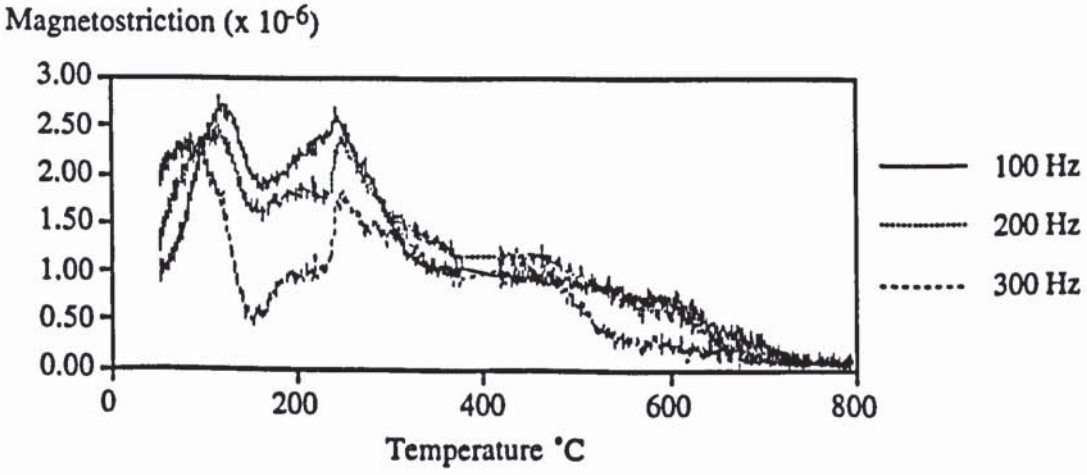

Figure 4.22 Magnetostriction as a Function of Temperature at 3000 A/m

The above test was repeated by sampling at 5 second intervals and the 800 sets of data are plotted on figure 4.23. The field strength was also higher at 4500 A/m.

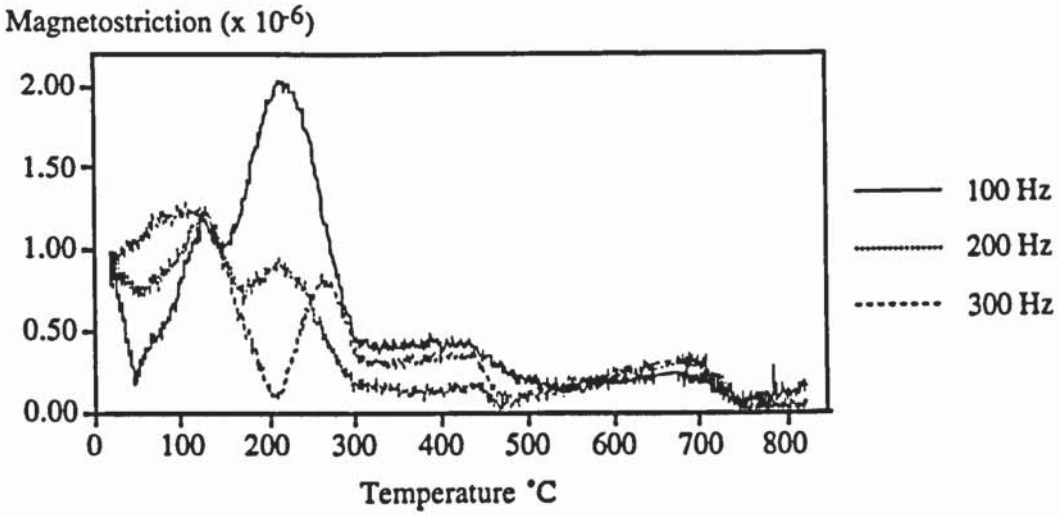

Figure 4.23 Magnetostriction as a Function of Temperature at 4500 A/m.

These figures indicate quite clearly that the general trend of magnetostriction, at all three frequencies, in fields of 3000 A/m and 4500 A/m was to decrease with an increase in temperature. The peaks at around 200°C may be associated with the Curie point of cementite, but without further investigation no comments can be made. A possible reason for the magnetostriction in the mild steel showing lower values in the higher field is that scale build up affected the measurements.

4.4 Discussion

Both methods of measuring magnetostriction produce results indicating that Joule magnetostriction is very small near the Curie point. The actual values of magnetostriction for the mild steel tested are not in good agreement over the lower temperature range. It is thought that this is due to inadequacies within the measuring equipment. For example with the strain gauge tests the results vary considerably from test to test, due to the build up of scale on the surface of the bar. The argon gas slowed down formation but did not prevent it.

The results show that magnetostriction is the most probable mechanism responsible for resonance at temperatures below about 600°C, but not for resonance near the Curie temperature. The data showing the behaviour of Joule magnetostriction as a function of temperature has been collected for the mild steel BS970-En3d. This data is believed to be fairly accurate because of the apparatus used to obtain the measurements, namely the high temperature strain gauge. It is suggested that the exact values would only

be obtained using single crystals and more specialised equipment. The results are assumed to be valid, if approximate in some cases such as the displacement apparatus.

4.5 Conclusions

Magnetostriction in mild steel has been measured using two different apparatus and found to decrease at the Curie point in fields up to 4500 A/m (rms). The result of calculating magnetostriction constants from the data shows that there is close agreement between the measured values on single crystals and theory. Differences are expected because of the assumptions made regarding the orientation of grains in a steel bar.

Vibration in steel heated electromagnetically is unlikely to be due to an increase in magnetostriction at the Curie point. However, it is known that magnetostriction changes with field strength and it may well only increase at the Curie point in much higher fields (50 kA/m and above). The apparatus needed to create fields of this size would be more difficult to construct, especially if low frequencies are required.

The magnetostriction measurements have shown good agreement with published data at low temperatures indicating that the measurements are valid at the higher temperatures.

Resonance in steel heated by induction is concluded to be caused by Joule magnetostriction at temperatures below 600°C. Resonance at or near the Curie point is unlikely to be due to Joule magnetostriction as this was found to diminish rapidly towards the Curie temperature when measured in lower fields.

Increases in magnetostriction at around 200°C are thought to be associated with the Curie point of cementite but further work is required to substantiate this.

CHAPTER FIVE

DISCUSSION

5.1 Introduction

In this chapter the experimental results will be discussed together with theory on causes of vibration not covered by experiment. Also included are references to results obtained by others and their hypotheses which may be related directly to this work. Finally, possible industrial applications of this phenomenon are included.

5.2 Vibration in Electromagnetically Heated Steel

Resonance was found to occur in steel during induction heating when the longitudinal natural frequency of a bar coincided with twice the heating frequency or subsequent harmonics. The mechanism responsible at temperatures below the Curie point is Joule magnetostriction since it was found that magnetostriction is significantly large in mild steel up to about 600°C.

The vibration at or near the Curie point (> 600°C) is likely to be caused by another mechanism since Joule magnetostriction is very small in mild steel at this temperature. However, results suggest that because the frequencies and magnitudes of resonance are similar at or below the Curie temperature, the mechanism responsible may well be some type of magnetostriction. It is postulated that volume magnetostriction may be the mechanism for resonance at the Curie point due to the destruction in spontaneous magnetisation. However, a change in volume ought to show changes in length, which were not detected using the high temperature strain gauge. This may have been because the tests on the mild steel in the furnace were in a much lower field and volume magnetostriction is only appreciable in higher fields.

The induction heating tests were found not to be repeatable since what were thought to be identical tests produced vast differences in the magnitude of resonance. However, the temperature at which resonance occurred was found to remain the same for identical tests. Generally the magnitude of resonance was found to be greatest for those resonances excited near the Curie temperature and was measured to be as high as 100g.

Published work on the subject of EMATs shows distinct similarities with work in this thesis. For many years researchers have been aware of an increase in amplitude of longitudinal ultrasonic waves in the vicinity of the Curie point, but no mechanism has been agreed upon (section 2.9). It is possible that the mechanism responsible for

resonance in steel heated by induction is the same as that responsible for the enhancement of ultrasound. It must be noted that there are many differences between the two areas of work such as:

i) frequency; the ultrasound was generated at 2 MHz whereas induction heating was at 3.2 kHz

ii) the steel heated by induction had large temperature differentials across the sample whereas the steel used for the ultrasound work had constant temperature profiles across the samples

iii) no steady magnetic fields were present in induction heating

iv) in the work reported here, vibration was detected using a non-contact laser, accelerometers and a high temperature strain gauge. Results of the amplitude of ultrasound were obtained using a non-contact electromagnetic acoustic transducer

If resonance and ultrasound enhancement were caused by an increase in volume magnetostriction near or at the Curie point, and was for some reason undetectable using the instrumentation available, then it has been reported that there is no known mechanism for the increase in volume magnetostriction as seen to occur in materials such as nickel, Ishio and Takahasi (1985).

5.3 Damping

It was reported by Cochardt (1953) that damping decreases rapidly at the Curie point in a large magnetic field. Even so there must be a driving force acting at this point for vibration to occur and this is the topic of interest involved in this work. The results from this work have shown damping to be small at resonance which is expected for any resonance. Damping in mild steel in a high alternating electromagnetic field was not investigated in great detail as it was difficult to measure with the induction heater switched on, which continuously produced vibration in the steel billet during heating.

5.4 Temperature Distribution in Steel Bars

The measured temperature distribution in a bar was found to be different from that predicted by Carslaw and Jaegar (1959) and Baker (1958). The surface and centre temperatures did not both rise at the same rate leading to a constant temperature differential. The reason for this was thought to be due to the forced cooling of the ends of the steel bars. This altered the heat flow causing the surface to heat at a slower rate than

the centre in the vicinity of the Curie point. It was believed that radiation and convection may also have altered the surface temperature at the Curie point, especially as the power density decreases and the losses increase. Resonance was still observed when lengths of mild steel bar shorter than the length of coil were heated which had a more even temperature distribution. Although it was not investigated experimentally it was assumed in the case of the short bars that the surface to centre temperature differential did remain constant because of no heat loss to the ends of the bar.

5.5 Possible Causes of Vibration In Steel Heated Electromagnetically

A number of possible mechanisms responsible for resonance in steel bars are discussed here. Magnetostriction as the most likely cause has already been covered in detail in chapter 4. The following were also investigated and found not to account for resonance in steel bars heated by induction:

i) forces due to the interaction between induced eddy currents and the magnetic field
ii) the alpha to gamma phase transformation in steel
iii) the existence of a thin ferromagnetic skin at the surface of a steel bar above the Curie temperature

5.5.1 Eddy Current Forces

The large eddy currents induced in steel bars when heated by electromagnetic induction produce forces directed along the length of the bar and towards the centre of the bar due to the interactions with the magnetic field.

Brown, Hoyler and Bierwirth (1948) show how to calculate the eddy current distribution in a conductor for a sheet. The method adopted uses Ampere's law applied to the simple case of a single thin current carrying conductor above and parallel to a conducting sheet.

$$J = H = \frac{I}{\pi h} \frac{1}{1 + (y/h)^2} \qquad (5.1)$$

where J is the current density (A/mm), H is the field strength (A/mm), h is the height of the conductor above the sheet (mm), and y is the distance from the conductor parallel to the surface of the sheet (mm).

Extending this to a coil consisting of 24 turns, which in reality is a helix but will be assumed to be 24 concentric turns, figure 5.1, the current density in a bar which is positioned inside this coil can be approximated.

The spacing between the centre of each turn of the coil is d millimetres. Each turn carries I amperes. It may be noted that y1 = z - 11.5d and y2 = z - 10.5d and so on. Also, from the other half of the coil (not shown) y13 = z + 0.5d and y24 = z + 11.5d.

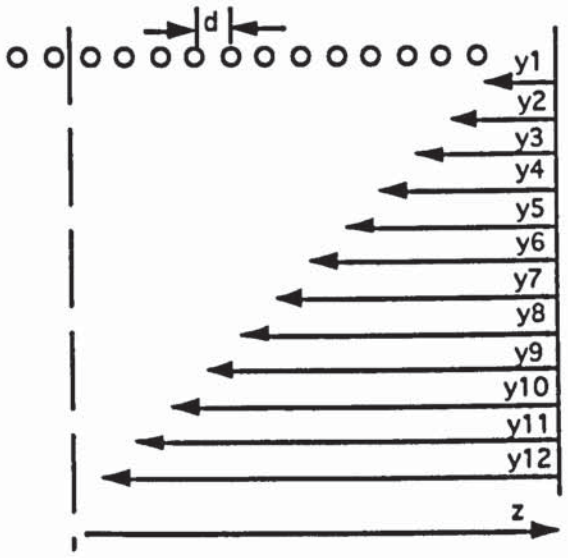

Figure 5.1 Diagram Showing the Eddy Current Calculation for a Cylindrical Bar.

The total current density in the bar, a distance z from the centre line, is found by applying equation 5.1 to each conductor and adding. For the simplest case of only two coils, at a distance $y = \pm (z - 0.5d)$, the equation becomes:

$$J = \frac{I}{\pi h}\left(\frac{1}{1 + \left(\frac{2z - d}{2h}\right)^2} + \frac{1}{1 + \left(\frac{2z + d}{2h}\right)^2}\right) \qquad (5.2)$$

For the case of a coil consisting of 24 turns a series is produced and when summed gives the eddy current density at a distance z from the centre of the coil due to all the turns of the coil:

$$J = \frac{I}{\pi h}\left[\frac{1}{1 + (z - 11.5d / h)^2} + \frac{1}{1 + (z - 10.5d / h)^2} + \ldots + \frac{1}{1 + (z - 0.5d / h)^2}\right.$$

$$\left. + \frac{1}{1 + (z + 0.5d / h)^2} + \ldots + \frac{1}{1 + (z + 11.5d / h)^2}\right] \qquad (5.3)$$

Appendix A.2.1 contains the solution to equation 5.3 using the software package Mathematica†. A graph was plotted for values of z from -240 mm to +240 mm to show the current distribution in a steel bar over this length. The values used were:

d = 12.4 mm
h = 40 mm
I =1033 A (rms)

It can be seen from figure 5.2 that the current density in the bar over the length of the coil (-160 mm to +160 mm) is maximum at the centre and decreases towards the ends of the coil. The most important point to notice is that the current density does not increase when directly opposite each conductor because the coils are close together.

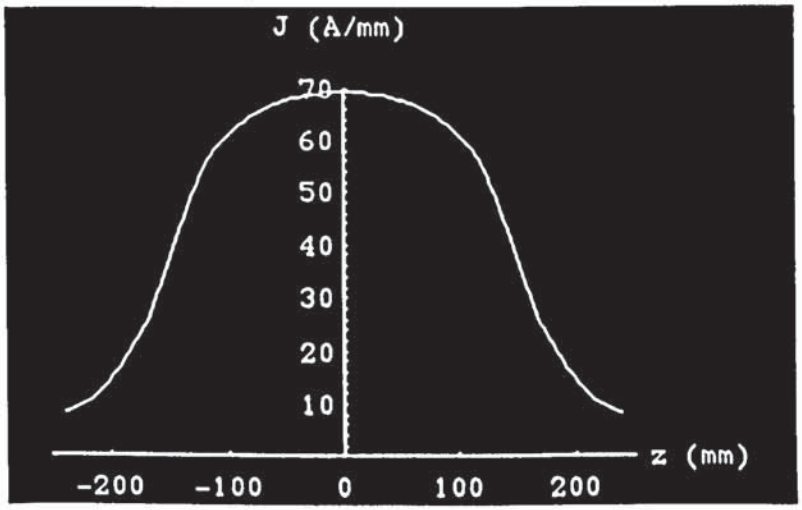

Figure 5.2 Calculated Eddy Current Density

Although this solution is more appropriate for thin conductors, the overall shape of the curve is similar if the conductors have width, as in this case, but there may be a slight change in the eddy current values. It may be noted that at the centre of the coil the eddy current density has a value of 70 A/mm from figure 5.2. This is in close agreement with the field strength measured at this position by experiment of 71 kA/m.

†Mathematica is a registered trademark of Wolfram Research, Inc.

There are two forces which act on a steel bar during induction heating. The first arises from the interaction between the eddy currents and the axial component of the magnetic field, H_z, producing a hoop stress which is directed towards the centre of the bar. The eddy current density is greatest at the centre of the coil and so the stress produced by this interaction will be calculated at the mid-point of the bar.

The second force arises from the interaction between the eddy currents and the radial component of the magnetic field, H_p, producing a longitudinal stress along the bar. Since the radial component of the field is greatest at the ends of the coil, figure 5.3, the stress will be calculated at a point on the bar at the end of the coil.

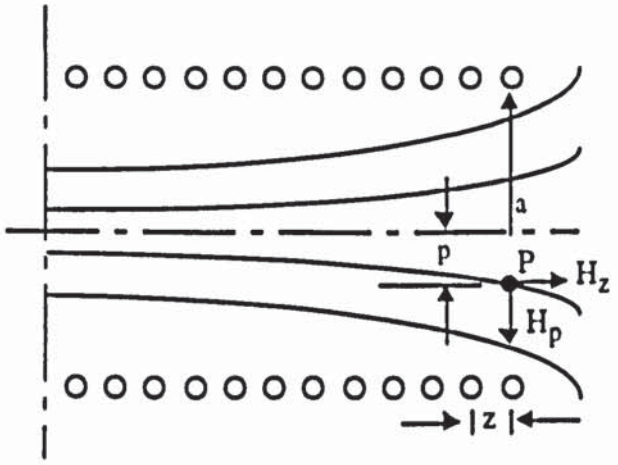

Figure 5.3 Field Components at the End of the Coil.

It can be shown, Hayt (1981), that the stress P between currents perpendicular to a field H is given by:

$$P = \frac{1}{2} BH \qquad (5.4)$$

where B is the flux density (T)
H = J is the field (A/m)
P is the stress (Pa)

For the case of heating a bar by induction at 60kW, the field is approximately equal to the eddy current density and from figure 5.2 is equal to 70450 Am^{-1} (rms) at the mid-point of the bar. The flux density, B at the centre of coil was measured by experiment to be 0.50 T at 50°C (Figure 4.19).

Using equation 5.3 and converting from rms values,

$$P = \frac{1}{2}\ 0.50\sqrt{2}\ .\ 70450\sqrt{2}\ \text{Pa} \tag{5.5}$$

$$P = 35225\ \text{Pa (max)} \tag{5.6}$$

Now, the force acts towards the centre of the bar and can be regarded as a uniform hoop stress. From Warnock (1943) it can be shown that strain arising from a hoop stress is given by:

$$\text{Strain} = \frac{1}{E}\ (-P + \nu P) \tag{5.7}$$

where ν is Poison's ratio (= 0.28 for steel)
P is the stress (Pa)
E is Young's modulus (207×10^9 Pa for steel)

$$\text{Strain} = \frac{1}{207 \times 10^9}\ (-39452 + 0.28\ .\ 39452) \tag{5.8}$$

$$\text{Strain} = -\ 1.23 \times 10^{-7} \tag{5.9}$$

The change in diameter of bar is simply the strain multiplied by the diameter:

$$\Delta d = -\ 1.23 \times 10^{-7} \times 0.02\text{m} = -\ 0.0025\ \mu\text{m} \tag{5.10}$$

The negative sign indicates that it is a decrease in diameter of the bar.

The radial component of field at the end of the coil (where it is assumed to be a maximum) can be calculated by considering each turn of the coil to be a circular loop and calculating the flux density at a given point P, figure 5.3 which is positioned a distance p from the centre line. The contribution from each turn at a distance z away from P was taken in turn and the total flux at P was found by summing the values.

From Smythe (1950) the flux density components are given by:

$$B_p = \frac{\mu I}{2\pi} \frac{z}{p[(a+p)^2 + z^2]^{0.5}} \left(-K + \frac{a^2 + p^2 + z^2}{(a-p)^2 + z^2} E\right) \quad (5.11)$$

$$B_z = \frac{\mu I}{2\pi} \frac{1}{[(a+p)^2 + z^2]^{0.5}} \left(K + \frac{a^2 - p^2 - z^2}{(a-p)^2 + z^2} E\right) \quad (5.12)$$

where B_p is the radial flux density (T)
B_z is the axial flux density (T)
μ is the permeability (Hm^{-1})
I is the rms coil current (A)
z is the axial distance of the centre of each turn to the point P (m)
a is the radius of the coil (m)
p is the radius to the point P (m)
K is the complete elliptic integral of the first kind of parameter m
E is the complete elliptic integral of the second kind of parameter m

and $$m = k^2 = 4ap[(a+p)^2 + z^2]^{-1} \quad (5.13)$$

The calculation was solved using Mathematica and the complete solution can be found in Appendix A.2.2.

Using the values: $I = 1033$ A
$a = 0.06$ m
$p = 0.02$ m
$z = 0, 0.013, 0.026, 0.039, \ldots\ldots, 0.299.$

Leads to: $B_z = 0.0536$ T
$B_p = 0.0072$ T

Knowing that $$B = \mu_0 H \quad (5.14)$$

$H_z = 42650\ Am^{-1}$
$H_p = 5730\ Am^{-1}$

Comparing the axial component of the field, H_z at the end of the coil with the value of the field, H (= J) calculated from equation 5.3 for the same point, we see that the two values are in close agreement. This shows that the method used to calculate the field components is valid. However it must be noted that these are approximate values.

The longitudinal stress, P on a steel bar was calculated from equation 5.4 using $B_p = 0.0072$ T(rms) and from figure 5.2, $H = 37450$ Am^{-1}(rms) at $z = 150$ mm:

$$P = \frac{1}{2}\ 0.0072\ \sqrt{2}.\ 37450\ \sqrt{2}\ \ Pa \tag{5.15}$$

$$P = 270\ Pa \tag{5.16}$$

Using Young's modulus, $E = 207 \times 10^9$ Pa:

$$Strain = P / E \tag{5.17}$$

$$Strain = 1.30 \times 10^{-9} \tag{5.18}$$

The values obtained for both the hoop and longitudinal strains due to the interactions between the eddy currents and magnetic field on a bar heated by induction are shown here to be one and three orders of magnitude respectively lower than the measured strain on a steel bar.

From these calculations it is fair to conclude that resonance is not simply due to forces between the eddy currents and field. No resonance occurred in the non-ferromagnetic materials such as stainless steel. If resonance was indeed due to the forces between eddy currents then it would have been expected to occur in these materials because eddy currents are responsible for induction heating and are present in any metallic material subjected to an alternating magnetic field.

5.5.2 The Alpha to Gamma Phase Transformation in Steel

The results collected show that resonance most frequently occurred at temperatures just below the Curie point or at 720°C to 740°C. This is approximately the temperature at which austenite formation begins in mild steel, ending at about 850°C. If resonance was as a result of this transformation occurring then it would be expected to:

i) exist at any temperature over the austenitic transformation range of 730°C to 850°C when a natural frequency of the bar was excited
ii) not exist at much lower temperatures e.g. 540°C with 500 mm long steel bars
iii) occur at a slightly higher temperature in the case of iron
iv) be different for the case of the 1.5% carbon steel because of its different structure to that of a mild steel
v) occur in the case of heating the titanium bar since it has a similar phase change at 902°C.

Reported by both Chaloupecky (1980) and Verhoeven, Downing and Gibson (1986) is also the possibility of changes in the transformation temperatures when using large electromagnetic fields. However, the results from section 3.21 show resonance to occur most often at around 740°C. If the increase in vibration was connected with the phase transformation, it should occur at a much higher temperature closer to the Curie point (760°C-770°C). Experimental work in chapter 3 failed to show any signs of a phase transformation in 0.4% carbon steel when heated by induction to various temperatures depending on the excitation of a resonance. It must be concluded that the resonances near the Curie point are not due to the phase transformation.

5.5.3 The Existence of a Thin Ferromagnetic Surface Layer

This hypothesis is a common explanation for the enhancement of ultrasonic waves generated using an EMAT in steel near the Curie point. It relies on the concentration of the steady field in a thin surface layer. This was applied to the case of induction heating a 600 mm long mild steel bar. However, it was found that when the bar was tightly wrapped in ceramic wool to minimise heat loss, there was no apparent cooling of the surface of the bar and no change in the resonance which occurred near the Curie point. The medium frequency electromagnetic field constantly created a skin layer in the steel bar and if the vibration was in some way connected to the flux in the skin, the increase in vibration would be most frequent at the start of heating when the skin depth was at its smallest.

Even without the insulation on the steel bar, the rate of heat lost by radiation and convection was far lower than that induced in the bar by the inverter up to temperatures of about 800°C when operating at maximum power. Surface cooling of the bar during heating did not occur. Therefore the existence of a thin ferromagnetic surface layer is an unlikely mechanism for resonance in steel bars heated by induction.

5.6 Magnetostriction

This research has produced results for magnetostriction in mild steel as a function of temperature which were found to be similar in magnitude to the published magnetostriction data for iron and silicon iron. The magnetostriction constant, λ_{100} for mild steel was calculated to be of similar magnitude, 40×10^{-6} at ambient temperature, as that measured by both Takaki (1937) and Tatsumoto and Okamoto (1959) in a single crystal of iron. The change in the calculated value of λ_{100} as a function of temperature in mild steel was different to that shown by the above authors although it had the same decreasing trend, diminishing towards the Curie point. This is most likely to be due to the

polycrystalline structure of the mild steel bar and the approximate formula used to calculate an average value of λ_{100} assuming an equal orientation of the grains.

Although volume magnetostriction was not measured directly, it was assumed that any changes in volume would also produce a change in dimension of the bar and would therefore be measurable using either accelerometers or strain gauges. However, in lower fields such as those used for magnetostriction measurement, volume magnetostriction may not have occurred and no dimension change would therefore have been apparent. Changes in dimension due to the form effect can be neglected since the ratio of length to diameter was greater than 5 for all the bars tested.

The results of Joule magnetostriction obtained using the two sets of apparatus are thought to show reasonable likeness, especially in the region of interest, the Curie point. Magnetostriction in iron is reported to be positive in low dc fields and negative in higher dc fields (above 40 kA/m). Mild steel showed a positive value in ac fields from zero to 3500 A/m.

5.7 Similarities with EMATs

A number of hypotheses have been put forward by authors who studied the phenomenon regarding the increase in amplitude of longitudinal ultrasonic waves in steel near the Curie point (chapter 2.9). The most popular theory being an increase in magnetostriction.

Trigubovich and Domorod (1984) produced a mathematical model for the amplitude of ultrasound generated by electromagnetic methods and calculated that there was an increase in the magnetostriction component with temperature rise whereas the Lorentz force component was calculated to decrease with temperature. The theory describing this was not compared directly to measurements of magnetostriction, only to the results of the amplitude of ultrasound. If the increase in vibration, or resonance, in steel heated by induction is caused by the same mechanism as that responsible using EMATs then it has been shown experimentally in this thesis that magnetostriction in relatively low fields does not increase in the region of the Curie point. However, to substantiate this claim it would be necessary to measure magnetostriction at the ultrasonic frequencies and field strengths.

Not only has ultrasound been generated by electromagnetic means, but also by lasers and conventional transducers in hot steel. Both produced similar results showing an increase in the amplitude of longitudinal ultrasonic waves near the Curie point. The phenomenon may therefore not be related to the presence of any type of magnetic field

(steady or alternating). It was postulated for the former technique that the alpha to gamma phase transformation in the steel had been brought about locally by the laser causing a dimension change. The latter comments on a number of possible explanations:

i) interaction of wave with magnetic properties of the material since the electron wave functions depend on the interatomic spacing which change in a longitudinal wave

ii) the alpha to gamma phase transformation

iii) solubility of carbides at 723°C and an interaction with the longitudinal wave

It must be noted that the increase in amplitude of ultrasound is not as a result of a resonance within the specimen being excited. During induction heating an increase in the magnitude of vibration at the Curie point only occurs when a resonance is excited.

Many authors refer to the region near the Curie point as an enhancement region for the generation of ultrasound using EMATs. The reason for it is as yet incomplete but has been investigated by many. Published speculation includes an increase in the magnetostrictive properties and magnetoelastic effect. Little is known about these effects which take place by means of a paraprocess. Papadakis, Lynnworth, Fowler and Carnevale (1972) obtained an increase in the amplitude of ultrasonic waves near the Curie point when no magnetic fields were present. If this is true then there can only be a few possible causes. Most of these will be specific to the interaction of longitudinal waves and magnetic properties of steel such as spontaneous magnetisation or the physical properties such as the solubility of carbides at 723°C. These interactions are beyond the scope of this work and have not been investigated as a result. Further work is required in this area in order to test these hypotheses.

5.8 Magnitude of Force Associated with Resonance

It is possible to estimate the magnitude of force required in a bar of steel to give a certain response at the face and compare this value to those obtained from experiment.

Bishop and Johnson (1960) examined the longitudinal vibration of uniform bars in great detail. They found that it was possible to calculate the harmonic longitudinal force applied at a section x = h, to give a response at any point x, figure 5.4 using:

$$u = \alpha_{xh} F e^{i\omega t} \tag{5.19}$$

where u is the longitudinal displacement in the direction of x (m)

α_{xh} is the receptance between sections x and h

$Fe^{i\omega t}$ is the harmonic force (N)

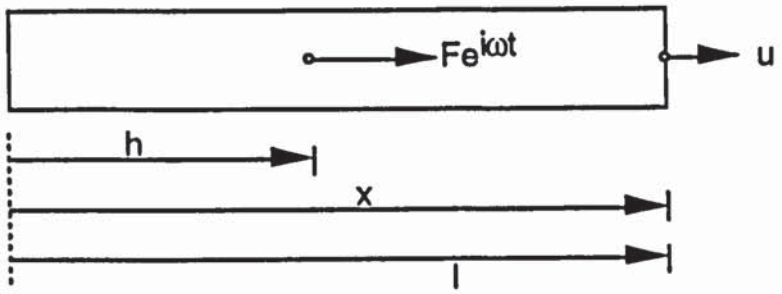

Figure 5.4 Force Applied at the Mid-Point of a Bar Leading to a Displacement at the Face

For a free-free bar, the receptance is obtained using:

$$\alpha_{xh} = - \frac{\cos \kappa h \cos \kappa(l - x)}{AE \kappa \sin \kappa l} \qquad (5.20)$$

where h is the value of x defining a section of the bar distant h from the origin (m) where $(0 \leq h \leq l)$

x is the distance along the bar (m)

l is the length of bar (m)

A is the cross section area (m^2)

E is Young's Modulus (Nm^{-2})

$\kappa = \omega \sqrt{(\gamma/E)}$

γ is the density (kgm^{-3})

ω is the angular frequency (rad s^{-1})

For a force applied at the centre of a 600 mm long mild steel bar, and the response measured at the face,

$$h = \frac{l}{2} = 0.3 \text{ m}$$

$$x = l = 0.6 \text{ m}$$

$$A = 1.257 \times 10^{-3} \text{ m}^2$$

Taking the case when the vibration of a bar increases near the Curie point due to resonance at 19.2 kHz,

$$\kappa = 19200 \times 2\pi \sqrt{\frac{7650}{124 \times 10^9}} = 29.96 \text{ ms}^{-2} \qquad (5.21)$$

$$\alpha_{xh} = - \frac{\cos 8.988}{1.257 \times 10^{-3} \cdot 124 \times 10^9 \cdot 29.96 \cdot \sin (17.98)} \qquad (5.22)$$

$$\alpha_{xh} = -2.53 \times 10^{-10} \tag{5.23}$$

$$Fe^{i\omega t} = -\frac{u}{2.53 \times 10^{-10}} \tag{5.24}$$

u was measured to be 0.05 μm from experiment (Table 3.3) and knowing that:

$$e^{i\omega t} = \cos \omega t + i \sin \omega t \tag{5.25}$$

and assuming that only the real part exists,

$$F_{(max)} = 197 \text{ N in the direction away from x.} \tag{5.26}$$

Comparing this value with those observed during induction heating and the measurement of magnetostriction using a strain gauge we see that:

i) Induction heating:

For a 40 mm diameter, 600 mm long mild steel bar, resonance at 740°C gave a strain of 0.67×10^{-6} (equation 3.9). Using Young's modulus of 168×10^9 Nm^{-2} at this temperature, then:

$$\sigma = \varepsilon E \tag{5.27}$$
$$\sigma = 112560 \text{ Nm}^{-2}$$

Cross section area $= \pi r^2 = 1.257 \times 10^{-3}$ m^2

$$F = \sigma A \tag{5.28}$$
$$\text{force, } F = 141 \text{ N}$$

ii) Magnetostriction

Total strain was measured to be 0.1×10^{-6} at 740°C in a field of 4500 Am^{-1} for a 50 mm diameter, 200 mm long sample of mild steel. Calculating force as above gives:

$$\text{force, } F = 33 \text{ N} \tag{5.29}$$

The theoretical value of the force required at the mid-point of the bar was calculated to be similar to the value obtained at resonance by experiment. Damping near the Curie point can be regarded as negligible since it was reported by Cochardt (1953) to be almost zero in a magnetic field. The force calculated from the magnetostriction

measurements was shown to be much smaller in magnitude and again reinforces the fact that Joule magnetostriction is unlikely to be responsible for resonance in steel bars near the Curie temperature. However, to be certain about this it will be necessary to repeat the measurements of magnetostriction in a much higher field similar to that produced by the induction heater.

5.9 Comments on Experimental Work

This project has been involved with the measurement of vibration in very harsh conditions, namely high electromagnetic fields and high temperatures. Even though induction heating is relatively simple in nature it produces a complex system with constantly changing temperatures and magnetic properties within the material heated. All these have made it very difficult to pin-point the exact mechanism responsible for resonance, especially in the vicinity of the Curie point.

The high temperatures reached by the repeatedly heated bars produced a build up of scale during heating which would certainly have affected the results to some degree. Scale may be responsible for the differences in magnitude of resonance observed during heating on separate occasions although it has been reported that the magnetostrictive properties of scale do not exist above about 500°C (Cole (1978)).

Although not directly investigated it is unlikely that the increase in vibration was due to the following which were first mentioned in chapter 2:

a) hysteresis - this was shown to diminish towards the Curie point
b) magnetocaloric effect - this would only exist at the Curie point and was reported to be a 2°C change in a field of 600 kAm^{-1}.

The following two results found during experimental work can also be neglected regarding the resonance in steel bars.

d) body forces, pushing or pulling the bar into or out of the coil
e) lateral vibration which was shown to be very small

Measurements were recorded using a number of different techniques and using more than one type of apparatus. This provided a certain degree of diversity into the method of measuring both vibration in steel bars and magnetostriction in a mild steel sample. Since the results showed the same trends with increase in temperature, the work conducted is assumed to be valid.

Measurements of temperature were difficult to check, but calibrated thermocouples were used throughout this work. Vibration was measured using accelerometers and a laser vibrometer and the results were of the same order of magnitude in terms of displacement. The tests using the two different instruments were carried out on different occasions and magnitude of vibration in the bar may well have been different and would account for the difference in the measured displacement. Taking the case of a 600 mm long mild steel bar heated at 35kW from ambient temperature, the displacement was calculated, (Table 5.1) using equation 3.8 and the measured magnitudes of acceleration at a frequency of 19.2 kHz. This was compared to the displacement calculated for the measurements of velocity from the laser vibrometer at the same frequency.

Instrument	Acceleration (g)	Velocity (mm/s)	Displacement (μm)
Accelerometer	51.2	-	0.035
Laser Vibrometer	-	2.09	0.017

Table 5.1 Comparison Between Accelerometer and Laser Vibrometer Measurements

As far as accuracy is concerned with all the results collected, the majority used equipment that was regularly calibrated. However, some equipment such as LabView was working very close to its frequency limit and it is not sure how reliable the data was from this equipment. The effect of this can be seen from the diagrams of the frequency spectra. The results were also recorded on a Hewlett-Packard F.F.T. analyser during the early stages of the experimental work for comparison and it was found that the results obtained using LabView showed occasional spurious readings at unexpected frequencies. However, the results from LabView gave a good overall indication of the longitudinal vibration of a bar.

The accuracy of the measurements collected in this work rely mainly on the instrumentation used but also, to a lesser degree, the design and construction of the apparatus involved with the measurements. For example, the displacement apparatus used to obtain information regarding magnetostriction in mild steel was cheap but crude. The measurement relied solely on how good a contact was made between the probe and surface of the steel ring.

Accuracy will also have been lost in the calculated values of the magnetostriction constants for mild steel because of the assumptions used. Since no data was found for the constants for any mild steel, it is difficult to assess how different they are from experimental values for single crystals.

5.10 Possible Industrial Uses

Induction heating processes are usually simple or repetitive in nature and require little instrumentation. It would be difficult to fix instrumentation to billets on a production line in order to measure a parameter such as surface temperature. Normally temperature is measured using either a pyrometer or contact thermocouple or estimated by heating the material for a fixed amount of time at a certain power level. Some processes do not require an accurate final temperature such as forging, but induction hardening can be more critical with regard to temperature.

5.10.1 Control

By controlling the power of an induction heater, it is possible to control the temperature and time relationship of the workpiece. The most widely used systems use either on/off switching or a continuous proportional controller. If temperature needs to be controlled, then a feedback signal is required from a measuring instrument. A pyrometer requires calibrating to each material and can give invalid readings if the emissivity is incorrectly set or if scale obscures the surface. Contact thermocouples cannot be used in a continuous heating process either.

At the out-set of this research it was envisaged that if the vibration occurred only at the Curie point then it would be possible to accurately monitor the heating of a steel billet and know exactly when its surface reached the Curie point. Temperature would not be the measured parameter, but longitudinal vibration. This would allow a completely encased heating coil to be used with no access for pyrometers, which would be ideal for a production line. Vibration would have been monitored using a laser vibrometer. However, lasers are expensive and this application would only have applied to the critical measurement of the Curie point. In this research resonance was found to occur at a range of temperatures during heating and so this application is unlikely for control purposes.

5.10.2 On-line Monitoring of Hot Steel

EMATs have been used in large processing industries to inspect the quality of steel immediately after it has been cast. Normal inspection techniques would require the steel to have cooled sufficiently and to be stationary. However, a technique that uses ultrasound to monitor steel up to 1200°C, and moving up to 1 m/s, has been investigated in detail by many engineers, section 2.9.

This technique can be used to measure the average temperature of a specimen through the relationship of ultrasound velocity against temperature. The internal

temperature distribution is important in solid and solidifying steel bodies. EMATs can be used also to measure the wall thickness of hot steel tube.

The type of flaw to be inspected depends upon the type of ultrasound generated within the material. The method of identifying the flaws inside a material depends on the ultrasound being deflected off of the flaw. However, if the flaw is parallel to the direction of ultrasound, it will not reflect the signal and will be missed. Only shear wave generation in steel is efficient over the whole temperature range 20°C to 1200°C. Longitudinal wave generation is very efficient around the temperature 600°C to 800°C. This method could then be used to detect the magnetic phase transformation or a particular type of flaw. If the mechanism responsible for the increase in longitudinal ultrasonic waves was discovered then it may be possible to produce more efficient generation at temperatures lower than 600°C or greater than 800°C. This would help in the non-contact inspection of hot steels after casting.

If resonance during induction heating is produced by the same or a similar mechanism as that responsible for the increase in ultrasound near the Curie point, then the most favourable industrial application would be to apply any findings from results obtained using induction heating to the case of the ultrasonic monitoring of hot steel.

5.11 Conclusions

The results of an investigation of vibration in electromagnetically heated steel have been discussed with reference to both magnetostriction and published work by others.

It appears that magnetostriction produces resonance in steel below about 600°C, but is unlikely to be responsible for resonance above this temperature. To be completely sure of this would require further work because of the differences in field strengths used for the induction heating and magnetostriction measurements.

Other possible causes such as eddy current forces due to an interaction with the magnetic field have been shown to be too small to be responsible for resonance.

CHAPTER SIX

CONCLUSIONS

6.1 Introduction

The longitudinal vibration of a number of ferromagnetic steels has been investigated in detail by experiment. At the start of the investigation very little was known about the behaviour of steel when heated by electromagnetic induction but this thesis has produced a solid background to the work. Not only is this thesis a representation of the work undertaken by the present author, it is also meant to be used as a comprehensive literature review combining all the work associated with this topic. It also brings together the possibility that resonance in steel heated by MF induction heating is similar to the enhancement of ultrasound in hot steel near the Curie point.

6.2 Background

After an extensive literature survey no previous work has been published, to the author's knowledge, describing resonance in steel heated by induction. There is also very little data on the subject of magnetostriction in steel, especially the mild steels, as a function of temperature.

It has been discovered that researchers investigating the reason for an increase in ultrasound amplitude at the Curie point in steel are unable to give one single explanation. Little work has actually been carried out to study the mechanism responsible.

It is concluded that this is most probably the first time that the two topics, resonance and ultrasound enhancement have been compared.

6.3 Resonance in Steel Bars Heated by Induction

It was discovered that when a length of ferromagnetic steel bar is heated in a standard industrial induction heater, longitudinal resonances are excited if a natural frequency of the bar coincides with twice the heating frequency or multiples of it. Resonance was seen to occur most frequently when the surface temperature was in the vicinity of the Curie point. It was also found that the rate of temperature rise of the surface at this temperature was lower than that of the remainder of the steel which gave the impression of resonance occurring most often at this temperature. By changing the length of the steel bars, it was possible to alter the temperature at which resonance occurred. This was possible because the inverter frequency was fixed.

It was found that resonance changed with changes in heating power, initial temperature, bar diameter, type of steel and frequency of heating. This has shown that the magnitude of resonance is related to the heating power, is greater for lower carbon steels (except iron), is inversely related to the initial temperature of the bar prior to heating and increases with increase in diameter (which is also an increase in power input to the workpiece). The temperature at which resonance occurs (when in the vicinity of the Curie point) is inversely related to both the initial temperature the power setting.

The most likely cause of resonance, magnetostriction, was investigated for several reasons. The main one being that no published data was located for mild steel, especially at high temperature. Experimental results also suggested that magnetostriction was responsible such as:

a) resonance was observed only at twice the heating frequency and its harmonics.
b) resonance was not observed after the whole bar had reached the Curie temperature.
c) resonance only occurred in ferromagnetic steel.
d) odd resonances were most frequently excited leading to vibrations at the faces of the bar being out of phase. Magnetostriction would produce similar results.

6.4 Magnetostriction

Magnetostriction was measured using two completely different methods, displacement measurements and strain measurements. Both were found to decrease with increase in temperature and approach zero at the Curie point. It is concluded that this is not the mechanism responsible for resonance in steel near the Curie point. However, since magnetostriction is greater at lower temperatures, it is concluded that it is the mechanism responsible for resonances below the Curie point.

The magnetostriction results obtained using the strain gauge show similar trends for the fundamental frequency, second and third harmonic of magnetostriction as a function of temperature. With an increase in temperature (maximum 800°C) magnetostriction was found to decrease steadily. The peaks at lower temperatures (between 100°C and 300°C) are thought to be associated with the Curie point of cementite although no direct experimental work was undertaken to prove this hypothesis. The results show no signs of an increase in magnetostriction at or in the vicinity of the Curie point.

6.5 Mechanisms Associated with The Generation of Ultrasound Using Electromagnetic Acoustic Transducers (EMATs)

Much published work has been studied concerning a similar phenomenon when using EMATs. Since it was envisaged that this and resonance during induction heating are related, tests were conducted on steel bars heated by induction regarding the various hypotheses put forward for increases in ultrasound amplitude.

It was found that many of these hypotheses, when applied to the case of heating steel by induction, were not responsible for resonance. These included the alpha to gamma phase transformation, the formation of a ferromagnetic surface layer at high temperatures due to surface cooling and an increase in magnetostriction. However, it is assumed that the two phenomena are related. If they turn out to be due to different mechanisms then the hypotheses would not apply to the case of resonance during induction heating anyway.

6.6 Industrial Applications

Work concerning a possible application of this phenomenon is limited because of the results obtained. Once the mechanism responsible for resonance near the Curie point has been found then it may be possible to find an appropriate use. At this early stage it is difficult to assess any use.

6.7 Overall Conclusions

Other work in this thesis has shown that resonance is:

- not due to eddy current forces within a steel bar
- only occurs in ferromagnetic steel
- is not produced as a result of a thin skin layer such as that proposed in connection with an increase in the amplitude of ultrasound at the Curie point
- not solely due to the alpha to gamma phase transformation

To sum up, the main conclusions of this thesis are:

- Resonance occurs in ferromagnetic steel, heated by induction, when a natural frequency coincides with twice the heating frequency and subsequent harmonics.

- Resonance is more likely to occur when the surface temperature is in the vicinity of the Curie point because of the slow rate of change in surface temperature.

- Magnetostriction of mild steel has been measured as a function of temperature up to 800°C.

- The magnetostriction constant λ_{100} has been calculated as a function of temperature to 800°C.

- Below about 600°C, resonance is caused by Joule magnetostriction.

- Above this temperature resonance is unlikely to be caused by Joule magnetostriction but further tests are required to be totally confident. Volume magnetostriction may be responsible, especially in high fields such as that produced by the induction heater.

Finally it is concluded that in order to obtain a more thorough understanding of this phenomenon further work is required.

CHAPTER SEVEN

PROPOSALS FOR FURTHER WORK

7.1 Introduction

There is much scope for further work regarding this topic since the mechanism responsible for resonance in the region of the Curie point was not fully determined in this work. The research was restricted to the investigation of resonance at medium frequencies in induction heaters and to the study of magnetostriction at low frequency in weaker fields. There are possibilities for further work involving different frequencies and different field strengths. This chapter evaluates some of these ideas and also proposes work relating to other phenomena which have been reported concerning similar work.

7.2 Striated Heating and Resonance

A phenomenon that was discovered by Babat (1944) and Lozinskii (1969) describe the occurrence of striated heating when using high frequency electromagnetic fields. It may well be that striated heating is in some manner related to the vibration which has been observed at medium frequencies although striated heating was not apparent. This could be tested by simply using an induction heater of greater frequency and repeating the tests used in this thesis. The difficulty arises in the measurement of any signal at these much higher frequencies. Accelerometers operate up to 50 kHz maximum, although the laser vibrometers are able to reach up to 1.5 MHz. The processing equipment such as a spectrum analyser would also need to cover this higher frequency range.

Although the striations are reported to disappear at the Curie point, it may be helpful to find out whether an increase in vibration occurs and if so, whether it coincides with the formation of striations. Resonance could be avoided using a high frequency heater by choosing a suitable length of steel bar.

7.3 Mechanical Excitation of Longitudinal Vibration in Steel Bars

It is necessary to investigate mechanical vibrations in hot steel when induced by purely mechanical means such as a shaker. By keeping the magnitude of the induced vibration constant and measuring the response it would be possible to detect any increases in the response as a function of temperature. A magnetic field would be absent for initial tests and later a steady field could be applied. This would not cause vibration but a constant change in the dimension of the specimen due to magnetostriction. The test

would have to be designed to allow for thermal expansion of the material and the frequency of mechanical vibration would be chosen so that no resonances would be excited in the test piece. The results would be directly comparable to those obtained using EMATs. If an increase in amplitude was detected near the Curie point, then the mechanism responsible would most likely be connected to the propagation of longitudinal waves in steel.

As an alternative method to test whether resonance in steel near the Curie point coincided with the alpha to gamma phase transformation, a test could be devised to measure both longitudinal vibration of the bar and expansion when heated by induction. A long thin rod would be the best sample to use as the test piece with an accelerometer attached to one end and the other end firmly fixed. The expansion could be measured using a displacement transducer. There should be a decrease in length as the phase transformation occurs and it would be interesting to see if the vibration increased at the same time.

7.4 Ferromagnetic Materials

In this research only three ferromagnetic materials were studied; iron, steel and monel 400. Monel 400 is weakly ferromagnetic and has a Curie point just above room temperature. It showed no resonance during induction heating. No other ferromagnetic materials such as nickel and cobalt were tested, primarily because of the cost of these materials.

It would be valuable to study the behaviour of these materials to discover whether the phenomenon occurs in these materials or if it is solely restricted to steels. If it did occur, then it would be necessary to investigate whether it occurred most frequently around the Curie temperature. This would help in assessing whether the phase transformation in steel could be ignored or whether it should be investigated in more detail.

7.5 Steels

Only a limited number of different steels were used in this research. Tests involving a whole range of different carbon steels should be examined. Also, the effect of different heat treatments to just one type of steel could be studied. The results may give more information as to the mechanism responsible for resonance during induction heating such as one particular phase, e.g. cementite or ferrite.

Much data has been published on the magnetostrictive properties of silicon-iron as a function of temperature. This material could be heated by induction and the longitudinal vibration measured. The results could be compared with the measurements of magnetostriction from Pike and Moses (1977) and also indicate whether results vary if the material is grain oriented or not.

7.6 Phase Transformation in Steel

The A_1 transition temperature at 723°C needs to be investigated in more detail regarding induction heating and resonance. The majority of resonances occurred just before the Curie point (760°C) and may be connected with this transition. Methods of investigation would involve the use of materials which are ferromagnetic and do not undergo this transformation. Examples of these are pure iron which has a body centred cubic structure and nickel which has a face centred cubic structure. Cobalt could be used to determine whether resonance is associated with the Curie temperature or a phase transition since it undergoes a phase transformation at 425°C and has a Curie point of 1130°C.

7.7 Measurement of Magnetostriction in High Fields

The alternating field used to create magnetostriction in samples of mild steel was small (4500 A/m) compared to that produced by the induction heater. Since it is unknown how magnetostriction varies with temperature in high fields (100 kA/m) tests need to be carried out to obtain a set of data, especially in the region of the Curie point. It may well be necessary to use low frequency or d.c. fields to minimise heating and prevent resonance. However it would be both expensive and difficult to design the necessary apparatus to create such high fields at low frequency.

Volume magnetostriction data in high fields near the Curie temperature is also required and may have to be obtained directly from experiment. Since volume magnetostriction also leads to a change in dimension it could be measured by similar techniques as used in this research. However, more than one measurement would need to be made to determine whether the volume remained constant or not. If it did remain constant then the mechanism would be Joule magnetostriction otherwise it would be volume magnetostriction. The main difficulty in the measurement of volume magnetostriction in high fields is the generation of the high fields with minimum heating effect.

7.8 Electromagnetic Generation of Ultrasound

Two types of ultrasonic wave can be generated in hot steel, the shear wave and the longitudinal wave. Both are important for the detection of flaws depending on their orientation. Although it is possible to generate the shear waves in steel from ambient temperatures to 1200°C, it is only possible to generate longitudinal waves in the region 600°C to 800°C due to enhancement of the signal. If the cause of this enhancement was discovered then it may be possible to use the longitudinal generation of ultrasound across a wider temperature range.

It is possible to heat steel by induction at high frequency such as 500 kHz which is approaching the common ultrasonic frequencies. Vibration should be investigated in steel at these frequencies to see if an increase occurs. There should be no excitation of resonances within a 600 mm long steel bar at this frequency and may lead to a result similar to that of the EMAT results. This work would also enable tests to be performed in high fields (100 kA/m) without a resonance being excited. If magnetostriction is highly dependent upon field strength, then it can be measured using this technique. Equipment may be expensive as magnetostriction will occur at twice the heating frequency and will need detectors able to measure vibration in the range of MHz.

It was discovered by many such as Whittington (1978), that only an increase in the amplitude of longitudinal ultrasonic waves occurred near the Curie point. Shear waves, produced using a different orientation of the steady field were found to increase only slightly in amplitude over the temperature range 300°C to 700°C before decreasing at the Curie point. By using a transverse flux induction heater it may be possible to produce similar types of shear wave in steel, such as a beam, figure 7.1. The transverse vibration produced by the heater could be measured to see whether there was an increase at the Curie point. Although the test is different to those conducted using EMATs because it uses no steady magnetic field, it would be interesting to discover how steel behaves regarding vibration when heated transversely. The results would help in determining whether the phenomena, produced using two different methods at different frequencies, were related.

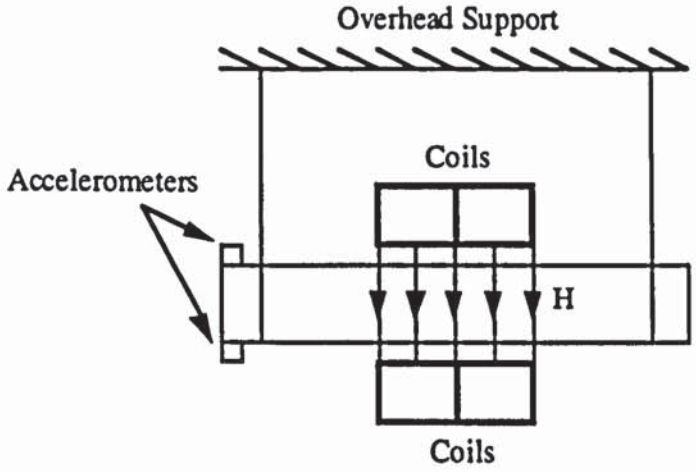

Figure 7.1 Transverse Induction Heating of A Steel Beam

7.9 Other Areas of Proposed Study

Much work on the subject of magnetostriction in steel as a function of temperature has been reported by researchers in Russia. The papers which are translated from their work mention the topic of the paraprocess. The actual meaning and explanation of the paraprocess has not appeared in the translations and it would be helpful if an explanation could be obtained. It is believed that the paraprocess is a type of energy exchange and in this case is from magnetic to elastic energy which takes place in steel near the Curie point.

This research has used two different induction heaters which were both load resonant systems. Tests ought to be conducted using a swept frequency inverter, just to ensure that the resonance is not produced as a result of an interaction between the load and resonant circuit.

Finally accurate measurements of damping in steel in large ac fields as a function of temperature are required. These measurements may be obtained by the test described in section 7.3 where the response of a mechanically excited bar is measured over the temperature range (20°C to 800°C).

REFERENCES

Akulov, N.S. (1930) On a Law Which Relates Different Properties of Ferromagnetic Crystals with Each Other. Z. Physik. **59**, 254-64.

Alers, G.A. and Burns, L.R. (1987) EMAT Designs for Special Applications. Materials Evaluation, **45**, 1184-1189.

Alers, G.A. (1991) EMATs as Noncontact Transducers for Tube Inspection. Mechanical Working and Steel Processing Conference Proceedings. Iron and Steel Soc. of AIME. **28**, 405-406.

BS970 Part 3 (1991) Bright Bars For General Engineering Purposes. British Standards Institution.

Babat, G. and Lozinskii, M.G. (1940) Heat Treatment of Steel by High Frequency Currents. Journal of the IEE. **86**, 161-168.

Babat, G.I. (1944) Some Peculiarities of Induction Heating, Journal of Applied Physics, **15**, 835-839.

Baker, R.M. (1958) Classical Heat Flow Problems Applied to Induction Billet Heating, AIEE Trans., **77**, 106-112.

Baker, R.T. and Oliver, T.N. (1994) Vibration in Electromagnetically Heated Steel. International Symposium on Electromagnetic Processing of Materials (EPM'94), Nagoya, Japan. Iron and Steel Institute of Japan. October 25-28. 541-546.

Baker, R.T. and Oliver, T.N. (1995) Magnetostriction and Vibration in Steel Heated by Induction. UPEC '95, Greenwich, UK. September 5-7.

Baker, R.T. and Oliver, T.N. (1996) Effect of Temperature on Vibration and Magnetostriction in Mild Steel. BNCE / UIE International Congress on Electricity Applications, Birmingham, UK. 16-20 June.

Barrett, W.F. (1882) On the Alterations in the Dimensions of the Magnetic Materials by the Act of Magnetisation. Nature **26**, 585-6.

Bidwell, S. (1886) Change in Length of Fe, Ni and Steel by Magnetisation. Proc. Roy. Soc. **40**, 109-34.

Bidwell, S. (1890) Effect of Tension on Magnetostriction of Fe, Co and Ni, Proc. Roy. Soc. (London), **47**, 469-80.

Bishop, R and Johnson, D. (1960) The Mechanics of Vibration, Cambridge University Press.

Boyd, D.M. and Sperline, P.D. (1988) Noncontact Temperature Measurements of Hot Steel Bodies Using an Electromagnetic Acoustic Transducer (EMAT). Review of Progress in Quantitative Non-Destructive Evaluation. **7B**, 1669-1676.

Bozorth, R.M. (1951) Ferromagnetism. Van Nostrand. Bell Telephone Series. Toronto, London.

Brown, G.E.; Hoyler, C.N. and Bierwirth, R.A. (1948) Theory and Application of Radio Frequency Heating. Van Nostrand, London.

Budenkov, G.A. and Maskaev, A.F. (1973) Excitation and Detection Mechanism for Ultrasonic Waves in Iron and Iron-Nickel Alloy Near The Curie Point. Defektoskopiya, **1**, 109-115.

Budenkov, G.A. and Maskaev, A.F. (1979) Electromagnetic Excitation of Ultrasound in Carbon Steels at High Temperatures. Defektoskopiya, **4**, 66-70.

Budenkov, G.A. and Gurevich, S.Yu (1982) Current Status of Contactless Methods and Facilities for Ultrasonic Inspection (Survey). Soviet Journal of Non-Destructive Testing. 325-347.

Carslaw, H.S. and Jaeger, H.C. (1959) Conduction of Heat in Solids, Oxford University Press, Oxford.

Chaloupecky, V.(1980) Analysis of the a - g Phase Transformation in Eutectoid Steel During Induction Heating, Metal Science and Heat Treatment, **22**, no. 3/4, 252-255.

Chikazumi, S. (1978) Physics of Magnetism, Robert E Krieger.

Chow, C.K. and Nembach, E. (1976) Magnetically and Thermally Activated Dislocation Motion in Ni Single Crystals, Acta Metallurgica, **24**, 453-461. Pergamon Press.

Cochardt, A. W. (1953) The Origin of Damping in High-Strength Ferromagnetic Alloys. Journal of Applied Mechanics, ASTM, 26, 196-200.

Cole, P.T. (1978) The Generation and Reception of Ultrasonic Surface Waves in Mild Steel at High Temperatures. Ultrasonics, **16** (4), 151-155.

Cook, J.R.; Jackson, J.F. and Droney, B.E. (1989) Sensing As-Cast Billet Temperatures with Electromagnetic Acoustic Transducers (EMAT). Iron and Steel Engineer. **66** (9), 17-22.

Cullity, B.D. (1972) Introduction To Magnetic Materials, Addison-Wesley.

Davies, J. and Simpson, P.(1979) Induction Heating Handbook, Mcgraw- Hill.

Dibben, D. (1991) Private Communication.

Dobbs, E.R. (1984) Electricity and Magnetism, Cox & Wyman Ltd, Reading.

Eingorn, I.Y. (1989) Magnetostriction of Electrical Steel and Transformer Noise. Soviet Electrical Engineering, C/C of Electrotekhnika, **60** (4), 28-30.

Esser, H. and Eusterbrock, H. (1941) Investigation of Thermal Expansion of Some Metals and Alloys with an Improved Dilatometer, Arch. Eisenhuttenw, **14**, 341-55.

Faraday, M. (1832) On the Induction of Electric Currents. On the Evolution of Electricity from Magnetism. On a New Electrical Condition of Matter. On Arago's Magnetic Phenomena. Phil. Trans. **122**: 125-62; ERE, 1, 1-139.

Ghosh, A.K. and Roy, M.N.(1987) Phase Transformation of Steel in Magnetic Field. Transactions, Indian Institute of Metals, **40** (4), 329-333.

Gillott, D.H. and Calvert, J.F. (1965) Eddy Current Loss in Saturated Solid Magnetic Plates, Rods and Conductors. IEEE Transactions on Magnetics, **MAG-1**, 126-137.

Gurevich, S.Yu. and Gal'tsev, Yu.G. (1993) Experimental Directional Patterns of EMA Transducers for High Temperature Ultrasonic Testing of Metals. Russian Ultrasonics. **23** (2), 66-75.

Harris, C.M. and Crede, C.E. (1976) Shock and Vibration Handbook, McGraw-Hill.

Hayt, W.H. (1981) Engineering Electromagnetics, McGraw-Hill.

Herbert, E.G. (1929) The Hardening of Superhardened Steel By Magnetism, Iron and Steel Institute, **Part 2**, 239-55.

Higgins, R.A. (1983) Engineering Metallurgy, Part I Applied Physical Metallurgy, Hodder and Stoughton.

Hoekstra, B.; Gyorgy, E.M.; Zydzik, G. and Flanders P.J. (1977) Magnetostriction Measurements with a Recording Rotating Field Magnetostrictometer. Review Scientific Instruments, **48**, 1253-1255.

Honda, R and Shimizu, S. (1903) Change of Length of Ferromagnetic Substances Under High and Low Temperatures and Magnetisation. Phil. Mag. [6], **6**, 392-400.

Horoszko, E. (1985) Induction Heating of Cylindrical Workpieces. Elektrowaerme International. Edition B. **43** (2), 69-76.

Hunter, L.P. (1970) Handbook of Semiconductor Electronics. McGraw-Hill.

Ishio, S. and Takahashi, M. (1985) Temperature Dependence of Forced Volume Magnetostriction in FCC Fe-Ni Alloys. Journal of Magnetism and Magnetic Materials, **50** (3), 271-277.

Joule, J.P. (1842) On a New Class of Magnetic Forces. Ann. Electr. Magn. Chem., **8**, 219-24.

Joule, J.P. (1847) On the Effects of Magnetism upon the Dimensions of Iron and Steel Bars. Phil. Mag. **[3] 30**, 76-87, 225-41.

Kaule, W. (1964) Magnetostrictive Ultrasonic Testing of Materials. Proceedings of the 4th International Conference of Non-Destructive Testing. 291-294.

Kawashima, K; Murota, S; Nakamori, Y; Soga, H; Suzuki, H. (1979) Electromagnetic Generation of Ultrasonic Waves in Absence of External Magnetic Field and its Applications to Steel Production Lines. Ninth World Conference on Non-Destructive Testing, Melbourne, Australia. 4H.3.

Langman, R.D. (1987) Worked Examples in Electroheat. The Electricity Council, London.

Lee, E.W. (1955) Magnetostriction and Magnetomechanical Effects. Rept. Prog. Phys. **18**, 184-229.

Lee, S.S. and Ahn, B.Y. (1992) EMAT Application at High Temperature. Non-Destructive Testing and Evaluation. **7** (1), 253-261.

Lenz, H.F.E. (1834) Ann. de Phys., **31**, 483.

Lozinskii, M. (1969) Industrial Applications of Induction Heating, Pergamon Press.

Meirovitch, L. (1967) Analytical Methods in Vibrations, The Macmillan Company.

Merkulov, L.G. (1965) Magnetic Head for Contactless Ultrasonic Flaw Detection. Ul'trazvukovaya Tekh. **3**, 31-33.

Metals Handbook (1985) Volume 8: Mechanical Testing, American Society for Metals.

Nagaoka and Honda (1902) On the Magnetostriction of Steel, Nickel, Cobalt and Nickel Steels. Phil Mag [6] **4**, 45-72.

Otroumov, B. and Polotovskii, L. (1933) Radio Engineering Method of Testing Metals. Vestn. Metalloprom. **5**, 14-19.

Papadakis, E.P.; Lynnworth, L.C.; Fowler, K.A. and Carnevale, E.H. (1972) Ultrasonic Attenuation and Velocity in Hot Specimens by the Momentary Contact Method with Pressure Coupling, and some Results on Steel to 1200°C. The Journal of the Acoustical Society of America. **52**, No. 3 (2), 850-857.

Pierce, G. (1929) Magnetostriction Oscillators. Proc. Inst. Radio Engineers, **17**, 42-88.

Pike, E.C. and Moses, A.J. (1977) Effects of Temperature on a.c. Magnetostriction in Grain-Oriented Silicon-Iron. Journal of Materials Science, **12**, 187-191.

Pravdin, L.S. and Burtseva, V.A. (1992) Special Features of Variation of Magnetisation and Magnetostriction from Small Increases of Elastic Stresses and Magnetic Field Using Low-Carbon Steel as an Example. Russian Journal of Non-Destructive Testing. **28** (4), 192-199.

Randell, R.; Zener, C. and Rose, F. (1939) Intercrystalline Thermal Current as a Source of Internal Friction. Phys. Rev. **56**, 343-348.

Rankin, J.S. (1932) Further Experiments on the Magnetostriction of Cold Drawn Wire. Journal Royal Technical College, Glasgow, 687-9.

Schmidt, W. (1933) Thermal Extension Measurements With X-rays, Ergeb.tech Rontgenkunde **III**, 194-201.

Simmons, G.H. and Thompson, J.E. (1971) Proc. IEE, **118**, 1302.

Smythe, W.R. (1950) Static and Dynamic Electricity. McGraw-Hill.

Takaki (1937) Uber die Magnetostriktion der Eisenkristalle bei Hoher Temperature, Zeitschrift für Physik. **105**, 92. (In German).

Tatsumoto, E. and Okamoto, T. (1959) Temperature Dependence of the Magnetostriction Constants of Iron and Silicon Iron. Journal Physics Society of Japan. **14**, 1588-1594.

Thompson, R.B. (1978) A Model for the Electromagnetic Generation of Ultrasonic Guided Waves in Ferromagnetic Metal Polycrystals. IEEE Transactions on Sonics and Ultrasonics. **Su-25** (1), 7-15.

Trigubovich, B.V. and Domorod, N.E. (1984) Theory of Electromagnetically Excited Ultrasound in Ferromagnetic Materials Near The Curie Point. Soviet Journal of Non-Destructive Testing, **20** (7), 469-475.

Verhoeven, J.D; Downing, H.L. and Gibson, E.D. (1986) Induction Case Hardening of Steel. Journal of Heat Treating. **4** (3), 253-264.

Warnock, F.V. (1943) Strength of Materials, Sir Isaac Pitman & Sons, London.

Webster, W.L. (1925) Magnetostriction in Iron Crystals. Proc. Roy. Soc., **109A**, 570-584.

Weiss, P (1907) Hypothesis of the Molecular Field and Ferromagnetic Properties. Journal Physics [4] **6**, 661-90.

Weiss, P. and Picard, A. (1918) On a New Magnetocaloric Phenomenon. Compt Rend, 166, 352-354.

Whittington, K.R. (1978) Ultrasonic Inspection of Hot Steel. British Journal of NDT. September 1978, 242-247.

Williams, S.R. (1933) Mechanical Hardness Influenced by Magnetism and Measured by Magnetostrictive Effects. Trans. American Soc. for Steel Treating. **21**, 741-768.

Yamano T., Nakagiri A., Shinke N. and Maeda H. (1990) Effects of Temperature on Magnetostriction due to Alternating Magnetic Field. Technology Reports of Kansai University, **32**, 45-54.

APPENDIX ONE

SPECIFICATIONS AND DATA

A.1.1 Specification of the Crossley 60kW, 3.2 kHz Induction Heater

Electrical Input

Input Voltage	380 / 440 V 3 Phase . 50 Hz
Input Power Factor	0.92 at full output voltage
Input Line Current	105 A at 415 V

Electrical Output

Inverter Output Voltage	800 V rms (maximum)
Output Frequency	2.5 - 3.5 kHz (depends on load circuit resonant frequency)

Note: the load must be tuned so that the highest operating frequency does not exceed the rating of the tank circuit capacitors.

Output Power Factor	0.92 Approx.
Output Voltage Waveform in Tank Circuit	Sinusoidal
Overall Efficiency	93%
Stability	± 3% for mains variations +10% or -5%

Water requirement

Flow	18 litres / minute
Inlet temperature	30°C

Dimensions

Height	1800 mm
Width	1200 mm
Depth	500 mm

A.1.2 Resistivity, Specific Heat and Thermal Conductivity Data for Mild Steel As Functions of Temperature (From Davies, 1979)

Below is an up to date table of data showing the changes in resistivity, specific heat and thermal conductivity with temperature for mild steel (0.23% carbon).

Temperature (°C)	ρ (Ωm)	cγ ($Wsm^{-3}K^{-1}$)	K ($Wm^{-1}K^{-1}$)
20	0.160×10^{-6}	3.65×10^{6}	52.0
100	0.220×10^{-6}	3.85×10^{6}	51.0
200	0.290×10^{-6}	4.10×10^{6}	49.0
300	0.380×10^{-6}	4.40×10^{6}	46.0
400	0.483×10^{-6}	4.77×10^{6}	43.0
500	0.610×10^{-6}	5.19×10^{6}	39.3
600	0.755×10^{-6}	5.66×10^{6}	35.5
700	0.922×10^{-6}	6.66×10^{6}	31.5
800	1.095×10^{-6}	6.73×10^{6}	26.0
900	1.135×10^{-6}	5.94×10^{6}	26.5
1000	1.168×10^{-6}	5.09×10^{6}	27.3
1100	1.195×10^{-6}	5.10×10^{6}	28.5

Table A.1.1 Some Physical Properties of Mild Steel As a Function of Temperature

A.1.3 Specification of Radyne 100kW Induction Heater

Number of Coils	3 in series
Number of turns per coil	29
Length of coil	0.35 m
Diameter of coil	0.045 m
Power supply	Tank circuit inverter
Rating	100kW
Nominal frequency	2400 Hz
Maximum field strength	100 000 A/m
High power setting	1500 A, 550 V
Low power setting	650 A, 240V

A.1.4 Accelerometer Specification

Make	Bruel & Kjaer
Accelerometer Type	4343
Weight	11 grams
Charge Sensitivity	10.15 pC/g
Voltage Sensitivity	8.91 mV/g
Mounted Resonance	42 kHz
Frequency Range	10% : 0.1 Hz - 12.6 kHz
Capacitance	1139 pF
Max. Transverse Sensitivity	2.6%
Transverse Resonance	15 kHz
Construction	Delta Shear
Typical Temperature Transient Sensitivity	0.04 g/°C
Typical Magnetic Sensitivity	0.04 g/kGauss
Typical Acoustic Sensitivity	0.001 g
Ambient Temperature Range	-74°C to 250°C
Max. Operational Shock	20 000 g
Max. Continuous Sinusoidal Acceleration	6000 g
Base Material	Titanium ASTM Gr. 2

A.1.5 Specification of the Conditioning Amplifier

Make	Bruel and Kjaer
Type	2626
Maximum Charge Input	10^5 pC
Sensitivity Conditioning	3 digit dial in of transducer sensitivity from 1 - 1099 pC/unit
Amplifier Sensitivity	0.1 to 1000 mV/pC corresponding to - 20 to + 60 dB with transducer capacitance of 1 nF
Calibrated Output Ratings	0.001 to 10V/unit selectable in 20dB steps
Accuracy	± 0.5% at 1 kHz increasing to ±1% at 10 kHz for input loads less than 60 nF and 20 nF respectively
Signal Output (Direct)	10 V (10mA) peak from 0.3 Hz to 30 kHz
DC Offset	± 10 mV max
Output Impedance	< 1 Ω at frequencies up to 10 kHz for all V/unit out settings
Frequency Range	0.3 Hz to 100 kHz

Low Pass Filter	Switchable: 3dB upper limits of 1 kHz, 3 kHz, 10 kHz, 30 kHz and Lin ≈ 100 kHz with attenuation slope of 40 dB/decade
High Pass Filter	Switchable: 3dB lower limits of 0.3 Hz, 1 Hz, 3 Hz, 10 Hz and 30 Hz with attenuation slope of 20 dB/decade
Distortion	< 1%
Inherent Noise (2Hz to 22 kHz)	$5x10^{-3}$ pC referred to input with maximum sensitivity and 1 nF transducer capacitance
Level Indicators	Overload - LED lights when input or output exceeds 10 V peak 20dB from Overload - LED lights when output is between 1 and 10 V peak
Rise Time	≈ 2.5 V/μs
Recovery Time	< 200μs

A.1.6 Specification of the Ometron VS100 Vibration Sensor

Laser Class	< 1 mW output, class II
Vibration Velocity	± 0.005 to ± 100 mm/s
Vibration Frequency	DC to beyond 50 kHz
Working Distance	Over 200 m dependent on surface coating
Spatial Resolution	1 mm diameter at 20 m working distance 0.1 mm diameter at 0.5 m working distance
Working Depth of Field	± 3 m at 10 m working distance
Signal Output	Analog velocity signal ± 10 V BNC Frequency shifted Doppler signal 0.1 V Square Wave Analog Doppler signals 1 and 2 (in quadrature)
Optical Unit Dimensions	325 x 210 x 85 mm
Weight	7 kg
Power Requirements	12 V or 110/240 V rms, 50/60 Hz

A.1.7 Specification of the Linear Variable Differential Transformer (LVDT) and Conditioning Amplifier

Transducer Type:	GTX1000 / 313
Make:	RDP Electronics Ltd
Calibrated Temperature:	20°C
Linear Range:	± 1 mm
Sensitivity:	150 mV / V / mm with 5 V rms 5 kHz Excitation
Linearity:	0.05%
Gain Range:	6
Single Input Equivalent to:	IN 1 mm OUT 1 mm
To Give an Instrument Output of:	- 5.0 V + 5.0 V

Conditioning Amplifier:	S7AC
Make:	RDP Electronics Ltd
Supply:	± 6 V to ± 18 V or +12 V to +36 V at 50 mA
Voltage Output - dual supply:	± 4 V to ± 10 V into 2 kΩ
- single supply:	± 4 V to ± 10 V into 10 kΩ
Current Output - both supplies:	4 - 20 mA into 100 / 550 Ω max. overload internally limited to 30 mA max.
Oscillator Output:	1 V rms at 5 kHz standard. 1 kHz - 10 kHz via resistor change. 25 mA maximum.
Oscillator Temp. Coefficient:	0.005% / °C typical
Demodulation:	Synchronous
Amplifier Gain:	x 0.07 to x 500 in 8 ranges with fine control
Zero Range:	± 5 V minimum
Linearity:	0.1% of full scale
Input Resistance:	130 kΩ differential
Zero Stability: Voltage O/P:	0.002% of f.s. typical / °C
Current O/P:	0.005% of f.s. typical / °C
Gain Stability: Voltage O/P:	0.005% of f.s. typical / °C
Current O/P:	0.01% of f.s. typical / °C
Bandwidth:	dc to 500 Hz (flat)
Noise: on Voltage Output:	5 mV peak to peak typical
on Current Output:	10 µA peak to peak typical
Temperature Range:	-10°C to 60°C
Dimensions:	150 x 64 x 34 mm
Weight:	0.35 kg
Gland Cable Diameter:	2 to 5 mm
Seals:	IP65 Specification

A.1.8 Strain Gauge Specification

Make:	Kyowa Electronic Instruments Co, Ltd
Model:	KHCS-10-120-G12
Gauge type:	Uniaxial, 2-element
Resistor element:	Special heat resistant alloy
Gauge resistance:	120 Ω ± 10 Ω (with 2 m long MI cable)
Difference between active and dummy gauge resistance:	± 5 Ω or less
Gauge length:	10 mm
Matchable linear expansion coefficients:	11, 13 and 16 ppm/°C
Highest operating temperature:	750°C
Gauge factor (at room temperature):	Approx. 2.0 (with 2 m long MI cable, after temperature compensation)
(at 750°C):	Approx. 1.8 (with 1 m heated component length, after temperature compensation)
Thermally induced apparent strain:	See data sheet
Compensated temperature range:	25 to 750°C
Leadwire (soft cable):	ϕ 1.7, 3-conductor 0.5 m ETFE shielded
(MI cable):	ϕ 1.6, Ni 3-conductor MI cable (2 m long)
Drift (at 750°C):	± 10 x 10^{-6} strain/hour or less
Strain limit (at 750°C):	10 000 x 10^{-6} strain
Fatigue life (750°C):	1 x 10^{6} or more operations
Insulation resistance (at room temperature):	1000 MΩ or higher
(at 750°C):	50 kΩ or higher (with 2 m long MI cable and 1 m long heated length)
Allowable maximum load:	50 mA
Allowable minimum radius of curvature for gauge installation:	20 mm
Materials (flange and tube):	Inconel 600 (NCF 600)
Gauge installation:	Spot-welds (P=0.8mm) in 2 rows on 2 sides

Aston University

Page removed for copyright restrictions.

APPENDIX TWO

CALCULATIONS

A.2.1 Eddy Current Density In A Bar Heated By Induction

Using the approximate formula, equation 5.2 to calculate the eddy current density in a sheet due to parallel conductors, it is possible to apply it to the situation of a bar inside a coil to obtain an approximation of the eddy current density distribution in a steel cylindrical bar.

Here the coil current is **i**, the eddy current density is **jtotal** and the field is **h**. The distance between each turn is **d** which are a height **h** above the suface of the bar.

The total eddy current density in the bar, a distance **z** from the centre line is found by applying equation 5.1 to each turn of the coil and adding.

Spliting the equation into three parts, denoted by **j**, **j2** and **j3**:

In[1]:=

```
j = i / (Pi h)
```

Out[1]=

$$\frac{i}{h\ Pi}$$

Taking one half of the coil only where **n** is the number of turns.

In[2]:=

```
j2 = Sum [1 / (1 + ((z -(0.16 + 0.31 n)h) / h)^2),
{n,0,11}]
```

Out[2]=

$$\frac{1}{1+\frac{(-3.57\,h+z)^2}{h^2}}+\frac{1}{1+\frac{(-3.26\,h+z)^2}{h^2}}+\frac{1}{1+\frac{(-2.95\,h+z)^2}{h^2}}+\frac{1}{1+\frac{(-2.64\,h+z)^2}{h^2}}+\frac{1}{1+\frac{(-2.33\,h+z)^2}{h^2}}+\frac{1}{1+\frac{(-2.02\,h+z)^2}{h^2}}+\frac{1}{1+\frac{(-1.71\,h+z)^2}{h^2}}+\frac{1}{1+\frac{(-1.4\,h+z)^2}{h^2}}+\frac{1}{1+\frac{(-1.09\,h+z)^2}{h^2}}+\frac{1}{1+\frac{(-0.78\,h+z)^2}{h^2}}+\frac{1}{1+\frac{(-0.47\,h+z)^2}{h^2}}+\frac{1}{1+\frac{(-0.16\,h+z)^2}{h^2}}$$

Calculating the second part of the summation:

In[3]:=

```
j3 = Sum [1 / (1 + ((z +(0.16 + 0.31 n)h) / h)^2),
{n,0,11}]
```

Out[3]=

$$\frac{1}{1+\frac{(0.16\,h+z)^2}{h^2}}+\frac{1}{1+\frac{(0.47\,h+z)^2}{h^2}}+\frac{1}{1+\frac{(0.78\,h+z)^2}{h^2}}+\frac{1}{1+\frac{(1.09\,h+z)^2}{h^2}}+\frac{1}{1+\frac{(1.4\,h+z)^2}{h^2}}+\frac{1}{1+\frac{(1.71\,h+z)^2}{h^2}}+\frac{1}{1+\frac{(2.02\,h+z)^2}{h^2}}+\frac{1}{1+\frac{(2.33\,h+z)^2}{h^2}}+\frac{1}{1+\frac{(2.64\,h+z)^2}{h^2}}+\frac{1}{1+\frac{(2.95\,h+z)^2}{h^2}}+\frac{1}{1+\frac{(3.26\,h+z)^2}{h^2}}+\frac{1}{1+\frac{(3.57\,h+z)^2}{h^2}}$$

The total eddy current density, **jtotal** is calculated from:

In[4]:=

```
jtotal = j (j2 +j3)
```

Out[4]=

$$
\begin{aligned}
(i\ (& \frac{1}{1+\frac{(-3.57\,h+z)^2}{h^2}}+\frac{1}{1+\frac{(-3.26\,h+z)^2}{h^2}}+\\
& \frac{1}{1+\frac{(-2.95\,h+z)^2}{h^2}}+\frac{1}{1+\frac{(-2.64\,h+z)^2}{h^2}}+\\
& \frac{1}{1+\frac{(-2.33\,h+z)^2}{h^2}}+\frac{1}{1+\frac{(-2.02\,h+z)^2}{h^2}}+\\
& \frac{1}{1+\frac{(-1.71\,h+z)^2}{h^2}}+\frac{1}{1+\frac{(-1.4\,h+z)^2}{h^2}}+\\
& \frac{1}{1+\frac{(-1.09\,h+z)^2}{h^2}}+\frac{1}{1+\frac{(-0.78\,h+z)^2}{h^2}}+\\
& \frac{1}{1+\frac{(-0.47\,h+z)^2}{h^2}}+\frac{1}{1+\frac{(-0.16\,h+z)^2}{h^2}}+\\
& \frac{1}{1+\frac{(0.16\,h+z)^2}{h^2}}+\frac{1}{1+\frac{(0.47\,h+z)^2}{h^2}}+\\
& \frac{1}{1+\frac{(0.78\,h+z)^2}{h^2}}+\frac{1}{1+\frac{(1.09\,h+z)^2}{h^2}}+\\
& \frac{1}{1+\frac{(1.4\,h+z)^2}{h^2}}+\frac{1}{1+\frac{(1.71\,h+z)^2}{h^2}}+\\
& \frac{1}{1+\frac{(2.02\,h+z)^2}{h^2}}+\frac{1}{1+\frac{(2.33\,h+z)^2}{h^2}}+\\
& \frac{1}{1+\frac{(2.64\,h+z)^2}{h^2}}+\frac{1}{1+\frac{(2.95\,h+z)^2}{h^2}}+\\
& \frac{1}{1+\frac{(3.26\,h+z)^2}{h^2}}+\frac{1}{1+\frac{(3.57\,h+z)^2}{h^2}}))\ /\ (h\ Pi)
\end{aligned}
$$

The current, **i** in each turn of the coil is 1033 Amps:

```
In[5]:=
  i = 1033
Out[5]=
  1033
```

The height, **h** between the surface of the bar and coil is 40 mm:

```
In[6]:=
  h = 40
Out[6]=
  40
```

Using these values the value of the total eddy current density at a distance **z** from the centre line is:

```
In[7]:=
  N[jtotal]
Out[7]=
```

$$8.22035\left(\frac{1}{1. + 0.000625\,(-142.8 + z)^2} + \frac{1}{1. + 0.000625\,(-130.4 + z)^2} + \frac{1}{1. + 0.000625\,(-118. + z)^2} + \frac{1}{1. + 0.000625\,(-105.6 + z)^2} + \frac{1}{1. + 0.000625\,(-93.2 + z)^2} + \frac{1}{1. + 0.000625\,(-80.8 + z)^2} + \frac{1}{1. + 0.000625\,(-68.4 + z)^2} + \frac{1}{1. + 0.000625\,(-56. + z)^2} + \frac{1}{1. + 0.000625\,(-43.6 + z)^2} + \frac{1}{1. + 0.000625\,(-31.2 + z)^2} +\right.$$

$$\frac{1}{1. + 0.000625\ (-18.8 + z)^2} +$$
$$\frac{1}{1. + 0.000625\ (-6.4 + z)^2} +$$
$$\frac{1}{1. + 0.000625\ (6.4 + z)^2} +$$
$$\frac{1}{1. + 0.000625\ (18.8 + z)^2} +$$
$$\frac{1}{1. + 0.000625\ (31.2 + z)^2} +$$
$$\frac{1}{1. + 0.000625\ (43.6 + z)^2} +$$
$$\frac{1}{1. + 0.000625\ (56. + z)^2} +$$
$$\frac{1}{1. + 0.000625\ (68.4 + z)^2} +$$
$$\frac{1}{1. + 0.000625\ (80.8 + z)^2} +$$
$$\frac{1}{1. + 0.000625\ (93.2 + z)^2} +$$
$$\frac{1}{1. + 0.000625\ (105.6 + z)^2} +$$
$$\frac{1}{1. + 0.000625\ (118. + z)^2} +$$
$$\frac{1}{1. + 0.000625\ (130.4 + z)^2} +$$
$$\frac{1}{1. + 0.000625\ (142.8 + z)^2})$$

Plotting a curve of eddy current density for values of **z** between -240 mm and 240 mm :

In[8]:=

```
bp = Plot[jtotal, {z, -240, 240}]
```

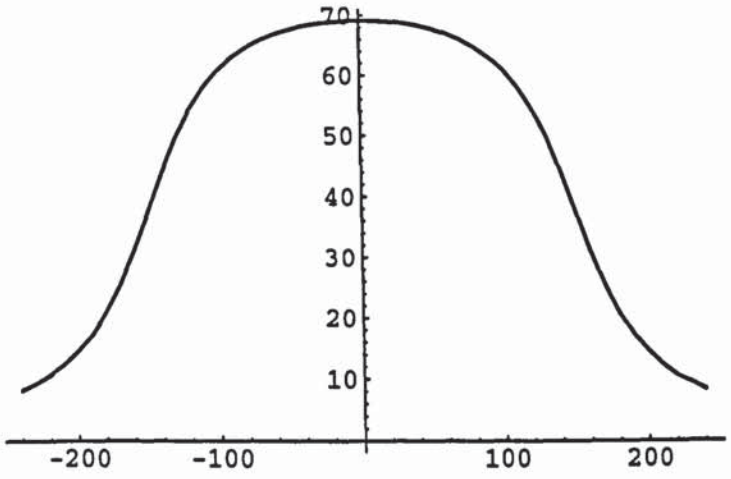

Out[8]=

-Graphics-

Adding labels:

In[9]:=

```
Show[bp, PlotRange->{0,70},
AxesLabel->{"z (mm)", "J (A/mm)"}]
```

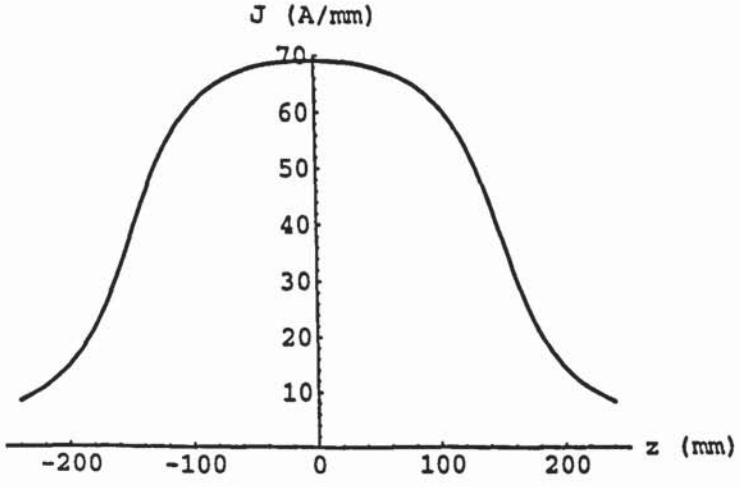

Out[9]=

-Graphics-

A.2.2 Field Produced By A Circular Loop

The flux density at a point P due to a circular loop of current can be found in texts such as Smythe (1950). The derivations are not given here, only the final equations.

The flux density in the radial direction, denoted by **bp** for a single loop is given by:

In[10]:=

```
bp = ((mu i) / (2 Pi)) (z / (r(Sqrt[(a + r)^2 +
z^2]))) (-EllipticK[m]+(EllipticE[m]((a^2+
r^2+z^2)/((a-r)^2+z^2))))
```

Out[10]=

$$(1033\ \text{mu}\ z\ (\frac{(a^2 + r^2 + z^2)\ \text{EllipticE[m]}}{(a - r)^2 + z^2} - \text{EllipticK[m]})) \ /\ (2\ \text{Pi}\ r\ \text{Sqrt}[(a + r)^2 + z^2])$$

where **i** is the coil current (A) rms
mu is the permeability of free space (H/m)
z is the axial distance between point P and the plane of the coil (m)
a is the radius of the coil (m)
r is the radius of point P (m)
K(m) is the complete elliptic integral of the first kind
E(m) is the complete elliptic integral of the second kind

The total flux density is found by calculating **bp** for each turn of the coil and adding.

The flux density in the axial direction, denoted by **bz** for a single loop is given by:

In[11]:=

```
bz = ((mu i) / (2 Pi)) (1 / (Sqrt[(a + r)^2 +
z^2])) (EllipticK[m]+(EllipticE[m]((a^2-r^2-
z^2)/((a-r)^2+z^2))))
```

Out[11]=

$$\frac{1033\ \text{mu}\ (\frac{(a^2 - r^2 - z^2)\ \text{EllipticE[m]}}{(a - r)^2 + z^2} + \text{EllipticK[m]})}{2\ \text{Pi}\ \text{Sqrt}[(a + r)^2 + z^2]}$$

The values for **r, a, m, mu** and **i** are introduced:

In[12]:=

```
r = 0.02;
```

In[13]:=

```
a = 0.07;
```

```
In[14]:=
  m = 4 a r((a + r)^2 + z^2)^-1
```

Out[14]=

$$\frac{0.0056}{0.0081 + z^2}$$

```
In[15]:=
  mu = 4 Pi 10^-7;
In[16]:=
  i = 1033;
```

The value of **bp** is then calculated for each of the 24 turns of the coil which was spaced 13 mm apart.

```
N[bp] /.{z->0}
0
N[bp] /.{z->0.013}
0.000780698
N[bp] /.{z->0.026}
0.00117714
N[bp] /.{z->0.039}
0.00118426
N[bp] /.{z->0.052}
0.000998193
N[bp] /.{z->0.065}
0.000773069
N[bp] /.{z->0.078}
0.000576193
N[bp] /.{z->0.091}
0.000423573
N[bp] /.{z->0.104}
0.0003112
N[bp] /.{z->0.117}
0.000230126
N[bp] /.{z->0.130}
0.000171899
N[bp] /.{z->0.143}
0.000129922
N[bp] /.{z->0.156}
0.0000994104
```

```
N[bp] /.{z->0.169}
0.0000770005
N[bp] /.{z->0.182}
0.000060352
N[bp] /.{z->0.195}
0.0000478381
N[bp] /.{z->0.208}
0.0000383227
N[bp] /.{z->0.221}
0.000031006
N[bp] /.{z->0.234}
0.0000253196
N[bp] /.{z->0.247}
0.000020855
N[bp] /.{z->0.260}
0.0000173162
N[bp] /.{z->0.273}
0.0000144858
N[bp] /.{z->0.286}
0.0000122028
N[bp] /.{z->0.299}
0.0000103466
```

The total is then found by addition to equal 0.00721 Tesla.

Similarly for the axial component of the flux density at P the values for each of the 24 turns of the coil are:

```
N[bz] /. {z->0}
0.00988707
N[bz] /. {z->0.013}
0.00926901
N[bz] /. {z->0.026}
0.0077873
N[bz] /. {z->0.039}
0.00610776
N[bz] /. {z->0.052}
0.00463687
```

```
N[bz] /. {z->0.065}
0.00348629
N[bz] /. {z->0.078}
0.00262856
N[bz] /. {z->0.091}
0.00199994
N[bz] /. {z->0.104}
0.00153999
N[bz] /. {z->0.117}
0.00120139
N[bz] /. {z->0.130}
0.000949616
N[bz] /. {z->0.143}
0.000760188
N[bz] /. {z->0.156}
0.000615889
N[bz] /. {z->0.169}
0.0005046
N[bz] /. {z->0.182}
0.000417734
N[bz] /. {z->0.195}
0.00034915
N[bz] /. {z->0.208}
0.000294414
N[bz] /. {z->0.221}
0.000250285
N[bz] /. {z->0.234}
0.000214371
N[bz] /. {z->0.247}
0.000184882
N[bz] /. {z->0.260}
0.000160471
N[bz] /. {z->0.273}
0.000140107
N[bz] /. {z->0.286}
0.000122998
```

```
N[bz] /. {z->0.299}
0.000108528
```

The total is found by addition to equal 0.0536 Tesla.

APPENDIX THREE

RESEARCH PUBLICATIONS

1) Vibration in Electromagnetically Heated Steel
Richard T. Baker and Trevor N. Oliver
Presented at the International Symposium on Electromagnetic Processing of Materials (EPM '94)
Nagoya, Japan.
25-28 October 1994

2) Magnetostriction and Vibration in Steel Heated by Induction
R.T. Baker and T.N. Oliver
Presented at the 30th Universities Power Engineering Conference (UPEC '95)
Greenwich University, UK.
5-7 September 1995

3) Effect of Temperature on Vibration and Magnetostriction in Mild Steel Heated by Induction
R.T. Baker and T.N. Oliver
To be Presented at the International Congress on Electricity Applications
International Convention Centre, Birmingham, UK.
16-20 June 1996

Aston University

Pageă removed for copyright restrictions.